



OpenAIR@RGU

The Open Access Institutional Repository at Robert Gordon University

<http://openair.rgu.ac.uk>

Citation Details

Citation for the version of the work held in 'OpenAIR@RGU':

HECTOR, E. E., 2007. Molecular mechanisms of nutrient mediated regulation of hypoxia inducible factor -1a(HIF-1a) in endothelial cells. Available from *OpenAIR@RGU*. [online]. Available from: <http://openair.rgu.ac.uk>

Copyright

Items in 'OpenAIR@RGU', Robert Gordon University Open Access Institutional Repository, are protected by copyright and intellectual property law. If you believe that any material held in 'OpenAIR@RGU' infringes copyright, please contact openair-help@rgu.ac.uk with details. The item will be removed from the repository while the claim is investigated.

**MOLECULAR MECHANISMS OF NUTRIENT
MEDIATED REGULATION OF
HYPOXIA INDUCIBLE FACTOR – 1 α (HIF-1 α)
IN ENDOTHELIAL CELLS**

Emma E. Hector

**Molecular mechanisms of nutrient mediated regulation of
Hypoxia inducible factor – 1 α (HIF-1 α) in endothelial cells.**

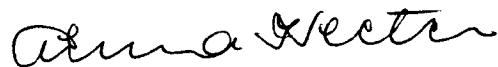
Emma E. Hector (Bsc. Hons) (Aberdeen)

A thesis submitted in partial fulfilment of the requirements of
The Robert Gordon University
for the degree of Doctor of Philosophy

February 2007

Declaration

This thesis in candidature for the degree of Doctor of Philosophy has been composed entirely by myself. The work which is documented was carried out by myself, with the exception of cryostat sectioning of tissues from the rat model of diabetes, which was done by Profs. Mary Cotter and Norman Cameron of Aberdeen University (section 2.1), and detection of HIF-1 α protein expression in the vasculature of the 24 week diabetic rat supplemented with α -lipoic acid (fig 3.4) which was carried out by Stuart Fergusson. All sources of information contained within which have not arisen from the results generated have been specifically acknowledged.

A handwritten signature in cursive script, reading "Emma Hector".

Emma E. Hector

**Dedicated to the memory of
my beloved Granny Jess
who would have been so very proud**

Contents		Page
(i) Acknowledgements		I
(ii) Abstract		III
(iii) Abbreviations		IV
Chapter 1	Introduction	
1.1	Overview	2
1.2	Diabetes mellitus	3
1.3	Vascular complications of diabetes	4
1.3.1	Microvascular complications	4
1.3.1.1	Neuropathy	4
1.3.1.2	Retinopathy	5
1.3.1.3	Nephropathy	5
1.3.2	Macrovascular complications	6
1.3.3	Pathogenic mechanisms of vascular complications of diabetes	6
1.3.3.1	Glycolysis and the Warburg effect	7
1.3.3.2	The sorbitol pathway	10
1.3.3.3	Kinase/phosphatase pathways	12
1.3.3.4	Advanced glycation end products (AGE)	15
1.4	Role of the vascular endothelium in diabetic complications	15
1.4.1	Physiology of the vascular endothelium	15
1.4.2	Mediators of dysfunction of the vascular endothelium	16
1.4.2.1	Reactive oxygen species (ROS)	16
1.4.2.2	Neutrophil attraction and adherence	16
1.4.2.3	Vasoactive substances	17
1.4.2.4	Growth factors	17
1.4.2.5	EC receptors	19
1.4.2.6	Hypoxia	20
1.5	Hypoxia inducible factor-1 (HIF-1)	21
1.5.1	The HIF family	21
1.5.1.1	HIF-2 and HIF-3	21
1.5.1.2	HIF-1	22
1.5.2	Role of HIF-1 in the induction of hypoxia-responsive genes	24
1.5.2.1	Growth factors and HIF-1	26
1.5.2.2	Glucose transporters and HIF-1	26
1.5.2.3	Glycolytic enzymes and HIF-1	27

1.5.3	Mechanisms involved in the hypoxic regulation of HIF-1 α expression	28
1.5.3.1	Oxygen sensing	28
1.5.3.2	Stabilisation of HIF-1 α	31
1.5.3.3	Inhibition and competitive binding	32
1.5.3.4	Modification of MAPK- and Pi3K-dependent pathways	35
1.5.3.5	Redox signalling	36
1.5.3.6	Time course of HIF-1 α expression	36
1.5.4	Non-hypoxic regulation of HIF-1 α expression	37
1.5.4.1	Positive regulation	37
1.5.4.2	Negative regulation	42
1.5.5	Role of HIF-1 α in the development of physiological and pathophysiological processes associated with disease and cell damage	42
1.5.5.1	Carcinogenesis	42
1.5.5.2	Apoptosis	44
1.5.5.3	Wound healing	44
1.5.5.4	Diabetic complications	44
1.5.6	Potential role of glucose in the regulation of HIF-1 α	46
1.6	<i>In vivo</i> and <i>in vitro</i> models of experimental diabetes mellitus	47
1.7	Aims of the study	48
Chapter 2	Materials and methods	50
2.1	Streptozotocin-induced diabetic rat model	51
2.1.1	Streptozotocin treatment of rats	51
2.1.2	Preparation of cryostat sections	51
2.2	Cell culture	52
2.2.1	Cell culture materials	52
2.2.2	Human umbilical vein endothelial cells (HUVEC)	52
2.2.2.1	Cell growth conditions	52
2.2.2.2	Routine subculture	53
2.2.2.3	Sub-culture for experimental procedures	53
2.2.2.3.1	Sub-culture of HUVEC into 75cm ² flasks	54
2.2.2.3.2	Sub-culture of HUVEC into chamber slides	54
2.2.2.3.3	Sub-culture of HUVEC into 96 well plates	54
2.2.3	Cell viability and proliferation	55
2.2.3.1	Trypan blue dye exclusion method	55
2.2.3.2	Alamar blue cell growth assay	55

2.2.4	Artificial induction of Hypoxia	56
2.2.4.1	Chemical induction of hypoxia	56
2.2.4.2	Non-chemical induction of hypoxia	57
2.2.5	Alteration of glucose concentration and substitution with glucose analogues	57
2.2.6	Inhibition of signalling pathways in cell culture	58
2.2.6.1	Transcription and translation	58
2.2.6.2	Protein kinase activity	58
2.2.6.3	Redox signalling	59
2.3	Immunochemical staining	59
2.3.1	Avidin-biotin complex /alkaline phosphatase (ABC/AP) procedure for use with monoclonal mouse antibody	59
2.3.1.1	Overview of ABC/AP	59
2.3.1.2	IHC using ABC/AP applied to cryostat sections of animal tissue	61
2.3.1.3	ICC using HUVEC grown on chamber slides	62
2.4	Polymerase chain reaction (PCR)	62
2.4.1	RNA extraction from whole cell preparations	63
2.4.1.1	Sample homogenisation using spin columns	63
2.4.1.2	RNA extraction using RNeasy midi kit	63
2.4.2	Assessment of concentration and purity of RNA	64
2.4.3	Preparation of complementary DNA (cDNA)	66
2.4.3.1	Reverse transcriptase polymerase chain reaction (RT-PCR)	66
2.4.3.2	cDNA priming	67
2.4.3.3	In vitro amplification of cDNA by PCR	70
2.4.3.3.1	Preparation of amplification reaction mix	70
2.4.3.3.2	Amplification of DNA sequence	70
2.4.4	Validation and analysis of double stranded DNA (dsDNA)	71
2.4.4.1	Agarose gel electrophoresis	71
2.4.4.2	PicoGreen dsDNA quantitation kit	71
2.4.4.3	Optimisation of amplification process	73
2.5	Riboprobe preparation	73
2.5.1	PCR product purification	73
2.5.1.1	Preparative agarose gel electrophoresis	73
2.5.1.2	WIZARD PCR preps DNA purification system	74
2.5.1.3	Quantification of purified DNA	75
2.5.2	Ligation mediated recombinant plasmid (LMRP) cloning	75

2.5.2.1	PCR product ligation into pGEM-T Easy Vector	77
2.5.2.2	Bacterial cell transformation	77
2.5.2.3	IPTG/X-Gal screening of transformed bacteria	78
2.5.2.4	Plasmid Purification	79
2.5.2.5	Restriction digest of plasmid DNA	80
2.5.3	RNA labelling with digoxigenin-UTP (DIG-UTP) by <i>in vitro</i> transcription with SP6 and T7 RNA polymerases	81
2.5.3.1	Standard transcription assay	82
2.5.3.2	Dot blot determination of labelling efficiency	83
2.5.3.3	DIG Luminescent Detection Kit	84
2.5.3.4	Exposure and development of chemiluminescent film	85
2.5.4	RNA labelling with biotin by <i>in vitro</i> transcription with SP6 and T7 RNA polymerases	85
2.5.4.1	MAXIscript <i>in vitro</i> transcription kit	85
2.5.4.2	BrightStar psoralen-biotin nonisotopic labelling kit	87
2.5.4.3	BrightStar BioDetect detection kit	87
2.6	<i>In situ</i> hybridisation (ISH)	88
2.6.1	Fixation of cells grown on glass slides	88
2.6.2	Hybridisation of antisense RNA probe	89
2.6.3	Washing and RNase digestion of unbound probe	89
2.6.4	Immunological detection of bound probe	90
2.7	Ribonuclease protection assay (RPA)	91
2.7.1	Hybridisation of probe and sample RNA	91
2.7.2	RNase digestion of unhybridised probe and sample RNA	91
2.7.3	Separation and detection of protected fragments	92
Chapter 3	HIF-1α protein expression in a rat model of diabetes	93
3.1	Introduction	94
3.2	Materials and methods	95
3.3	Results	95
3.3.1	HIF-1 α expression 4 weeks after STZ-induction of diabetes	95
3.3.2	HIF-1 α expression 10 weeks after STZ-induction of diabetes	98
3.3.3	HIF-1 α expression 24 weeks after STZ-induction of diabetes	98
3.3.4	Effect of α -lipoic acid dietary supplementation on the level of HIF1 α protein in the sciatic nerve of the 24 week diabetic rat	98
3.4	Discussion	105

Chapter 4	Evaluation of methods for the detection of HIF-1α mRNA	107
4.1	Introduction	108
4.2	Materials and methods	109
4.2.1	<i>In situ</i> hybridisation (ISH)	109
4.2.2	Ribonuclease protection assay (RPA)	109
4.2.3	Quantitative Picogreen analysis of RT-PCR	110
4.3	Results	110
4.3.1	Riboprobe synthesis for detection of HIF-1 α mRNA	110
4.3.2	<i>In situ</i> detection of HIF-1 α mRNA	114
4.3.3	Ribonuclease protection of HIF-1 α mRNA	114
4.3.4	Optimum conditions for Picogreen detection of HIF-1 α mRNA	119
4.4	Discussion	124
Chapter 5	Effect of glucose and hypoxia on HIF-1α expression in HUVEC	127
5.1	Introduction	128
5.2	Materials and methods	129
5.2.1	Determination of cell growth and viability	129
5.2.2	Incubation of HUVEC with altered glucose and oxygen concentration	129
5.2.3	Determination of gene expression by Picogreen quantification of PCR products	130
5.2.4	Inhibition of RNA transcription and protein translation	130
5.2.5	Immunocytochemical detection of HIF-1 α protein expression in HUVEC	130
5.2.6	Data Analysis	131
5.3	Results	131
5.3.1	Effect of altered glucose and oxygen concentration on HUVEC growth	131
5.3.2	Effect of altered glucose and oxygen concentration on HIF-1 α mRNA expression	133
5.3.3	Contribution of transcription and translation pathways to regulation of HIF-1 α mRNA	133
5.3.4	Effect of altered glucose and oxygen concentration on expression of genes induced by HIF-1 α , and its natural antisense, aHIF	137
5.3.5	Effect of altered glucose and oxygen concentration on HIF-1 α protein expression	140
5.4	Discussion	143

Chapter 6	Mechanism of regulation of HIF-1α mRNA level in HUVEC	147
6.1	Introduction	148
6.2	Materials and methods	149
6.2.1	Effect of the antioxidant α -lipoic acid on level of HIF-1 α mRNA detected	149
6.2.2	Effect of inhibition of protein kinase activity on level of HIF-1 α mRNA detected	149
6.2.3	Effect of glucose analogues, 2-deoxyglucose and 3-orthomethylglucose, on HUVEC growth and HIF-1 α mRNA level detected	149
6.2.3.1	Determination of cell growth and viability	149
6.2.3.2	Determination of HIF-1 α mRNA level	150
6.2.4	Data Analysis	150
6.3	Results	150
6.3.1	Effect of the antioxidant α -lipoic acid on level of HIF-1 α mRNA level detected	150
6.3.2	Effect of protein kinase inhibition on level of HIF-1 α mRNA detected	152
6.3.3	Effect of the glucose analogues, 2-deoxyglucose and 3-orthomethylglucose, on HIF-1 α expression in HUVEC	154
6.3.4	Effect of the glucose analogues on HIF-1 α mRNA expression at 24 hours	154
6.4	Discussion	157
Chapter 7	General Discussion	160
7.1	Summary of findings	161
7.2	Discussion	
7.2	Future work	162
Appendix 1	References	176
Appendix 2	Buffers and solutions	216

Figures

Chapter 1	Introduction	
1.1	The anaerobic glycolytic pathway	8
1.2	The sorbitol pathway	11
1.3	Interaction between protein kinase signalling pathways in response to elevated glucose	14
1.4	Structure of HIF-1	23
1.5	Control of signalling through HIF-1 α in response to changing O ₂ levels	30
1.6	Schematic representation of HIF-1 α mRNA and its natural antisense, aHIF	34
1.7	Signal transduction pathways leading to the expression of HIF-1 and the transactivation of downstream target genes	39
Chaper 2	Materials and methods	
2.1	Schematic diagram of preformed avidin-biotin-alkaline phosphatase complex reacting with biotinylated secondary antibody	60
2.2	pGEM-T Easy Vector circle map	76
Chapter 3	HIF-1α protein expression in a rat model of diabetes	
3.1	Immunohistochemical detection of HIF-1 α in the sciatic nerve vasculature of 4 week control and diabetic rats	96
3.2	Immunohistochemical detection of HIF-1 α in the sciatic nerve vasculature of 10 week control and diabetic rats	99
3.3	Immunohistochemical detection of HIF-1 α in the sciatic nerve vasculature of 24 week control and diabetic rats	101
3.3	Effect of α -lipoic acid dietary supplementation on the level of HIF1 α protein in the sciatic nerve of the 24 week diabetic rat	103
Chapter 4	Evaluation of methods for the detection of HIF-1α mRNA	
4.1	Electrophoretically resolved HIF-1 α PCR product	111
4.2	Ligation mediated recombinant plasmid cloning	112
4.3	Dot blot demonstrating the quantitation of DIG-labelled riboprobe	113
4.4	<i>In situ</i> detection of mRNA expression in HUVEC	115
4.5	Ribonuclease protection of HIF-1 α mRNA	117
4.6	Determination of optimum cycle number for HIF-1 α amplification	120
4.7	Optimum expression of β_2 M as an internal control for HIF-1 α	122

Chapter 5 Effect of glucose and hypoxia on HIF-1 α expression in HUVEC

5.1	HUVEC growth curves in response to altered glucose and oxygen concentration	132
5.2	Effect of time, glucose and oxygen concentration on HIF-1 α mRNA expression	134
5.3	Effect of Act D on HIF-1 α expression at 24h in 20mM glucose	135
5.4	Effect of CHX on HIF-1 α expression at 24h in 20mM glucose	136
5.5	Electrophoretically resolved aHIF, GLUT-1 and IGF-1R PCR product	138
5.6	Expression of GLUT-1, IGF-1R and aHIF mRNA compared to that of HIF-1 α in response to 20mM glucose	139
5.7	Immunocytochemical detection of HIF-1 α protein expression in HUVEC	141

Chapter 6 Mechanism of regulation of HIF-1 α mRNA level in HUVEC

6.1	Effect of α -lipoic acid on HIF-1 α mRNA level detected	151
6.2	Effect of Pi3Ki and MAPKi on HIF-1 α mRNA level detected	153
6.3	HUVEC growth in response to glucose analogues at 24h	155
6.4	Effect of glucose analogues 2DG and 3OMG on HIF-1 α mRNA detection	156

Tables

Chapter 1 Introduction

1.1	Genes targeted for HIF-1-induced expression	25
-----	---	----

Chapter 2 Materials and methods

2.1	Summary of cDNA primers used for PCR amplification of gene products	68
2.2	Summary of components required for PicoGreen quantification of dsDNA standards	72
2.3	Components contained in the pGEM-T Easy Vector kit	77
2.4	Dilution of control RNA of known concentration	83
2.5	SP6 directed in vitro transcription of LMRP RNA	86
2.6	Components of ISH mix buffer	89

(i) Acknowledgements

Without the following people, I would not be where I am today, so to them I offer my most sincere thanks;

Firstly, to my Director of Studies, Dr. Rachel M. Knott, for her expert knowledge and guidance on the academic issues, and also her support and understanding on a more personal level. To my co-supervisor, Dr. Stephen M. MacManus, for the encouragement shown throughout this project, for proof reading this thesis and providing invaluable advice.

To Dorothy Moir, technician and good friend, who helped me find my feet in the early days, and provided great company as we muddled through the practicalities of life in the lab.

For the collaboration of Profs. Mary A. Cotter and Norman E. Cameron, Department of Biomedical Sciences, Aberdeen University, who kindly provided the diabetic rat tissues used in this study.

To Prof. John V. Forrester and his team at the Department of Ophthalmology, Aberdeen University, especially Marie Robertson and Liz Muckersie, for allowing me the use of their facilities and providing expert advice on cell culture methods.

To my fellow PhD students, both past and present, for their good humour and camaraderie, particularly Anita and Julie who shared the ups and downs of life in PC14.

In my new life as a post-doc (almost), I thank my new boss, Prof. Cherry L. Wainwright, for being so understanding and allowing me extra time to complete my write-up. Also, to my colleagues in PC9, Nelson, Margaret, Ciprian, Nicola and

double-trouble in the form of Sarah and Karen, without whom, I would probably get far more work done.

Last, but by no means least, I give love and thanks for the support of my family, Mum and Dad, mum-in-law Margaret, my husband Neil (who feared I had become a professional student) and our two beautiful little girls, Amelia and Arwen.

(ii) Abstract

Poorly controlled diabetes mellitus is associated with the development of chronic vascular complications which cause morbidity and premature mortality. Many studies have highlighted maintenance of normal blood glucose levels in all people with diabetes as the most effective way in which chronic complications can be reduced and prevented .

Presently, the underlying mechanisms associated with the manifestation and progression of vascular complications are poorly defined. Therefore, this study considered how the increased oxidative demand placed upon cells by high glucose concentration would result in a state of pseudohypoxia, and potentially the expression of hypoxia inducible factor- α (HIF-1 α).

In an animal model of diabetes, HIF-1 α protein expression was seen to increase in the vasculature surrounding the sciatic nerve at 10 and 24 weeks diabetes duration, which was seen to be reversed at 24 weeks in response to treatment with the antioxidant α -lipoic acid.

In vitro, exposure of HUVEC to 20mM glucose for 24h induced perinuclear expression of HIF-1 α protein, as opposed to nuclear expression evident under hypoxic conditions. Furthermore, at 24h in 20mM glucose, HIF-1 α mRNA level detected was significantly higher than that seen in all other conditions ($p < 0.001$).

The increase in HIF-1 α mRNA detected was seen to be dependent upon mRNA stability, and potentially its association with RNA-binding proteins and/or the natural antisense, aHIF. Pi3K and to a lesser extent p42/44 MAPK signalling pathways were also implicated, and α -lipoic acid treatment reversed the stability of HIF-1 α mRNA. The effect of high glucose on HIF-1 α mRNA level was not seen in response to partially/non-metabolisable glucose analogues, indicating glucose metabolism to be central to the stabilisation of HIF-1 α mRNA.

In conclusion, regulation of HIF-1 α at the level of mRNA and protein by the metabolism of high concentrations of glucose, may contribute to the generation of chronic vascular disease associated with diabetes, and should be further explored as a potential mechanism by which such complications may be prevented.

(iii) Abbreviations

ABC/AP	Avidin-biotin complex /alkaline phosphatase
Abs ₂₆₀	Absorbance at 260nm wavelength
Abs ₂₈₀	Absorbance at 280nm wavelength
Act D	Actinomycin D
ADP	Adenosine diphosphate
AGE	Advanced glycation end products
Amp ^r	Ampicillin resistant
Ang-2	Angiopoietin-2
Ang-4	Angiopoietin-4
ANOVA	One-way analysis of variance
aHIF	Natural antisense of HIF-1 α
AR	Aldose reductase
ARNT	Aryl hydrocarbon receptor nuclear translocator
Asn	Asparagine
ATP	Adenosine triphosphate
BAEC	Bovine aortic endothelial cells
BCEC	Bovine corneal endothelial cells
BDR	Background diabetic retinopathy
bFGF	Basic fibroblast growth factor
bHLH/PAS	basic helix-loop-helix/ Per-ARNT-Sim
β_2 -M	β_2 -microglobulin
bp	Base pairs
BREC	Bovine retinal endothelial cells
BSA	Bovine serum albumin
cAMP	Cyclic adenosine monophosphate
CBP	CREB binding protein
cDNA	Complementary DNA
CHX	Cyclohexamide
CO	Carbon monoxide

CO ₂	Carbon dioxide
COX-2	Cyclo-oxygenase-2
C-TAD	C-terminal transactivation domain
DAG	Diacylglycerol
DCCT	The Diabetes Control and Complications Trial
DEPC	Diethylpyrocarbonate
DFO	Desferrioxamine
2-DG	2-Deoxyglucose
dH ₂ O	Distilled water
DIG	Digoxigenin
DIG-AP	Anti-digoxigenin-alkaline phosphatase
DIG-UTP	Digoxigenin-uridine-5'-triphosphate
DM	Diabetes mellitus
DMSO	Dimethylsulphoxide
DNA	Deoxyribose nucleic acid
dNTP	Deoxynucleotide triphosphate
DR	Diabetic retinopathy
dsDNA	Double-stranded DNA
DTT	Dithiothreitol
EC	Endothelial cells
ECACC	The European Collection of Cell Cultures
<i>E. coli</i>	<i>Escherichia coli</i>
EDHF	Endothelium-derived hyperpolarising factor
EDTA	Ethyl diaminetetra-acetic acid
EGF	Epidermal growth factor
EGFR	Epidermal growth factor receptor
EMSA	Electrophoretic mobility shift assay
eNOS	Endothelial NOS
Epo	Erythropoietin
ET	Electron transport
iNOS	Inducible NOS

ET-1	Endothelin-1
F-2, 6-BP	Fructose-2, 6 bisphosphate
FAK	Focal adhesion kinase
FCS	Foetal calf serum
FIH-1	Factor inhibiting HIF-1
g	Gravity
GAPDH	Glyceraldehyde 3-phosphate dehydrogenase
GF/SF	Glucose-free/serum-free
GlcRE	Glucose response element
GLUT-1	Glucose transporter type-1
GLUT-3	Glucose transporter type-3
GMEM	Glasgow's Minimal Essential Medium
GSH	Glutathione
H	Hypoxia
h	Hours
HAT	Histone acetyl-transferase
HBSS	Hank's balanced salt solution
HCl	Hydrochloric acid
HDMEC	Human dermal microvascular endothelial cells
HIF-1	Hypoxia inducible factor-1
HIF-1 α	Hypoxia inducible factor-1 subunit α
HIF-1 β	Hypoxia inducible factor-1 subunit β
HK	Hexokinase
HKII	Hepatoma type II hexokinase
HRE	Hypoxia response element
HREC	Human retinal endothelial cells
HUVEC	Human umbilical vein endothelial cells
Hyp	Hypoxia
i	Inhibitor
ICAM-1	Intercellular adhesion molecule-1
ICC	Immunocytochemistry

ID	Inhibitory domain
IDDM	Insulin-dependent diabetes mellitus
IgG1	Immunoglobulin isotype 1
IGF-1	Insulin-like growth factor-1
IGF-1R	Insulin-like growth factor-1 receptor
IGFBP	IGF binding protein
IHC	Immunocytochemistry
IL	Interleukin
ISH	<i>In situ</i> hybridisation
JNK	NH-2 terminal kinase
KCl	Potassium chloride
LA	Alpha-lipoic acid
LB	Luria-Bertani
LMP	Low melting point
LMRP	Ligation mediated recombinant plasmid
L-PK	L-type pyruvate kinase
MAPK	Mitogen activated protein kinase
MCT-1	Monocarboxylate transporter type-1
MgCl ₂	Magnesium chloride
M-MLV	Murine Moloney leukaemia virus
mRNA	Messenger RNA
N	Normoxia
n	Number of experiments
NaCl	Sodium chloride
NADH	Nicotinamide adenine dinucleotide
NADPH	Nicotinamide adenine dinucleotide phosphate
NaOAc	Sodium acetate
NBF	Nerve blood flow
NBT/BCIP	Nitro blue tetrazolium chloride/5-bromo-4-chloro-3-indolylphosphate
NFκB	Nuclear factor κB
NIDDM	Non insulin-dependent diabetes mellitus

NLS-C	carboxyl- terminal nuclear localisation signal
NLS-N	amino- terminal nuclear localisation signal
NO	Nitric oxide
Norm	Normoxia
NOS	Nitric oxide synthase
N-TAD	N-terminal transactivation domain
O ₂	Oxygen
OD	Optical density
ODDD	Oxygen dependent degradation domain
4-OHE2	4-hydroxy estradiol
3-OMG	3-Orthomethylglucose
ONOO	Peroxynitrite
PAF	Platelet-activating factor
PAI-1	Plasminogen activator inhibitor-1
PBS	Phosphate buffered saline
PCR	Polymerase chain reaction
PDR	Proliferative diabetic retinopathy
PDH	Pyruvate dehydrogenase
PFA	Paraformaldehyde
PFK-1	Phosphofructokinase-1
PGK-1	Phosphoglycerate kinase-1
PHD	Prolyl hydroxylases
Pi3K	Phosphoinositol -3 protein kinase
PKC	Protein kinase C
PPP	Pentose phosphate pathway
PSTD	proline-serine-threonine-rich protein stability domain
PTEN	Phosphatase tensin homologue
pVHL	von Hippel Lindau tumour suppressor protein
RAGE	Endothelial AGE receptors
RBP	RNA-binding proteins
REDOX	Oxidation-reduction

REF-1	Redox factor-1
ROS	Reactive oxygen species
RNA	Ribose nucleic acid
RPA	Ribonuclease protection assay
RT-PCR	Reverse transcriptase polymerase chain reaction
SDH	Sorbitol dehydrogenase
SDS	Sodium dodecylsulphate
SRC-1	Steroid-receptor coactivator-1
SSC	Standard saline citrate
Strep-AP	Streptavidin-alkaline phosphatase
STZ	Streptozotocin
t	Time point
TAD	Transactivation domain
TAE	Tris-acetate EDTA
TBE	Tris-borate EDTA
TBS	Tris-buffered saline
TE	Tris-EDTA
TGF- β	Transforming growth factor- β
TIF-2	Transcription intermediary factor-2
TNF- α	Tumour necrosis factor- α
Trk-A	Tyrosine kinase receptor-A
tRNA	Transfer RNA
TRX	Thioredoxin
v/v	Volume/volume
VEGF	Vascular endothelial growth factor
VSMC	Vascular smooth muscle cells
vWF	von Willebrand factor
Ub	Ubiquitin
UKPDS	The United Kingdom Prospective Diabetes Survey
UTP	Uridine-5'-triphosphate
UTR	Untranslated region

UV	Ultra violet
w/v	Weight/volume

Chapter 1

Introduction

1.1 Overview

Poorly controlled diabetes mellitus is associated with the development of chronic vascular complications which cause morbidity and premature mortality. The need for maintaining normal blood glucose levels in all diabetic patients has been highlighted, as blood glucose which is elevated for several years is a major factor in the development and progression of vascular complications (The Diabetes Control and Complications Trial (DCCT), 1993; The UK Prospective Diabetes Survey (UKPDS), 1998).

The underlying mechanisms associated with the manifestation and progression of vascular complications, however, are still poorly defined. This thesis considers how a state of functional hypoxia arising from the need to metabolise elevated levels of glucose, resembling that experienced in poorly controlled diabetes, may contribute to the development of vascular disease associated with diabetes. This state of pseudohypoxia arises even though oxygen supply to the cells may be physiologically normal. However, the increased demand for oxidative phosphorylation of high concentrations of glucose will inevitably create a state of functional hypoxia, and potentially the expression of hypoxia-inducible genes associated with angiogenesis, glucose transport and metabolism.

A critical regulator of gene expression in response to hypoxia is a heterodimeric transcription factor termed hypoxia-inducible factor-1 (HIF-1), the inducible subunit of which is HIF-1 α . By investigating the expression of HIF-1 α in a rat model of diabetes, and in response to high glucose concentration under normal and decreased oxygen levels in cell culture, it may then be possible to determine the level at which any regulation is occurring, and also the mechanism(s) and signalling pathway(s) involved.

The outcome of this work is potentially very important, as it may help to elucidate whether glucose itself, glucose metabolite(s) or particular steps within the metabolic pathway could be targeted by therapies to prevent and treat the chronic vascular complications associated with diabetes.

1.2 Diabetes mellitus

Diabetes mellitus is a long term progressively debilitating disease, the only known insulin-independent therapy for which remains to be successful pancreatic transplantation, first performed in 1966 (Kelly *et al.*, 1967). Advancements made in pancreatic transplant technology in the past 10 years have resulted in a steady rise in graft function and patient survival rates (Gruessner *et al.*, 2005). However, post-operative vascular complications resulting in graft dysfunction do present a significant problem (Freund *et al.*, 2004).

According to a recent report from Diabetes UK (Diabetes: State of the nations 2005), the number of people in the UK diagnosed with the condition has risen from 1.4 million in 1996 to over 2 million in 2005. Of this figure, close to 250,000 have type 1 diabetes, also known as early onset, juvenile or insulin-dependent diabetes, and is the most severe, requiring insulin therapy to sustain life. Non insulin-dependent diabetes mellitus (NIDDM) or type 2, also known as adult or late-onset diabetes, affects approximately 1.8 million of those suffering from the disease. The incidence rate of diabetes is not significantly different between men and women until age 75, at which point diabetes affects more men than women (Watkins, 2003).

Diabetes is characterised by the inability of the body to maintain levels of glucose in the blood, which would normally be regulated by insulin secretions from the pancreas. The person with diabetes either produces no insulin, or produces it in levels that are inadequate. In the case of type 1 diabetes, the body's autoimmune system destroys insulin-producing cells. Type 2, whereby the body becomes resistant to insulin although it still may be producing insulin normally, is highly correlated with age, and may be controlled effectively with diet and lifestyle changes.

The person with diabetes is susceptible to a series of late stage complications that cause morbidity and premature mortality. Onset of symptoms develop on average 15 - 20 years after the appearance of overt hyperglycaemia. However, this time period may be decreased if diagnosis is delayed, which can

occur in the case of type 2 diabetes. Therefore, the identification of risk markers for vascular disease in diabetes is significant in preventing long term disabilities. Several studies have highlighted the importance of good blood glucose control in the prevention of diabetic complications (DCCT, 1993; UKPDS, 1998), and it would appear that maintenance of tight blood glucose control is critical for the prevention of early cellular damage which can lead to blindness, end-stage renal disease, amputation and fatality from myocardial infarction. As a result, much work has gone into furthering the understanding of the mechanisms by which either high or low glucose levels impair normal cell growth, and how this impacts upon the development of complications of diabetes (Ng *et al.*, 2005; Yamagishi *et al.*, 2004; Caldwell *et al.*, 2003).

1.3 Vascular complications of diabetes

1.3.1 Microvascular complications

1.3.1.1 Neuropathy

Neuropathy is a common complication associated with diabetes mellitus (Akbari *et al.*, 1997). Signs and symptoms of the disease include reduced nociception and burning sensation in the peripheral extremities. The DCCT of 1993 demonstrated that intensive blood sugar control resulted in a 60% decrease in clinically detected neuropathy, however, at the moment, little is known about the mechanisms underlying such abnormalities in nerve function.

Metabolic abnormalities in diabetes appear to affect nerve function through vascular effects, and improving neural blood flow corrects nerve function in experimental diabetes (Cameron *et al.*, 2003a). Potential factors involved include increased protein glycation, accumulation of polyols, altered lipid metabolism, decreased myoinositol content, abnormal Schwann cell function, microangiopathy resulting in ischaemia and/or lack of neurotrophic factors (Thomas *et al.*, 1993; Dyck *et al.*, 1996).

Assessment of the microvasculature accompanying the diabetic nerve has uncovered pathological changes including basement membrane thickening, pericyte degeneration and increased endothelial cell proliferation, which correlate strongly with the degree of nerve fibre defect (Gianinni & Dyck 1995; Malik, 1997).

1.3.1.2 Retinopathy

Diabetic retinopathy (DR) is the commonest cause of blindness in the working population of the Western world. The incidence and severity of DR has also been shown to correlate closely with poor glucose control (DCCT, 1993). The pathophysiology of DR involves basement membrane thickening and retinal oedema as a result of poor glucose control, causing local ischaemia within the retina associated with microaneurysms and excessive vascular permeability. At the advanced stage, the disease is known as proliferative diabetic retinopathy (PDR) characterised by the development of new blood vessels which grow in an attempt to perfuse ischaemic areas. Other factors that contribute to the retinopathic condition include increased platelet adhesiveness, erythrocyte aggregation, and increased blood viscosity. As the disease progresses, the proliferation of new blood vessels and fibrous tissue on the surface of the retina may increase the risk of vitreous haemorrhage and retinal detachment (Winters & Jernigan 2000). The retinal microvasculature appears to be the main target of glucose mediated damage in PDR (Forrester *et al.*, 1993), and angiogenesis initiated by vascular endothelial growth factor (VEGF) occurs in response to ischaemia in the retina of patients with diabetes (Shima *et al.*, 1995).

1.3.1.3 Nephropathy

Diabetic nephropathy is a major cause of end-stage renal disease and even in the early stages is associated with increased death rates. The early stages of nephropathy are asymptomatic. Microalbuminuria related to endothelial dysfunction (Verrotti *et al.*, 2003), is the first clinical sign of nephropathy, and only

detectable after the onset of severe renal damage. However, some 50% of patients with microalbuminuria die from cardiovascular disease before progressing to end-stage renal disease (Deckert *et al.*, 1992).

1.3.2 Macrovascular complications

Though the incidence of microvascular disease is higher in people with diabetes compared to the general population, it is macrovascular disease which accounts for most fatalities. Macrovascular diseases are characterised by atherosclerosis and involve vessels of the heart, cerebrum and peripheral arteries. People with diabetes have a three-fold higher risk of developing atherosclerosis and its associated clinical complications compared to those without diabetes, which in the case of type 2 coexists with other contributing factors such as hypertension and obesity (Fumeron *et al.*, 2006).

1.3.3 Pathogenic mechanisms of vascular complications of diabetes

Diabetes through hyperglycemia is widely known to be a major factor leading to microvascular and neural complications (Brownlee, 2001). Hyperglycemia-induced end-organ damage in diabetes is thought to be associated with increased flux of glucose by means of the polyol metabolic pathway (Yagihashi *et al.*, 2001; Obrosova *et al.*, 2002), accumulation of advanced glycation end products (Soulis *et al.*, 1999), increased oxidative stress (Cameron & Cotter, 1999; Coppey *et al.*, 2001), and activation of the protein kinase C pathway (Cameron *et al.*, 1999; Booth *et al.*, 2002). However, the pathogenesis of the vascular complications of diabetes remains controversial (Stehouwer *et al.*, 1997).

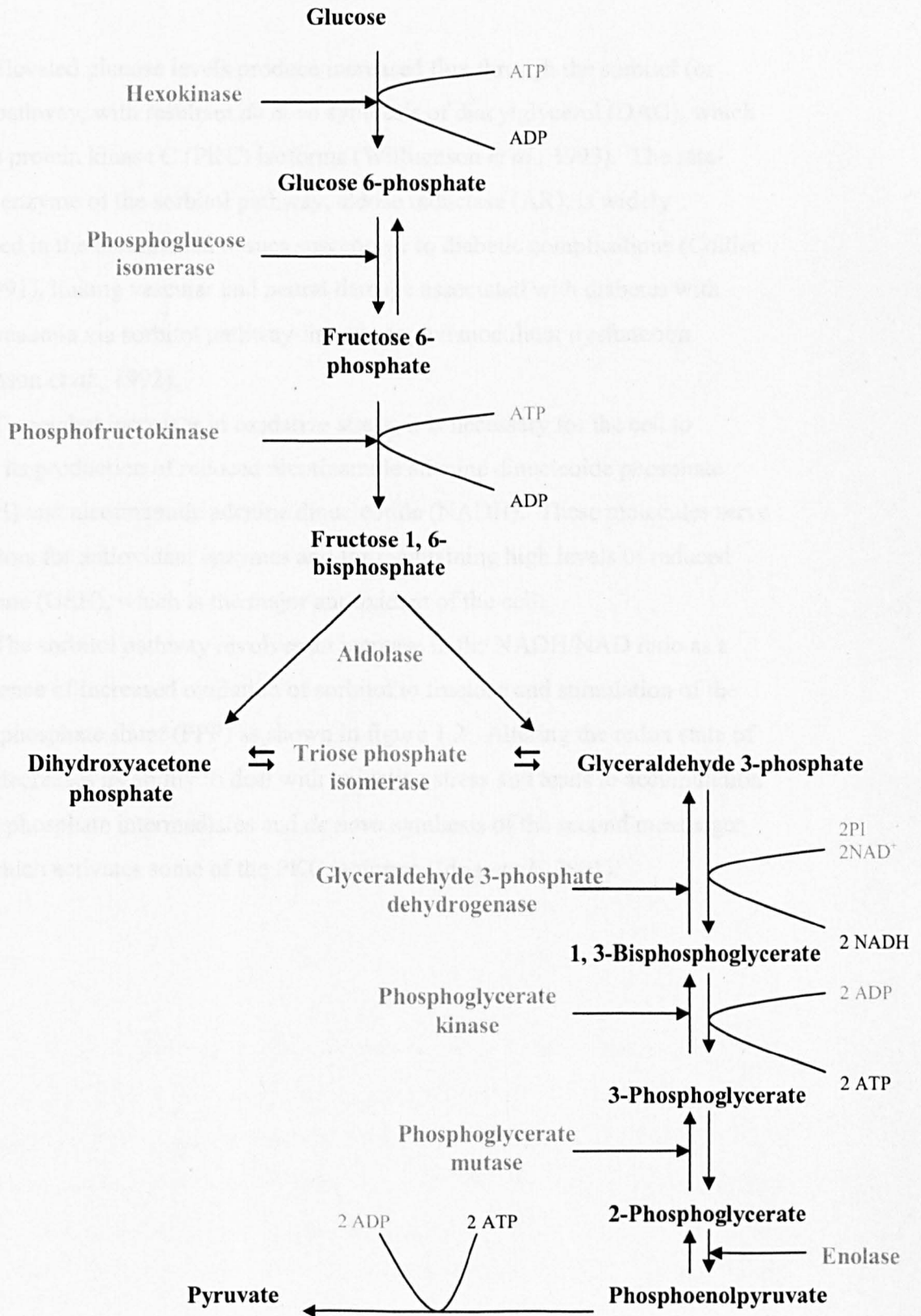
1.3.3.1 Glycolysis and the Warburg effect

Under hypoxic conditions, energy release by means of oxidative phosphorylation becomes impaired. Metabolic requirements are therefore met by a shift to anaerobic glycolysis, as shown in figure 1.1. As anaerobic glycolysis generates less adenosine triphosphate (ATP) than oxidative phosphorylation, the enzymatic activity and gene expression of glycolytic enzymes is increased during hypoxia (Webster *et al.*, 1987). Hypoxia-induced upregulation of anaerobic glycolysis is demonstrated in the expression of the monocarboxylate transporter type-1 (MCT-1) in an ischemic human retinal model, in response to the high concentrations of lactate generated via enhanced anaerobic glycolysis (Knott *et al.*, 1999). This adaptive response to hypoxia also involves the activation of genes that facilitate glucose transport and utilisation (Gleadle & Ratcliffe, 1998).

However, hypoxia is not the only trigger for anaerobic glycolysis. In cancer, the preferred pathway of energy production is anaerobic glycolysis, even under normoxic conditions, a phenomenon known as the Warburg effect (reviewed by Semenza, 2000b). Elevated hexokinase (HK) and phosphofructokinase (PFK) activity are hallmarks of many cancer cells. PFK is also stimulated by insulin and other growth factors under normoxic conditions (Feldser *et al.*, 1999).

Figure 1.1 The anaerobic glycolytic pathway. Anaerobic glycolysis is the transformation of glucose to lactate when limited amounts of oxygen (O₂) are available. It is less efficient than aerobic glycolysis, producing only 2 ATP molecules per glucose molecule, or about 5% of glucose's energy potential (38 ATP molecules). The pH in the cytoplasm quickly drops when lactic acid accumulates, eventually inhibiting enzymes involved in glycolysis. The liver later gets rid of this excess lactate by transforming it back into an important glycolysis intermediate called pyruvate.

1.4.3.2 The carbon pathway



1.3.3.2 The sorbitol pathway

Elevated glucose levels produce increased flux through the sorbitol (or polyol) pathway, with resultant *de novo* synthesis of diacylglycerol (DAG), which activates protein kinase C (PKC) isoforms (Williamson *et al.*, 1993). The rate-limiting enzyme of the sorbitol pathway, aldose reductase (AR), is widely distributed in the mammalian tissues susceptible to diabetic complications (Collier *et al.*, 1991), linking vascular and neural damage associated with diabetes with hyperglycaemia via sorbitol pathway-linked enzyme modulator dysfunction (Williamson *et al.*, 1992).

To combat increases in oxidative stress, it is necessary for the cell to increase its production of reduced nicotinamide adenine dinucleotide phosphate (NADPH) and nicotinamide adenine dinucleotide (NADH). These molecules serve as cofactors for antioxidant enzymes and for maintaining high levels of reduced glutathione (GSH), which is the major antioxidant of the cell.

The sorbitol pathway involves an increase in the NADH/NAD ratio as a consequence of increased oxidation of sorbitol to fructose and stimulation of the pentose phosphate shunt (PPP) as shown in figure 1.2. Altering the redox state of the cell decreases its ability to deal with oxidative stress and leads to accumulation of triose phosphate intermediates and *de novo* synthesis of the second messenger DAG, which activates some of the PKC isoforms (Idris *et al.*, 2001).

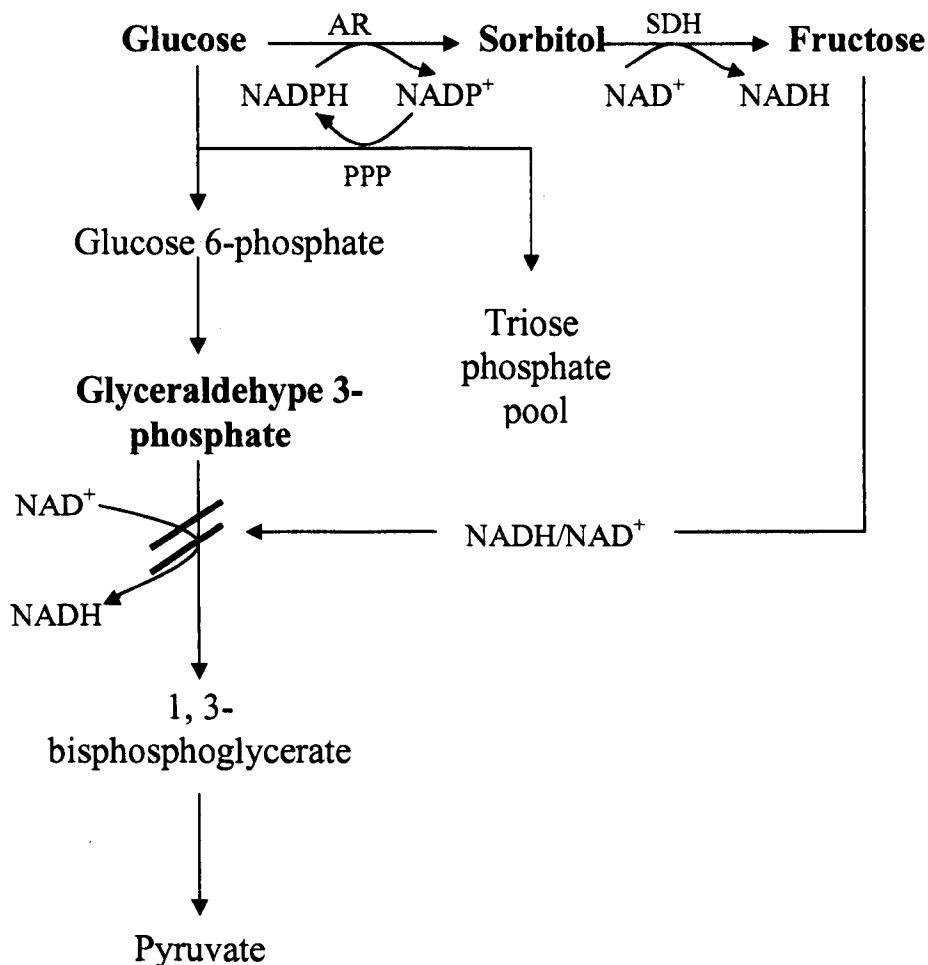


Figure 1.2: The sorbitol pathway. Alteration in redox state as a result of oxidation of NADH to NAD^+ during conversion of glucose to fructose. Increased fructose levels result in osmotic changes and formation of advanced glycation end products and non-enzymatic fructosylation. AR- aldose reductase, SDH- sorbitol dehydrogenase, PPP-pentose phosphate pathway.

1.3.3.3 Kinase/phosphatase pathways

Mitogen activated protein kinase (MAPK) pathways, phosphoinositol-3 protein kinase (Pi3K) pathways and protein kinase C (PKC) are sensitive to elevated glucose levels (Campbell *et al.*, 2003; Nakamura *et al.*, 2001).

The p42/44 MAPKs are believed to play a major role in the manner by which many mitogens transduce their extracellular signals into intracellular responses. These kinases are ubiquitously expressed and activated in response to many different growth factors by a cascade of sequential protein phosphorylation. Other MAPK homologs such as c-jun, NH-2 terminal kinase (JNK) and p38 MAPK are activated by distinct but parallel phosphorylation cascades. The transcriptional and post-transcriptional response of c-jun to hypoxia has been reported in various normal and transformed cells (Ausserer *et al.*, 1994; Alfranca *et al.*, 2002). The relationship between c-jun, glucose and oxygen is seen in the superinduction of c-jun mRNA and protein expression during simultaneous oxygen and glucose deprivation by an apparent oxidative stress related pathway (Ausserer *et al.*, 1994).

Oncogenic transformation is characterised by the gain of function in growth promoting oncoproteins and loss of function in growth attenuating tumour suppressor proteins, both of which are seen in the signalling pathway mediated by Pi3K (Jiang *et al.*, 2000). Pi3K acts through phosphorylating inositol lipids, producing phosphatidylinositol 3,4-bisphosphate and phosphatidylinositol 3,4,5-trisphosphate. Pi3K is linked via its regulatory subunit p85 to upstream receptors that are activated by growth factors or insulin. A downstream target of Pi3K is the serine threonine-kinase, Akt, that is activated by phosphatidylinositol-dependent kinase 1 (Chan *et al.*, 1999; Vanhaesebroeck & Alessi, 2000). The mammalian target of rapamycin, mTOR, situated downstream of Akt is also subject to enhanced kinase activity in response to elevated glucose, resulting in upregulation of protein translation and cell cycle progression (Xu *et al.*, 2003).

Studies performed *in vivo* and *in vitro* have established a link between the cell-damaging effects of high glucose concentration and/or elevation in intracellular PKC (Shiba *et al.*, 1993). The activation of PKC in the presence of high glucose

concentrations has already been shown to be an important pathway by which glucose toxicity may be mediated in retinal cells. This is also suggested by the finding that increased glucose metabolism increases intracellular calcium and cAMP linked to p42/44 MAPK and p70 activation in pancreatic beta cells (Briaud *et al.*, 2003). Glucose-potentiated vascular smooth muscle cell (VSMC) chemotaxis and associated morphological changes are dependent on the Pi3K and p42/44 MAPK pathways, and also on cross-talk between these pathways (Campbell *et al.*, 2004). VSMC speed and direction of migration, and adhesion via focal adhesion kinase (FAK) in response to elevated glucose is modified by PKC, and therefore has implications for the formation of atherosclerotic plaques in the diabetic patient (Campbell *et al.*, 2005).

Several mechanisms are known to be responsible for upregulation of the Pi3K pathway in human cancer, for example the gene coding for the catalytic subunit of Pi3K is amplified in cervical carcinoma (Ma *et al.*, 2000) while the tumour suppressor phosphatase and tensin homologue (PTEN) is frequently lost in glioblastoma and endometrial cancer (Cantley *et al.*, 1999; Besson *et al.*, 1999).

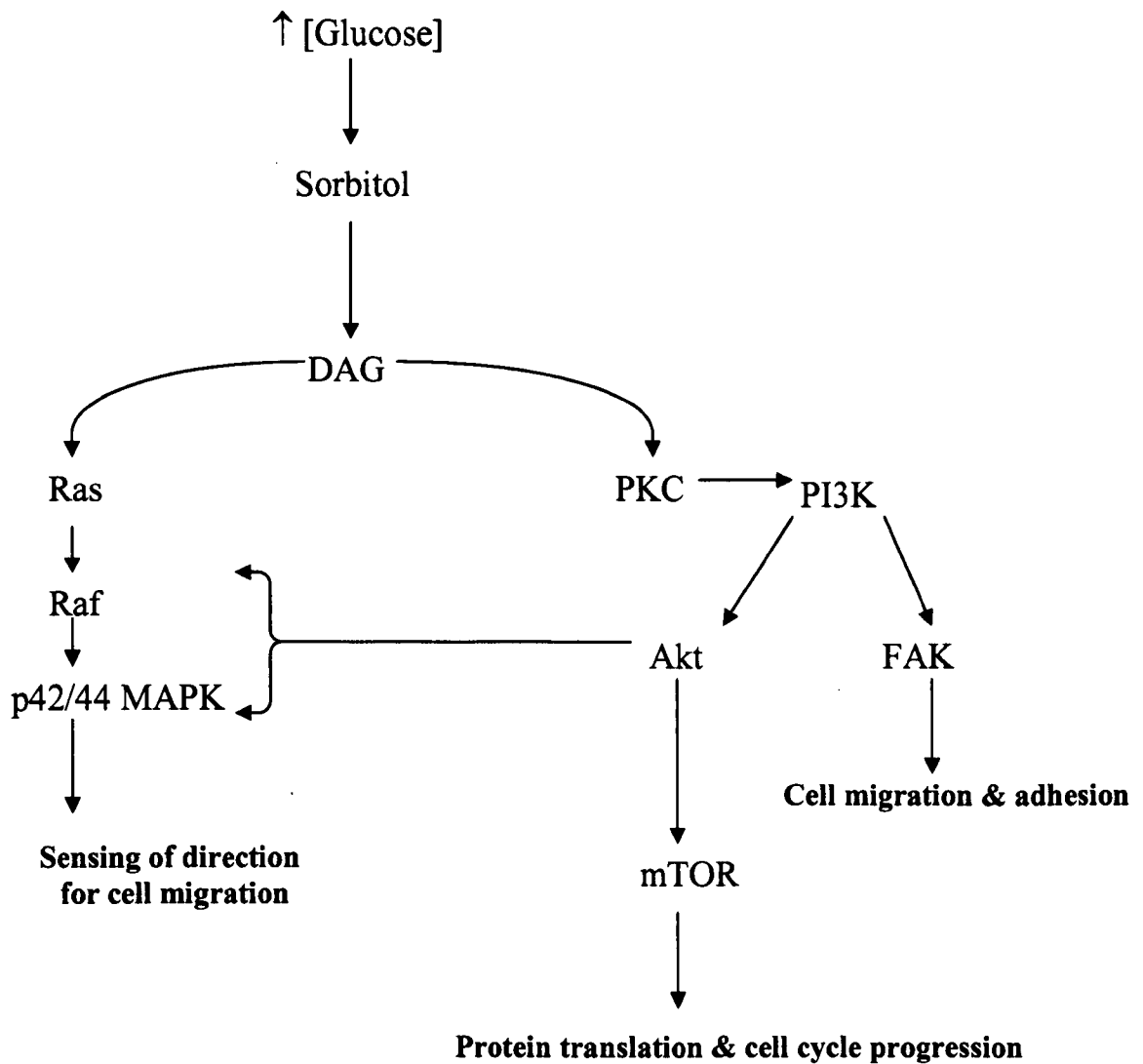


Figure 1.3: Interaction between protein kinase signalling pathways in response to elevated glucose. Synthesis of DAG via the sorbitol pathway stimulates PKC dependent induction of MAPK and Pi3K cascades, which, through the activation of downstream targets, may contribute to the pathogenesis of atherosclerosis, a significant complication associated with diabetes (as adapted from Campbell *et al.*, 2005).

1.3.3.4 Advanced glycation end products (AGE)

Advanced glycation end products (AGE) result from the non-enzymatic glycation of amines in response to glucose binding to protein which accumulates in vascular tissue during diabetes and aging. At the tissue and cellular level, AGE affects many biochemical processes, including increased cell membrane permeability and matrix changes. Diabetic nephropathy is seen to be synergistic with atherosclerosis, whereby accumulation of AGE in blood vessel walls and on lipoproteins may result in increased vascular permeability, increased uptake of cholesterol and acceleration of atherogenesis (Manske, 1993). In experimental diabetes, the interaction of circulating AGE and endothelial AGE receptors (RAGE) appear to mediate microvascular leakage, possibly via AGE-RAGE-dependent enhanced oxidant stress (Bonnardel-Phu *et al.*, 1999).

1.4 Role of the vascular endothelium in diabetic complications

1.4.1 Physiology of the vascular endothelium

The vascular endothelium primarily has a barrier function, whereby endothelial cells (EC) make up the continuous layers of cells linked by tight junctions which line the blood vessels. It has enormous power of regeneration, as seen through the reassembly of its cytoskeletal F-actin filaments within a 3 hour recovery period following almost complete destruction by energy depletion (Kuhne *et al.*, 1993).

Numerous endothelial cell derived products, such as vasoactive mediators, affect the functioning of other cells, including muscle, leukocyte and platelet cells (reviewed by Michiels *et al.*, 2000). Due to its location as the first line of contact with the blood, ECs are susceptible to changes in the substances contained in blood. As such, poorly controlled blood glucose promotes endothelial cell dysfunction and is a major factor in the development of micro and macrovascular disease associated with diabetes mellitus.

1.4.2 Mediators of dysfunction of the vascular endothelium

Glucose concentration and oxygen availability are able to influence a number of parameters within the endothelium, including regulation of the expression and responsiveness of cells to reactive oxygen species (ROS), adhesion molecules, vasoactive enzymes and growth factors, all of which in turn mediate changes in cell growth.

1.4.2.1 Reactive oxygen species (ROS)

ROS are elevated by metabolic changes in diabetes, including auto-oxidation and increased advanced glycation. Local formation of ROS by ECs initiates a host of unwanted effects, and free radical generation has been implicated in various pathological changes associated with hyperglycaemia. Dietary antioxidants may be effective in combating diabetic pathologies. This is further elucidated through the findings that antioxidant treatment with lipophilic scavengers such as butylated hydroxyl-toluene, probucol and vitamin E, or more hydrophilic agents such as α -lipoic acid and acetyl cysteine, can prevent or reverse nerve conduction velocity deficits in diabetic rats (Cameron & Cotter, 1999) and lessen the oxidative damage caused by dysregulation of glucose metabolism in NIDDM (Ruhe & McDonald, 2001).

1.4.2.2 Neutrophil attraction and adherence

Perhaps the most marked effect of hypoxia on ECs is the increased ability to attract neutrophils. The binding of leukocytes to the ECs is mediated by several adhesion molecules such as intercellular adhesion molecule-1 (ICAM-1), along with chemoattractant/activator molecule interleukin-8 (IL-8) or platelet-activating factor (PAF). PAF is a neutrophil activating agent, promoting neutrophil adherence to the endothelium following hypoxia or ischaemia. During conditions of inflammation, endothelial E-selectin also mediates transient adhesion between

ECs and leukocytes (Bevilacqua *et al.*, 1989), an action which may be attributable to hypoxia-induced upregulation of E-selectin during states of inflammation (Zund *et al.*, 1996). The contact of neutrophils with the activated endothelium not only results in adherence and activation, but also delays apoptosis, thereby prolonging the life of the endothelial cell in a hypoxic environment (Ginis & Faller, 1997).

1.4.2.3 Vasoactive substances

Hypoxia differentially affects vascular tone by regulating the release of vasorelaxing molecules e.g. nitric oxide (NO) and prostacyclin, and vasoconstricting molecules, such as endothelin-1 (ET-1). The result of this regulation is to create conditions favourable to vasoconstriction (Kourembanas & Bernfield, 1994), inhibiting the release of vasorelaxing molecules, possibly through a decrease in endothelial nitric oxide synthase (eNOS) expression. In hypoxic ECs, an initial decrease in the second messenger cyclic adenosine monophosphate (cAMP) levels may be linked to increased vascular leakage, resulting in an increase in cytosolic calcium, which in turn may activate vasoactive enzymes such as bradykinin, histamine or phospholipase A₂. It has also been suggested that cyclooxygenase-2 (COX-2) expression is induced via nuclear factor κ B (NF- κ B) in hypoxic ECs (Schmedtje *et al.*, 1997).

1.4.2.4 Growth factors

Glucose-mediated increased levels of transforming growth factor- β (TGF- β) protein and mRNA levels have been demonstrated in human retinal endothelial cells (HREC) (Pascal *et al.*, 1999). TGF- β inhibits endothelial cell proliferation by blocking progression through the cell cycle to the S-phase. Therefore, decreased TGF- β bioavailability and the resultant reduction in endothelial growth inhibition may also allow uncontrolled cell growth in response to other growth factors, as observed in the proliferative phase of DR. TGF- β is also a potent chemotactic agent for peripheral blood monocytes (Wahl *et al.*, 1987) thus representing an

indirect role for TGF- β in the disease process within retinal endothelial cells, due to the association between monocytes and microaneurysms in the retina.

Hypoxic regulation of vascular endothelial growth factor (VEGF) occurs in most cell lines and tissues, and is widely recognised as the primary angiogenic factor responsible for EC mitogenesis and capillary proliferation (Shweiki *et al*, 1992). The ability of VEGF to induce ICAM-1 and eNOS, clearly demonstrates the involvement of VEGF in the initiation of early diabetic retinal leukocyte adhesion and consequent vascular damage in vivo (Joussen *et al.*, 2002).

Expression of the components of the insulin growth factor (IGF) system, including IGF-1, IGF binding proteins (IGFBP) and IGF-1 receptor (IGF-1R) in ECs is regulated by various conditions, including vascular origin, hypoxia (Tucci *et al.*, 1998), TGF- β 1 and VEGF (Dahlfors *et al.*, 2000).

Hyperglycaemia and IGF-1 stimulate EC migration and tubular formation (Shigematsu *et al.*, 1999). The relationship between hyperglycaemia and IGF-1 may therefore account for the observation of a strong migratory response of bovine corneal endothelial cells (BCEC) toward D-glucose at concentrations exceeding 10mM (Vogel *et al.*, 1993). IGF-1 has also been reported to inhibit phosphorylation pathways in bovine retinal endothelial cells (BREC) exposed to high glucose, thereby exerting a protective effect on the cell (McBain *et al.*, 2003) through coupling cell proliferation with glucose delivery (DeBosch *et al.*, 2001).

The role of the IGF-1 system in diabetic retinopathy is unclear (Wang *et al.*, 1995). Although IGFs are important modulators of cellular proliferation and differentiation, it has been suggested that the insulin-like growth factor binding protein (IGFBP), as opposed to IGF, may be the dominant paracrine regulator of proliferation of EC, as well as maintenance of endothelium integrity during hypoxia (Tucci *et al.*, 1998) as bovine macro and microvessel ECs widely display IGFBP-2 through to BP-6 (Moser *et al.*, 1992). Furthermore, in human retinal ECs, long term exposure to high concentrations of glucose was able to reduce IGF-1-induced mitogenesis by decreasing the expression of stimulatory IGFBPs, while leaving the concentration of the inhibitory IGFBP-4 constant (Giannini *et al.*, 2001).

1.4.2.5 EC receptors

In the diabetic endothelium, the activity of receptors is central to the tissue's ability to regenerate following assault from the complications associated with poor glucose control.

In human diabetic ischaemic cardiomyopathy, expression of the VEGF receptors, flt-1 and flk-1, were significantly lower compared to non-diabetic coronary heart disease patients, although VEGF expression was higher. This was accompanied by reduced signal transduction, which may account for the reduced neoangiogenesis in diabetic patients with ischaemic cardiomyopathy (Sasso *et al.*, 2005).

Diabetic ulcers display distinct alterations in reparative angiogenesis. This is demonstrated in dermal endothelial cells through the down-regulation of tyrosine kinase receptor-A (Trk-A) in cutaneous wounds of type 1 diabetic mice, thus preventing endothelial cell proliferation (Graiani *et al.*, 2004).

Both macrovessel and microvessel ECs express the IGF-1 receptor (IGF-1R) (Boes *et al.*, 1991) to which IGF-1 binds to exert all of its known physiological effects (LeRoith *et al.*, 1995). Although ECs express both IGF-1R and the insulin receptor (IR), the vasodilation induced by insulin might be mediated primarily via its stimulatory effect on the IGF-1R, which in certain micro and macrovascular EC lines is more abundant than IR (Chisalita *et al.*, 2004). In STZ-diabetic rats, aortic IGF-1 mRNA has been seen to be unaffected, whereas IGF-1R mRNA was greatly increased, and aortic vasorelaxation was significantly greater in STZ- rats compared to age-matched control. Furthermore, insulin treatment not only reduced endothelial dysfunction in these rats, but also further increased IGF-1R expression (Kobayashi *et al.*, 2002).

In a spontaneous rat model of diabetes, vascular TGF- β receptor type II was expressed to a greater extent in pre and early stages of diabetes compared to age matched controls, which was associated with hyperinsulinaemia and vascular thickening (Hosomi *et al.*, 2002). Recently, the TGF- β receptor type V signalling cascade, which co-expresses with TGF- β receptors I, II and III, was found to cross-

talk with other TGF- β receptor, insulin receptor and IGF-1 receptor cascades, which may represent a new level of control over the responsiveness of the vascular tissue to diabetes-induced assault (Huang & Huang, 2005).

1.4.2.6 Hypoxia

In differentiated human umbilical vein endothelial cells (HUVEC) exposed to reduced oxygen, the initiating event of EC activation is a decrease in the activity of the mitochondrial respiratory chain activity (Janssens *et al.*, 1995). The inhibition of mitochondrial oxidative phosphorylation alone, however, is not always sufficient to produce the effects of hypoxia. This is true in the case of gene expression in response to activation of the mediator of hypoxia inducible transcription, hypoxia inducible factor-1 (HIF-1).

HIF-1 is directly responsible for the induction of several hypoxia-inducible genes, many of which are potential contributors to the development of diabetic endothelial dysfunction, due to their central role in glucose transport and metabolism, angiogenesis, cell proliferation and survival.

As already considered in this section, activation of ROS and subsequent redox-sensitive expression of VEGF, ET-1, inflammatory cytokines and adhesion molecules, combined with diminished NO bioavailability, leads to exaggerated endothelial cell damage and dysfunction. This process, at least in part, is thought to involve the participation of HIF-1 (Lavie, 2003).

Therefore, expression of the factors implicated in the generation of endothelial cell dysfunction may be subject to HIF-1-mediated regulation, triggered by a state of pseudohypoxia generated in response to increased metabolic demand placed upon the cells subjected to pathologically high concentrations of glucose, such as would occur in poorly controlled diabetes.

1.5 Hypoxia Inducible Factor-1 (HIF-1)

1.5.1 The HIF family

HIF belongs to the basic helix-loop-helix (bHLH) /Per-ARNT-Sim (PAS) superfamily of eukaryotic transcription factors, which are made up of two proteins known as α , or the inducible sub-unit, and the aryl hydrocarbon receptor nuclear translocator (ARNT) or β sub-unit. On activation, the two sub-units heterodimerise forming the functional HIF transcription factor. Under certain conditions, classically hypoxia, the functional transcription factor persists. Under normoxic conditions, it is targeted for degradation via the von Hippel-Lindau (pVHL) tumour suppressor protein (Maxwell *et al.*, 1999).

1.5.1.1 HIF-2 and HIF-3

Although HIF-1 has been the most thoroughly researched, and will be the subject of the following investigation, there are two further members of the HIF family, termed HIF-2 and HIF-3.

HIF-2 α has a close sequence homology and similar properties to HIF-1 α , and was initially described as endothelial and foetal specific (Wenger & Gassman, 1997). Subsequently, along with HIF-1 α , HIF-2 α was seen to be involved in the promotion of oncogene transformation, via induction of VEGF in human breast cancer (Blancher *et al.*, 2000), and human bladder cancer (Jones *et al.*, 2001). Moreover, target gene expression and migration of renal carcinoma cells has been reported to be critically dependent upon HIF-2 α (Sowter *et al.*, 2003). Target genes dependent upon HIF-2 α expression in renal carcinoma include VEGF, GLUT-1 and plasminogen activator receptor (Carroll & Ashcroft, 2006). In non-cancerous cells, marked hypoxic induction of HIF-2 α has also been identified in distinct cell populations of different organs in the rat, including brain, heart, lung, liver, pancreas and intestine (Wiesner *et al.*, 2002). In the ischaemic brain, HIF-2 α was

seen to mediate the transcriptional activation of EPO expression in astrocytes, thereby promoting neuronal survival during ischaemia (Chavez *et al.*, 2006).

The third α -class of HIF subunit, HIF-3 α , was first isolated in mouse in 1998. The human homologue subsequently revealed high homology to HIF-1 α and HIF-2 α (Hara *et al.*, 2001), and was shown to have at least 6 alternatively splicing variants. Human HIF-3 α is strongly expressed in heart, placenta and skeletal muscle, and weakly expressed in lung, liver and kidney. As is the case with HIF-1 α and -2 α , the von Hippel-Lindau tumour suppressor (pVHL) is intricately involved in the regulation of HIF-3 α . It is not yet known whether the splice variants of HIF-3 α are capable of transcriptional activation of genes not regulated by HIF-1 α or HIF-2 α (Maynard *et al.*, 2003).

1.5.1.2 HIF-1

HIF-1 α is the inducible subunit of the heterodimer, the regulation of which controls dimerisation and transactivation of HIF-1, as opposed to HIF-1 β which is constitutively expressed in the nucleus (Wang & Semenza, 1995). The N-terminal half of HIF-1 α contains bHLH and PAS domains that are required for dimerisation and DNA binding. The C-terminal half contains domains required for degradation and transactivation; these are the oxygen dependent degradation domain (ODDD) which confers oxygen-dependent instability, two independent transactivation domains (TAD), N-TAD and C-TAD, separated by an inhibitory domain (ID) that negatively regulates the transactivation domains (Jiang *et al.*, 1996).

1.4.2 Role of HIF-1 in the induction of hypoxia-responsive genes

Hypoxia induces the expression of different genes whose products promote survival response of cells. The oxygen-sensing pathway is located in the nucleus and mainly comprises of hypoxia-inducible transcription factors. All of these

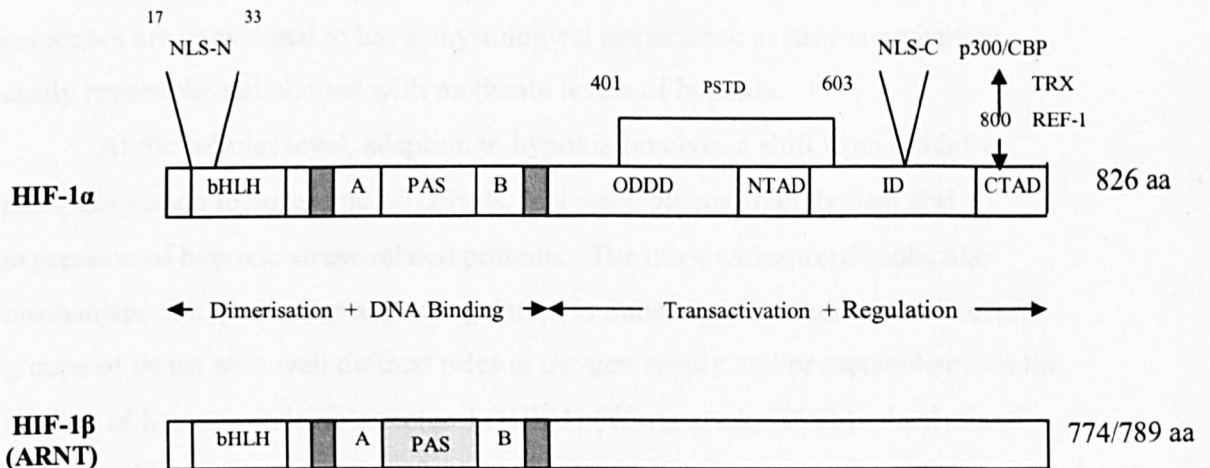


Figure 1.4: Structure of HIF-1. Important functional domains of the HIF-1 α and HIF-1 β subunits are indicated as follows: bHLH, basic-helix-loop-helix domain; ID, inhibitory domain; NLS-N and NLS-C, amino- and carboxyl- terminal nuclear localisation signal; PAS, Per-ARNT-Sim homology domain with internal A and B repeats; PSTD, proline-serine-threonine-rich protein stability domain which is targeted by the prolyl hydroxylases; ODDD, oxygen dependent degradation domain; C-TAD and N-TAD, amino- and carboxyl-terminal transactivation domain; REF-1, redox factor 1; TRX, thioredoxin. The double headed arrow indicates that reduction of Cys800, which is mediated by REF-1 and TRX, is required for the interaction of the C-TAD with co-factor p300 or C terminal binding protein (CBP) (as adapted from Semenza, 2000b).

1.5.2 Role of HIF-1 in the induction of hypoxia-responsive genes

Hypoxia induces the expression of different genes whose products augment non-oxidative synthesis of ATP, increase the oxygen-carrying capacity of blood and multiply the number of capillaries irrigating the hypoxic tissue. All of these responses are considered to have physiological importance as they are adaptive, easily reversible and elicited with moderate levels of hypoxia.

At the cellular level, adaption to hypoxia involves a shift from oxidative phosphorylation to anaerobic glycolysis, increased glucose metabolism and expression of hypoxic stress-related proteins. The most widespread molecular mechanism of hypoxia-dependent regulation is transcriptional induction of several groups of genes with well defined roles in oxygen supply and/or metabolism via the binding of hypoxia-inducible factor-1 (HIF-1) (Wang *et al.*, 1995b). Analysis of the 5' flanking region of many of these genes revealed a sequence consensus to HIF-1 (5'-RCGTG-3'), termed the hypoxia response element (HRE) situated upstream of the transcription initiation site.

Over 70 HIF-1 regulated genes have been identified to date, the protein products of which play key roles in angiogenesis, vascular reactivity and remodelling, glucose and energy metabolism, along with cell proliferation and survival, shown in table 1.1 (Semenza, 2000c).

Gene Product	Function
Adenylate kinase 3	Nucleotide metabolism
α_{18} -adrenergic receptor	Vascular tone
Adrenomedullin	Vascular tone, cell survival
Aldolase A	Glucose metabolism
Aldolase C	Glucose metabolism
Carbonic anhydrase 9	pH regulation
Ceruplasmin	Iron metabolism
Endothelin-1 (ET-1)	Vascular tone and remodelling
Enolase-1	Glucose metabolism
Erythropoietin	Erythropoiesis, cell survival
Glucose transporter 1	Glucose metabolism
Glucose transporter 3	Glucose metabolism
Glyceraldehyde-3-P-dehydrogenase (GAPDH)	Glucose metabolism
Haem oxygenase-1	Vascular tone, cell survival
Hexokinase 1	Glucose metabolism
Hexokinase 2	Glucose metabolism
Insulin-like growth factor (IGF)	Cell proliferation and survival
IGF-binding protein 1	Cell proliferation and survival
IGF-binding protein 2	Cell proliferation and survival
IGF-binding protein 3	Cell proliferation and survival
Lactate dehydrogenase A	Glucose metabolism
Nitric oxide synthase 2 (NOS 2)	Vascular tone, cell survival
NIP3	Apoptosis
p21	Cell proliferation
p35srj	Regulation of HIF-1 activity
Phosphofructokinase L	Glucose metabolism
Phosphoglycerate kinase 1	Glucose metabolism
Plasminogen activator inhibitor 1	Angiogenesis
Prolyl-4-hydroxylase α	Collagen metabolism
Pyruvate kinase M	Glucose metabolism
Transferrin	Iron metabolism
Transferrin receptor	Iron metabolism
Transforming growth factor β_3 (TGF- β_3)	Angiogenesis, cell proliferation
Triosephosphate isomerase	Glucose metabolism
Vascular endothelial growth factor (VEGF)	Angiogenesis, cell survival
VEGF receptor flt-1	Angiogenesis

Table 1.1 Genes targeted for HIF-1-induced expression (as adapted from Semenza, 2000c)

1.5.2.1 Growth Factors and HIF-1

The activity of HIF-1 as the control centre for the hypoxic response was first observed through its ability to bind to the HRE of the primary regulator of mammalian erythropoiesis, erythropoietin (EPO) (Semenza & Wang 1992). Further to this, HIF-1 and its recognition sequence were found to be a common component of the mammalian cellular response to hypoxia, due to its activation in a variety of cell lines in which EPO is not expressed (Wang & Semenza 1993).

The potent and specific endothelial cell mitogen, vascular endothelial growth factor (VEGF) is also activated by HIF-1 in hypoxic cells (Forsythe *et al.*, 1996). Hypoxia regulates expression of VEGF by increasing its transcription and by stabilizing its mRNA, through interaction with HIF-1 α (Liu *et al.*, 2002). As the primary angiogenic factor responsible for endothelial cell mitogenesis and capillary proliferation (Shweiki *et al.*, 1992), inhibition of VEGF may prove useful in the treatment of proliferative diabetic retinopathy, indicated by the ability of VEGF to induce ICAM-1 and endothelial NOS which initiate early diabetic retinal leukocyte adhesion and consequent vascular damage *in vivo* (Joussen *et al.*, 2002).

1.5.2.2 Glucose Transporters and HIF-1

A family of glucose transporters (GLUT) mediate the entry of glucose into cells; therefore an important factor in glucose delivery would involve the regulation of the expression and subcellular distribution of the glucose transporters. Two specific isoforms, GLUT-1 (Mandarino *et al.*, 1994) and GLUT-3, have both been detected in bovine retinal endothelial cells at the mRNA and protein levels (Knott *et al.*, 1993). Later, both were detected at the level of mRNA (Knott *et al.*, 1996a) and protein (Knott *et al.*, 1996b) in human retinal endothelial cells (HREC), although, to date, only GLUT-1 has been detected *in vivo*.

Upregulation of the insulin-independent GLUT-1 is stimulated during hypoxia in order to deliver more glucose for glycolysis. Through immunohistochemical staining, GLUT-1 protein expression has been demonstrated

to be absent in the neovascular retina of people with PDR. As GLUT-1 expression is characteristic of tissues that possess a barrier function, the loss of selective permeability characteristic of PDR may be associated with an absence of facilitated glucose transport (Kumagai *et al.*, 1994).

In the endothelium of hypoxic brain tissue, expression of GLUT-1 and GLUT-3 has been seen to increase via HIF-1 induced transcription (Vannucci *et al.*, 1996). More recently, GLUT-1 has been found to be up-regulated under low oxygen in placental cell lines through HIF-1 interaction with a consensus HRE site of the GLUT-1 promoter (Hayashi *et al.*, 2004).

1.5.2.3 Glycolytic enzymes and HIF-1

As anaerobic glycolysis generates less ATP than oxidative phosphorylation, the enzymatic activity and gene expression of glycolytic enzymes is increased during hypoxia (Webster *et al.*, 1987). This adaptive response to hypoxia involves the activation of genes that facilitate glucose transport and utilisation (Gleadle & Ratcliffe 1998).

The rate-limiting enzyme in glucose metabolism, hexokinase II (HKII) is selectively regulated by HIF-1-dependent mechanisms in both normal and transformed cell lines (Riddle *et al.*, 2000; Mathupala *et al.*, 2001). In liver cancer, induction of HIF-1 α and HKII was not accompanied by an increase in VEGF, therefore indicating increased anaerobic glycolysis to be the primary target, as opposed to increased vascularisation (Yasuda *et al.*, 2004).

Anaerobic glycolysis is highly dependent upon the key regulator of carbon flux through glycolysis, fructose-2, 6 bisphosphate (F-2, 6-BP) (Kawaguchi *et al.*, 2001), which is a potent allosteric regulator of the key enzyme in glycolysis, phosphofructokinase (PFK-1). The activity of F-2, 6-BP has been shown to be dependent upon HIF-1 α expression, as both share many common induction pathways, including the hypoxia mimicking agents, cobalt and DFO. Induction was also replicated by inhibiting the prolyl hydroxylases responsible for the pVHL-dependent destabilisation of HIF-1 α . The apparent dependence of F-2,6-BP on

HIF-1 α was further confirmed by its over-expression in pVHL-deficient cells, and lack of hypoxic induction in HIF-1 α null mouse embryo fibroblasts (Minchenko *et al.*, 2002).

Cultured ECs exposed to hypoxia upregulate glyceraldehyde-3-phosphate dehydrogenase (GAPDH). GAPDH catalyses the sixth step in glycolysis: the conversion of glyceraldehydes-3-phosphate to 1, 3 bisphosphoglycerate, generating a high energy phosphate compound in an oxidation-reduction reaction. Although not a primary regulatory site for glycolysis, the activity of GAPDH is inhibited by several glycolytic metabolites, other small molecules and by association with cell membranes (Wang *et al.*, 1980). GAPDH expression is regulated by hypoxia primarily at the level of transcription. The regulation of GAPDH by hypoxia appears to be cell-specific and involves HIF-1 α (Graven *et al.*, 2003). For glycolytic function, GAPDH is upregulated in the cytosolic fraction of hypoxic EC. However, increased levels of GAPDH has also been detected within the nuclear fraction, suggesting a non-glycolytic function, which may be related to the relative hypoxia tolerance of EC, which can survive for at least 96 hours in 0% oxygen (Graven & Farber, 1995).

1.5.3 Mechanisms involved in the hypoxic regulation of HIF-1 α expression

1.5.3.1 Oxygen sensing

Diverse oxygen sensing mechanisms have been proposed to mediate the hypoxic transcriptional response of HIF-1 α (Semenza, 1999). A number of these models implicate an iron-containing unit, in the form of either a haem group or an iron/sulphur cluster, which undergoes change on activation (Goldberg *et al.*, 1998).

The support for such a model is seen in the response to cobalt, which causes similar induction of hypoxia responsive genes through replacing iron in the synthesized porphyrines, but due to its poor ability to bind O₂, it locks the haem protein into the deoxy form, thus mimicking hypoxia. Furthermore, the iron chelator desferrioxamine (DFO) is also able to stabilise HIF- α under non-hypoxic

conditions (Semenza, 1999) by replacing or removing the central iron of the putative haem oxygen sensor (Wenger, 2000). Carbon monoxide has a high binding affinity for the iron in haem molecules, also locking the haem protein in the deoxy conformation and substantially attenuating the hypoxic induction of EPO and VEGF mRNAs (Goldberg & Schneider, 1994). CO and NO are both haem binding ligands, both target the internal oxygen dependent degradation domain of HIF-1 α and repress the C-terminal transactivation domain, therefore abrogating the hypoxic accumulation of HIF-1 α protein (Huang *et al.*, 1998).

However, the lack of identification of specific proteins with this role in mammalian cells may discount this as a stand alone mechanism. It has been hypothesised that activation of HIF-1 α associated with iron deficiency may be responsible for increased glucose tolerance in iron-deficient animals (McCarty, 2003). This theory would rationalize previous studies in which glucose uptake was increased in iron-deficient animals and cells (Brooks *et al.*, 1987). Increases in both haematocrit and body iron stores appear to be associated with hyperinsulinaemia and increased IGF-1, both characteristics of insulin resistance. Activation of HIF-1 α in this case may rationalise the finding that iron excess mediates some of the increased cancer risk associated with insulin resistance (Facchini *et al.*, 1998).

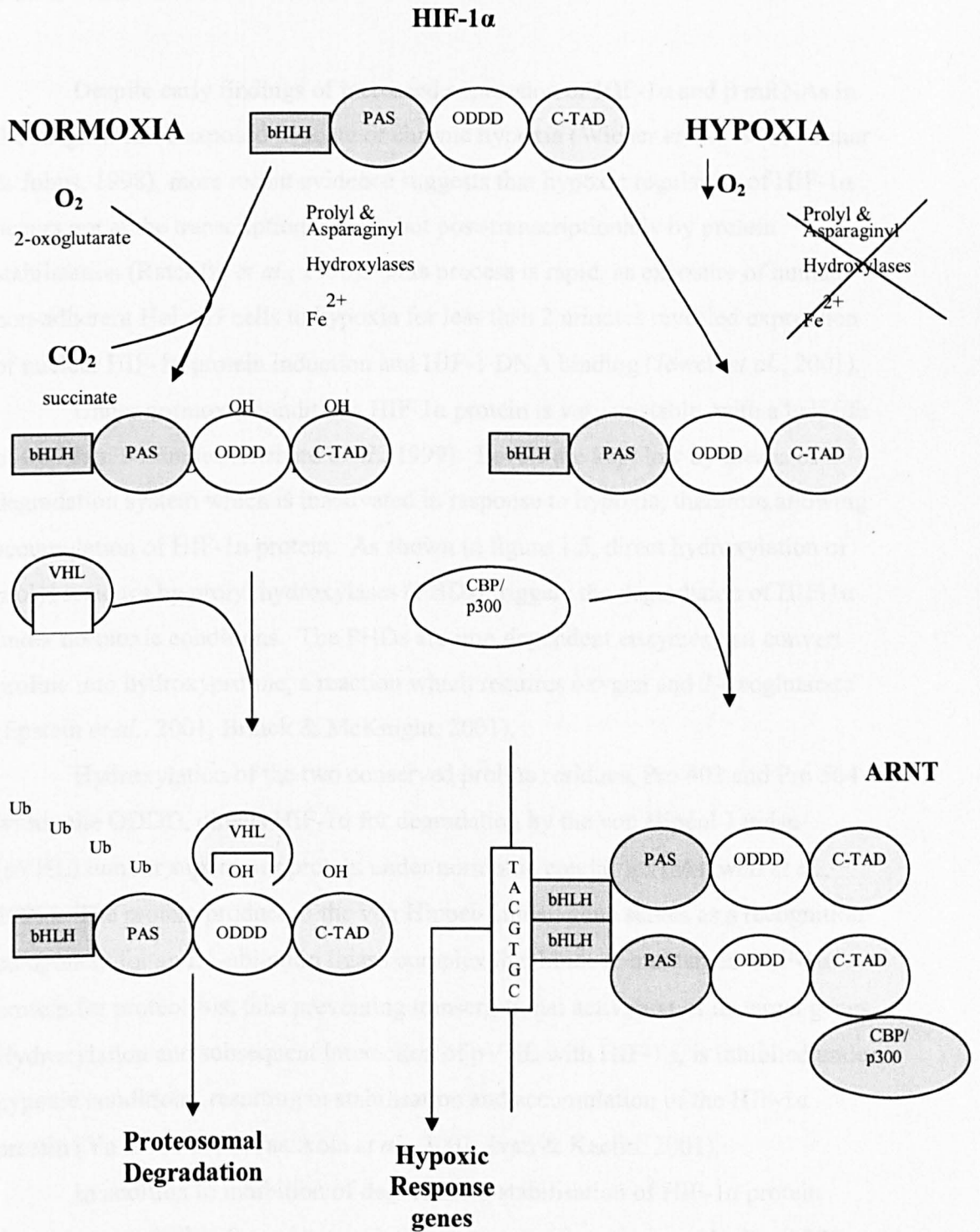


Figure 1.5: Control of signalling through HIF-1 α in response to changing O_2 levels (as adapted from a review by Kewley *et al.*, 2004).

1.5.3.2 Stabilisation of HIF-1 α

Despite early findings of increased expression of HIF-1 α and β mRNAs in the lungs of mice exposed to acute or chronic hypoxia (Wiener *et al.*, 1996; Palmer & Johns, 1998), more recent evidence suggests that hypoxic regulation of HIF-1 α occurs not at the transcriptional level, but post-transcriptionally by protein stabilisation (Ratcliffe *et al.*, 1998). This process is rapid, as exposure of human non-adherent HeLaS3 cells to hypoxia for less than 2 minutes revealed expression of nuclear HIF-1 α protein induction and HIF-1 DNA binding (Jewell *et al.*, 2001).

Under normoxic conditions HIF-1 α protein is very unstable, with a half life of less than 5 minutes (Richard *et al.*, 1999). Levels are kept low by means of a degradation system which is inactivated in response to hypoxia, therefore allowing accumulation of HIF-1 α protein. As shown in figure 1.5, direct hydroxylation of prolyl residues by prolyl hydroxylases (PHDs) triggers the degradation of HIF-1 α under normoxic conditions. The PHDs are iron dependent enzymes that convert proline into hydroxyproline, a reaction which requires oxygen and 2-oxoglutarate (Epstein *et al.*, 2001, Bruick & McKnight, 2001).

Hydroxylation of the two conserved proline residues, Pro 402 and Pro 564 within the ODDD, directs HIF-1 α for degradation by the von Hippel-Lindau (pVHL) tumour suppressor protein under normoxic conditions (Maxwell *et al.*, 1999). The protein product of the von Hippel-Lindau gene serves as a recognition component for an E3-ubiquitin ligase complex that binds to and targets HIF-1 α protein for proteolysis, thus preventing transcriptional activation of its target genes. Hydroxylation and subsequent interaction of pVHL with HIF-1 α , is inhibited under hypoxic conditions, resulting in stabilisation and accumulation of the HIF-1 α protein (Yu *et al.*, 1998; Jaakkola *et al.*, 2001; Ivan & Kaelin, 2001).

In addition to inhibition of degradation, stabilisation of HIF-1 α protein depends upon the binding of transcriptional co-activator proteins. Nuclear p300 and CREB binding protein (CBP) are homologues of ubiquitously expressed proteins which possess histone acetyl-transferase activity (HAT) (Carrozza *et al.*, 2003). Transactivation of HIF-1 α requires the C-TAD of HIF-1 α to interact with

transcriptional co-activator proteins, such as CBP and p300. This high affinity binding involves almost the entire C-TAD of HIF-1 α and extensive intermolecular hydrophobic interactions are formed between the C-TAD and CBP/p300, thus contributing to the stability of the complex (Dames *et al.*, 2002). The binding of these proteins serves two functions, as a physical link between HIF-1 α and the initiation complex of the target gene, and chromatin remodelling through their intrinsic acetyltransferase activity, which is required for gene transcription (reviewed by Semenza, 1998). Under normoxic conditions this interaction is blocked by hydroxylation of the asparagine residue Asn-803 within the C-TAD (Lando *et al.*, 2002). Other histone acetyltransferases, steroid-receptor coactivator-1 (SRC-1) and transcription intermediary factor-2 (TIF-2) also interact with HIF-1 α , enhancing activity in a synergistic manner with p300 (Carrero *et al.*, 2000).

1.5.3.3 Inhibition and competitive binding

Originally considered to be a factor inhibiting HIF-1 (FIH-1) (Mahon *et al.*, 2001), FIH-1, which is an asparaginyl hydroxylase, has more recently been identified as an oxygen sensor involved in HIF-1 α regulation (Lando *et al.*, 2002). FIH-1 targets the asparagine 803 (Asn-803) residue for hydroxylation, thereby repressing transactivation of HIF-1 α through preventing binding of the transcriptional co-factor p300/CBP to the HIF-1 α C-TAD (Lando *et al.*, 2002). Like the PHDs, this hydroxylation enzyme is a member of the 2-oxoglutarate and iron-dependent dioxygenase family (Safran & Kaelin, 2003).

Competition for binding to HIF-1 β also regulates the ability of HIF-1 α to activate target genes. Full length HIF-1 α mRNA contains 15 exons, but a spliced variant of HIF-1 α mRNA lacking exon 14 (sHIF-1 α) has also been discovered (Gothie *et al.*, 2000). The truncated HIF-1 α protein translated from the shorter mRNA is able to compete with normal HIF-1 α protein for HIF-1 β , and therefore decrease HIF-1 transcriptional activity.

In renal carcinoma, a natural antisense of the HIF-1 α transcript (aHIF) which is complementary to the 3' untranslated region (UTR) of HIF-1 α has been

described (Thrash-Bingham & Tartof, 1999). This sequence does not encode a protein, yet it is widely expressed in normal and foetal tissues and has been found in breast cancer (Rossignol *et al.*, 2002). The aHIF sequence contains several putative HREs so has the ability to create a negative loop of regulation of HIF-1 α expression through exposing the AU instability regions within the 3' UTR of HIF-1 α , thus increasing its degradation speed. Previous to these findings, only artificial antisense of HIF-1 α was known to inhibit mRNA translation in this manner (Caniggia *et al.*, 2000). This potentially has implications for cell growth in a chronically hypoxic environment, where long term transcriptional regulation could be achieved through greater control via aHIF, rather than post-translational modifications of HIF-1 α , which are more suited to short term adaptations (Rossignol *et al.*, 2002).

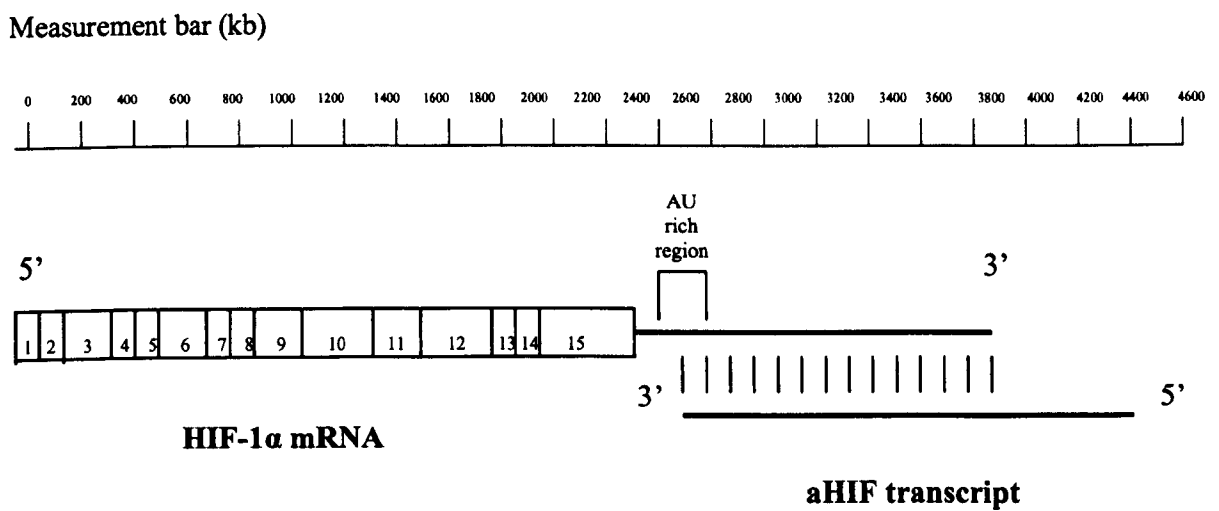


Figure 1.6: Schematic representation of HIF-1 α mRNA and its natural antisense, aHIF. The position of the 15 exons of the coding region of HIF-1 α , the AU rich region of HIF-1 α (Genbank accession: U22431) is shown relative to aHIF, along with their respective lengths in kb. aHIF is complementary upon at least 1027 bases of the HIF-1 α 3'UTR (as adapted from Rossignol *et al.*, 2002).

1.5.3.4 Modification of MAPK- and Pi3K-dependent pathways

The relationship between MAPK signalling and HIF-1 protein expression was first observed by Wang and colleagues in 1995, through the use of the MAPK inhibitor Genistein, which resulted in decreased levels of the α and β subunits along with blocking of the DNA binding complex. MAPK is required for the transactivation activity of HIF-1 α , and inhibition of MAPK disrupts the HIF-1 α -p300 interaction, suppressing the transactivation activity of p300. However, this regulation of HIF-1 transactivation may have little effect on the hypoxic accumulation of HIF-1 α (Sang *et al.*, 2003). This theory is supported by reports that p42/44 MAPK directly phosphorylate HIF-1 α and regulate its transcriptional activity with no effect on HIF-1 α protein levels induced by hypoxia (Richard *et al.*, 1999), thus demonstrating co-operation between hypoxia and growth factor signals, which ultimately lead to an increase in HIF-1-mediated gene expression (Salceda *et al.*, 1997; Conrad *et al.*, 1999; Richard *et al.*, 1999).

Recently, a functional relationship was found between induction of c-jun mRNA, c-jun N-terminal phosphorylation and the presence of HIF-1 α . Furthermore, JNK activity was seen to be dependent on enhanced glucose utilization mediated by HIF-1, therefore indicating that intracellular glucose levels link hypoxia-inducible JNK activity with oxygen sensing (Laderoute *et al.*, 2004).

Hypoxia-induced HIF-1 α expression can also be blocked in certain cell types, using Pi3K inhibitors such as LY294002 and wortmannin (Chandel *et al.*, 2000; Zhong *et al.*, 2000). Further to this, several reports have demonstrated that the Pi3K/Akt pathway modulates HIF-1 activation and activity in non-hypoxic cells (Zhong *et al.*, 2000, Zundel *et al.*, 2000; Mazure *et al.*, 1997). Subsequently, it has been shown that insulin, epidermal growth factor (EGF), mutation in the tumour suppressor PTEN (Jiang *et al.*, 2001), IGF-1 (Liu *et al.*, 2001), 4-hydroxy estradiol (Gao *et al.*, 2004), HER2/neu and other tyrosine kinases such as EGFR and V-SRC (Hudson *et al.*, 2002) specifically increase the protein levels of HIF-1 α in human cancer cell lines via Pi3K-dependant pathways. Amplified signalling through Pi3K, and its downstream target mTOR, enhanced HIF-1 α gene expression in PC-3

prostate cancer cell line, also indicating mTOR to be a potential upstream activator of HIF-1 (Hudson *et al.*, 2002).

1.5.3.5 Redox signalling

HIF-1 must remain in the reduced state in order to be able to bind to target DNA (Wang *et al.*, 1995). Furthermore, redox sensitive stimulation of the HIF-1 α subunit may be critical for the activation of HIF-1 (Huang *et al.*, 1996). The hypoxia inducible coactivators of HIF- α are SRC-1 and CREB-binding protein. These enhance the transactivation potential of HIF-1 α through binding to specific domains within the C terminus, the activity of which is strongly potentiated by the nuclear redox regulatory protein, redox factor-1 (Ref-1) (Carrero *et al.*, 2000). This finding proved logical, as it had already been established that Ref-1 is implicated in the up-regulation of HIF-1 α -dependent induction of gene expression (Huang *et al.*, 1996).

However, non-hypoxic induction of HIF-1-mediated gene expression may not follow this trend, as later studies showed VEGF mRNA and HIF-1 α induction to be independent of ROS in arsenite-induced ovarian carcinoma (Duyndam *et al.*, 2001), or ROS production by nickel or cobalt (Salnikow *et al.*, 2000).

1.5.3.6 Time course of HIF-1 α expression

As previously described, stabilisation of HIF-1 α protein in response to hypoxia is a rapid process, with nuclear expression and target DNA binding evident after less than 2 minutes in HeLa cells (Jewell *et al.*, 2001). The time course of expression of HIF-1 α may be a significant factor underlying hypoxic disease. An extended time course of HIF-1 α expression is thought to be an important factor in pre-eclampsia (PE), whereby PE villous explants subjected to hypoxia showed significantly impaired HIF-1 α degradation compared to non-PE tissue after 90 minutes re-oxygenation (Rajakumar *et al.*, 2003). In a model of neonatal rat brain hypoxia-ischaemia, HIF-1 α protein expression peaked at 8h following 90 minute

occlusion of the middle cerebral artery, then declined subsequently at 24h in injured cortex (Mu *et al.*, 2003). However, Li *et al* (2005) reported that 1h global ischaemia-hypotension in the rat produced a marked increase in HIF-1 α protein expression in the hippocampus and cortex at 6h, which subsequently peaked at 48-96h. In a mouse dorsal skin flap model of segmental hypoxia, HIF-1 α mRNA expression was enhanced at 4h hypoxia, maximal at 6h and decreased back to normal levels at 8h (Vihanto *et a.*, 2005). A previous study, however, reported that permanent focal ischaemia in rat brain induced a significant increase in HIF-1 α mRNA which increased up to 20h (Rosenberger *et al.*, 1999). The Vihanto study also showed that after 24h, strong accumulation of HIF-1 α protein occurred in endothelial and adjacent cells.

1.5.4 Non-hypoxic regulation of HIF-1 α expression

1.5.4.1 Positive regulation

HIF-1 activity in several cell types has been reported to be regulated by diverse non-hypoxic stimuli including, NO (Kimura *et al.*, 2000), tumour necrosis factor- α (TNF- α) (Sandau *et al.*, 2001), insulin, IGF-1 (Zelzer *et al.*, 1998), and mechanical stress (Kim *et al.*, 2002).

Non-hypoxic agents have the capacity to induce HIF-1 activity to an equal or greater extent than hypoxia alone, and in contrast to the post-transcriptional control of hypoxia-induced HIF-1 α stability, these non-hypoxic stimuli have been reported to regulate HIF-1 α through transcriptional and translational mechanisms, some involving PKC and/or Pi3K signalling (Kim *et al.*, 2002; Kimura *et al.*, 2000; Page *et al.*, 2002; Sandau *et al.*, 2001; Zelzer *et al.*, 1998; Zhong *et al.*, 2000).

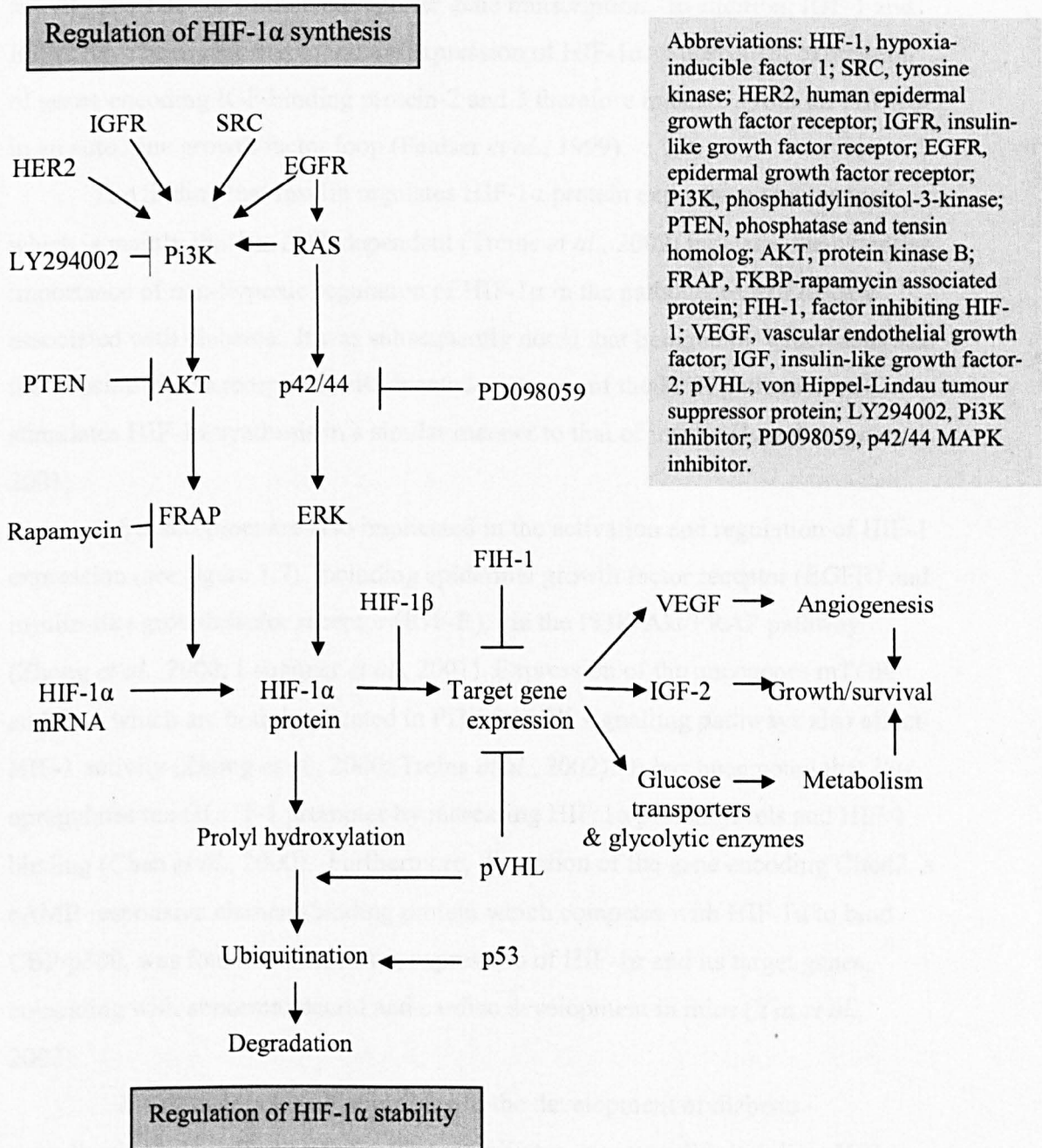
Epidermal growth factor (EGF), basic fibroblast growth factor (bFGF) and tumour necrosis factor- α (TNF- α) have all been shown to increase HIF-1 α expression (Agani & Semenza, 1998; Zelzer *et al.*, 1998; Jeong *et al.*, 2003) by pathways which are independent and parallel to that of hypoxia (Feldser *et al.*, 1999).

Hypoxia-independent mechanisms by which HIF-1 α and HIF-1-dependent transcriptional activity are induced, could play a major role in vascular remodelling, as substantially elevated levels of HIF-1 α in response to Angiotensin II, thrombin and platelet-derived growth factor (PDGF) have been detected in vascular smooth muscle cells independent of the oxygen environment (Richard *et al.*, 2000).

HIF-1 α is also potently induced by the dietary flavonoid, quercetin, under normoxic conditions, in a manner similar to that of hypoxia. This may be attributable to the subsequent finding that HIF-1 α contains potential serine/threonine phosphorylation sites for a variety of kinases, including casein kinase II, which is potently inhibited by quercetin, therefore stabilising HIF-1 α and allowing nuclear localisation of the protein in a transcriptionally active state (Wilson & Poellinger, 2002).

Non-hypoxic activation of HIF-1 α may involve the Warburg effect. By this mechanism, cancer cells produce lactate and pyruvate, the end products of anaerobic glycolysis, even in the presence of oxygen. Lu and colleagues observed that lactate and pyruvate were responsible for HIF-1 α expression in the absence of hypoxia, thereby demonstrating the potential implication for regulation of HIF-1 α via the Warburg effect (Lu *et al.*, 2002).

Figure 1.7. Signal transduction pathways leading to the expression of HIF-1 and the transactivation of downstream target genes (as adapted from Semenza, 2002 and Zhong *et al.*, 2000). Co-operative induction of signalling pathways in response to growth factors modulate the expression of HIF-1 α and subsequent transactivation or degradation.



Unlike hypoxia, insulin does not stimulate HIF-1 α accumulation through the inhibition of its degradation, but through a translation dependent mechanism resulting in increased HIF-1 α protein expression, augmented HIF-1 α DNA binding activity and HIF-1 α stimulated reporter gene transcription. In addition, IGF-1 and IGF-2 have been reported to induce expression of HIF-1 α . Subsequent expression of genes encoding IGF-binding protein-2 and 3 therefore indicate a role for HIF-1 α in an autocrine growth factor loop (Feldser *et al.*, 1999).

The finding that insulin regulates HIF-1 α protein expression in a manner which is mainly Pi3K/mTOR-dependent (Treins *et al.*, 2002) indicates the potential importance of non-hypoxic regulation of HIF-1 α in the pathogenesis of disease associated with diabetes. It was subsequently noted that heregulin, which activates the tyrosine kinase receptor HER2 located upstream of the Pi3K pathway, stimulates HIF-1 α synthesis in a similar manner to that of insulin (Laughner *et al.*, 2001).

Other receptors are also implicated in the activation and regulation of HIF-1 expression (see figure 1.7), including epidermal growth factor receptor (EGFR) and insulin-like growth factor receptor (IGF-R), via the Pi3K/Akt/FRAP pathway (Zhong *et al.*, 2000; Laughner *et al.*, 2001). Expression of the oncogenes mTOR and *Ras*, which are both implicated in Pi3K/MAPK signalling pathways also affect HIF-1 activity (Zhong *et al.*, 2000; Treins *et al.*, 2002). It has been noted that *Ras* upregulates the GLUT-1 promoter by increasing HIF-1 α protein levels and HIF-1 binding (Chen *et al.*, 2000). Furthermore, disruption of the gene encoding Cited2, a cAMP-responsive element-binding protein which competes with HIF-1 α to bind CBP/p300, was found to cause over expression of HIF-1 α and its target genes, coinciding with abnormal neural and cardiac development in mice (Yin *et al.*, 2002).

Many factors which contribute to the development of diabetic complications also affect HIF-1 α . The vasodilator, prostacyclin, stabilises HIF-1 α by downregulating ROS production in HUVEC (Chang *et al.*, 2005) and the chemoattractant interleukin-1 β (IL-1 β), is able to activate HIF-1 α mediated expression of VEGF and its receptor VEGF-2 (Amano *et al.*, 2004). In diabetes,

the plasminogen activator inhibitor-1 (PAI-1) gene is expressed in the arterial wall during cell adhesion (Chang *et al.*, 2003) decreasing fibrinolysis and increasing thrombogenicity. HIF-1 is a down-stream molecule of PAI-1, and is also increased in the arterial wall in human diabetes (Pandolfi *et al.*, 2001), therefore representing a potential mechanism contributing to accelerated atherosclerosis.

1.5.4.2 Negative regulation

Tumour suppressor gene products, including pVHL, PTEN and p53 are known to inhibit HIF-1 α protein expression (Semenza, 2002a). Interaction of the tumour suppressor protein p14^{ARF} with HIF-1 can directly inhibit its transcriptional activity by sequestering the α -subunit into the nucleolus (Fatyol & Szalay, 2001). Progression of colorectal adenocarcinoma correlates with the loss of PTEN tumour suppressor activity, increase in HIF-1 α protein and mRNA and VEGF expression, which increased gradually as the pathological stage of cancer advanced (Jiang *et al.*, 2003). This action of PTEN may be due to it encoding a specific phosphatase which negatively regulates Pi3K/Akt, thus interfering with the activation of HIF-1 α (Zhou *et al.*, 2002).

1.5.5 Role of HIF-1 α in the development of physiological and pathophysiological processes associated with disease and cell damage.

1.5.5.1 Carcinogenesis

HIF-1 α has a complex role in carcinogenesis. In adult animals HIF-1 α is over-expressed in epithelial cancers and high grade pre-malignant lesions (Zhong *et al.*, 1998). Involvement of HIF-1 α in the vascularisation of tumours is clearly seen by means of its role in the activation of angiogenic mechanism(s). The increasing tissue mass results in areas of tumour that have reduced oxygen tension as a result of inadequate blood supply.

The inevitable hypoxia activates HIF-1 α , which then induces VEGF to drive the proliferation of endothelial cells. In Ha-*ras* transformed cells, analysis of the 5' flanking region of the VEGF promoter, indicates that a HIF-1-like sequence promotes a 15 fold increase in reporter gene activity (Mazure *et al.*, 1996).

In pancreatic cancer, HIF-1 α confers resistance to apoptosis and induction of metabolism-associated genes, GLUT-1 and aldolase A (Akakura *et al.*, 2001). The tumour suppressor gene p53 promotes ubiquitination and proteosomal degradation of the HIF-1 α subunit (Ravi *et al.*, 2000), therefore the loss of p53 during tumourigenesis results in a HIF-1 α dependent switch to an angiogenic phenotype.

A common trait of highly malignant tumours is the capacity to metabolise more glucose to lactate than their tissue of origin. It has been observed that the distal region of the hepatoma type II hexokinase (HKII) promoter displays consensus sequences for HIF-1, which overlap the E-box sequences known to be related to glucose response. Combined stimulation with glucose and hypoxia upregulate the expression of HKII- 7-fold, compared to the 2-fold induction by glucose alone. This suggests responsiveness to hypoxia by a process that is modulated by glucose in rapidly proliferating hepatoma cells (Mathupala *et al.*, 2001).

Both MAPK and the Pi3K/Akt pathways enhance HIF-1 α levels in tumour cells or mitogen stimulated cells under normoxia (Zhong *et al.*, 2000; Stiehl *et al.*, 2002) and such enhancement is deemed to involve control of HIF-1 α translation (Laughner *et al.*, 2001). It has been suggested that Pi3K signalling is neither required nor sufficient for stabilisation of HIF-1 α (Arsham *et al.*, 2002), however, it was later observed that Pi3K/Akt/FRAP signalling is required for HIF-1 α and VEGF-A expression in 4-hydroxy estradiol (4-OHE2) induced carcinogenesis (Gao *et al.*, 2004). Several mechanisms are known to be responsible for upregulation of the Pi3K pathway in human cancer, for example the gene coding for the catalytic subunit of Pi3K is amplified in cervical carcinoma (Ma *et al.*, 2000) while the tumour suppressor PTEN is frequently lost in glioblastoma and endometrial cancer (Cantley *et al.*, 1999; Besson *et al.*, 1999).

1.5.5.2 Apoptosis

Paradoxically, HIF-1 α also participates in hypoxic cell death which may arise from activation of proapoptotic mediators, the Bcl-2-binding proteins BNIP3 and NIX which can inhibit the anti-apoptotic effect of Bcl-2 and stabilise wild type p53 (Bruick, 2000). Another cell-death molecule activated by HIF-1, simply known as HGTD-P, is situated downstream of HIF-1 α and triggers apoptosis via mitochondrial pathways. These cell death mediators may be activated by separate HIF-1-dependent pathways, as HGTD-P is stimulated in response to acute hypoxic insult, while BNIP3 responds to chronic hypoxia (Lee *et al.*, 2004).

1.5.5.3 Wound healing

Wound healing proceeds through various stages of proliferation and tissue remodelling. In a mouse model of epidermal wounding, HIF-1 α , GLUT-1 and phosphoglycerate kinase-1 (PGK-1) mRNAs were detectable immediately after wounding (Elson *et al.*, 2000). Coordinate gain of HIF-1 α expression and HIF-1 function at specific stages of wound healing suggests that regulation of HIF-1 α gene expression in this circumstance may occur at the level of mRNA and protein (Wang *et al.*, 1995; Huang *et al.*, 1996). The induction of HIF-1 α mRNA in the proliferative compartment of the epidermis in wound healing (Zhong *et al.*, 1999) along with the close proximity of the underlying dermal capillaries to where expression is centred in the epidermal basal cells (Smith-McCune *et al.*, 1997) suggests that the affected area is not necessarily hypoxic, therefore HIF-1 α activation in this instance may be hypoxia independent.

1.5.5.4 Diabetic complications

Vascular expression of HIF-1 α has been suggested to contribute to the manifestation of diabetic retinopathy (Ozaki *et al.*, 1999; Lukiw *et al.*, 2001). This in turn activates VEGF, which is a major factor in the development of uncontrolled

cell growth and vascular permeability of the retinal microvasculature characteristic of diabetic retinopathy (reviewed by Caldwell *et al.*, 2003). On the other hand, diabetes coincides with a marked decrease in VEGF expression in ischaemic muscle (Rivard *et al.*, 1999) and skin wounds (Frank *et al.*, 1995) suggesting negative regulation of HIF-1 α .

The exact cause of this regulation, however, is not clear. Reduction in VEGF receptor expression in response to hyperglycaemia, and subsequent abnormal VEGF signalling, has also been noted (Pinter *et al.*, 2001). Therefore, gain of HIF-1 α function may be advantageous in diabetic peripheral vascular disease, frequently complicated by chronic leg ulcers which can precipitate amputation. An undesirable hallmark of VEGF activity, however, is its ability to increase blood vessel permeability (Dvorak *et al.*, 1999). In order to produce a healthy vasculature free from vascular leakage, oedema and inflammation, endothelial VEGF clearly needs to work in conjunction with other angiogenic factors (Bruick & McKnight, 2001).

The co-ordinating role which HIF-1 α may have in such regulation is seen in transgenic mice which over-express epidermal HIF-1 α . These mice develop a microvasculature which, in spite of induction of VEGF and an increase in microvascular density, is non-leaky at base line, and somewhat leakage resistant in response to acute inflammation (Elson *et al.*, 2001), thereby implicating HIF-1 α as a global mediator of the angiogenic response. This action may be achieved through the ability of HIF-1 α to regulate Angiopoietin-2 and Angiopoietin-4 (Ang-2 and Ang-4), which when expressed in conjunction with VEGF exhibit marked hypervascularity without excess vascular leakage, producing morphologically and functionally normal vessels (Yamakawa *et al.*, 2003).

Regulation of VEGF in response to hyperglycaemia via HIF-1 α , however, remains controversial. It has been observed that insulin-induced HIF-1 α -dependent VEGF expression requires p38 MAPK and Pi3K, whereas hyperglycaemia-induced regulation of VEGF expression is HIF-1 α -independent, requiring instead PKC and p42/p44 MAPK (Poulaki *et al.*, 2002).

1.5.6 Potential role of glucose in the regulation of HIF-1 α

The changes in oxygen tension and glucose concentration play an important role in metabolism, angiogenesis, tumorigenesis and embryonic development. However, little is known about the interaction of these two signals. Since HIF-1 itself promotes glycolytic metabolism, enhancement of HIF-1 by glucose metabolites may constitute a novel feed-forward signalling mechanism (Lu *et al.*, 2005). The effect of altered glucose and oxygen availability to tissues, and the subsequent effect this has on HIF-1 expression, is recognised in several disease states. However, the mechanisms underlying this association are largely unknown.

In spontaneously diabetic rats, early induction of VEGF in liver and kidney at the onset of disease was shown to be associated with HIF-1 and CREB-1 both binding to the hypoxia response element (HRE) and/or the CREB response element (CRE) (Braun *et al.*, 2001). In STZ-induced diabetic rats, high glucose was seen to blunt the HIF-HRE pathway and subsequent VEGF response to hypoxia (Katavetin *et al.*, 2006). Diabetic kidney disease has shown excess glucose metabolism under normoglycaemic conditions to involve an increase in GLUT-1 levels coincident with increased nuclear HIF-1 α protein expression (Pfafflin *et al.*, 2006). In human fibrosarcoma and pharyngeal carcinoma cell lines, absence of glucose and serum resulted in no hypoxic accumulation of HIF-1 α protein in the nuclear fraction of either cell line, with normal glucose concentrations proving more important than normal serum in restoring the full response to hypoxia (Vordermark *et al.*, 2005). HIF-1-dependent increase in glucose metabolism and consumption has also been suggested as a mechanism by which cell death may occur in renal epithelial cells exposed to severe hypoxia (Biju *et al.*, 2005). However, hypoxia induced changes in vascular cell growth have been seen to be altered by hyperglycaemia via inhibition of HIF-1 α expression and activity (Gao *et al.*, 2007).

Cross-talk between oxygen and glucose is seen in the regulation of L-type pyruvate kinase (L-PK) gene expression in the liver, whereby reduction of glucose-dependent induction of L-PK under low oxygen tension appears to be mediated by interference between HIF-1 α and an upstream stimulating factor at the glucose

response element (GlcRE). Furthermore, the GlcRE also functions as a hypoxia response element (HRE), as demonstrated through its ability to bind HIF-1 α (Krones *et al.*, 2001; Kietzmann *et al.*, 2002).

Such evidence suggests co-operation between oxygen and glucose dependent control of metabolism at the level of transcription factors, therefore implicating HIF-1 α activation and consequent signalling to be the common feature linking the two.

1.6 *In vivo* and *in vitro* models of experimental diabetes mellitus

Diabetes is a multifactorial disease, the long-term consequences of which are the result of a multitude of metabolic and structural abnormalities occurring concomitantly. Therefore, it is very difficult to establish causal relationships between observed changes and the chronic complications associated with human diabetes (Bone *et al.*, 1997).

In vivo and *in vitro* models of experimental diabetes are powerful tools in the study of the pathophysiology of the disease, yet advantages and disadvantages are associated with both. The *in vivo* streptozotocin (STZ)-induced rat model of diabetes can never mimic the human disease exactly, especially in terms of longevity and development of chronic complications. However, it has proved to be very useful in the study of the initial metabolic and vascular insults which can trigger diabetic neuropathy (Cameron *et al.*, 2001), retinopathy (Yu *et al.*, 2001) and nephropathy (Sodhi *et al.*, 2001), displaying many of the morphological and functional changes evident in human diabetic complications.

To be able to fully investigate the pathways and mechanisms contributing to human diabetic complications, *in vitro* human cell culture models are perhaps preferable. However, vascular cells grown in culture form flat monolayers, not vessels as in nature, have no blood supply and no cooperation from other cell types. Therefore, such a simple system can never accurately represent that of a complex *in vivo* model. Nevertheless, by employing the cell culture model, the extracellular environment can easily be manipulated and monitored, which is not possible *in*

vivo, and specific cell lines which are relevant to pathogenesis of vascular complications are readily available for these studies. Furthermore, unlike the animal model, the human cell culture model is not hampered by the issue of species specificity, and therefore should yield findings which are more clinically relevant to human diabetes.

1.7 Aims of the study

Although the mechanisms involved in the regulation and expression of HIF-1 α are becoming increasingly clear, the signalling pathways that determine HIF-1 α stabilisation, nuclear translocation and HIF-1 transactivational ability under hypoxic or normoxic conditions remain confusing and often contradictory.

It is now widely accepted that non-hypoxic stimuli contribute to HIF-1 α expression. Furthermore, it is also becoming more apparent that several factors which are proposed to initiate and sustain the development of the chronic complications of diabetes are either upstream mediators or downstream effectors of HIF-1 α expression.

Glucose has been inextricably linked to the development and progression of diabetic complications. Tissues subjected to poorly controlled blood glucose levels, such as those experienced in diabetes, develop a state of pseudohypoxia due to the increased demand for the expression of metabolic enzymes and pathways which are classically associated with reduced oxygen tension.

By establishing whether glucose or a product of glucose metabolism has the ability to modulate HIF-1 α expression independently of or in conjunction with hypoxia, we would then be able to dissect some of the signalling pathways which may be contributing to this regulation, and perhaps represent a novel target to which logical strategies aimed at therapeutic intervention could be developed.

Therefore, using an *in vivo* model of experimental diabetes (i) and an *in vitro* endothelial cell culture model thereafter (ii-vi), the aims of this study were the following;

- (i) To determine the expression of HIF-1 α *in vivo*, within the vasculature of a chemically-induced rat model of experimental diabetes. As the endothelium is the first line of defence to substances contained within the blood, this could highlight regulation of endothelial expression of HIF-1 α to be a significant vascular response to diabetic insult.
- (ii) To investigate the significance of endothelial HIF-1 α expression in response to elevated glucose *in vitro* using HUVEC. This would then allow the levels of HIF-1 α protein and mRNA to be measured directly, in cells exposed to high glucose combined with normoxia or hypoxia.
- (iii) Use chemical inhibitors of transcription/translation pathways in cell culture to determine whether any change in expression of HIF-1 α mRNA in response to altered glucose concentration observed in (ii) is occurring at the level of transcription, mRNA stability or translation. Furthermore, assess whether the stability elements within the 3'UTR of HIF-1 α mRNA are being targeted and modulated by RNA-binding proteins.
- (iv) To assess the effect of any change in HIF-1 α expression on mRNA levels of the HIF-1-responsive genes GLUT-1 and IGF-1R and the natural antisense of HIF-1 α , termed aHIF.
- (v) To investigate the potential influence of Pi3K and MAPK signalling cascades on glucose mediated regulation of HIF-1 α , and also determine the effect of altered redox status through use of antioxidant compounds.
- (vi) Use of non-metabolizable analogues of glucose to determine whether any observable influence which elevated glucose concentration is having on HIF-1 α expression is attributable to glucose itself, or a product of its metabolism.

Chapter 2

Materials and Methods

2.1 Streptozotocin-induced diabetic rat model

Tissue samples taken from a rat model of chemically induced diabetes were kindly provided by Prof. M. A. Cotter and Prof. N. E. Cameron, of the Department of Biomedical Sciences, Aberdeen University.

2.1.1 Streptozotocin treatment of rats

The pancreatic beta-cell toxin streptozotocin (STZ) was administered to rats by single injection in order to produce a chemically-induced model of experimental type 1 diabetes.

Adult Sprague Dawley stock rats were maintained by the Biological Services Unit at Aberdeen University, in accordance with the British Home Office Code of Practice for the housing and care of animals used in scientific procedures. Chemical induction of diabetes was carried out at Aberdeen University, using an established method involving the administration of STZ by intraperitoneal injection at a concentration of 45mg/kg in sterile saline administered at 19 weeks. Regular blood sugar monitoring was used to detect the onset of diabetes, and animals were then sacrificed at 4 weeks (body weight (g): 362 ± 8 ; plasma glucose (nM): 49.9 ± 5.5), 10 weeks (body weight (g): 328 ± 13 ; plasma glucose (nM): 54.2 ± 2.9) and 24 weeks (body weight (g): 310 ± 10 ; plasma glucose (nM): 49.8 ± 4). Time matched control littermates were treated with an injection of saline alone (body weight (g): 443 ± 4 ; plasma glucose (nM): 7.6 ± 0.5).

2.1.2 Preparation of cryostat sections

Tissue bundles were prepared from the treated and control animals. These consisted of aorta and sciatic nerve surrounded by skeletal muscle. For cryostat sectioning, the tissue bundles were frozen in isopentane pre-cooled in liquid nitrogen, and stored at -80°C . Prior to cutting, the temperature of the frozen tissue bundles was allowed to rise to -20°C .

2.2 Cell culture

2.2.1 Cell culture materials

Cell culture reagents were purchased from Invitrogen (Paisley, UK), all cell culture plastics and glassware from Fisher Scientific UK Ltd. (Loughborough, UK) and chemical agents from Sigma-Aldrich (Poole, UK), unless stated otherwise, and all were used as supplied.

2.2.2 Human umbilical vein endothelial cells (HUVEC)

All in vitro investigations were carried out using human umbilical vein endothelial cells (HUVEC), cultured from an immortalised cell line, purchased from The European Collection of Cell Cultures (ECACC).

2.2.2.1 Cell growth conditions

All procedures involving cells were carried out in a dedicated cell culture lab, under aseptic conditions in an Aura 2000 laminar flow air hood (Bioair Instruments). All solutions, plastics and glassware used in cell culture were sterile prior to use. Cells were routinely cultured in glucose-free Glasgow's Minimal Essential Medium (GMEM) containing 10% foetal calf serum (FCS), 1 unit/ml penicillin, 1µg/ml streptomycin, 2mM L-glutamine and 5mM glucose. Standard growth conditions were maintained at 37°C in a humidified atmosphere of 5% CO₂ /95% room air in a Galaxy S incubator (Wolf Laboratories).

Cell monolayers were propagated in 75cm² culture flasks. Subculture was carried out using sub-confluent colonies of cells which displayed the characteristic cobblestone morphology when visualised with an inverted light microscope, and stained positive for von Willebrand factor (vWF) using immunocytochemistry (IHC). The media was replaced approximately twice weekly as indicated by a

colour change in the pH sensitive indicator. Used medium was poured away and the cell monolayer rinsed with Hank's balanced salt solution (HBSS), before adding 15ml fresh growth medium to the flask.

2.2.2.2 Routine sub-culture

To harvest cells for subculture, growth medium was poured off and the monolayer rinsed three times with 10ml calcium and magnesium free HBSS. The final wash was incubated for 10 minutes to remove all traces of medium.

The cell monolayer was removed from the flask by adding 10ml 0.25% trypsin solution, and by gentle agitation the flask for no longer than 2 minutes. An equal volume of medium containing FCS was then added to the cell suspension to neutralize the enzymatic activity of the trypsin. The cell suspension was removed to a sterile universal tube, and the flask rinsed with 3ml medium which was also poured into the same tube. Cells in suspension were pelleted by centrifugation at 8000-9000 x g for 8 minutes prior to removing the supernatant and resuspending the cell pellet in 1ml fresh medium. The cell suspension was then split at the desired ratio. For subculture, a split ratio of 1 to 4 was used, therefore 250µl cell suspension was added to sterile 75cm² flasks, and supplemented with 15ml fresh medium. The flasks containing HUVEC were transferred to an incubator set to conditions as previously described and left undisturbed overnight to allow the cells to adhere and begin to grow. Growth was checked daily under the microscope and by observation of any change in the colour of medium, indicative of pH changes.

2.2.2.3 Sub-culture for experimental procedures

For all experimental procedures, cells were harvested from 75cm² stock flasks as detailed in 2.2.2.2., under normal growth conditions, as laid out in 2.2.2.1.

2.2.2.3.1 Sub-culture of HUVEC into 75cm² flasks

The cell suspension obtained from 1 x 75cm² flask routinely contained sufficient cells to allow a 1 in 10 split into subsequent 75cm² flasks, therefore 100µl from 1ml cell suspension was added to the 75cm² flask and supplemented with 15ml growth medium. Flasks were then incubated under normal conditions and checked regularly under microscopy. On reaching 60% confluence, the cells were stepped down overnight in glucose-free/serum-free (GF/SF) GMEM, to facilitate synchronisation of cell growth at the start of the experimentation.

2.2.2.3.2 Sub-culture of HUVEC into chamber slides

Chamber slides containing two chambers of 2cm² area were used for immunocytochemical analysis of HUVEC. To seed the chambers, the cell count was obtained using the trypan blue dye exclusion method (2.2.3.1). Each well on the 2 well chamber slide was seeded with HUVEC at a density of 0.025 x 10⁶ cells/ml in a volume of 2ml. On reaching 60% confluence, the slides were stepped down over night in order to synchronise growth prior to treatment.

2.2.2.3.3 Sub-culture of HUVEC into 96 well plates

Cell number was counted as above, and each well in the 96-well culture plate was seeded with HUVEC at a density of 0.025 x 10⁶ cells/ml, in a volume of 200µl. The cells were allowed to adhere and start to grow overnight, before being used in the alamar blue assay, as described in 2.2.3.2.

2.2.3 Cell viability and proliferation

2.2.3.1 Trypan blue dye exclusion method

On reaching a suitable stage of proliferation, the cells were harvested as laid out in 2.2.2.2., and the viable cell number determined by means of trypan blue dye exclusion, in order to seed growth chambers with the appropriate number of cells.

An aliquot of cell suspension was mixed with trypan blue dye at a 1:1 ratio, mixed gently and left to stand for 2 minutes to allow the dye to penetrate any non viable cells. During this time, the haemocytometer was assembled with a glass coverslip. Using a Pasteur pipette, a small volume of the cell suspension was applied to the edge of the coverslip and allowed to fill the area under the coverslip by means of capillary action.

Using a microscope to see the two grids etched on either side of the haemocytometer, viable and non viable cells were counted in the 25 squares contained within the large square edged by double lines on both grids. The mean of the two sides of the slide was taken before calculating total viable cell number as follows;

$$\text{Number of cells/ml} = \frac{\text{cell count per large square} \times \text{dilution factor} \times 10^{-4} \text{ cm}^3}{\text{(volume of large square)}}$$

2.2.3.2 Alamar blue cell growth assay

Alamar blue is an indicator dye, formulated to quantitatively measure the proliferation of cells in culture. It consists of an oxidation-reduction (REDOX) indicator that yields a colorimetric change evident in the growth media (dark blue to pink) in response to metabolic activity. The assay plate is read using a colorimeter, to measure absorbance at 570nm (reduced) and 600nm (oxidised) wavelengths.

For the assay, cells were harvested from 75cm² flasks, as described in 2.2.2.2, and the cell count was then obtained using trypan blue (section 2.2.3.1).

Cells were seeded in clear flat bottomed 96 well sterile cell culture plates, at a density of 0.025×10^6 cells/ml. The plates were then incubated overnight under conditions as laid out in 2.2.2.1. The following morning, the plates were checked for cell adherence and initial growth by microscopy. The old growth medium was carefully removed and replaced with fresh media combined with 10% (v/v) alamar blue (Serotec). Plates were returned to the appropriate incubation conditions, and absorbance readings taken using an FL600 microplate reader (Bio-tec) after 0, 1, 6, 24 and 29 hours.

2.2.4 Artificial induction of Hypoxia

A hypoxic environment was created artificially *in vitro* by subjecting the cells in culture to a chemical mimic of hypoxia, the iron-chelator desferrioxamine (DFO) (Sigma), or by incubation in a 5% O₂/5% CO₂/air environment created by a Galaxy S CO₂ incubator (Wolf Laboratories).

2.2.4.1 Chemical induction of hypoxia

HUVEC were cultured in GMEM, containing 10% FCS and other cell growth supplements, at 37°C under 5% CO₂ /95% room air (normoxia) in 75cm² flasks (2.2.1.1). The cells were harvested and 2ml of cells at 1×10^6 cells/ml were seeded to each chamber of a 2 well chamber slides (2.2.2.3.2).

On reaching approximately 60% cell confluence, the growth medium was removed and the cell monolayer rinsed twice with HBSS. Growth medium was then replaced with GF/SF GMEM in order to step-down the cells overnight. The following morning, the GF/SF GMEM was removed, and replaced with fresh growth medium containing 130µM DFO for 0-6 hours. After treatment, the test medium was removed, and slides rinsed three times in sterile phosphate buffered saline (PBS). The slides were then left to air dry before storing at -20°C until required.

2.2.4.2 Non-chemical induction of hypoxia

Cells were cultured in the appropriate container depending on the procedure being undertaken, following methods described previously. The effect of hypoxia alone or in conjunction with other test agents was assessed through exposing the cells to lowered oxygen tension for the desired length of time, by means of an incubator that allowed for regulation of oxygen level, set to 5% O₂/5% CO₂/air, as opposed to 18% O₂ normal air incubations.

These conditions were created and maintained by purging O₂ from the incubator with nitrogen. After exposure to hypoxia, the containers were rapidly removed and placed on ice, before washing three times with ice cold PBS to remove all traces of media.

2.2.5 Alteration of glucose concentration and substitution with glucose analogues

The response of the cells to altered glucose level was observed, along with the response to equivalent concentrations of selected glucose analogues. Incubation with D-glucose and analogues were also combined with non-chemical induction of hypoxia, as described in section 2.2.4.2., in order to investigate any synergism between the two stimuli.

Routine subculture and maintenance of the cells was carried out in GMEM supplemented with 5mM glucose, thus simulating physiologically normal blood glucose level (euglycaemia).

Glucose was made up at 1M concentration in GF/SF GMEM. The solution was sterilised by filtration using a 0.2µm filter (Nunc). The glucose in solution could then be stored at 4 °C before adding to GMEM to produce glucose concentrations of either 5mM or 20mM.

Similarly, the glucose analogues 2-deoxyglucose (2-DG) and 3-orthomethylglucose (3-OMG) were used at equivalent concentrations. 2-DG can only be metabolised

by the first step of glycolysis before becoming trapped within the cell, while 3-OMG is not metabolised by the cell, and is free to enter and leave through active transport.

2.2.6 Inhibition of signalling pathways in cell culture

2.2.6.1 Transcription and translation

Inhibition of mRNA transcription and protein translation were studied using the chemical inhibitors actinomycin D (Act D) and cyclohexamide (CHX), respectively.

Act D was prepared under sterile conditions in dimethylsulphoxide (DMSO) and used in cell culture at a final concentration of 10µg/ml. A commercially prepared solution of CHX dissolved in DMSO was used in cell culture at a final concentration of 10µg/ml.

Prior to use, either Act D or CHX was added to 100ml GMEM + 10% FCS + supplements before applying the medium to the cells. The cells were then incubated with the separate inhibitors for 1, 6 and 24h with either 5mM or 20mM glucose, in normoxic and hypoxic conditions. The test agent solvent was controlled for by treating the cells as above with DMSO alone at an equivalent concentration in the media.

2.2.6.2 Protein kinase activity

PD98059 (Calbiochem), a mitogen activated protein kinase (MAPK) inhibitor, and LY294002 (Promega) a phosphoinositol-3 kinase (Pi3K) inhibitor were purchased as commercially prepared solutions dissolved in DMSO.

PD98059 was added to culture media to a final concentration of 2µg/ml, and LY294002 to a final concentration of 10µg/ml. Each inhibitor was incubated in cell culture and controlled for as described in section 2.2.6.1.

2.2.6.3 Redox signalling

The antioxidant α -lipoic acid was dissolved in ethanol then added to GMEM + 10% FCS + supplements to a final concentration of 250 μ g/ml. The media containing α -lipoic acid was then incubated with cells for 1, 6 and 24 h with either 5mM or 20mM glucose in normoxia and hypoxia. The solvent was controlled for by incubating the cells as above with an equivalent concentration of ethanol.

2.3 Immunochemical staining

Immunohistochemistry (IHC) was employed to detect protein expression within cryostat sections of diabetic and control rat tissue. Immunocytochemistry (ICC) was used similarly for detection within cultured cell preparations.

2.3.1 Avidin-biotin complex /alkaline phosphatase (ABC/AP) procedure for use with monoclonal mouse antibody

2.3.1.1 Overview of ABC/AP

The ABC/AP procedure is an immunoenzymatic staining method for detection of an antigen by light microscopy. This method utilises the high affinity of avidin for a biotinylated secondary antibody linked to a primary antibody directed against the antigen.

Alkaline phosphatase, which is used as the enzyme label for antigen detection, lyses a chromogenic substrate producing a red colour, thus indicating detection of the antigen.

2.3.1.2 IHC using ABC/ABC applied to cryostat sections of mouse brain

Sections of rat tissue were prepared and stored as detailed in section 2.1. Previously prepared sections of rat tissue mounted on glass slides were removed from the -20°C freezer, and allowed 2-3 hours to come up to room temperature.

Sections were fixed in ice cold acetone for 30 minutes in a fume cupboard, air-drying off the batch for 30 minutes. Tissue sections were then defatted with a wax pen. Slides were oxidized in one-buffered saline (50mM NaCl, 0.1M Tris, pH 7.5) (TBS) for 3 minutes, before tapping off excess liquid, to prevent or damage the tissue sections.

Non-specific binding of the secondary antibody was blocked by pre-adsorption of the secondary antibody with a mixture of bovine serum albumin (BSA) and casein. The primary antibody was applied to the sections. The primary antibody was applied to the sections. The primary antibody was applied to the sections.

Key:

✖ avidin

▲ biotin

● alkaline phosphatase

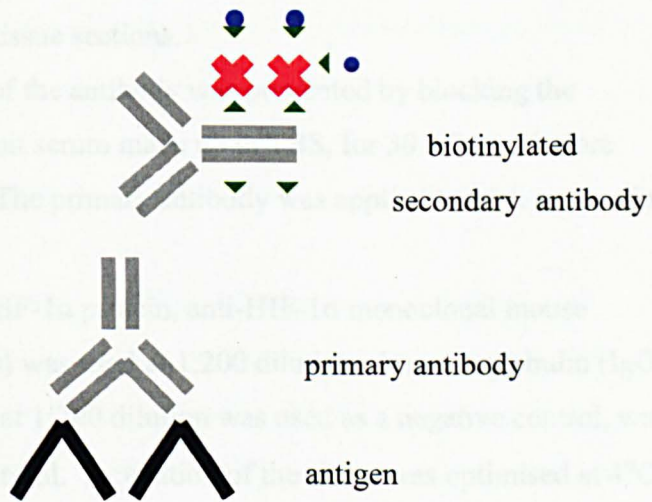


Figure 2.1. Schematic diagram of preformed avidin-biotin-alkaline phosphatase complex reacting with biotinylated secondary antibody (as adapted from 'Immunochemical Staining Methods Handbook', Dako Corporation, 1989)

The ABC/ABC solution was applied to each section, and incubated for 30 minutes in the humidified chamber at room temperature.

2.3.1.2 IHC using ABC/AP applied to cryostat sections of animal tissue

Sections of rat tissue were prepared and stored as detailed in section 2.1. Previously prepared sections of rat tissue mounted on glass slides were removed from the -20°C freezer, and allowed 2-3 hours to come up to room temperature.

Sections were fixed in ice cold acetone for 30 minutes in a fume cupboard, before air-drying on the bench for 10 minutes. Tissue sections were then delineated with a wax pen. Slides were equilibrated in tris-buffered saline (50mM tris, 40mM HCl, 0.9% NaCl, pH 7.5) (TBS) for 5 minutes, before tapping off excess liquid, taking care not to damage the tissue sections.

Non-specific binding of the antibody was prevented by blocking the sections with 50µl of 10% rabbit serum made up in TBS, for 30 minutes before tapping off the excess liquid. The primary antibody was applied to each section in 50µl aliquots.

For the detection of HIF-1α protein, anti-HIF-1α monoclonal mouse antibody (Affinity Bioreagents) was used at 1:200 dilution. Immunoglobulin (IgG1 isotype, Affinity Bioreagents) at 1:200 dilution was used as a negative control, with TBS alone as a background control. Incubation of the slides was optimised at 4°C overnight in a humidified chamber. After the incubation was complete, excess liquid was tapped off, and the slides were washed in TBS for 3 x 5 minutes at room temperature.

The secondary antibody, biotinylated rabbit anti-mouse (Dako), was made up in TBS with 5% rat serum to 1:300 dilution and applied in 50µl aliquots to the sections, before incubating in a humidified chamber at room temperature for 20-30 minutes.

The avidin-biotin-alkaline phosphatase complex (ABC/AP) solution was prepared following manufacturers instructions, and incubated at room temperature for 30 minutes. During this time, the slides were washed 3 x 10 minutes in TBS. The ABC/AP solution was applied to each section, and incubated for 30 minutes in the humidified chamber at room temperature.

Slides were then washed for 3 x 10 minutes in TBS. During this time, the chromogenic Fast Red substrate solution was prepared according to manufacturers instructions, and haematoxylin solution (Fisons) filtered to be used for counter-staining the slides.

After washing was complete, the substrate was applied to the sections until a red colour was present, which was routinely 2-3 minutes. Counter-staining was carried out in filtered haematoxylin for 3 seconds, before rinsing the slides in distilled water and allowing to dry.

Once dry, the slides were mounted by adding 3 drops of Ultra-mount (Dako) to cover the section before placing on coverslips. The slides were then viewed under light microscopy.

2.3.1.3 ICC using HUVEC grown on chamber slides

The ABC/AP procedure using HUVEC grown on chamber slides was employed using the same protocol as for the cryostat sections of rat tissue, detailed in 2.3.1.2. The only alteration involved substituting the 5% rat serum in the secondary antibody solution with 5% human serum.

2.4 Polymerase chain reaction (PCR)

The expression of specific genes was investigated in HUVEC by producing complementary DNA (cDNA) from cell samples and subjecting these to polymerase chain reaction (PCR) amplification.

PCR produces multiple copies of the gene of interest, by targeting short complementary primer sequences to specific regions within the gene. By optimising the amplification process for any given DNA sequence, it is then possible to measure the level of mRNA expressed by the gene of interest as a function of PCR product concentration.

2.4.1 RNA extraction from whole cell preparations

RNA extraction from whole cell preparations was carried out using commercially available kits from Qiagen. Buffers used in the procedure were provided with the kit, unless specified, full details of which are included in the manufacturer's handbook.

2.4.1.1 Sample homogenisation using QIAshredder spin columns (Qiagen)

Phosphate buffered saline (PBS) (Sigma) was treated with 0.01% diethylpyrocarbonate (DEPC) (Sigma) prior to autoclaving, in order to destroy any RNAase activity within the solution. Cell lysis buffer RLT was treated with 10µl/ml β-mercaptoethanol (Sigma) prior to use, in order to disrupt cell walls and aid lysis.

Cells were grown in 75cm² flasks (2.2.1.3.1) and treated as previously specified. Flasks were rinsed twice with chilled DEPC treated PBS on ice, before disrupting cell walls by adding 600µl buffer RLT. Cell lysates were then collected with a cell scraper. A maximum of 700µl cell lysate was applied to a QIAshredder column sitting in a 2ml collection tube before centrifuging for 2 minutes at 12,000 x g to fully disrupt the cells.

2.4.1.2 RNA extraction using RNeasy midi kit (Qiagen)

One volume of 70% ethanol was added to the homogenised lysate, and mixed by pipetting. Up to 700µl homogenised sample, including any precipitate which formed on addition of ethanol, was applied to an RNeasy spin column sitting in a 2ml collection tube.

The tubes were centrifuged for 15 seconds at 8000 x g, and the RNA was bound to the membrane in the spin column. Where the sample volume exceeded 700µl, subsequent aliquots were loaded into the same spin column, discarding the flow through after each centrifugation. Washing buffer RW1 was applied to the

RNeasy column, and centrifuged for 15 seconds at 8000 x g to wash. The RNeasy column was then transferred into a new 2ml collection tube, and 500µl of the second wash buffer RPE added before centrifuging for 15 seconds at 8000 x g to wash. The wash was repeated, and the tube centrifuged for 2 minutes at 12,000 x g to dry the RNeasy membrane. To eliminate any chance of possible buffer RPE carryover, the column was placed in a new 2ml collection tube and centrifuged at 12,000 x g for 1 minute.

To collect the RNA from the membrane, the column was placed into a new 1.5ml collection tube, and 30-50µl of RNase free water was pipetted directly on to the RNeasy membrane. The tubes were centrifuged for 1 minute at 8000 x g to elute the sample. The RNA was then ready for use, or stored at -20°C for 1 to 2 months, or at -80°C for more long term storage in ethanol.

2.4.2 Assessment of concentration and purity of RNA

Samples of extracted RNA were electrophoresed on agarose gel prepared at 1.4%(w/v) in 50ml Tris borate EDTA buffer (TBE) (130mM Tris, 35mM boric acid, 2.5mM EDTA). The agarose powder in TBE was melted by heating in a boiling water bath. A horizontal mini gel electrophoresis tank (Biorad) was prepared, containing the gel mould set up with well forming comb.

Prior to pouring, ethidium bromide was added to the molten agarose at a final concentration of 5ng/ml, to allow visualisation of the DNA under UV light. The well forming comb was removed along with the mould sealing gaskets when set, and electrophoresis buffer (TBE) was applied to just above the surface of the gel.

To 8µl of RNA, 2.5 µl of loading buffer (7 parts water to 3 parts glycerol plus two tracking dyes, bromophenol blue and xylene cyanol, both at 0.25% (w/v)) was added, then applied to the gel. The gel was then run for 1 hour at 100 volts.

Observation of 2 bands under UV light, representing the 28S and 18S ribosomes, indicated the presence of undegraded RNA.

The concentration of RNA in solution was measured spectrophotometrically at 260nm wavelength. The solution was diluted as follows in DEPC treated water.

4µl RNA + 996µl DEPC dH₂O (Dilution factor = 250)

The concentration of RNA in solution was calculated taking into account that at 260nm, absorbance of 1 = 40 µg/ml RNA

Abs₂₆₀ x dilution factor x 40 = X µg/ml RNA concentration

Absorbance was also measured at 280nm, in order to determine the purity of the RNA in solution, where a 260/280nm ratio of 2.00 indicated pure RNA. Samples were routinely found to have a ratio of 1.9 to 2.1, which was within an acceptable range.

Where the RNA concentration in solution was too dilute (ie. less than 455ng/µl which was the minimum required for reverse transcription, as described in section 2.4.3.1) samples were reprecipitated, before reconstituting in a smaller volume of sterile DEPC treated water. Two and a half times volume of ice-cold ethanol was added to the nucleic acid solution. The solution was then adjusted to 0.3M sodium acetate (NaOAc) by adding 1/10 volume 3M NaOAc, pH5.2 (Sigma). The solution was then mixed thoroughly and stored at -20°C for a minimum of one hour. The reprecipitated nucleic acid was centrifuged at 8000 x g for 5 minutes at 4°C before decanting the supernatant.

The pellet was then washed twice with 70% ethanol and centrifuged at 8000 x g at 4°C for 2 minutes. After removing the ethanol, the pellet was allowed to air dry, before reconstituting in an appropriate volume of DEPC treated dH₂O.

2.4.3 Preparation of complementary DNA (cDNA)

2.4.3.1 Reverse transcriptase polymerase chain reaction (RT-PCR)

For RT-PCR, RNA was prepared at a concentration of 5 μ g in 11 μ l in a thin walled PCR tube, to which 1 μ l of a 0.5 μ g/ μ l 15-mer oligo-dT primer (Sigma-Genosys) was added. Using a thermocycler (Techne Genius), the reaction was incubated at 70°C for 10 min, then 4°C for 2 minutes. Tubes were removed to ice for 1-2 minutes to cool, before pulse spinning. From a commercially available RT-PCR kit (Sigma), the following components were then added to each tube, according to the manufacturer's instructions:

4 μ l - 5x first strand buffer (250mM Tris-HCl pH 8.3, 375mM KCl, 15mM MgCl₂)

1 μ l - 10mM deoxynucleotide triphosphate mix (dNTP) (Roche)

2 μ l - 0.1M dithiothreitol (DTT)

1 μ l - 200units/ μ l murine Moloney leukaemia virus (M-MLV) reverse transcriptase

The mixture was mixed gently, pulse spun and incubated for 10 minutes at room temperature. The tubes were then returned to the thermocycler set to the following program:

Cycle 1; amplification - 50 minutes at 42°C

Cycle 2; inactivation of reverse transcriptase - 5 minutes at 95°C

The cDNA samples were made up to 100 μ l volume with sterile DEPC treated dH₂O prior to use or storage at -20°C.

2.4.3.2 cDNA priming

The following table (2.1) contains details of the oligonucleotides used in priming amplification of specific sequences within the cDNA. Primer sequences were generated through use of Genbase primer design software available via the Human Genome Mapping Project (web site; www.hgmp.mrc.ac.uk).

All primers were then synthesised by Sigma-Genosys, except for β_2 -microglobulin and insulin-like growth factor-1 receptor which were synthesized by Oswell DNA service, University of Southampton.

Table 2.1 Summary of cDNA primers used for PCR amplification of gene products. The amplification of each target gene sequence was achieved by binding of specific primers to their consensus sequences within the cDNA, allowing polymerase chain reaction (PCR) replication of the specific sequence.

Name	Primer	Product size (bp)	Length	T _m °C	% GC	Acc. No	Ref
Hypoxia Inducible Factor type 1 Alpha (HIF-1 α)	5' TCCATCTCCTACCCACATAC 3' 3' CTTTGGCTCCATTCCATTC 5'	365	20 19	54.8 55.7	50 42.1	U22431	Wang <i>et al.</i> , 1995
Antisense HIF-1 α (aHIF)	5' TGCTTCACTCATCCATTCA 3' 3' TTTTGGCTCTTTGTGGTTGGA 5'	390	20 20	64.3 63.1	45 40	U85044	Rossignol <i>et al.</i> , 2002
Glucose transporter type 1 (GLUT-1)	5' TGAACCTGCTGGCCTTC 3' 3' GCAGCTTCTTTAGCACA 5'	398	17 17	62.7 54.9	58.8 47.1	K03195	Mueckler <i>et al.</i> , 1985
Insulin like growth factor 1 receptor (IGF-1R)	5' GCCTCTCCGGGTTTAAAATG 3' 3' CCGGAGCCAGACTTCATTCT 5'	381	21 21	54.2 56.2	52.4 57.1	M73724	Ulrich 1991
β_2 -Microglobulin (β_2 -M)	5' CCTTGAGGCTATCCAGCGTACTCC 3' 5' CCATGATGCTGCTTACATGTCTC 3'	321	24 23	60.7 55.2	58.3 47.8	M17987	Gussow <i>et al.</i> , 1987

2.4.3.3 In vitro amplification of cDNA by PCR

2.4.3.3.1 Preparation of amplification reaction mix

Specific sequences of interest within the cDNA were amplified using the primers listed in table 2.1. The reaction mix was prepared in a thin walled DNase free PCR tube from the following components supplied as a commercially available kit, as recommended by the manufacturer.

5 μ l 10x reaction buffer (50mM KCl, 10mM Tris-HCl, pH 8.3 and 1.5mM MgCl₂)

1 μ l 10mM dNTP mix

33.5 μ l dH₂O

0.5 μ l *Taq* DNA Polymerase (*Thermus aquaticus*) (Roche)

The components were mixed and pulse spun. To the reaction mix, the specific primer and cDNA were then added and mixed gently.

2.4.3.3.2 Amplification of DNA sequence

The reaction tubes prepared in section 2.4.3.3.1 were transferred to the thermocycler (Techne Genius) and subjected to the following programs of sequential annealing, extension and denaturation.

1. Primer annealing to target sequence for amplification -
2 min at 94°C, 1 min at 55°C and 1 min 30 sec at 72°C
2. Extension of primed sequence -
10 to 30 cycles of 1 min at 94°C, 1 min at 55°C and 1 min 30 sec at 72°C
3. Denaturation of polymerase on completion -
50 sec at 94°C, 1 min at 55°C and 5 min at 72°C

Samples were then cooled to 4°C before briefly centrifuging to collect contents.

2.4.4 Validation and analysis of double stranded DNA (dsDNA)

2.4.4.1 Agarose gel electrophoresis

Regions of interest within the cDNA were amplified by PCR, as detailed in section 2.4.3.3. Once samples were amplified, the PCR product was determined by means of analytical agarose gel electrophoresis.

Agarose gel was prepared at 1.4% (w/v) as described in section 2.4.2. The following components were mixed then added to the wells.

- 8µl PCR sample
- 3µl dH₂O
- 2.5µl loading buffer (7 parts water to 3 parts glycerol plus two tracking dyes, bromophenol blue and xylene cyanol, both at 0.25% (w/v)).

In addition, two commonly used markers, PCR marker showing band sizes of 50 – 1000 bp and *Hind*III digested λ-DNA showing band sizes of 125 – 23,130 bp, were also loaded. The gel was run for 1 hour at 100 volts to separate fragments, then visualised under UV light using a gel documentation system (Uvi-pro).

2.4.4.2 PicoGreen dsDNA quantitation kit

PicoGreen quantitation reagent (Molecular Probes, Invitrogen) is an ultrasensitive fluorescent nucleic acid stain for quantifying dsDNA in solution. The stain will not measure single-stranded DNA, RNA or protein contaminants, therefore allowing highly accurate measurement of PCR product concentration as low as 25pg/ml. Therefore, combined with the presence of a single band on the agarose gel, we can be certain that only the DNA sequence of interest is measured.

PicoGreen reagent was diluted to 1:200 from stock in Tris EDTA (TE) buffer (10mM Tris-HCl, 1mM EDTA, pH 7.5) supplied with the kit. The dsDNA standards were prepared in TE buffer according to the manufacturer's instructions, as detailed in table 2.3, and loaded into a black 96 well microtitre plate.

2 µg/ml DNA stock (µl)	TE buffer (µl)	PicoGreen reagent	Final DNA conc in assay (ng/ml)
250	0	250	1000
25	225	250	100
2.5	247.5	250	10
0.25	249.75	250	1
0	250	250	0

Table 2.2 Summary of components required for PicoGreen quantification of dsDNA standards.

The amplified PCR products of unknown concentration, as prepared in section 2.4.3.3, were diluted by adding a 10µl aliquot of PCR product to 90µl sterile dH₂O and also applied to the microtitre plate. A 100µl volume of PicoGreen reagent was then added to each well containing unknown sample to give a final volume of 200µl.

The plate was read using a FL600 fluorescence microplate reader (Bio-tek) and recordings were handled using KC4 software (Thistle Scientific). Fluorescence was measured at excitation and emission wavelengths of 485 and 590, respectively. The concentration of dsDNA in the unknown samples was then measured by direct comparison to the known concentration in the standards.

2.4.4.3 Optimisation of amplification process

In order for amplification of the sequence of interest to be within the linear phase, the volume of cDNA and number of cycles were varied. This was carried out by adding 1-5 μ l cDNA plus 5 μ l specific primer to the reaction buffer, before amplifying for 10, 15, 20, 25 or 30 cycles of the extension program (section 2.4.3.3.2).

For each number of extension cycles carried out, a graph of resultant concentration of PCR product, as measured by PicoGreen (section 2.4.4.2) was plotted against volume of cDNA used. The number of cycles for the optimum program was chosen by selecting the plot which produced a normal sigmoid curve, and from that plot the optimum volume of cDNA was considered to be that which fell within the most linear phase of the plot.

2.5 Riboprobe preparation

DNA fragments generated by PCR amplification of the HIF-1 α sequence, the primer for which is detailed in table 2.1, were obtained by the process described in section 2.4.3.3 then subjected to ligation mediated recombinant plasmid (LMRP) amplification by means of a bacterial cell host, in order to transcribe a single stranded RNA probe complimentary to the HIF-1 α sequence.

By the incorporation of a label into the RNA probe during transcription, detection of consensus HIF-1 α RNA expression within a cell preparation was then possible by means of enzymatic digestion of a substrate and formation of a colour precipitate.

2.5.1 PCR product purification

2.5.1.1 Preparative agarose gel electrophoresis

The HIF-1 α sequence was amplified from cDNA prepared from HUVEC RNA, following the protocol as laid out in section 2.4.3.3. Product size was

then validated using analytical agarose gel electrophoresis (section 2.4.1.1). Preparative agarose gel electrophoresis was used to extract the PCR product from the reaction mixture.

Low melting point (LMP) agarose gel was prepared at 1.8 % concentration (w/v) in 35ml Tris-acetate EDTA (TAE) buffer (40mM Tris-acetate, 1mM EDTA, pH 8.3). The gel was prepared as laid out in section 2.4.4.1, using a preparative comb. The single central well was loaded with 250 μ l consisting of 200 μ l sample and 50 μ l loading dye, before carrying out the electrophoresis and visualising the gel, as described earlier.

Following electrophoresis, a clean blade was used to excise the single band of DNA from the gel. Agarose containing the DNA was then aliquoted into 0.3g portions, and stored in 1.5ml tubes at 4°C for purification of the PCR product from the agarose.

2.5.1.2 WIZARD PCR preps DNA purification system (Promega)

The 1.5ml tubes containing 0.3g agarose prepared in section 2.5.1.1, were transferred to a water bath at 70°C, and incubated until the agarose was completely melted. Purification resin (Promega) was added to each melted agarose slice in a volume of 1ml. The solution was then mixed thoroughly for 20 sec by pipetting and each sample was purified using a vacuum manifold. The minicolumn/syringe barrel assembly supplied with the kit was inserted into the vacuum manifold, and the DNA /resin mix was applied to the syringe barrel. Briefly, a vacuum was applied to draw the mixture into the minicolumn, before immediately breaking the vacuum.

To wash the minicolumn, 2ml of 80% isopropanol was added to the syringe barrel, followed by a replication of the vacuum to draw the isopropanol through the minicolumn. The resin was dried by continuing to draw a vacuum for 30 seconds after the solution was pulled through the minicolumn. The minicolumn was then removed from the barrel to a 1.5ml microcentrifuge tube and centrifuged for 2 minutes at 8000 x g to remove any residual isopropanol. The minicolumn was transferred to a new microcentrifuge tube, and 50 μ l dH₂O applied.

After incubation at room temperature for 1 minute, the minicolumn was centrifuged for 20 seconds at 8000 x g to elute the DNA fragment from the column. The purified DNA was then stored in the microcentrifuge tube at -20°C.

2.5.1.3 Quantification of purified DNA

Quantification of DNA was carried out as for RNA (section 2.4.2), but using the following equation;

Abs₂₆₀ x dilution factor x 50 (Abs₂₆₀ of 1 = 50 µg/ml DNA) = X µg/ml DNA concentration

2.5.2 Ligation mediated recombinant plasmid (LMRP) cloning

Cloning of the PCR product was carried out using the pGEM-T Easy Vector System (Promega), which is a plasmid DNA vehicle into which the PCR product is ligated, enabling the replication of the PCR product upon transformation of a bacterial cell host.

The site of ligation in the plasmid is within the *lacZ* gene coding for the enzyme β-galactosidase, therefore successful ligation will interrupt this gene and prevent production of the enzyme. The plasmid also contains an uninterrupted gene conferring ampicillin resistance to the host cell on transfection. The cloning region of the vector also contains T7 and SP6 polymerase initiation sites allowing 5' or 3' transcription of the cloned insert, respectively, and multiple restriction sites, allowing digestion and release of the cloned insert.

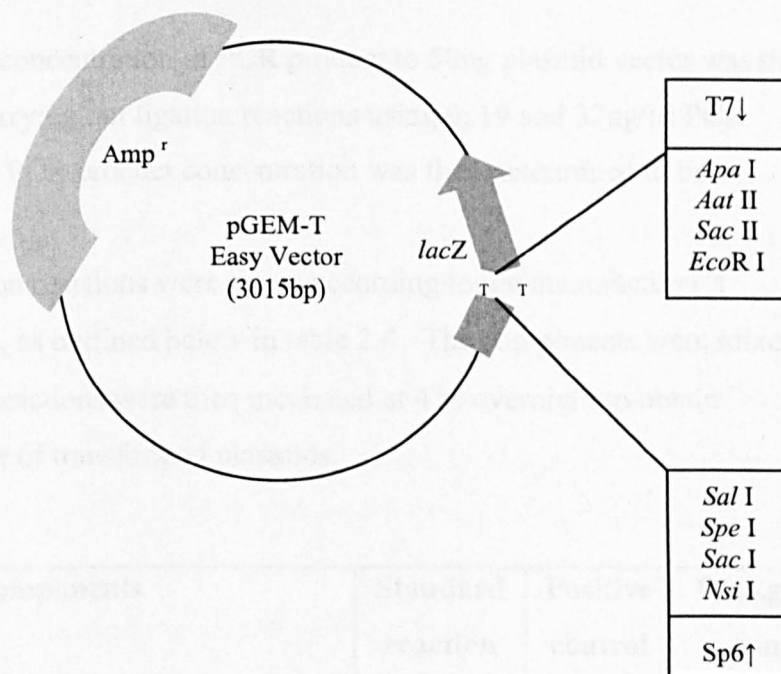


Figure 2.2 pGEM-T Easy Vector circle map. The schematic diagram shows the location of the intact ampicillin resistance gene (*Amp^r*) and the *lacZ* sequence which codes for the enzyme β -lactamase. The *lacZ* gene contains the PCR product insertion site, and therefore is disrupted by ligation. Single 3' terminal thymidines added to both ends at the insertion site greatly improves the efficiency of ligation by providing a compatible overhang for PCR products. The cloning region of the vector contains recognition sites for multiple restriction enzymes, including *Apa* I near the T7 RNA polymerase transcription initiation site, and *Sal* I near the SP6 RNA polymerase transcription initiation site, allowing for release of the cloned insert by enzymatic digestion (as adapted from pGEM-T Easy Vector Technical Manual, Promega 1999).

2.5.2.1 PCR product ligation into pGEM-T Easy Vector (Promega)

The sequence to be cloned was amplified by PCR as described in section 2.4.3.3, followed by quantitation and purification (sections 2.4.4.1 and 2.5.2, respectively).

Optimum concentration of PCR product to 50ng plasmid vector was then established, by carrying out ligation reactions using 6, 19 and 32ng/ μ l PCR product. Optimal PCR product concentration was then determined to be 32ng/ μ l.

All ligation reactions were set up according to the manufacturer's recommendations, as outlined below in table 2.4. The components were mixed by pipetting and reactions were then incubated at 4°C overnight to obtain maximum number of transformed plasmids.

Components	Standard reaction	Positive control	Background control
2X Rapid Ligation Buffer	5 μ l	5 μ l	5 μ l
pGEM-T Easy Vector (50ng)	1 μ l	1 μ l	1 μ l
PCR product (for 32ng/ μ l)	X μ l	-	-
Control insert DNA	-	2 μ l	-
T4 DNA Ligase	1 μ l	1 μ l	1 μ l

Table 2.3. Components contained in the pGEM-T Easy Vector kit (Promega). Proportions required for the PCR product ligation reaction are as recommended by the manufacturer.

2.5.2.2 Bacterial cell transformation

Tubes containing the ligation reactions were briefly centrifuged to collect contents at the bottom. A 2 μ l volume of each ligation reaction was then added to separate 1.5ml tubes on ice. Another tube was then set up on ice with

0.1ng uncut plasmid for determination of transformation efficiency of the competent cells.

Vials containing the bacterial strain *Escherichia coli* (*E-coli*) JM109 high efficiency competent cells (Promega) were removed from -70°C storage and placed on ice until thawed. The cells were then mixed by gentle agitation of the tubes. Aliquots of 50µl of cells were transferred to the tubes for standard, positive control and background ligation reactions, and 100µl was removed for determination of transformation efficiency.

Tubes containing cells plus the ligation products (section 2.5.2.1) were gently agitated to mix, and placed on ice for 20 minutes. The tubes were then transferred to a water bath at exactly 42°C, in order to heat-shock the cells thus allowing the plasmid vectors to permeate the cell membrane. Tubes were then immediately returned to ice for 2 minutes. At room temperature, SOC growth medium (2% Bacto-tryptone, 0.5% Bacto-yeast extract, 10mM NaCl, 2.5mM KCl, 20mM Mg²⁺, 20mM glucose) was added in 950µl aliquots to the ligation reactions, and 900µl to the tube containing the cells transformed with uncut plasmid. All reactions were then incubated for 1.5 hours at 37°C with shaking at 150 x g.

2.5.2.3 IPTG/X-Gal screening of transformed bacteria

Transformation efficiency was evaluated by the process of blue-white colony screening. Cells containing recombinant plasmid vector were unable to metabolise the synthetic substrate of β-galactosidase, X-Gal (Promega), which produces a blue colour on cleavage, due to the disruption of the *lacZ* gene. Therefore, cells containing an untransformed plasmid will appear blue and those containing transformed plasmid remain white.

To ensure that only the cells containing the plasmid are able to grow, the antibiotic ampicillin is included in the growth medium, as the plasmid confers ampicillin resistance which is naturally absent from these cells.

Two culture plates containing Luria-Bertani (LB) agar (1.5% agar, 1% Bacto-tryptone, 0.5% Bacto-yeast extract, 0.5% NaCl, pH 7.0)/ampicillin (100µg/ml)/ IPTG (0.5mM)/X-Gal (80µg/ml) were prepared for each reaction,

plus two plates for determining transformation efficiency. Aliquots of 100µl of each transformed culture was spread on duplicate plates. For the transformation control (transformed with 0.2µg/µl pAMP plasmid, which is also ampicillin resistant), a 1:10 dilution with SOC medium was used for plating, owing to an expectation of high colony number. The plates were then incubated overnight at 37°C.

2.5.2.4 Plasmid Purification Midi Kit (Qiagen)

A single white colony was picked from a freshly streaked selective plate and used to inoculate a starter culture of 2-5ml LB medium also containing ampicillin. The medium containing the colony was incubated for approximately 8 hours at 37°C with vigorous shaking at 300 x g. The starter culture was then inoculated into 50ml fresh selective LB medium, and grown at 37°C for 12-16 hours with vigorous shaking at 300 x g.

Plasmid purification was carried out using a commercially available kit (Qiagen) in which all buffers and details of their composition were supplied. The bacterial cells were harvested by centrifugation at 6000 x g for 15 minutes at 4°C prior to addition of 4ml of resuspension buffer (50mM Tris-HCl, 10mM EDTA, 100µg/ml RNase A, pH8.0). A 4ml volume of lysis buffer (200mM NaOH, 1% sodium dodecylsulphate (SDS)) was then added and mixed gently but thoroughly by inverting 4-6 times before incubating at room temperature for 5 minutes. Chilled neutralisation buffer P3 (3M potassium acetate, pH 5.5) was subsequently added in 4ml volume and mixed immediately by inverting 4-6 times, and incubated on ice for 15 minutes. The solution was centrifuged at 15,000 x g for 30 minutes at 4°C, before removing the supernatant containing plasmid DNA. A QIA-tip (Qiagen) was equilibrated by applying 4ml equilibration buffer (750mM NaCl, 50mM MOPS, 15% isopropanol, 0.15% Triton-X100, pH 7.0), and allowing the column to empty by gravity flow. Next, the supernatant was applied to the QIA-tip and allowed to enter the resin by gravity flow. The QIA-tip was subsequently washed with 2 x 10ml of wash buffer QC (1M NaCl, 50mM MOPS, 15% isopropanol, pH 7.0) before eluting

DNA with 5ml elution buffer QF (1.25mM NaCl, 50mM MOPS, 15% isopropanol, pH 7.0).

The DNA was precipitated by adding 3.5ml (0.7 volumes) isopropanol at room temperature to the eluted DNA, mixing and centrifuging immediately at 15,000 x g for 30 min at 4°C before carefully decanting the supernatant.

The DNA pellet was washed with 2ml 70% ethanol at room temperature, and centrifuged at less than 15,000 x g for 10 min. The pellet was allowed to air dry for 5-10 minutes, before reconstituting in 10µl TE buffer. DNA concentration in ng/µl was then quantified using a spectrophotometer at 260nm wavelength, as detailed in section 2.5.1

2.5.2.5 Restriction digest of plasmid DNA

The plasmid vector DNA purified from the bacterial cell culture was then restricted at two sites using enzymes *ApaI* and *SalI* (Promega), which cut cDNA near the SP6 and T7 restriction sites respectively, located at either side of the ligated PCR product. A double digest using both enzymes was performed in order to remove the insert DNA from the plasmid. The following components were contained within a commercially available kit (Promega) and mixed in a 0.5ml sterile tube, in accordance with the manufacturers instructions;

Sterile water	16.3µl
10 x Restriction enzyme buffer (60mM Tris-HCl pH 9.7, 1.5M NaCl, 60mM MgCl ₂ , 10mM DTT)	2.0µl
Acetylated bovine serum albumin (BSA), 10µg/µl	0.2µl
cDNA (plasmid DNA) 1µg/µl	1.0µl
<i>ApaI</i> , 10µg/µl	0.5µl
<i>SalI</i> , 10µg/µl	0.5µl

The components were mixed gently by pipetting, then the tubes were placed in a thermocycler, and incubated for 1 hour at 37°C enhancing enzyme activation followed by 10 minutes at 70°C to promote enzyme denaturation.

The restricted samples were run on an analytical agarose gel, as detailed in section 2.4.4.1, along with a single digest ie; *ApaI* or *SalI* alone and unrestricted plasmid DNA, for comparison. The plasmid contained only one site at which *ApaI* or *SalI* could cut, as detailed below. These flanked the ligation site, therefore allowing the portion of the vector containing the insert to be removed.

T7 (*Apa* 1) recognition sequence:

5'...G GGCC↓C...3'

3'...C ↑CCGG G...5'

Sp6 (*Sal* 1) recognition sequence:

5'...G↓TCGA C...3'

3'...C AGCT↑G..5'

A preparative agarose gel (section 2.5.1.1) was used to isolate and purify the plasmid after linearisation by single restriction enzyme digest as previously described, and cut out of the gel for further analysis.

2.5.3 RNA labelling with digoxigenin-uridine-5'-triphosphate (DIG-UTP) by *in vitro* transcription with SP6 and T7 RNA polymerases (Roche)

For the generation of RNA probes utilizing *in vitro* transcription, the sequence to be detected, in this case HIF-1 α , was cloned into a vector containing phage transcription promoters that can initiate transcription in the presence of the corresponding RNA polymerase.

When two different phage transcription promoters are placed on either side of the polylinker cloning sites of the vector in opposite orientations, it is possible to selectively transcribe sense and anti-sense RNA probes. Transcribing only one strand at a time prevents re-annealing of complimentary strands during hybridization. By inclusion of either labeled or unlabeled nucleotides, it is possible to make labeled or unlabeled probes for detection of specific RNA.

A digoxigenin (DIG)-labelled riboprobe consensus to the ligated PCR

product was synthesised from an RNA polymerase reaction incorporating a DIG label directed by the T7 or SP6 initiation sites contained in the pGEM-T vector, producing sense or antisense riboprobes, respectively. This assay was conducted using a commercially available kit. Antisense probes were then be used to detect complementary sequences within tissue or cells, with the sense probe acting as a control.

2.5.3.1 Standard transcription assay

One microgram of purified template DNA, from the single restriction digest outlined in section 2.5.3.2, or 4µl control DNA (Promega) was added to a sterile, RNase free tube, before adding DEPC treated water to a final volume of 13µl.

The standard transcription assay was carried out using a commercially available T7/SP6 RNA polymerase kit (Roche), the exact content of which is included in the manufacturers instructions. The following components were then added on ice, as recommended by the manufacturer;

10 X DIG-UTP labelling mixture	2µl
10 X transcription buffer	2µl
RNase inhibitor	1µl
RNA polymerase SP6 or T7	2µl

The contents of the tube were then mixed gently and centrifuge briefly, prior to incubating for 2 hours at 37°C. After this time the reaction was terminated by adding 2µl of 0.2M EDTA (pH 8). The resulting DIG labelled RNA transcripts were then stored at -20°C.

Based on the cDNA map information provided by the manufacturer of the pGEM-T vector (Promega), the anti-sense probe was that transcribed from the *SaII* linearised plasmid DNA with SP6 polymerase (*SaII*/SP6), and the *ApaI*/T7 transcript was the sense control.

2.5.3.2 Dot blot determination of labelling efficiency

The samples of T7 or SP6 transcribed RNA were quantified by applying 1 μ l aliquots directly on to a strip of positively charged nylon membrane (Hybond). To determine concentration of the sample, a series of dilutions of DIG-labelled control RNA (supplied with the kit) were also applied in 1 μ l aliquots, as indicated in table 2.5. Dilution and content of tubes 1-7 are as specified in the manufacturers instructions.

RNA immobilised on the membrane was then fixed using a short wavelength (254nm) UV light crosslinker (Uvi-pro) at 12 Joules for 60 seconds, prior to enzyme immunoassay detection with anti-digoxigenin-alkaline phosphatase (DIG-AP) and the chemiluminescent substrate CSPD, detailed in 2.5.3.3.

Assay Tube	RNA(μ l)	From tube supplied with kit	RNA dilution buffer (μ l)	Dilution	Final Concentration
1	-	dilution of probe and unlabeled control RNA	-	-	10 ng/ μ l
2	2	1	18	1:10	1 ng/ μ l
3	2	2	198	1:100	10 pg/ μ l
4	15	3	35	1:3.3	3 pg/ μ l
5	5	3	45	1:10	1 pg/ μ l
6	5	4	45	1:10	0.3 pg/ μ l
7	5	5	45	1:10	0.1 pg/ μ l
8	5	6	45	1:10	0.03 pg/ μ l
9	5	7	45	1:10	0.01 pg/ μ l
10	0	-	50	-	0

Table 2.4 Dilution of control RNA of known concentration. As specified in the manufacturer's guidelines.

2.5.3.3 DIG Luminescent Detection Kit (Roche)

DIG-based chemiluminescence was used to detect RNA. All solutions are as specified in the manufacturers instructions (Roche).

The hybridised probes were immunodetected with anti-DIG-AP, which are Fab fragments conjugated to alkaline phosphatase, and visualised with the chemiluminescence substrate CSPD.

Nylon membrane containing the fixed RNA sample was briefly washed (1-5 min) in washing buffer (0.1M maleic acid, 0.15M NaCl, pH 7.5, 0.3% Tween). The following incubations were then performed at 37°C with constant, gentle agitation;

- 30 minutes in 100ml blocking solution (1% (w/v) blocking reagent (Roche), 0.1M maleic acid, 0.15M NaCl, pH 7.5)
- 30 minutes in 20ml DIG-AP antibody solution (75 mU/ml anti-DIG-AP, 1% (w/v) blocking reagent, 0.1M maleic acid, 0.15M NaCl, pH 7.5)
- 2 x 15 minutes in 100ml washing buffer
- Equilibrate 2-5 minutes in 20ml detection buffer (0.1M Tris-HCl, 0.1M NaCl, pH 9.5)

The membrane was then placed with the RNA side facing up on one sheet of a plastic film folder and 2ml diluted CSPD solution was applied. The membrane was immediately covered with the second sheet of the folder to spread the substrate evenly and without air bubbles. The membrane was then incubated for 5 minutes at 15 - 25°C, before squeezing out the excess liquid and sealing the folder. The damp membrane was incubated for a further 5-15 minutes at 37°C, to enhance the luminescent reaction.

Enzymatic dephosphorylation of CSPD by alkaline phosphatase then led to light emission at a maximum wavelength of 477nm which was recorded on chemiluminescent detection film (Roche), as detailed in section 2.5.3.4

2.5.3.4 Exposure and development of chemiluminescent film

All steps were carried out at room temperature in a designated dark room. The CSPD treated membrane was exposed to chemiluminescent detection film for 15 - 25 minutes at room temperature. Multiple exposures were taken to achieve the desired signal strength. After exposure of the film, it was developed and fixed according to the manufacturers' directions as follows;

- 4 minutes in developer fluid (Kodak)
- 4 minutes in dH₂O
- 4 minutes in fixing fluid (Fisons)

The developed films were then rinsed thoroughly under running water and allowed to dry before inspection. A light box was used to aid visualisation of the resulting image.

2.5.4 RNA labelling with biotin by *in vitro* transcription with SP6 and T7 RNA polymerases

2.5.4.1 MAXIscript *in vitro* transcription kit (Ambion)

LMRP preparation was carried out as before, in sections 2.5.1 to 2.5.3. *In vitro* transcription was employed in order to produce an anti-sense RNA probe, by using *Sal* 1 to linearise the recombinant plasmid and SP6 directed polymerisation.

Using the MAXIscript protocol as detailed in the manufacturers instructions, components were mixed to produce sample, control and marker set transcripts, as detailed in table 2.6.

Component	LMRP reaction	Control reaction	Marker
Nuclease free water	Up to 20 μ l	Up to 20 μ l	Up to 20 μ l
<i>Apa</i> 1 restricted LMRP DNA template	1 μ g	-	-
pTRI-Actin-mouse control DNA template	-	1 μ g	-
Century Marker Plus Template Set (Ambion)	2 μ l	2 μ l	0.5 μ g
10X transcription buffer	1 μ l	1 μ l	1 μ l
10mM ATP	1 μ l	1 μ l	1 μ l
10mM CTP	1 μ l	1 μ l	1 μ l
10mM GTP	2 μ l	2 μ l	2 μ l
10mM UTP			
SP6 RNA polymerase			

Table 2.5 SP6 directed in vitro transcription of LMRP RNA. The anti-sense probe was compared with a 'no transcription' reaction control (pTRI-Actin-mouse control DNA template contains no SP6 polymerase promoter site) and Century Marker Plus Template Set reaction (Ambion) producing 100-1000 nucleotide RNA molecular weight markers.

2.5.4.2 BrightStar psoralen-biotin nonisotopic labelling kit (Ambion)

The transcripts produced in section 2.5.4.1 were then labelled with a 5' terminal biotin, linked via a planar psoralen conjugate which has high affinity for nucleic acid, using the BrightStar psoralen-biotin nonisotopic labelling kit (Ambion) following the manufacturers instructions.

Concentrations of 0.5-50ng/ μ l RNA transcript were denatured by heating at 100°C for 10 minutes then applied to a clean untreated 96 well plate on ice. In a dimly lit room, the vial containing psoralen-biotin dissolved in dimethylformamide was briefly centrifuged, and 1 μ l added to each sample in 96 well plate and mixed. The samples were irradiated with 365nm UV light for 45 minutes to activate biotinylation by means of long wavelength UV light catalysed covalent binding of psoralen to nucleic acids. Samples were then transferred to sterile RNase free microfuge tubes, and made up to 100 μ l volume with TE buffer.

Dot blot analysis of labeling efficiency, as described in section 2.5.3.2, was performed using serial dilutions of known concentration labelled control DNA (1ng – 10fg) along with the transcripts from section 2.5.5.1. The biotinylated nucleic acids were then stored at -20°C short term or -80°C long term.

2.5.4.3 BrightStar BioDetect detection kit (Ambion)

Detection of biotinylated nucleic acids immobilised on nylon membrane was then carried out. All steps were performed at room temperature with gentle agitation using commercially available buffers supplied with the kit.

The membrane was washed 2 x 5 min in wash buffer before incubating for 2 x 5 min in blocking buffer. An extended incubation was then carried for 30 min in blocking buffer. The biotin label was detected firstly by binding to strepavidin-alkaline phosphatase (strep-AP), which will bind to the biotin, was diluted in blocking buffer (10 μ l/10ml) and mixed gently before applying to the membrane and incubated for 30 min. The membrane was exposed to a further 10 min in blocking buffer prior to 2 x 2 min incubations in assay buffer to equilibrate the membrane.

Five millilitres of the chemiluminescent substrate CDP-star solution was then applied and incubated for 5 min. Cleavage of CDP-star by AP bound to biotin produced chemiluminescence which could be detected on film. The membrane was then quickly blotted and wrapped in a single layer of plastic.

CDP-star reached peak emission after 2-4 hours, and exposure times were varied in order to detect optimum signal. Development and fixation of the exposed film was then carried out, as detailed in section 2.5.3.4.

2.6 *In situ* hybridisation (ISH)

A DIG-labeled single stranded RNA probe, synthesised as described in section 2.5.3, complementary to HIF-1 α was used to probe whole cell HUVEC preparations for expression of HIF-1 α RNA

2.6.1 Fixation of cells grown on glass slides

HUVEC were grown on glass slides as detailed in section 2.2.2.3.2. After treatment, the slides were removed from the incubator, and washed 3 x 5 min in DEPC treated PBS. Cells were then fixed with 4% paraformaldehyde (PFA) for 10 minutes in a fume cupboard, before further washing in PBS for 2 x 5 min. Cells were dehydrated in 70% ethanol at 4°C for 30 min then washed 2 x 5 min on ice before incubating with 4% PFA/0.2% Triton X for 10 min on ice. Another washing step was carried out, then incubation with 50% formamide/2 x standard saline citrate (SSC) buffer (0.9% NaCl, 0.4% sodium citrate) (50 μ l/well) for 10 min at 55°C.

2.6.2 Hybridisation of antisense RNA probe

The *in situ* hybridisation (ISH) mix was prepared fresh in a 5ml volume prior to hybridisation, by mixing components as detailed below;

Chemical	Final concentration in mix
2.5ml deionised formamide	50%
0.09g NaCl	0.3M
100µl Tris HCl (1M, pH 7.5)	20mM
50µl EDTA (0.5M, pH 8)	5mM
50µl NaH ₂ PO ₄ (1M)	10mM
1ml dextran sulphate	10%
1ml 5 x Derrhardt's reagent (1% w/v Ficoll, 1% w/v polyvinylpyrrolidone, 1% w/v BSA, 800µl denatured salmon sperm, 400µl 10% SDS, 2.4ml 20XSSC)	1 x
250µl tRNA (12.5mg/ml)	0.5mg/ml

Table 2.6 Components of ISH mix buffer

The slides were pre-hybridised in the ISH mix for 1h, before incubating the cells with DIG-labeled antisense probe, transcribed from LMRP cut with *Sal* I and polymerised by SP6 polymerase, the preparation of which is detailed in section 2.5, diluted 1 in 40 in ISH mix. The slides were then covered with parafilm cut to well sized coverslips and incubated overnight at 55°C.

2.6.3 Washing and RNase digestion of unbound probe

After overnight incubation, slides were incubated in 5 x SSC for 30 min at 55°C to allow the coverslips to come off. Fifty percent formamide/2 x SSC

(50µl/well) was added for 30 min at 55°C. Slides were then washed twice in ISH wash buffer at 37°C.

RNase digestion of unbound single-stranded probe was achieved by adding 2µl RNase (20µg/µl) to 998µl wash buffer (0.4M NaCl, 10mM Tris-HCl, 5mM EDTA) and applying 100µl/well. This was then allowed to incubate for 30 min at 37°C, prior to washing 2 x 10 min in 2X SCC at the same temperature.

2.6.4 Immunological detection of bound probe

Prior to immunological detection, the slides were equilibrated in wash buffer (0.1M Tris-HCl, 0.15 NaCl, pH 7.5), then incubated for 30 min in blocking buffer (5% bovine serum albumin (BSA), 0.1M Tris-HCl, 0.15 NaCl, pH 7.5) with agitation. The DIG-AP conjugate was prepared 1:500 in blocking buffer, and 50µl/well added before incubating in a humidified chamber at room temperature for 30 minutes. Slides were then washed 2 x 15 min in wash buffer before equilibrating in substrate buffer (0.1M Tris HCl, 0.1M NaCl, 0.05M MgCl₂).

The colorimetric AP-substrate NBT/BCIP (18.75 mg/ml nitro blue tetrazolium chloride, 9.4 mg/ml 5-bromo-4-chloro-3-indolylphosphate) which was purchased as a ready made stock solution (Roche) was diluted by adding 200µl stock solution to 10ml substrate buffer. The dilute NBT/BCIP solution was then applied 100µl/well and the slides incubated in a humidifier box in the dark for up to 1 hour, until a purple/blue coloured precipitate was detected. At this point, the reaction was halted by washing the slides in distilled water. The slides were then allowed to dry, before mounting with Aquamount (DAKO) and applying coverslips. Samples were then ready to be observed by light microscopy.

2.7 Ribonuclease protection assay (RPA)

The ribonuclease protection assay (RPA) probed whole cell RNA extracted from treated cells using the procedure detailed in section 2.4.1. A biotin-labelled probe complementary to HIF-1 α RNA, synthesised as described in section 2.5.5, was mixed with the whole cell RNA in solution to allow binding of the probe to its consensus sequence.

2.7.1 Hybridisation of probe and sample RNA

An RPA III kit (Ambion) was used to hybridise biotin-labelled RNA probe to RNA from treated cells. For the hybridisation reaction, a probe concentration of 150 -600pg per10 μ g total RNA was used. For each reaction, sample and probe were mixed in sterile RNase free microfuge tubes. Two control tubes were also included, containing the same concentration of probe plus 10 μ g yeast RNA. The probe and sample RNA were co-precipitated, by adjusting conditions to 0.5M ammonium acetate, before adding 2.5 x volume of ethanol and mixing thoroughly. The tubes were then incubated at -20 $^{\circ}$ C for 15 minutes before centrifuging at 12,000 x g at 4 $^{\circ}$ C and discarding the supernatant. The resulting pellet was then resuspended in 10 μ l hybridisation buffer (supplied with kit), vortexed, then centrifuged briefly.

To allow the probe to hybridise to its complementary RNA sequences in the sample RNA, the tubes were incubated overnight at 42 $^{\circ}$ C

2.7.2 RNase digestion of unhybridised probe and sample RNA

To prevent unhybridised single-stranded probe from interfering with the detection of bound probe, it was removed by enzymatic digestion by RNase. RNase recognised and lysed unbound single stranded RNA but not hybridised double-stranded RNA.

The RNase mixture was prepared using the following kit components, as instructed by the manufacturer;

RNase digestion III buffer (supplied with kit) - 150µl/tube
RNaseA/T1 mix (250 units/ml RNase A, 10,000 units/ml RNase T1) - 1.5µl/tube

After briefly centrifuging the hybridisation tubes, 150µl of the RNase mixture was added to each of the sample RNA tubes and to one of the two yeast RNA tubes, to serve as a “no target” control. Tubes were briefly vortexed. Hybridisation buffer alone (minus RNase) was added to the second yeast RNA tube to provide a “no RNase” control for confirmation of probe integrity.

All tubes were incubated at 37°C for 30 minutes before terminating the reaction with 225µl RNase inactivation/precipitation III solution (supplied with kit). The samples were then incubated at -20°C for 15 minutes and microfuged at 10,000 x g for 15 min at 4°C before removing the supernatant.

2.7.3 Separation and detection of protected fragments

The pelleted protected fragments were resuspended in gel loading buffer (95% formamide, 0.025% xylene cyanol and bromophenol blue, 18mM EDTA, 0.2% SDS) then incubated for 3 minutes at 90-95°C. Samples were loaded onto a 5% TBE-urea ready gel (Bio-rad) in a Mini Protean (Bio-rad) vertical gel system. Samples were then electrophoresed for 1h at 250 volts in TBE buffer.

The nucleic acids within the gel were transferred to positively charged nylon membrane (Ambion) by electroblotting for 1h at 250 volts in 0.5 x TBE buffer. The nucleic acids were then immobilised on the membrane by UV crosslinking, before being subjected to chemiluminescent detection following the protocol detailed in section 2.5.5.3.

Chapter 3

HIF-1 α protein expression in a rat model of diabetes

3.1 Introduction

Neuropathy is the most common complication associated with diabetes mellitus, affecting more than half of all patients (Tesfaye *et al.*, 1996).

Hyperglycaemia, which is a fundamental metabolic insult associated with diabetes, contributes greatly to incidence and severity of peripheral neuropathy. Complex interactions between metabolic and vascular factors associated with diabetes appear to affect nerve function through vascular effects (Cameron *et al.*, 2001). Such abnormalities are more severe in endoneurial capillaries than in the epineurium, skin or muscle, indicating interaction between the endoneurium and the neurovasculature to be a strong regulatory factor in the manifestation of hyperglycaemia associated disease (Malik *et al.*, 1993).

A growing body of evidence indicates that the prevalence of tissue hypoxia is associated with the development of diabetic neuropathy (Cameron & Cotter, 1997). The effect of diabetes on endothelial cells may be particularly significant, as increased endothelial cell proliferation in response to hypoxia is in itself a trigger for maintenance of endothelial cell growth (Hudlicka *et al.*, 2002). However, although there is greater impairment of diabetic nerve function with increased ischemia, reversal of hypoxia alone does not result in any significant improvement in nerve function measurements (Veves *et al.*, 1996). Therefore, this may indicate a role for HIF-1 α in the co-operation between the signals of glucose and hypoxia in the diabetic vasculature.

Vascular expression of HIF-1 α has previously been suggested to contribute to the manifestation of diabetic retinopathy (Ozaki *et al.*, 1999; Lukiw *et al.*, 2001). However, despite the initiation of similar responses in the vasculature accompanying the diabetic nerve, expression of HIF-1 α has not been investigated in diabetic neurovasculature.

Therefore, the aim of this study was to determine whether induction of HIF-1 α protein was occurring within the vasculature supplying the sciatic nerve of a streptozotocin (STZ) diabetic rat, and if so, whether the level of expression correlated with duration of disease.

3.2 Materials and methods

Diabetes was induced in groups of rats by administering a 45mg/kg intraperitoneal injection of streptozotocin (STZ). STZ-induction of diabetes was controlled for by saline injection in a separate group of age-matched littermates. The STZ rats were then euthanized 4, 10 and 24 weeks after onset of diabetes, as detailed in section 2.1.1, along with the age-matched controls.

Cryostat sections of sciatic nerve surrounded by skeletal muscle were prepared as in section 2.1.2, and mounted on glass slides. Sections of diabetic and non-diabetic age-matched control were subjected to immunohistochemical detection of HIF-1 α protein with HIF-1 α monoclonal mouse primary antibody, using the avidin-biotin complex/alkaline phosphatase procedure (section 2.3.1.2).

Immunodetected slides were subsequently counterstained and mounted before viewing under light microscopy. Specificity of the biotinylated secondary antibody was controlled for using IgG1 as the primary antibody control and TBS alone as the buffer control.

For each test group, n=3 was analysed, and in all cases images shown are representative of that group.

3.3 Results

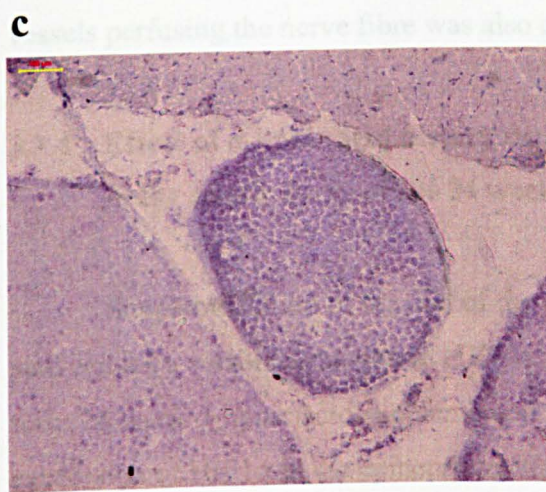
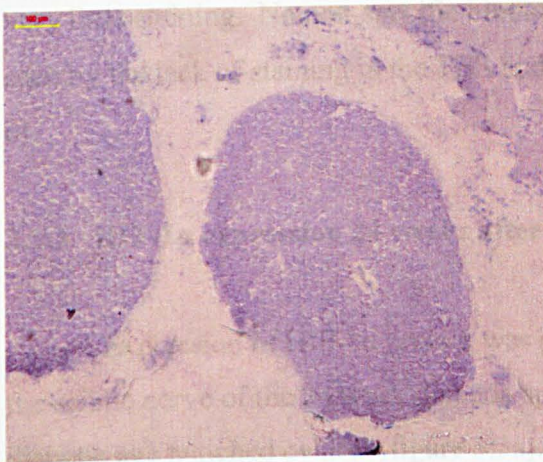
3.3.1 HIF-1 α expression 4 weeks after STZ-induction of diabetes

Only small localised areas of intense HIF-1 α staining were evident within the vasculature surrounding the sciatic nerve in the diabetic sample after 4 weeks of disease (figure 3.1d). At this time point, very little difference in HIF-1 α protein expression was seen between STZ and control samples (figures 3.1b and d, respectively). No staining of vessels was observed within the nerve fibre of STZ or control samples at 4 weeks, and no non-specific binding was detected, as shown by the lack of staining in the IgG1 control antibody samples (figures 3.1a and c).

Figure 3.1. Immunohistochemical detection of HIF-1 α in the sciatic nerve vasculature of 4 week control and diabetic rats. For the diabetic and non-diabetic control, rats were given an intraperitoneal injection of 45mg/g streptozotocin or saline, respectively. Four weeks after onset of diabetes in the STZ rats, both the treated and age-matched controls were euthanized. Sciatic nerve sections were subsequently mounted on slides for immunohistochemical detection of HIF-1 α protein expression. The photomicrographs are; **a)** non-diabetic control treated with IgG1 as antibody control. **b)** non-diabetic treated with HIF-1 α antibody. **c)** diabetic treated with IgG1 as antibody control. **d)** diabetic treated with HIF-1 α antibody. Photomicrographs are representative of 3 separate experiments, and the micron bar in the top left hand corner of each photomicrograph represents 100 μ m.

3.3.2 HIF-1 α expression 10 weeks after STZ-induction of diabetes

A large accumulation of HIF-1 α protein confined to the vasculature surrounding the sciatic nerve was detected in the 10 week diabetes sample. Staining was seen to be particularly intense in the capillaries providing blood to the sciatic nerve (figure 3.29). This staining was considerably more intense than that seen in both the 4 week diabetes sample (figure 3.18) and the 10 week diabetic control (figure 3.2c) which again displayed



3.3.2 HIF-1 α expression 10 weeks after STZ-induction of diabetes

A large accumulation of HIF-1 α protein confined to the vasculature surrounding the sciatic nerve was detected in the 10 week diabetic sample. Staining was seen to be particularly intense in the capillaries providing blood to the sciatic nerve (figure 3.2f). This staining was considerably more intense than that seen in both the 4 week diabetic sample (figure 3.1d) and the 10 week diabetic control (figure 3.2c) which again displayed very little staining. No non-specific binding of the secondary antibody was evident, as seen by the lack of staining in the TBS and IgG1 control samples (figures 3.2a, b, d and e).

3.3.3 HIF-1 α expression 24 weeks after STZ-induction of diabetes

Expression of HIF-1 α protein was still abundant in the vasculature surrounding the sciatic nerve of the 24 week diabetic specimen (figure 3.3c) compared to the non-diabetic age matched control (figure 3.3a). At the 24 week time point, expression in the vessels perfusing the nerve fibre was also evident for the first time (figure 3.3d).

3.3.4 Effect of α -lipoic acid dietary supplementation on the level of HIF1 α protein in the sciatic nerve of the 24 week diabetic rat.

Supplementation of the diet of the STZ-diabetic rat with the antioxidant α -lipoic acid caused a visible reduction in HIF-1 α protein expression at 24 weeks. Samples taken from 24 week α -lipoic acid supplemented STZ-diabetic rats revealed a decrease in the expression of HIF1 α in the epineurium (figure 3.4c) compared to the unsupplemented STZ- diabetic animals (figure 3.4b).

Figure 3.2. Immunohistochemical detection of HIF-1 α in the sciatic nerve vasculature of 10 week control and diabetic rats. For the diabetic and non-diabetic control, rats were given an intraperitoneal injection of 45mg/g streptozotocin or saline, respectively. Ten weeks after onset of diabetes in the STZ rats, both the treated and age-matched controls were euthanized. Sciatic nerve sections were subsequently mounted on slides for immunohistochemical detection of HIF-1 α protein expression. The photomicrographs are; **a)** non-diabetic treated with TBS as buffer control. **b)** non-diabetic treated with IgG1 as antibody control. **c)** non-diabetic treated with HIF-1 α . **d)** diabetic treated with TBS as buffer control. **e)** diabetic treated with IgG1 as antibody control **f)** diabetic treated with HIF-1 α . Photomicrographs are representative of 3 separate experiments, and the micron bar in the top left hand corner of each photomicrograph represents 100 μ m.

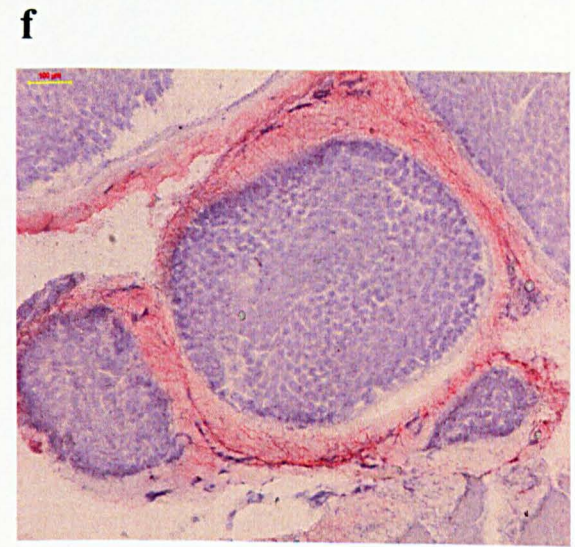
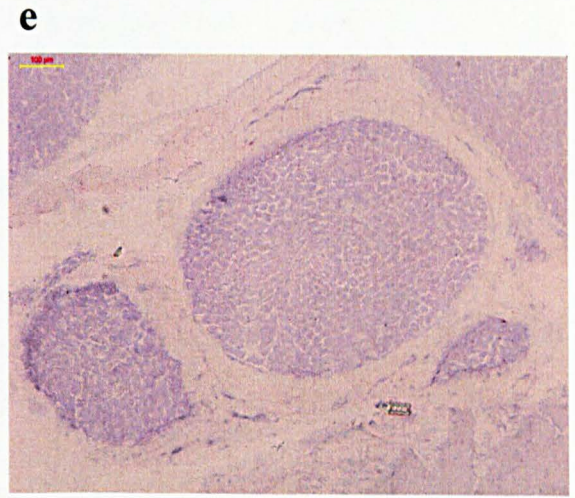
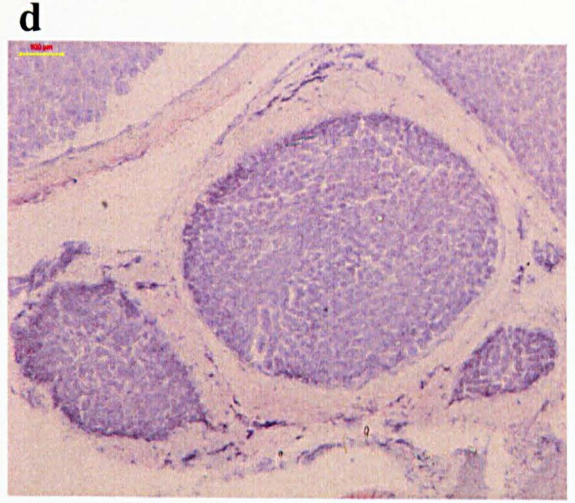
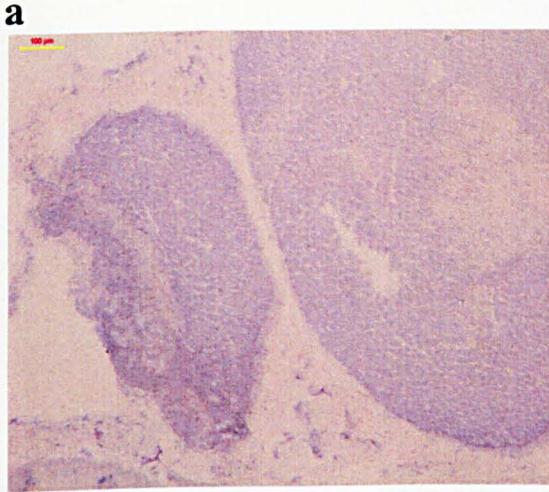
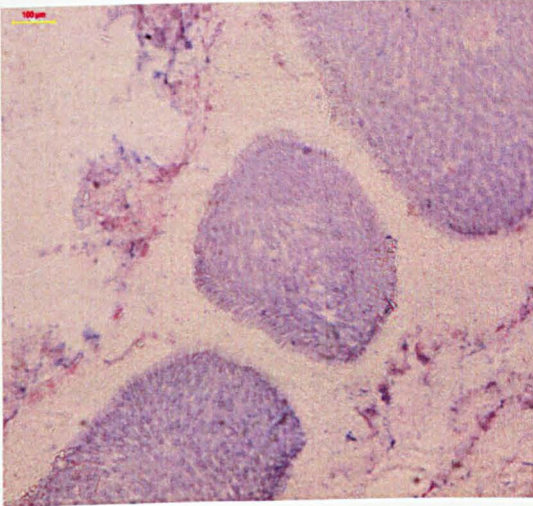
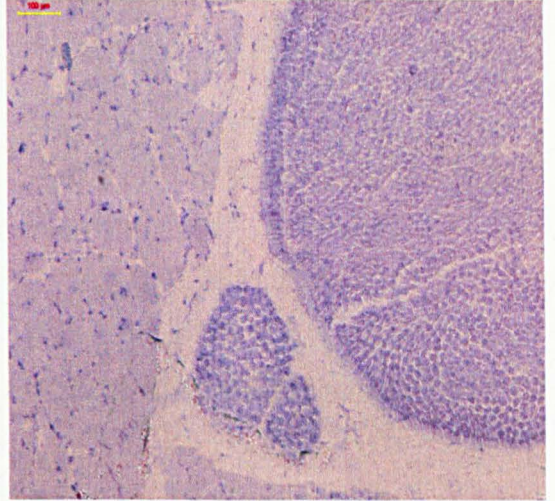


Figure 3.3. Immunohistochemical detection of HIF-1 α in the sciatic nerve vasculature of 24 week control and diabetic rats. For the diabetic and non-diabetic control, rats were given an intraperitoneal injection of 45mg/g streptozotocin or saline, respectively. Twenty-four weeks after onset of diabetes in the STZ rats, both the treated and age-matched controls were euthanized. Sciatic nerve sections were subsequently mounted on slides for immunohistochemical detection of HIF-1 α protein expression. The photomicrographs are; **a)** non-diabetic nerve and vasculature treated with HIF-1 α antibody. **b)** diabetic nerve and vasculature treated with negative antibody control IgG1. **c & d)** diabetic nerve and vasculature treated with HIF-1 α antibody, the latter showing intense staining within the nerve fibre. The micron bar in the top left hand corner of each micrograph represents 100 μ m.

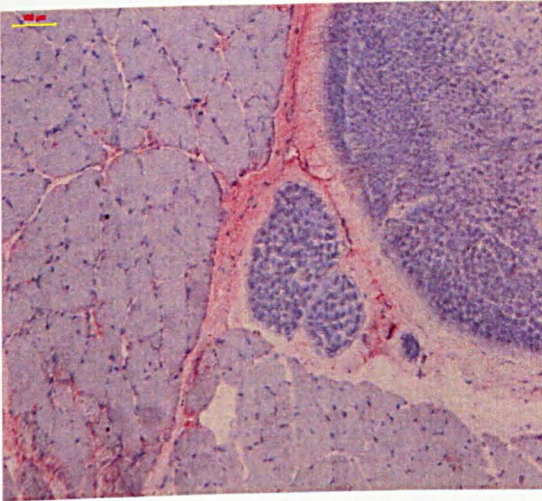
a



b



c



d

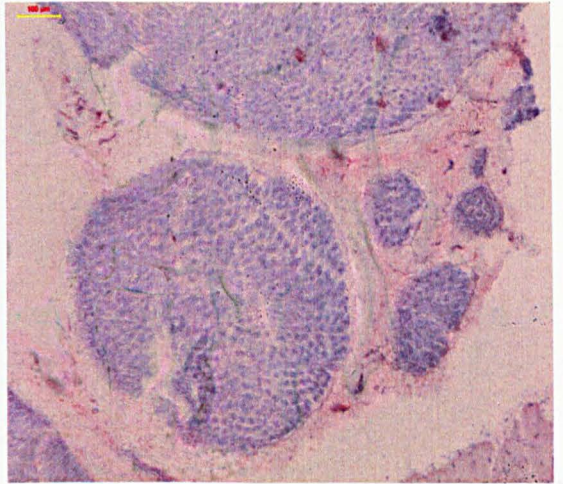
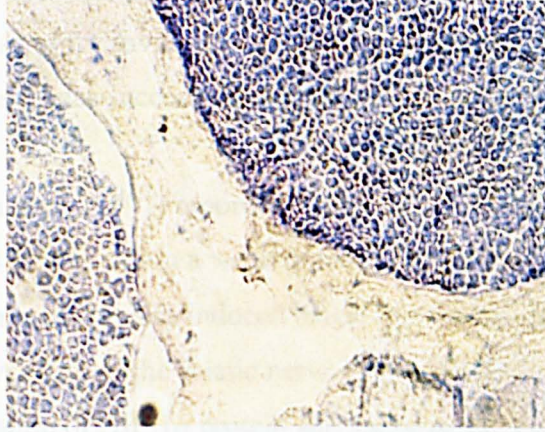


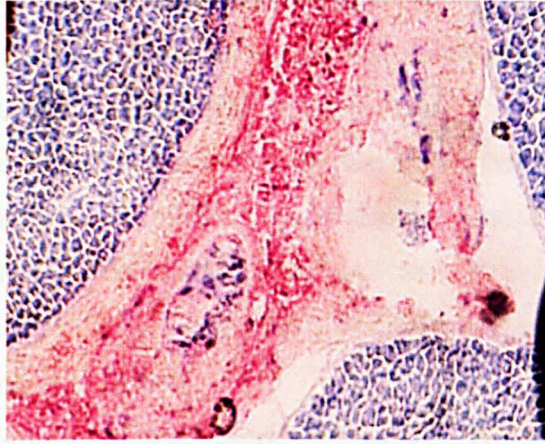
Figure 3.4. Effect of α -lipoic acid dietary supplementation on the level of HIF1 α protein in the sciatic nerve of the 24 week diabetic rat. Immunohistochemical detection of HIF-1 α protein revealed a significant decrease in the expression of HIF1 α in the epineurium of the diabetic animals treated with α -lipoic acid (c) compared to the non-treated diabetic animals (b). A negative control sample indicates the specificity of the HIF1 α staining (a). All photomicrographs are magnification of original X 420.

3.4 Discussion

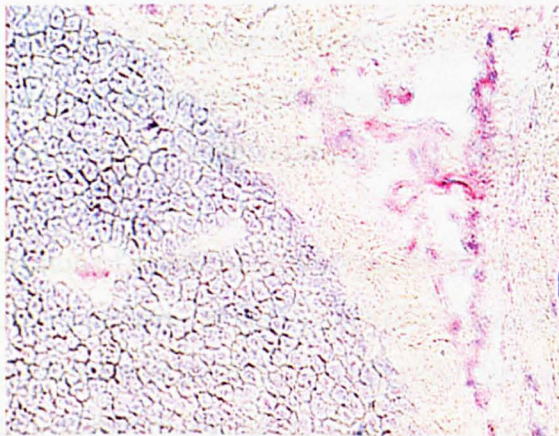
a



b



c



3.4 Discussion

This phase of the investigation has demonstrated the chronic expression of HIF-1 α within the vasculature accompanying the sciatic nerve of a rat model of experimental diabetes.

Cameron *et al.* (1991) reported that in STZ diabetic rats, sciatic nerve blood flow is reduced by 40 – 50% within a week or two of diabetes induction, leading to endoneural hypoxia due to hyperglycemia-induced blood flow reduction and subsequent decrease in the conduction velocity of the sciatic nerve (Cameron & Cotter, 1992). However, hypoxic stabilisation of HIF-1 α protein and subsequent DNA binding of target genes is a very rapid process (Jewell *et al.*, 2001) therefore the delayed induction of HIF-1 α which was observed at 10 and 24 weeks, may suggest that high glucose is somehow interfering with the upregulation of HIF-1 α under hypoxic conditions, pushing back the threshold at which hypoxia is able to induce HIF-1 α expression.

Vascular complications in diabetes are almost certainly predated by endothelial dysfunction (Wautier *et al.*, 1996). One mechanism that has been implicated, is reduced nitric oxide synthase (NOS) activity (Stevens *et al.*, 1994) caused by increased oxidative stress (Baynes, 1991; Ceriello *et al.*, 1993) resulting in impaired vasodilator response (Rodriguez-Manas *et al.*, 1998).

Endothelium-dependent vasodilation of arterioles that provide circulation to the sciatic nerve is impaired by diabetes (Terata *et al.*, 1999). However, in contrast to larger vessels in the rat where acetylcholine-induced dilation is mediated solely by NO (Sobey & Faraci, 1997), dilation of arterioles adjacent to the sciatic nerve is not dependent solely on NO, but involves a combination of endothelial derived factors (Terata *et al.*, 1999) which may potentially include endothelium-derived hyperpolarising factor (EDHF) and prostacyclin.

The production of reactive oxygen species (ROS) is known to increase in people with poorly controlled diabetes, which is particularly significant for diabetic neuropathy, the etiology of which has a large vascular component (reviewed by Yorek, 2003). This is further enhanced by advanced glycation end product formation and polyol pathway

activation, along with PKC activation and omega-6 essential fatty acid dysmetabolism (reviewed by Cameron *et al.*, 2001).

Antioxidants have been shown to improve neuronal blood flow and motor nerve conduction velocity in diabetic rats (Cameron *et al.*, 1993). Data obtained from STZ rats fed the antioxidant α -lipoic acid as a dietary supplement, revealed visibly reduced accumulation of HIF-1 α protein at 24 weeks diabetes (figure 3.4c). The role of HIF-1 α in the development of diabetes-induced vascular and neural dysfunction may therefore be linked to redox signalling cascades activated in response to hyperglycaemia, and therefore will affect the availability of NO in the endothelium.

To summarise, this chapter showed regulation of HIF-1 α protein expression in the vasculature of a rat model of diabetes, which may demonstrate a level of interference by hyperglycaemia related metabolic events in the induction of HIF-1 α in the diabetic vasculature. Endothelium-dependent vasodilation of arterioles that provide circulation to the sciatic nerve is impaired by diabetes (Terata *et al.*, 1999). Therefore, at this point, it is of interest to employ a vascular endothelial cell line model of diabetes, in order to further the understanding of pathways and mechanisms contributing to the regulation of HIF-1 α within the diabetic vasculature. By having the ability to manipulate the extracellular environment, the potential mechanisms by which oxygen and glucose regulate expression HIF-1 α can then be investigated.

Chapter 4

Evaluation of methods for the detection of HIF-1 α mRNA

4.1 Introduction

Technical advances in the study of molecular genetics are making it possible to study the temporal, spatial, histological and cytological expression of many genes. For this study, evaluation of HIF-1 α mRNA expression in HUVEC exposed to altered glucose and oxygen concentration was undertaken, due to the potential transcriptional regulatory effect this may have on the expression of HIF-1 α protein.

It is widely accepted that HIF-1 α is not regulated at the level of transcription in response to hypoxia alone (Wenger *et al.*, 1997; Ratcliffe *et al.*, 1998). However, various other stimuli do have positive and negative effects on HIF-1 α mRNA (Kim *et al.*, 2002; Kimura *et al.*, 2001; Page *et al.*, 2002; Sandau *et al.*, 2001; Zelzer *et al.*, 1998; Zhong *et al.*, 2000). Little is known about the effect of the combined stimuli of oxygen and glucose on HIF-1 α mRNA expression, therefore determining a method by which this potential transcriptional regulation could be measured was central to the aim of this chapter.

The most established method for detecting nucleic acid concentration is by UV absorbance spectroscopy, as pioneered by Beaven and colleagues in 1955. However, modern technologies are allowing more accuracy and less consumption of precious nucleic acid samples through the use of labelled probes and intercalating fluorochromes, which increase sensitivity and laboratory efficiency due to the high through-put nature of such formats (Ahn *et al.*, 1996).

The various methods have relative advantages and disadvantages. By assessing HIF-1 α mRNA by means of *in situ* hybridisation, ribonuclease protection assay (RPA) and reverse transcriptase polymerase chain reaction (RT-PCR), the suitability of each method will be addressed in terms of sensitivity, specificity and reproducibility.

4.2 Materials and methods

4.2.1 *In situ* hybridisation (ISH)

Detection of HIF-1 α mRNA by *in situ* hybridisation was carried out on HUVEC grown on chamber slides, as described in section 2.2.2.3.2. A DIG-labelled riboprobe containing the HIF-1 α anti-sense sequence was produced as described in 2.5.3.

After stepping down overnight, HUVEC were treated with the chemical inducer of hypoxia, desferrioxamine (DFO) (130 μ M) for 0, 1, 2, 4 and 6 hours (section 2.2.4.1). Slides were then incubated with the anti-sense probe (positive control), sense strand (probe control) or β -actin (internal control) before chromogenic detection of bound probe, as described in section 2.6. The slides were then viewed microscopically for intracellular location of probe binding, as indicated by a purple coloured precipitate.

4.2.2 Ribonuclease protection assay (RPA)

RPA utilised a biotin labelled RNA probe produced by *in vitro* transcription of the HIF-1 α sequence labelled with biotin (section 2.5.4). HUVEC were grown in 75cm² flasks (section 2.2.2.3.1) and stepped down overnight prior to incubating with 5mM or 20mM glucose or mannitol (osmotic control) in normoxia or hypoxia (ambient or 5% O₂, respectively) for 1 and 6 hours. After treatment, the cells were harvested and the whole cell RNA extracted (section 2.4.1). The sample RNA and single stranded probe were co-precipitated then separated by electrophoresis, as detailed in section 2.7. Protected HIF-1 α mRNA was then visualised by transferring the gel to nitrocellulose membrane for chemiluminescent detection (section 2.5.3.3).

4.2.3 Quantitative Picogreen analysis of RT-PCR

PCR based quantitative analysis of HIF-1 α mRNA was carried out by measuring fluorescence emitted by the binding of Picogreen nucleic acid stain to double stranded complementary DNA (cDNA) reverse transcribed from HIF-1 α mRNA.

As described in section 2.4.3, cDNAs containing the HIF-1 α sequence were produced from HUVEC treated with 5mM or 20mM glucose in hypoxia or normoxia for 1, 6 and 24 hours. This was also carried out for β_2 -microglobulin (β_2M), using the relative primers, which would serve as an internal control to normalise HIF-1 α expression. The PCR products were mixed with Picogreen reagent, and fluorescence measured against dsDNA standards on a microplate reader, as described in section 2.4.4.2.

4.3 Results

4.3.1 Riboprobe synthesis for detection of HIF-1 α mRNA

PCR amplification of HIF-1 α yielded a 365 bp product (figure 4.1) which was ligated into the pGEMT plasmid. After bacterial cloning of the ligated plasmid and double digest of the cloned fragment from the plasmid vector, a 467 bp product was visualised, consisting of the ligated HIF-1 α fragment plus 102 extra bases included in the cut from both ligation sites, as seen in lane 2 of figure 4.2. The full length plasmid DNA seen in lanes 3 and 4 resulted from a single restriction digest with *Apa* I and *Sal* I, respectively.

The incorporation of DIG-labelling during *in vitro* transcription of the probe resulted in a concentration of 0.01ng/ μ l labelled probe for both SP6 and T7 samples, as determined by dot blot analysis (figure 4.3). The biotin probe, which was labelled post-transcriptionally, produced a concentration of 1ng/ μ l labelled probe in both SP6 and T7 samples.

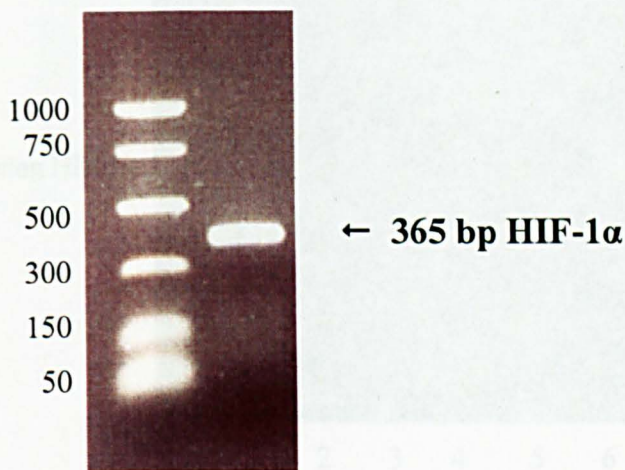


Figure 4.1 Electrophoretically resolved HIF-1 α PCR product. Amplification of HIF-1 α mRNA was achieved by PCR using primers specific for HIF-1 α . The PCR product was then resolved using a 1.4% agarose gel containing ethidium bromide visualised under UV light. The position of the 365 bp HIF-1 α fragment, which has 96% sequence identity shown by product sequencing (University of Aberdeen), is indicated and compared to the PCR marker (bp) positioned on the left.

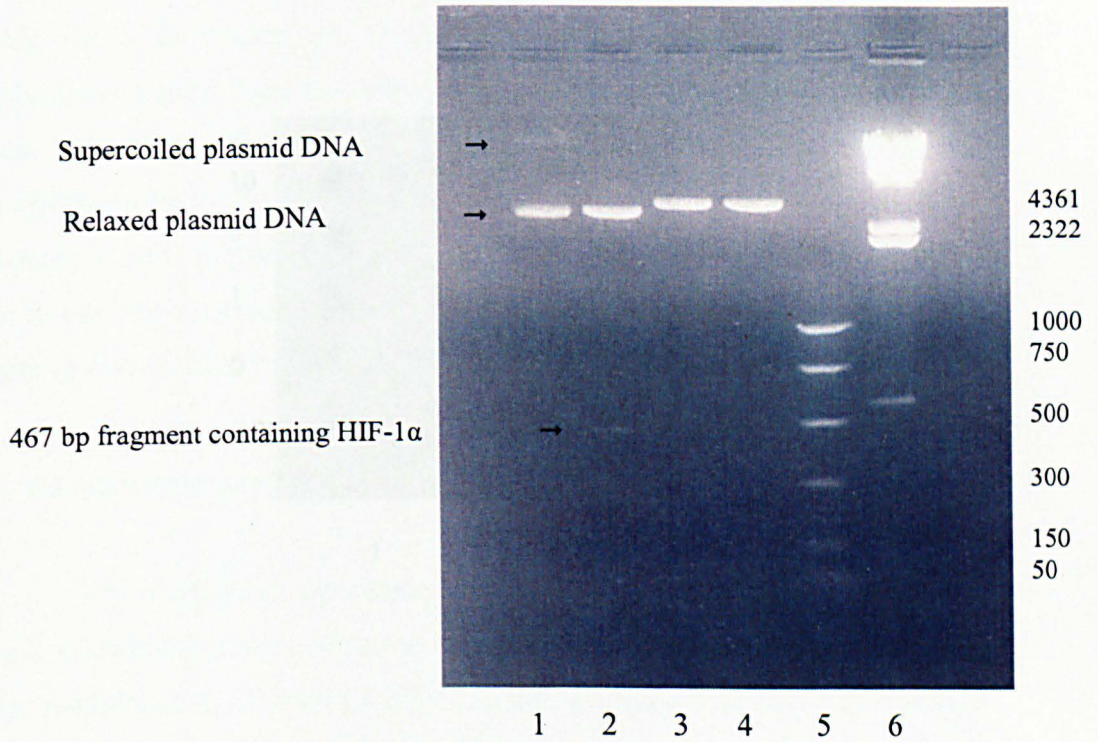


Figure 4.2 Gel electrophoresis demonstrating the quantification of DNA-PCR product

Figure 4.2 Ligation mediated recombinant plasmid cloning. After PCR amplification, the HIF-1 α fragment was ligated into a plasmid vector which was then used to transfect bacterial cells for cloning. Plasmid DNA was recovered and purified before samples were run on 1.4% agarose containing ethidium bromide and visualised under UV light. The samples are; 1) intact plasmid DNA migrating in supercoiled (faint upper band) and relaxed form, 2) double digested plasmid DNA – lower band 467 bp fragment containing the cloned HIF-1 α insert excised from plasmid DNA, 3) linearised 3015 bp plasmid DNA - single digest with *Apa* I, 4) linearised 3015 bp plasmid DNA - single digest with *Sal* I, 5) PCR marker and 6) *Hin* d III digested lambda DNA marker, both measured in base pairs.

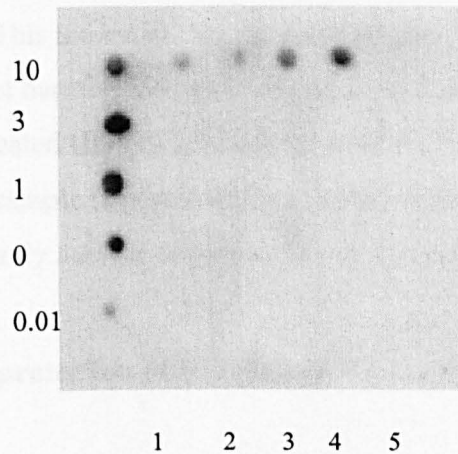


Figure 4.3 Dot blot demonstrating the quantitation of DIG-labelled riboprobe. The transformed plasmid DNA containing the PCR product insert was linearised with a single restriction enzyme digest. Polymerisation directed by the T7 promoter generated a sense strand probe (negative control) and polymerization directed by the SP6 promoter generated an anti-sense strand probe (positive control). SP6 and T7 polymerisation was also carried out using control yeast DNA containing no insert. The blots from left to right represent; 1) control labelled DNA of known concentration (ng/ μ l), 2) SP6 promoter anti-sense transcript, 3) T7 promoter sense transcript, 4) SP6 promoter control transcript and 5) T7 promoter control transcript. By comparison to the DNA of known concentration, the transcripts were both 0.01 ng/ μ l concentration.

4.3.2 *In situ* detection of HIF-1 α mRNA

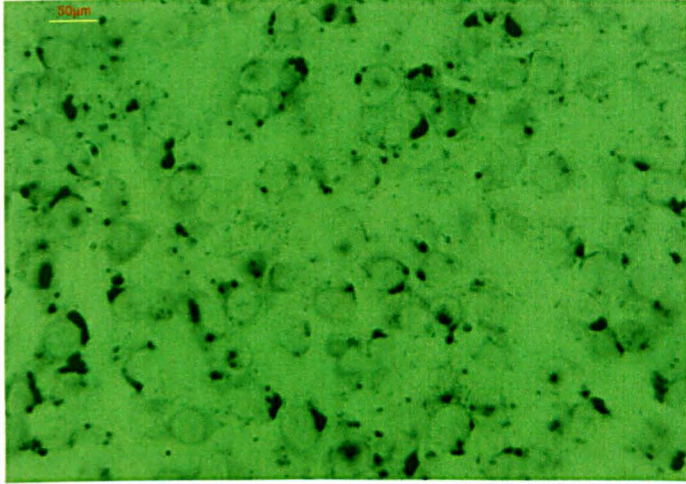
Expression of the internal control, β -actin (figure 4.4a) was abundant in HUVEC treated for 6 hours with DFO. Staining was particularly concentrated in the cytoplasm at the polar regions of many cells, indicating those which may be in the process of division. This indicated that the concentration of DFO and time period of incubation were not harming cell replication. *In situ* detection of HIF-1 α mRNA expression in DFO treated HUVEC did appear to show the presence of binding in the antisense treated sample (figure 4.4b) compared to the sense (figure 4.4c), and staining appeared mainly nuclear or perinuclear in the antisense treated sample.

4.3.3 Ribonuclease protection of HIF-1 α mRNA

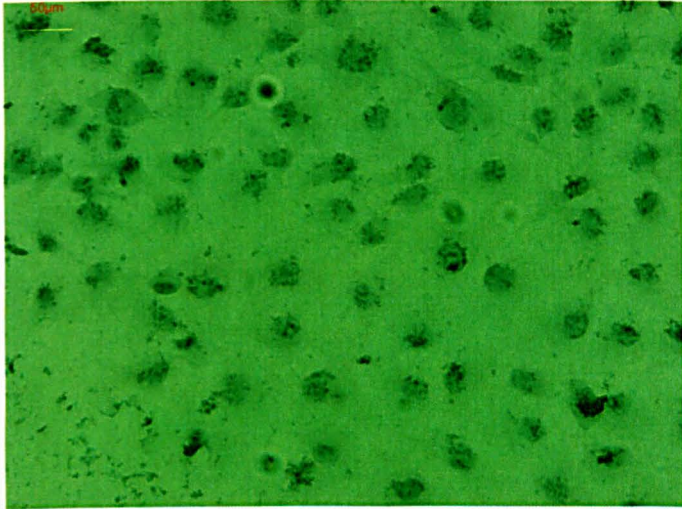
Whole cell RNA was extracted from HUVEC treated with 5mM or 20mM glucose or mannitol (osmotic control) in normoxia or hypoxia (5% O₂) for 1 and 6 hours. Samples of RNA were then run on 1.8% agarose gel stained with ethidium bromide and visualised using UV light. Detection of 28S and 18S ribosomal RNA in an approximate ratio of 2:1 demonstrating no degradation of the sample is evident in figure 4.5a. The RNA samples were then co-precipitated with the biotin-labelled probe at a concentration of 10 μ g RNA to 240pg labelled probe. None of the treated RNA samples showed any sign of mRNA fragment protection when resolved on 5% acrylamide gel. The marker set and full length 467 bp non-hybridised probe were both detected as shown in figure 4.5b.

Figure 4.4: *In situ* detection of mRNA expression in HUVEC. Cells were treated with growth medium supplemented with 130 μ M desferrioxamine for 6 hours, then incubated with the respective DIG-labelled riboprobe for detection of a) β -actin mRNA b) HIF-1 α mRNA antisense c) HIF-1 α mRNA sense. In all images the micron bar represents 50 μ m.

a



b



c

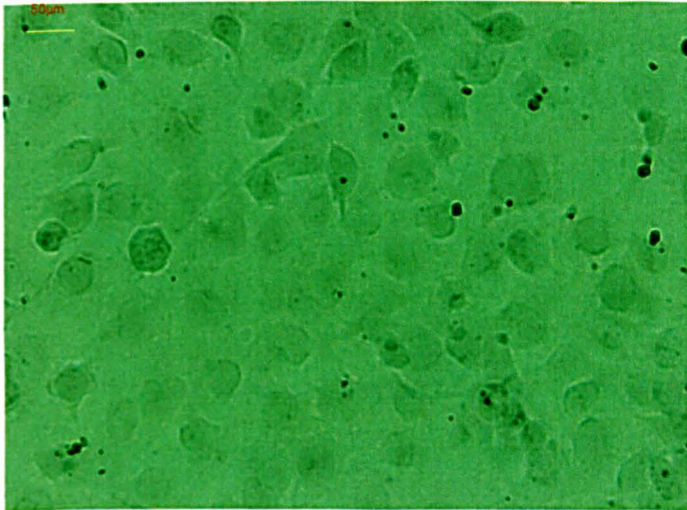


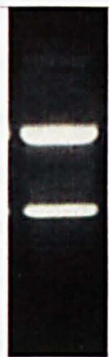
Figure 4.5 Ribonuclease protection of HIF-1 α mRNA. a) RNA extracted from 6h treated HUVEC was resolved on a 1.8% agarose gel stained with ethidium bromide and visualised under UV light, showing the presence of the 28S and 18S subunits. b) The transcribed biotin labelled riboprobe containing the anti-sense HIF-1 α RNA sequence was run on a 5% denaturing polyacrylamide gel along with a marker set. Full length probe was seen to be 467 bases in length.

4.3.4 Optimum conditions for RT-PCR

a

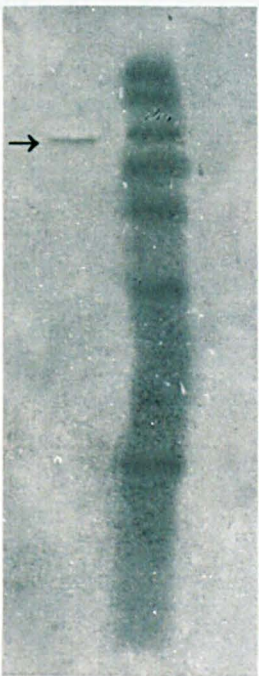
The optimum amplification conditions for the genes β_2 -microglobulin (β_2M) and β -actin (β actin) were determined in order to obtain baseline expression levels. For the β_2M gene, optimum amplification was equivalent to 0.01 μ g total RNA. For the β actin gene, the linear phase (figures 4.6b and 4.6c) was used for the amplification of HIF-1 α products. In the agarose gel (figure 4.6e) the sensitive nature of the assay was demonstrated. At 15 cycles, β_2M mRNA was not detected. At 16 cycles, β_2M mRNA was detected. At 17 cycles, β_2M mRNA was detected. At 18 cycles, β_2M mRNA was detected. At 19 cycles, β_2M mRNA was detected. At 20 cycles, β_2M mRNA was detected. At 21 cycles, β_2M mRNA was detected. At 22 cycles, β_2M mRNA was detected. At 23 cycles, β_2M mRNA was detected. At 24 cycles, β_2M mRNA was detected. At 25 cycles, β_2M mRNA was detected. At 26 cycles, β_2M mRNA was detected. At 27 cycles, β_2M mRNA was detected. At 28 cycles, β_2M mRNA was detected. At 29 cycles, β_2M mRNA was detected. At 30 cycles, β_2M mRNA was detected. At 31 cycles, β_2M mRNA was detected. At 32 cycles, β_2M mRNA was detected. At 33 cycles, β_2M mRNA was detected. At 34 cycles, β_2M mRNA was detected. At 35 cycles, β_2M mRNA was detected. At 36 cycles, β_2M mRNA was detected. At 37 cycles, β_2M mRNA was detected. At 38 cycles, β_2M mRNA was detected. At 39 cycles, β_2M mRNA was detected. At 40 cycles, β_2M mRNA was detected. At 41 cycles, β_2M mRNA was detected. At 42 cycles, β_2M mRNA was detected. At 43 cycles, β_2M mRNA was detected. At 44 cycles, β_2M mRNA was detected. At 45 cycles, β_2M mRNA was detected. At 46 cycles, β_2M mRNA was detected. At 47 cycles, β_2M mRNA was detected. At 48 cycles, β_2M mRNA was detected. At 49 cycles, β_2M mRNA was detected. At 50 cycles, β_2M mRNA was detected. At 51 cycles, β_2M mRNA was detected. At 52 cycles, β_2M mRNA was detected. At 53 cycles, β_2M mRNA was detected. At 54 cycles, β_2M mRNA was detected. At 55 cycles, β_2M mRNA was detected. At 56 cycles, β_2M mRNA was detected. At 57 cycles, β_2M mRNA was detected. At 58 cycles, β_2M mRNA was detected. At 59 cycles, β_2M mRNA was detected. At 60 cycles, β_2M mRNA was detected. At 61 cycles, β_2M mRNA was detected. At 62 cycles, β_2M mRNA was detected. At 63 cycles, β_2M mRNA was detected. At 64 cycles, β_2M mRNA was detected. At 65 cycles, β_2M mRNA was detected. At 66 cycles, β_2M mRNA was detected. At 67 cycles, β_2M mRNA was detected. At 68 cycles, β_2M mRNA was detected. At 69 cycles, β_2M mRNA was detected. At 70 cycles, β_2M mRNA was detected. At 71 cycles, β_2M mRNA was detected. At 72 cycles, β_2M mRNA was detected. At 73 cycles, β_2M mRNA was detected. At 74 cycles, β_2M mRNA was detected. At 75 cycles, β_2M mRNA was detected. At 76 cycles, β_2M mRNA was detected. At 77 cycles, β_2M mRNA was detected. At 78 cycles, β_2M mRNA was detected. At 79 cycles, β_2M mRNA was detected. At 80 cycles, β_2M mRNA was detected. At 81 cycles, β_2M mRNA was detected. At 82 cycles, β_2M mRNA was detected. At 83 cycles, β_2M mRNA was detected. At 84 cycles, β_2M mRNA was detected. At 85 cycles, β_2M mRNA was detected. At 86 cycles, β_2M mRNA was detected. At 87 cycles, β_2M mRNA was detected. At 88 cycles, β_2M mRNA was detected. At 89 cycles, β_2M mRNA was detected. At 90 cycles, β_2M mRNA was detected. At 91 cycles, β_2M mRNA was detected. At 92 cycles, β_2M mRNA was detected. At 93 cycles, β_2M mRNA was detected. At 94 cycles, β_2M mRNA was detected. At 95 cycles, β_2M mRNA was detected. At 96 cycles, β_2M mRNA was detected. At 97 cycles, β_2M mRNA was detected. At 98 cycles, β_2M mRNA was detected. At 99 cycles, β_2M mRNA was detected. At 100 cycles, β_2M mRNA was detected.

28S
18S



b

Full length probe



1000
750
500
400
300
200
100

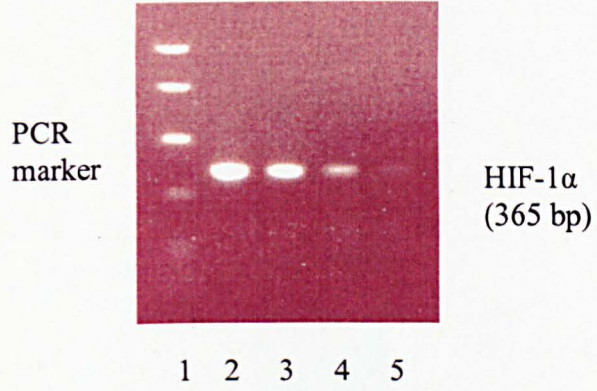
4.3.4 Optimum conditions for Picogreen detection of HIF-1 α mRNA

The optimum amplification conditions for HIF-1 α and the housekeeping gene β_2 microglobulin (β_2 M) were determined using cDNA from untreated HUVEC in order to obtain baseline expression. Single bands were detected for HIF-1 α (365bp) and β_2 M (321bp) when subjected to agarose gel electrophoresis. For both genes, optimum amplification was obtained with 15 cycles using 2 μ l cDNA, which was equivalent to 0.01 μ g cDNA, resulting in mRNA concentration values within the linear phase (figures 4.6b and 4.7b, respectively). Despite a 15 cycle amplification of HIF-1 α producing a barely visible band when resolved on agarose gel (figure 4.6a) the sensitive nature of picogreen binding easily detected this sample. At 15 cycles, β_2 M mRNA bands were easily visible on agarose gel (figure 4.7a). Picogreen binding to β_2 M mRNA became saturated at higher amplification cycles than 15, therefore preventing measurement of change in expression between samples.

Figure 4.6 Determination of optimum cycle number for HIF-1 α amplification.

a) PCR was carried out using primers specific for HIF-1 α and 2 μ l untreated HUVEC cDNA. The cycle number of the PCR program was altered and amplified HIF-1 α samples visualised on ethidium bromide stained agarose gel under UV light produced a single 365bp band. The resolved samples represent; 1) PCR marker, 2) 30 cycles, 3) 25 cycles, 4) 20 cycles and 5) 15 cycles. b) The optimum volume of cDNA required for 15 cycle amplification was quantified by Picogreen analysis of DNA concentration. This was determined to be 2 μ l, equivalent to 0.01 μ g cDNA, due to its position within the linear phase of amplification.

a



b

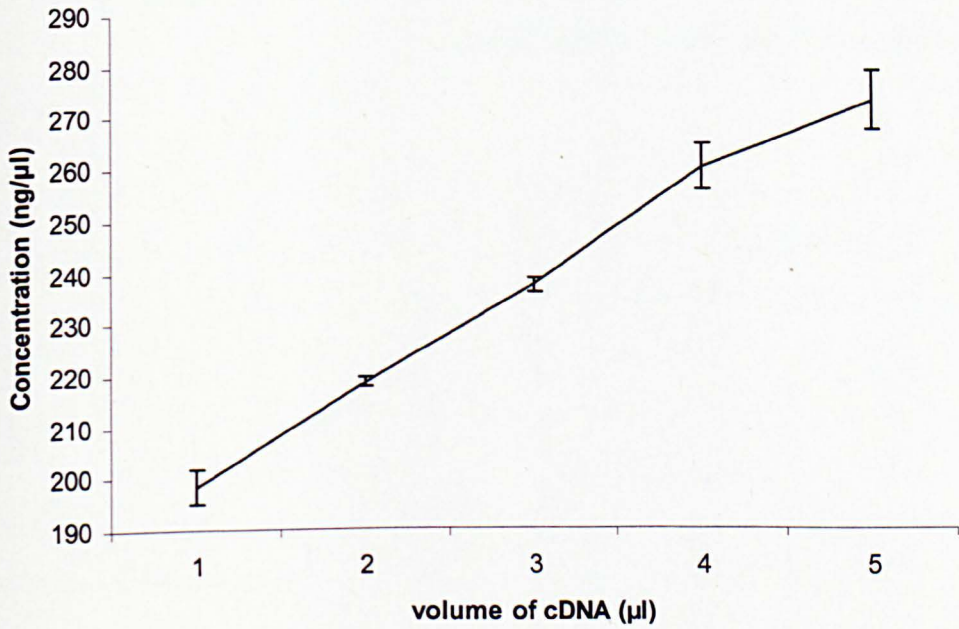


Figure 4.7 Optimum expression of β_2M as an internal control for HIF-1 α

a) A single 321bp band of β_2M detected after 15 amplification cycles of an untreated cDNA. b) The optimum volume of cDNA required for 15 cycle amplification of β_2M was quantified by Picogreen analysis of DNA concentration. This was determined to be 2 μ l cDNA, equivalent to 0.01 μ g, due to its position within the linear phase of amplification.

4.4 Discussion

a

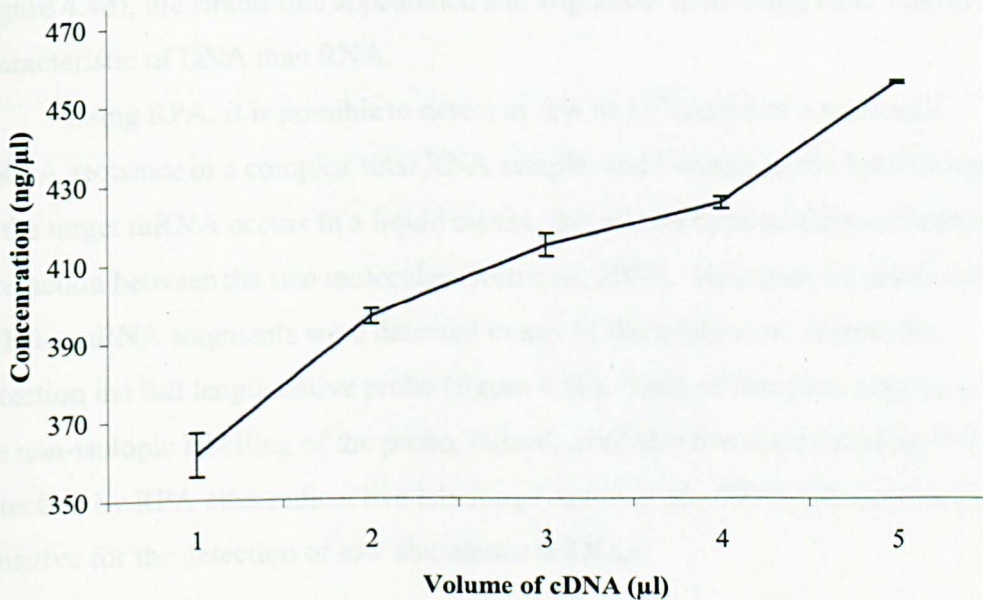
Method. In the detection of mRNA are important for investigations of the role of transcriptional pathways in HIV-1 gene expression. In situ hybridisation (ISH) has proved a powerful tool, as seen in a mouse model of cerebral ischemia where changes in sub-cellular location of HIV-1 mRNA expression were observed, even though the total level of expression was unchanged (Mard *et al.*, 2000). ISH has been used to detect HIV-1 mRNA in a mouse model of cerebral ischemia (Elsan *et al.*, 2000).



← β_2M
321 bp

b

in this study, in the detection of HIV-1 mRNA in HUVEC. HUVEC grown with the presence of HIV-1 showed evidence of binding (data not shown) to the HIV-1 RNA. The location of the binding in this case was not cytoplasmic, as expected for HIV-1, but nuclear. On a closer inspection of the apparent HIV-1 RNA binding (Figure 4.4b), the strand-like appearance and alignment with the HIV-1 RNA characteristic of DNA-RNA hybrids.



4.4 Discussion

Methods for the detection of mRNA are important for investigation of the role of transcriptional pathways in HIF-1 α gene expression. *In situ* hybridisation (ISH) has proved a powerful tool, as seen in a mouse model of cerebral ischemia where changes in sub-cellular location of HIF-1 α mRNA expression were observed, even though the total level of expression as detected by RT-PCR remained unchanged (Marti *et al.*, 2000). ISH has also been used to detect an increase in HIF-1 α mRNA in a mouse model of epidermal wound healing and carcinogenesis (Elson *et al.*, 2000).

In this study, *in situ* detection of β -actin mRNA using a commercially prepared riboprobe (figure 4.4a) showed ISH to be a suitable method for detecting the presence of mRNA in HUVEC. HUVEC probed with the synthesised HIF-1 α antisense showed evidence of binding (figure 4.4b) compared to that of the HUVEC probed with the HIF-1 α mRNA sense sequence (figure 4.4c). However, the location of the binding in this case was not cytoplasmic, as was the case for β -actin, but nuclear. On closer inspection of the apparent HIF-1 α mRNA antisense binding (figure 4.4b), the strand-like appearance and alignment in dividing cells was more characteristic of DNA than RNA.

Using RPA, it is possible to detect as few as 10^5 copies of a particular mRNA sequence in a complex total RNA sample, and because probe hybridisation to the target mRNA occurs in a liquid matrix, this allows optimal three-dimensional interaction between the two molecules (Rottman, 2002). However, no protected HIF-1 α mRNA fragments were detected in any of the treatments, despite the detection the full length native probe (figure 4.5b). Lack of detection may be due to the non-isotopic labelling of the probe, indeed, available literature detailing HIF-1 α detection by RPA cites radioactive labelling (Ameri *et al.*, 2004), which is more sensitive for the detection of low abundance mRNAs.

Even more sensitive than RPA, is RT-PCR, which can detect 50–100 copies of mRNA. This method has proved favourable for the detection of HIF-1 α mRNA, being frequently cited in the literature for detection in a variety of tissues and cell lines including human placental tissue (Caniggia *et al.*, 2000) human ovarian carcinoma (Nakayama *et al.*, 2002), glioblastoma (Sondergaard *et al.*, 2002) and mouse wound cells (Albina *et al.*, 2001). Measurement of RT-PCR by optical density (OD) has shown HIF-1 α mRNA expression levels to be significantly higher in colorectal adenocarcinoma SW480 cells in hypoxic compared to normoxic conditions. The OD method, however has been found to have the highest variance contributable to laboratory sample handling, compared to the fluorogenic Picogreen method which has the least (Haque *et al.*, 2003).

Picogreen measurement of RT-PCR was determined to be the most suitable for measurement of HIF-1 α mRNA in this study. This was based upon the ease with which the experimental conditions could be optimised and the speed at which multiple samples could be read using a plate reader, resulting in a quantifiable measurement of mRNA expression with low standard error between replicates. RT-PCR also allowed the measurement of a control to which HIF-1 α expression could be normalised. Studies examining gene expression with RT-PCR typically normalise their mRNA data to a constitutively expressed housekeeping gene. A gene frequently chosen to normalise expression is β -actin, which is often found to be the most stable gene in diabetic glomeruli and in primary mesangial cells exposed to 20mM glucose (Biederman *et al.*, 2004). However, β -actin, GAPDH and cyclophilin vary widely in hypoxia, with GAPDH considered particularly unsuitable as its transcription in hypoxia has been correlated in cancer cell lines with upregulation of HIF-1 α protein levels (Zhong *et al.*, 1999).

The choice of β_2 microglobulin (β_2 M) as a control compared favourably with reports of it as a control for mRNA expression in hypoxic placental endothelium (Orange *et al.*, 2003) and more specifically for HIF-1 α mRNA measurement in breast cancer biopsy (Cayre *et al.*, 2003). Expression of β_2 M also remains unchanged following endurance or resistance exercise in skeletal muscle (Mahoney *et al.*, 2004) negating the possible effect of lactic acid on control gene expression,

which was important to this study due to the potential for increased anaerobic glycolysis under hypoxic conditions.

A notable limitation of RT-PCR, however, exists in the fact that it is the cDNA which is measured and not the mRNA directly, as is the case for the other methods investigated. It was for this reason that it was important that we determine the optimum profile for amplification of the target sequence prior to taking experimental measurements. Furthermore, any changes in the level of HIF-1 α mRNA cannot be attributed to any difference in sub-cellular location. This would require the complementary experimental conditions using ISH.

Chapter 5

Effect of glucose and hypoxia on HIF-1 α expression in HUVEC

5.1 Introduction

Induction of HIF-1 α in response to diabetes, such as that observed in this study within the neurovasculature of the STZ rat, and by others in the manifestation of diabetic retinopathy (Ozaki *et al.*, 1999; Lukiw *et al.*, 2001), may be occurring in response to a variety of non-hypoxic stimuli implicated in the manifestation of diabetic complications. Such stimuli may include growth factors, cytokines, NO, thrombin and angiotensin (Agani *et al.*, 2002; Amaral *et al.*, 2001; Kim *et al.*, 2002; Kimura *et al.*, 2000; Sandau *et al.*, 2001; Zelzer *et al.*, 1998; Zhong *et al.*, 2000).

Despite the many metabolic and haemodynamic changes elicited by diabetes, sustained exposure of vascular tissues to hyperglycaemia is the main contributor to the pathogenesis of diabetic angiopathy. The role of HIF-1 α in the induction of vascular angiogenic factors and expression of genes involved in glucose transport and metabolism is clear, however, little is known of the ability of glucose to regulate expression of HIF-1 α . Although most reports cite HIF-1 α regulation to be post-translational, transcriptional regulation has been indicated as a potential mechanism by which HIF-1 α is regulated, such as in the induction of HIF-1 α mRNA in wound healing detected in a transgenic mouse model of neoplasia (Elson *et al.*, 2000). Wound healing is an example of a physiological process impaired by hyperglycaemic disease, thus indicating that transcriptional events may be central to glucose-regulated expression of HIF-1 α .

Due to their location within the intimal layer of the vessel wall and their predisposition to glucose induced injury, as demonstrated by previous groups (Knott *et al.*, 1996; Hammes, 2003, Creager *et al.*, 2003), vascular endothelial cells are a prominent target for high ambient glucose induced injury which may be responsible for triggering the induction of structural and functional alterations associated with diabetes.

Human umbilical vein endothelial cells (HUVEC) which are known to express HIF-1 (Gaddipati *et al.*, 1999) would provide a suitable model in which to study the effect of hypoxia and high glucose on HIF-1 α mRNA and protein expression *in vitro*. By employing an established vascular cell line, such as

HUVEC, we are ensuring a reproducible and robust system as required for the identification of molecular markers of gene expression. This is preferable to the technically difficult and time consuming isolation of endothelium from the *in vivo* rat model, which would probably yield an insufficient cell number for the varied and complex experimental requirements proposed. However, the caveats to using a cell line are fully recognised.

5.2 Materials and Methods

5.2.1 Determination of cell growth and viability

Human umbilical vein endothelial cells (HUVEC) maintained in 75cm² flasks (section 2.2.2.3.1) were harvested as detailed in section 2.2.2.2, before reseeded in 96 well plates, as described in section 2.2.2.3.3. Alamar blue indicator was added to growth medium containing either 5mM or 20mM glucose, and cells incubated under normoxia or hypoxia, as described in section 2.2.4.2. Cell growth was then measured at 0, 1, 6, 24 and 29 hours by determination of absorbance at 570nm using an automated plate reader (section 2.2.3.2).

5.2.2 Incubation of HUVEC with altered glucose and oxygen concentration

HUVEC were grown in 75cm² flasks (section 2.2.2.3.1) then incubated in growth media as prepared in section 2.2.5, containing 5mM glucose or 20mM glucose in normoxia or hypoxia for 1, 6 and 24 hours, as described in section 2.2.4.2. Total RNA was then extracted from the HUVEC (section 2.4.1) and cDNAs produced by reverse transcription (section 2.4.3.1).

5.2.3 Determination of gene expression by Picogreen quantification of PCR products

The cDNAs transcribed from treated HUVEC were subsequently primed for specific target gene amplification by PCR, as detailed in section 2.4.3.3. Expression of HIF-1 α , HIF-1 α antisense (aHIF), glucose transporter type 1 (GLUT-1) and insulin-like growth factor-1 receptor (IGF-1R) mRNAs were determined by PCR directed by short nucleotide primer pairs specific for the amplification of the target gene, as laid out in table 2.1. Amplification of the target gene was then measured quantitatively on a plate reader using Picogreen fluorogenic substrate and read using a microplate reader (section 2.4.4.2). Data shown in figures 5.2, 5.3, 5.4 and 5.6 represent the mean of 3 separate PCR reactions for each time point and condition. Each of the 3 separate PCR reactions for each time point and condition were carried out using cDNA produced from a different cell population. The PCR product resulting from each of the 3 reactions was subsequently read in triplicate on the multi-well plate reader, in order to account for intra-experimental error.

5.2.4 Inhibition of RNA transcription and protein translation

HUVEC grown in 75cm² flasks (section 2.2.2.3.1), were then exposed to concentrations of glucose and oxygen as described previously in the presence of either an inhibitor of RNA transcription, actinomycin D (Act D) or an inhibitor of protein translation, cyclohexamide (CHX) for 1, 6 and 24 hours, as described in section 2.2.6.1. cDNAs were then produced from the treated cells as described in section 2.4.3.1, subjected to PCR amplification of HIF-1 α mRNA (section 2.4.3.3) and measured using Picogreen fluorogenic reagent (section 2.4.4.2).

5.2.5 Immunocytochemical detection of HIF-1 α protein expression in HUVEC

HUVEC maintained in 75cm² flasks (section 2.2.2.3.1) were harvested as previously described and seeded on 2 well chamber slides (2.2.2.3.2). The HUVEC grown on chamber slides were then incubated for 24 hours in concentrations of glucose and oxygen as described previously (2.2.4.2).

The slides were then subjected to immunocytochemical detection of HIF-1 α protein with HIF-1 α monoclonal mouse primary antibody, using the avidin-biotin

complex/alkaline phosphatase procedure (sections 2.3.1.2 and 2.3.1.3). Immunodetected slides were subsequently mounted before viewing by light microscopy.

5.2.6 Data Analysis

Statistical analysis of data was carried out using one-way analysis of variance (ANOVA) followed by post-hoc tests. Level of significance was then conveyed using the following notation; * ($p < 0.05$), ** ($p < 0.01$), *** ($p < 0.001$).

5.3 Results

5.3.1 Effect of altered glucose and oxygen concentration on HUVEC growth

Prior to experimentation, it was important to ascertain what effect the test conditions which were to be employed would have on HUVEC proliferation and viability. Growth curves obtained from measurement of oxidation of Alamar blue substrate in culture, as demonstrated in figure 5.1, showed that in all treatments, proliferation of HUVEC continued beyond 24 hours, which was to be the maximum incubation period used in this study.

Up to 6 hours, no significant difference in proliferation was detected between growth conditions. Throughout the entire growth period monitored, HUVEC incubated in media containing a high concentration of glucose and those incubated in hypoxic conditions produced very similar growth curves, both of which demonstrated a higher rate of proliferation than cells subjected to standard growth conditions (5mM glucose, normoxia). The combination of high glucose and hypoxia had an additive effect on the proliferation rate after 6h incubation, which by 24h was significantly greater than that of all other conditions, most notably the normal growth conditions ($p < 0.001$).

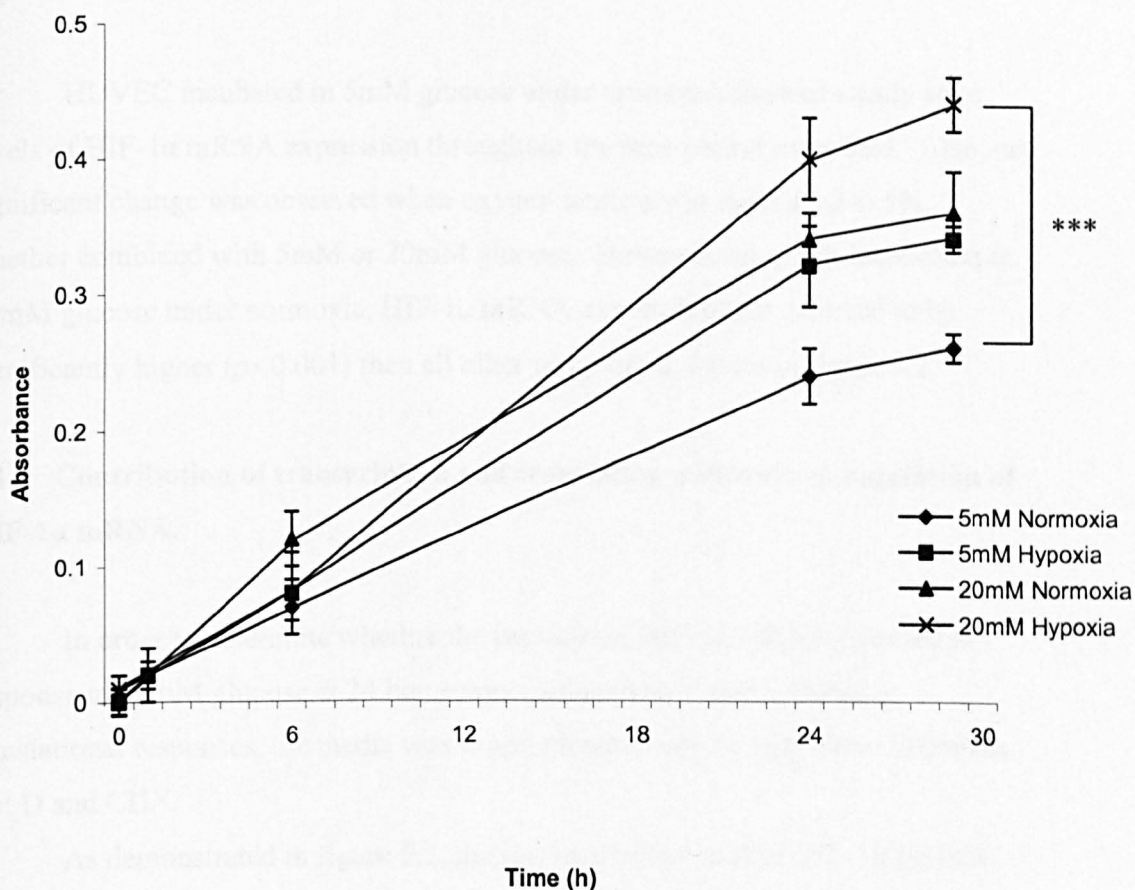


Figure 5.1. HUVEC growth curves in response to altered glucose and oxygen concentration. HUVEC were seeded at a density of 0.025×10^6 cells/ml on a microtitre plate and allowed to grow overnight under standard conditions. Cells were then incubated with fresh growth media supplemented with either 5mM or 20mM glucose and 10% (w/v) Alamar blue substrate. The plates were subsequently incubated under normoxic or hypoxic conditions (ambient or 5% O₂, respectively), and cell proliferation measured at 0, 1, 6, 24 and 29 hour intervals on a colorimetric microplate reader as absorbance at 570nm. Results shown are the mean of n=3.

5.3.2 Effect of altered glucose and oxygen concentration on HIF-1 α mRNA expression.

HUVEC incubated in 5mM glucose under normoxia showed steady state levels of HIF-1 α mRNA expression throughout the time period examined. Also, no significant change was observed when oxygen tension was decreased to 5%, whether combined with 5mM or 20mM glucose. However, after 24h incubation in 20mM glucose under normoxia, HIF-1 α mRNA expression was detected to be significantly higher ($p < 0.001$) than all other samples, as shown in figure 5.2

5.3.3 Contribution of transcription and translation pathways to regulation of HIF-1 α mRNA.

In order to determine whether the increase in HIF-1 α mRNA detected in response to 20mM glucose at 24 hours was mediated by transcriptional or translational responses, the media was supplemented with the respective inhibitors, Act D and CHX.

As demonstrated in figure 5.3, the increase in the level of HIF-1 α mRNA detected in response to 20mM glucose is unaffected by blocking transcription. However, the mRNA level in the correlating hypoxic sample, which was not seen to change in the absence of Act D, now appears to decrease indicating that transcription of HIF-1 α mRNA does occur in these conditions.

In figure 5.4, it can be seen that the elevated expression of HIF-1 α mRNA in response to 20mM glucose is blocked by the inhibitor of protein translation, CHX. Unlike Act D, CHX was not observed to have a significant effect on any of the hypoxic responses at 24 hours.

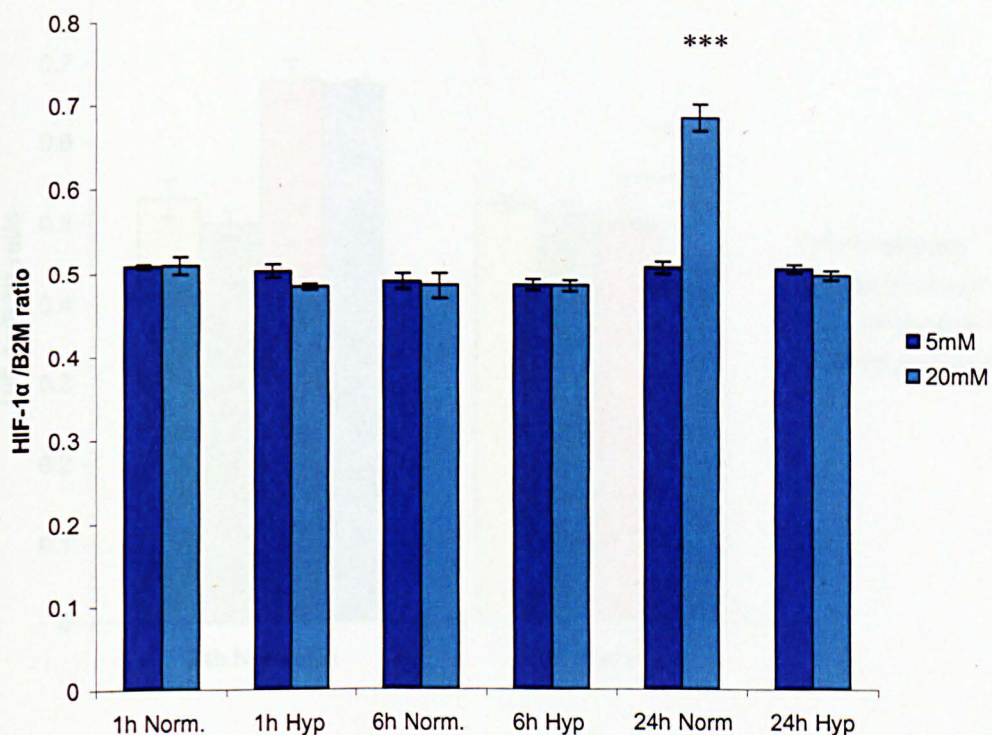


Figure 5.2: Effect of time, glucose and oxygen concentration on HIF-1 α mRNA expression. HUVEC were exposed to 5mM or 20mM glucose under 5% or ambient O₂ for 1, 6 and 24 hours. Total RNA was then extracted and used for reverse transcription. The resultant cDNAs were subsequently primed for HIF-1 α and B₂ microglobulin (B₂M) amplification by PCR, which was measured quantitatively on a plate reader using Picogreen. At 24 hours, expression in the normoxic 20mM sample is significantly higher than all other samples. Results shown are expressed as the ratio of HIF-1 α PCR product measured (ng) to that of B₂M (ng). Data shown are representative of n=3.

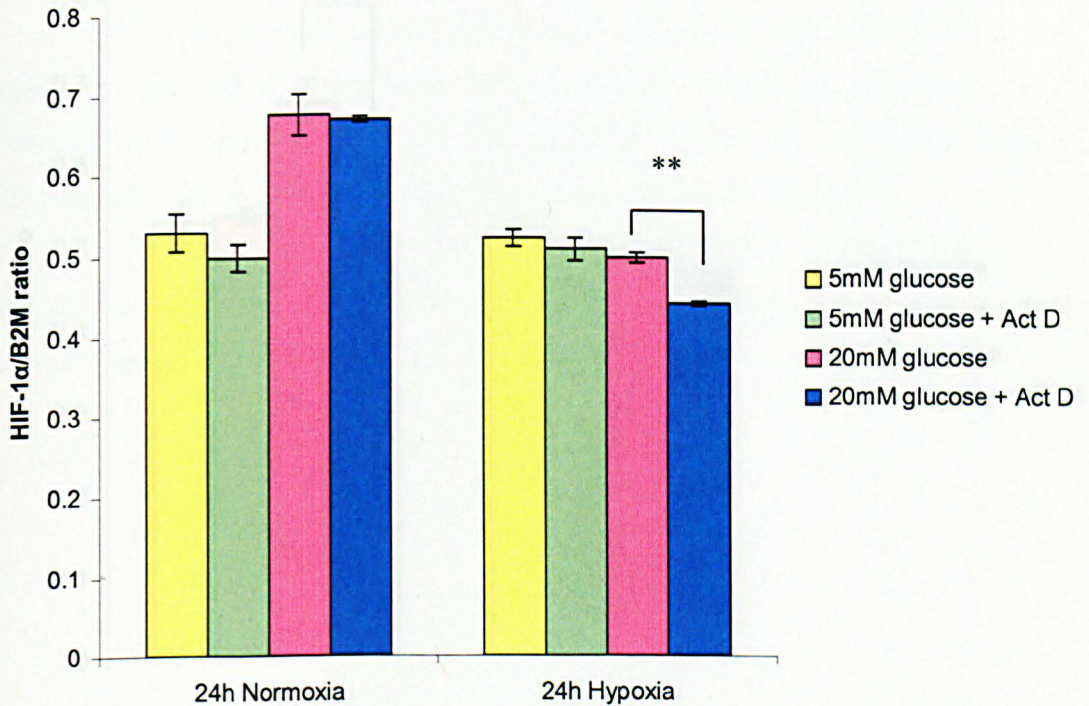


Figure 5.3: Effect of Act D on HIF-1 α expression at 24h in 20mM glucose.

HUVEC were incubated for 24h in media containing 20mM glucose with or without Act D under normoxic conditions. Total RNA was then extracted and used for reverse transcription. The resultant cDNAs were subsequently primed for HIF-1 α and B₂M amplification by PCR, which was measured quantitatively on a plate reader using Picogreen. Act D did not affect the stability of HIF-1 α expression detected with 20mM glucose under normoxia. Results shown are expressed as the ratio of HIF-1 α PCR product measured (ng) to that of B₂M (ng). Data shown are representative of n=3.

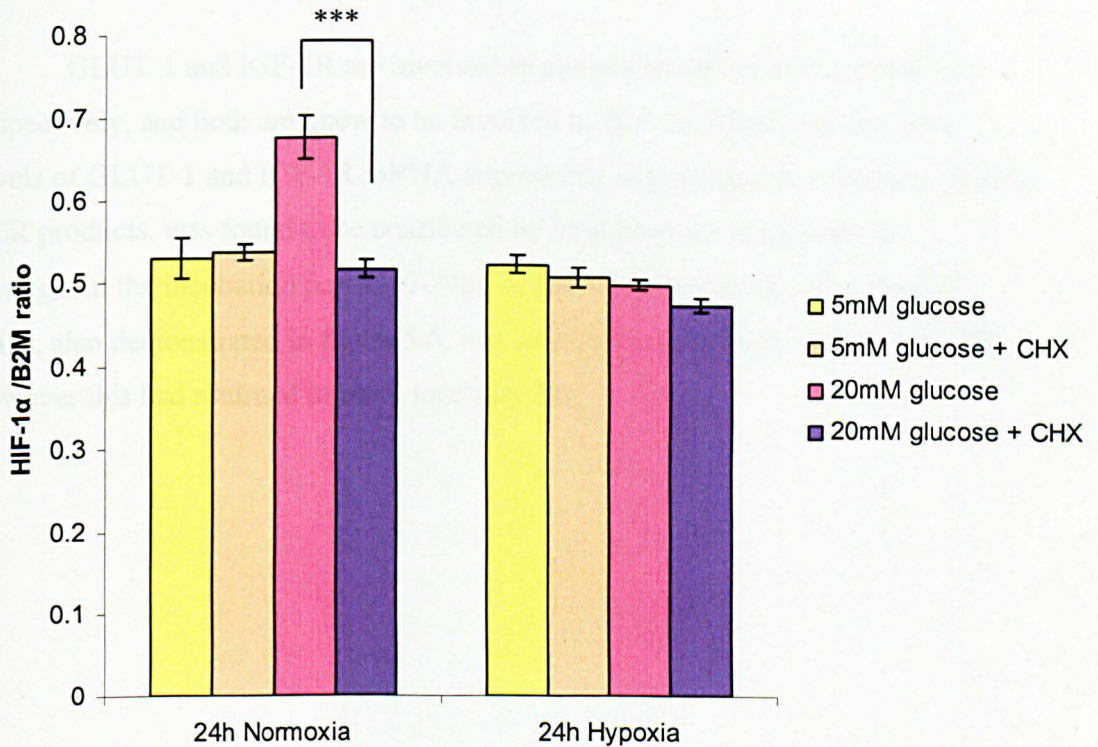


Figure 5.4: Effect of CHX on HIF-1 α expression at 24h in 20mM glucose.

HUVEC were incubated for 24h in media containing 20mM glucose with or without CHX under normoxic conditions. Total RNA was then extracted and used for reverse transcription. The resultant cDNAs were subsequently primed for HIF-1 α and B₂M amplification by PCR, which was measured quantitatively on a plate reader using Picogreen. CHX significantly decreased the stability of HIF-1 α expression detected with 20mM glucose under normoxia. Results shown are expressed as the ratio of HIF-1 α PCR product measured (ng) to that of B₂M (ng). Data shown are representative of n=3.

5.3.4 Effect of altered glucose and oxygen concentration on expression of genes induced by HIF-1 α , and its natural antisense, aHIF.

GLUT-1 and IGF-1R are involved in glucose transport and metabolism, respectively, and both are known to be involved in HIF-1 α signalling. Relative levels of GLUT-1 and IGF-1R mRNA expression, as measured by detection of their PCR products, was found to be unaffected by high glucose concentration throughout the incubation period (0-24h), as shown in figure 5.6. The level of aHIF, also demonstrated in figure 5.6, was seen to increase slightly at 6h ($p < 0.05$), however this had returned to basal levels by 24h.

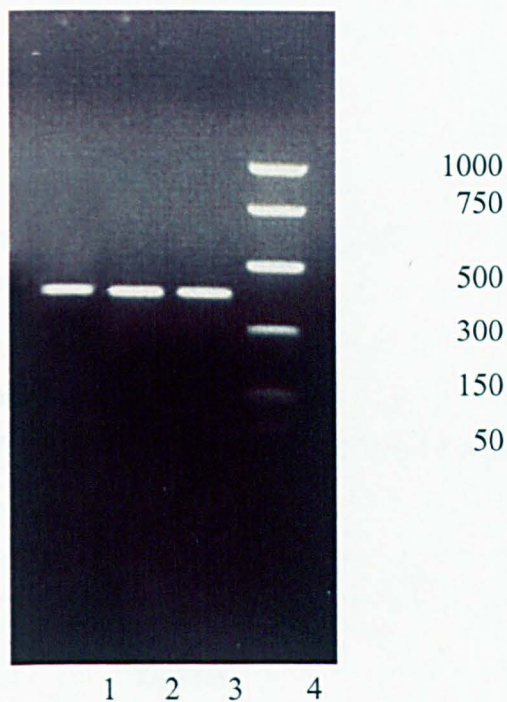


Figure 5.5 Electrophoretically resolved aHIF, GLUT-1 and IGF-1R PCR product. The position of the 1) 398 bp GLUT-1, 2) 390 bp aHIF and 3) 381 bp IGF-1R fragments are indicated and compared to 4) the PCR marker (bp) positioned on the right.

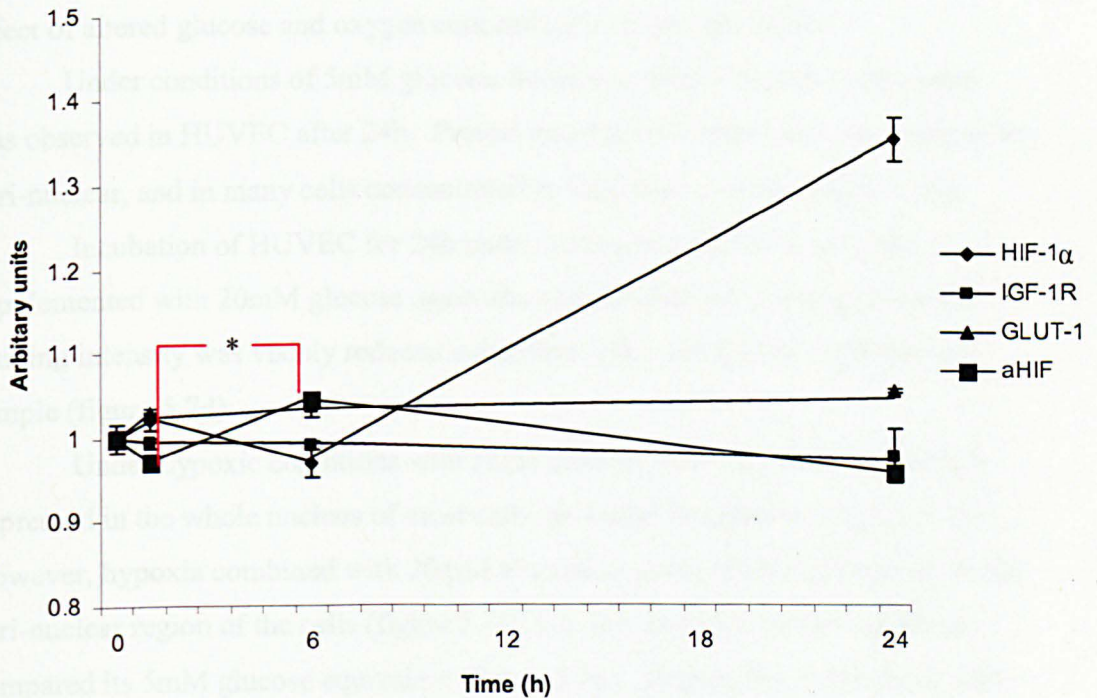


Figure 5.6: Expression of GLUT-1, IGF-1R and aHIF mRNA compared to that of HIF-1 α in response to 20mM glucose. HUVEC were incubated in media containing 20mM glucose under normoxia for 0, 1, 6 and 24 hours. Total RNA was then extracted and used for reverse transcription. The resultant cDNAs were subsequently primed for HIF-1 α , GLUT-1, IGF-1R, aHIF and B₂ microglobulin amplification by PCR, which was measured quantitatively on a plate reader using Picogreen. Unlike HIF-1 α , GLUT-1 and IGF-1R mRNA levels remained unchanged throughout the experiment. The level of aHIF increased slightly ($p < 0.05$) at 6h compared to 0h, then dropped at 24h. Results shown are in relation to the value obtained at t=0 expressed as arbitrary units, and are representative of n=3.

5.3.5 Effect of altered glucose and oxygen concentration on HIF-1 α protein expression

HIF-1 α protein expression was then investigated, in order to ascertain the effect of altered glucose and oxygen concentration on protein at 24h.

Under conditions of 5mM glucose, normoxia, HIF-1 α protein expression was observed in HUVEC after 24h. Protein expression in these cells was seen to be peri-nuclear, and in many cells concentrated at the poles, as seen in figure 5.7c.

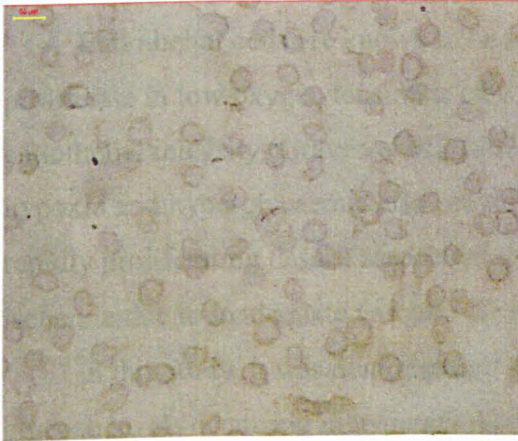
Incubation of HUVEC for 24h under normoxic conditions in media supplemented with 20mM glucose again showed peri-nuclear staining, however staining intensity was visibly reduced compared to the correlating 5mM glucose sample (figure 5.7d).

Under hypoxic conditions with 5mM glucose, HIF-1 α protein is strongly expressed in the whole nucleus of most cells, as would be expected (figure 5.7e). However, hypoxia combined with 20mM glucose not only shifted expression to the peri-nuclear region of the cells (figure 5.7f), but also caused a visible reduction compared its 5mM glucose equivalent (figure 5.7e). Despite this, expression did appear greater than in the equivalent normoxic sample (figure 5.7d).

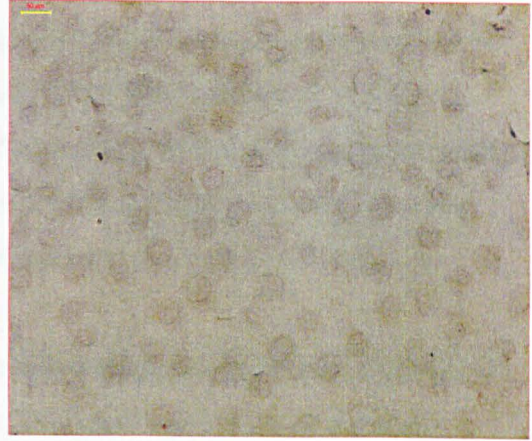
Figure 5.7: Immunocytochemical detection of HIF-1 α protein expression in HUVEC. HUVEC were seeded on chamber slides at 0.025×10^6 cells/ml. After an initial growth period, cells were then exposed to 5mM or 20mM glucose under normoxic (ambient O₂) or hypoxic (5% O₂) conditions for 24h before immunodetection of HIF-1 α protein expression. The following photomicrographs show; a) HUVEC probed with control antibody (IgG1) in order to determine antibody specificity, b) HUVEC incubated with TBS alone as buffer control, c) HIF-1 α protein detected in HUVEC treated with 5mM glucose under normoxia, d) 20mM glucose under normoxia, e) 5mM glucose under hypoxia and f) 20mM glucose under hypoxia. The micron bar in top left hand corner of each micrograph represents 50 μ m. Images shown are representative of n=3.

5.3 Discussion

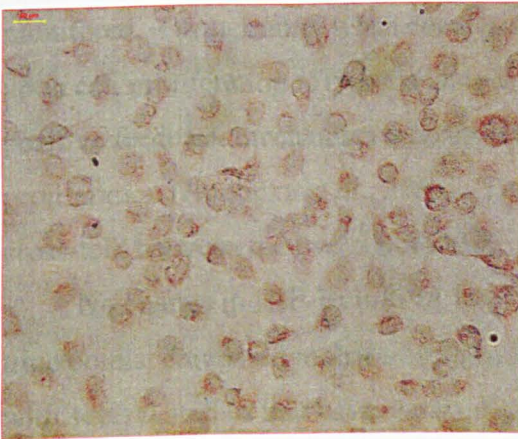
a



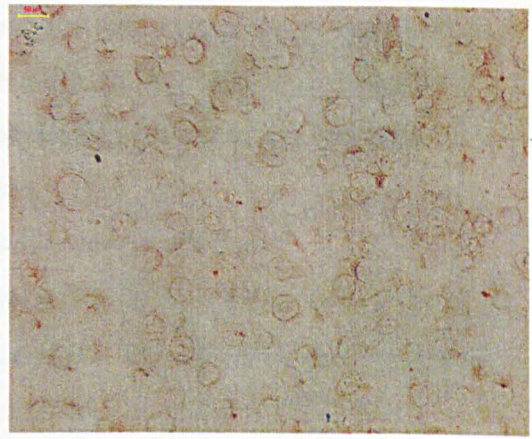
b



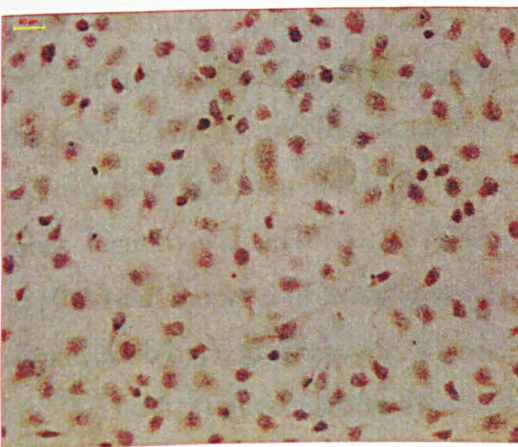
c



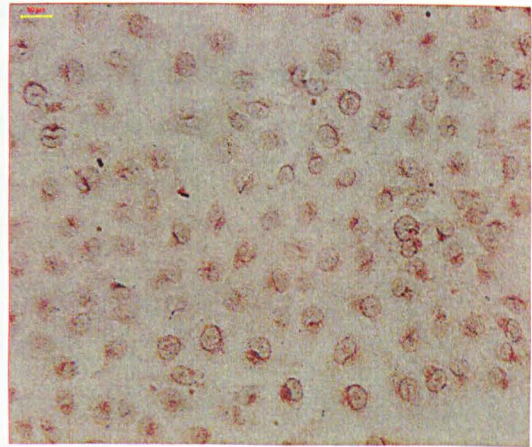
d



e



f



5.3 Discussion

Endothelial cells are known to be largely hypoxia-tolerant, as their ability to proliferate in low oxygen tension is essential for the maintenance of vascular endothelial integrity (Graven *et al.*, 1993, Tucci *et al.*, 1996). The combination of hypoxia and hyperglycaemia also occurs frequently in diabetic disease, whereby rapidly proliferating tissues associated with secondary complications become ischemic due to inadequate vascular supply.

In this study, it was demonstrated that when applied individually, hypoxia or glucose levels occurring in hyperglycaemia, stimulate cell growth to a greater extent than that seen under standard growth conditions over the 29h period monitored. Furthermore, when combined the two stimuli have an additive effect upon cell proliferation. Hypoxia has previously been identified as a trigger for a positive feedback mechanism whereby changes in endothelial cells maintain proliferation (Hudlicka *et al.*, 2002). Therefore, these observations suggest that cross-talk between the two signals may enhance this mechanism.

No change in HIF-1 α mRNA level was observed in response to hypoxia at all time points, compared to that of standard growth conditions. This is in agreement with several studies that have shown that under these conditions, HIF-1 α is regulated at the level of the protein, with mRNA remaining stable (Huang *et al.*, 1996., Gradin *et al.*, 1996., Hara *et al.*, 1999).

However, 20mM glucose under normoxic conditions significantly increased the level of HIF-1 α mRNA detected at 24 hours. This response may therefore indicate that regulation of mRNA expression by elevated glucose represents a mechanism by which HIF-1 α is regulated in endothelial cells. As such, regulation of HIF-1 α at the level of transcription may represent a coordinative adaptive responses to hyperglycaemia in the diabetic milieu.

To further understand the observation of increased HIF-1 α mRNA expression in cells exposed to high glucose in normoxia at 24 h, assessment of transcriptional and translational regulation of HIF-1 α mRNA was necessary. It was found that inhibition of transcription using Act D had no significant effect on the increase in

HIF-1 α mRNA expression detected, suggesting that increased levels are due to enhanced mRNA stability, as opposed to increased transcription. Interestingly, although high glucose combined with hypoxia had no effect on HIF-1 α mRNA level, treatment with Act D did cause a small yet significant reduction in the level of HIF-1 α mRNA detected in this sample.

Inhibition of protein translation using CHX did prevent increased detection in 20mM glucose with normoxia. This indicates the requirement for *de novo* protein synthesis for the hypoxia-independent stimulation of HIF-1 α mRNA by high glucose, which has also been implicated in the action of other non-hypoxic stimuli on HIF-1 α expression (Shi *et al.*, 2005; Frede *et al.*, 2005).

The natural antisense of the HIF-1 α transcript (aHIF), which is complementary to the 3' untranslated region of HIF-1 α , does not encode a protein, but is implicated in the degradation of HIF-1 α mRNA (Thrash-Bingham & Tartof, 1999). At 6h, exposure of HUVEC to high glucose under normoxia caused a small but significant increase in the level of aHIF detected. This did not coincide with any change in HIF-1 α mRNA at the same time point; however, it may have contributed to the maintenance of baseline level HIF-1 α mRNA. Therefore, increased aHIF may keep the HIF-1 α mRNA levels in check in response to increasing levels of stimulation. The return of aHIF levels to baseline at 24h exposure to high glucose may indicate that such a level of exposure to glucose is out with the control of aHIF, thus offering an explanation for the increase in HIF-1 α mRNA level detected at this time.

In order to determine whether observed changes in the level of HIF-1 α mRNA were specific for HIF-1 α or due to a generalised change in mRNA level, the expression of GLUT-1 and IGF-1R mRNA was measured in equivalent samples.

As an inherent effect of increased extracellular glucose concentration is altered uptake, it was therefore important to investigate the effect of high glucose on GLUT-1 mRNA in relation to that of HIF-1 α . It was subsequently shown that exposure of HUVEC to high glucose had no significant effect on GLUT-1 mRNA levels, although high extracellular glucose has been shown to decrease GLUT-1 mRNA levels in fibroblasts and pericytes (Whitesell *et al.*, 1990, Mandarino *et al.*, 1994). Previous groups have observed no reduction in expression of GLUT-1

protein in response to elevated glucose in human retinal endothelial cells (Knott *et al.*, 1996), bovine retinal endothelial cells (Mandarino *et al.*, 1994) or bovine aortic endothelial cells (BAEC) (Kaiser *et al.*, 1993). Although in this study protein levels were not measured, the mRNA data obtained does elude to a general endothelial cell response to high glucose, such as that described by previous groups.

The critical balance between the positive metabolic and negative angiogenic properties of IGF-1 in the prevention and treatment of diabetic complications has been highlighted (Knott, 1998). HIF-1 α may participate in the responsiveness of the tissue to IGF-1, as previous studies have indicated functional IGF-1 receptor (IGF-1R) to be essential for chemically induced non-hypoxic induction of HIF-1 α (Agani *et al.*, 1998). This study found that 20mM glucose in the presence of normoxia had no effect on the level of IGF-1R mRNA detected. Although this does not tell us anything about IGF-1, it may indicate that elevated glucose is not affecting the sensitivity of the tissue to IGF-1.

The lack of change in GLUT-1 or IGF-1R mRNA levels coincident with elevated HIF-1 α mRNA demonstrates that increase in mRNA level detected in response to high glucose is specific to HIF-1 α . Therefore, this poses the question as to what is happening to HIF-1 α protein expression at 24h in elevated glucose.

In this study, abundant detection of HIF-1 α protein in the nucleus of endothelial cells exposed to hypoxia agrees with expression found in endothelial cells derived from heart tissue in response to myocardial hypoxia (Lee *et al.*, 2000). It was also shown that HUVEC are very sensitive to hypoxia, due to the large increase in HIF-1 α protein expression in response to 5% oxygen with 5mM glucose, compared to ambient oxygen levels, a response which is not evident under the same conditions in human lung epithelial cells (Uchida *et al.*, 2004). When 5mM glucose was replaced with 20mM, HIF-1 α protein expression detected in HUVEC was not only visibly reduced, but also appeared primarily in the peri-nuclear region rather than within the nucleus.

Elevated HIF-1 α mRNA level detected at 24h in 20mM glucose under normoxia actually coincided with visibly reduced protein expression at this time, compared to standard growth conditions. The observation of reduced expression of

HIF-1 α protein in HUVEC treated with 20mM glucose combined with hypoxia, may represent a negative feedback mechanism by which HIF-1 α protein is down regulated under conditions of high glucose. However, in normoxia, increased HIF-1 α mRNA level as a result of increased stability in 20mM glucose suggested a block on translation of mRNA to protein, resulting in absolute levels of mRNA building up within the cell, and protein decreasing. Therefore, reduced HIF-1 α protein in response to 20mM glucose may be elicited via different mechanisms under hypoxic and normoxic conditions.

The effect of elevated glucose on HIF-1 α expression are in partial agreement with those of Catrina and colleagues (2004), who reported hyperglycaemia to reduce hypoxia induced protein stability in human dermal microvascular endothelial cells (HDMEC). Catrina's observation of no change in mRNA expression or protein expression in response to high glucose alone is not contradictory to our findings, but may highlight the different responses to glucose which are elicited in a microvascular EC line (HDMEC) compared to a macrovascular EC line (HUVEC).

This information therefore requires the consideration of mechanisms responsible for the induction of HIF-1 α mRNA in the presence of high glucose. As the significance of mRNA stability has already been highlighted in the course of this study, the next stage will address the question of which signalling pathways are initiating this stability, what is the contribution of glucose metabolism and, as protein translation is implicated in the response, are RNA binding proteins being expressed which will interact with the instability element of HIF-1 α mRNA.

Chapter 6

Mechanism of regulation of HIF-1 α mRNA level in HUVEC

6.1 Introduction

In this study, it has been seen that incubation of HUVEC with high glucose stabilised HIF-1 α mRNA levels at 24 hours under normoxic conditions. As this was not seen in the equivalent hypoxic sample, it was therefore important to determine the mechanism/s by which glucose may be regulating HIF-1 α mRNA independently of hypoxia.

Signalling by reactive oxygen species (ROS) is a potential mechanism by which high glucose may be regulating the stability of HIF-1 α mRNA, as hyperglycaemia is known to increase oxidative stress beyond the protective capabilities of the cell. ROS are also able to feed into and enhance other signalling pathways, such as p42/44 MAPK (Chess *et al.*, 2005). In clinical trials, the potent antioxidant α -lipoic acid has been reported to improved glucose metabolism in human diabetes (Jacob *et al.*, 1995) and be beneficial in the treatment of diabetic neuropathy (Ziegler *et al.*, 1999). Indeed, this study has shown that supplementing the feed of STZ rats with α -lipoic acid diminishes HIF-1 α protein expression in the vasculature supplying the sciatic nerve, as shown in chapter 3.

Pi3K and MAPK signalling pathways are implicated in the action of non-hypoxic mediators of HIF-1 α protein stabilisation, including that of AGEs (Treins *et al.*, 2001) and cytokines (Hellwig-Burgel *et al.*, 2005). In order to understand the implication of high glucose in the stabilisation of HIF-1 α mRNA via these signalling pathways, the effects of specific inhibitors of p42/44 MAPK (PD98059) and the p110 subunit of Pi3K (LY294002) on HIF-1 α mRNA level detected in HUVEC exposed to high glucose under normoxia were studied.

Finally, in order to elucidate the contribution of hexose metabolism to the regulation of HIF-1 α mRNA stability, the influence of replacing D-glucose with the glucose analogues, 2-deoxyglucose (2-DG) and 3-orthomethylglucose (3-OMG) was also studied. These analogues can be transported into the cell but not fully metabolised, therefore allowing the ability to distinguish whether hexose transport

or metabolism is mediating the permissive effect of high glucose on the stability of HIF-1 α mRNA.

6.2 Materials and Methods

6.2.1 Effect of the antioxidant α -lipoic acid on level of HIF-1 α mRNA detected.

HUVEC were grown in 75cm² flasks (section 2.2.2.3.1) then incubated in growth media containing 20mM glucose supplemented with 250 μ g/ml α -lipoic acid (2.2.6.3) under normoxic conditions for 1, 6 and 24 hours. HIF-1 α mRNA level was then measured by Picogreen detection of PCR product (2.4.3.3 and 2.4.4.2).

6.2.2 Effect of inhibition of protein kinase activity on level of HIF-1 α mRNA detected.

HUVEC were cultured in 75cm² flasks as before, and exposed to either 5 or 20mM glucose in conjunction with normoxia were supplemented with either PI3K inhibitor, LY294002 or p42/44 MAPK inhibitor, PD98059, at 10 μ g/ml and 2 μ g/ml respectively, as detailed in section 2.2.6.2. The effect of inhibition of each kinase on HIF-1 α mRNA expression in HUVEC after 1, 6 or 24h was then assessed by PCR and Picogreen detection, as detailed earlier in this chapter.

6.2.3 Effect of glucose analogues, 2-deoxyglucose and 3-orthomethylglucose, on HUVEC growth and HIF-1 α mRNA level detected.

6.2.3.1 Determination of cell growth and viability

HUVEC growth was measured using alamar blue (section 2.2.3.2), when incubated in either 5mM or 20mM of 2-deoxyglucose (2DG) or 3-orthomethylglucose (3OMG) (2.2.5) in place of glucose, combined with normoxia

or hypoxia. Measurements were then taken at 0, 1, 6, 24 and 29 hours using a plate reader (section 2.2.3.2).

6.2.3.2 Determination of HIF-1 α mRNA level

HUVEC were grown in 75cm² flasks (section 2.2.2.3.1), then incubated in 20mM 2DG or 3OMG in place of D-glucose (2.2.5) under normoxic conditions for 24h. cDNAs were then produced from the treated cells as described in section 2.4.3.1, which were then subjected to PCR amplification of HIF-1 α mRNA (section 2.4.3.3) and measured using Picogreen detection (section 2.4.4.2).

6.2.4 Data Analysis.

Statistical analysis of data was carried out using one-way analysis of variance (ANOVA) followed by post-hoc tests. Level of significance was then conveyed using the following notation; * ($p < 0.05$), ** ($p < 0.01$), *** ($p < 0.001$).

6.3 Results

6.3.1 Effect of the antioxidant α -lipoic acid on level of HIF-1 α mRNA level detected

Incubation of HUVEC in media containing 20mM glucose supplemented with α -lipoic acid resulted in reduced detection of HIF-1 α mRNA compared to that detected in the α -lipoic acid-free media, as shown in fig 6.1. This reduction was most significant at 24h ($p < 0.001$), with resultant detection level similar to that seen in samples where HIF-1 α mRNA was not subject to stabilisation by high glucose.

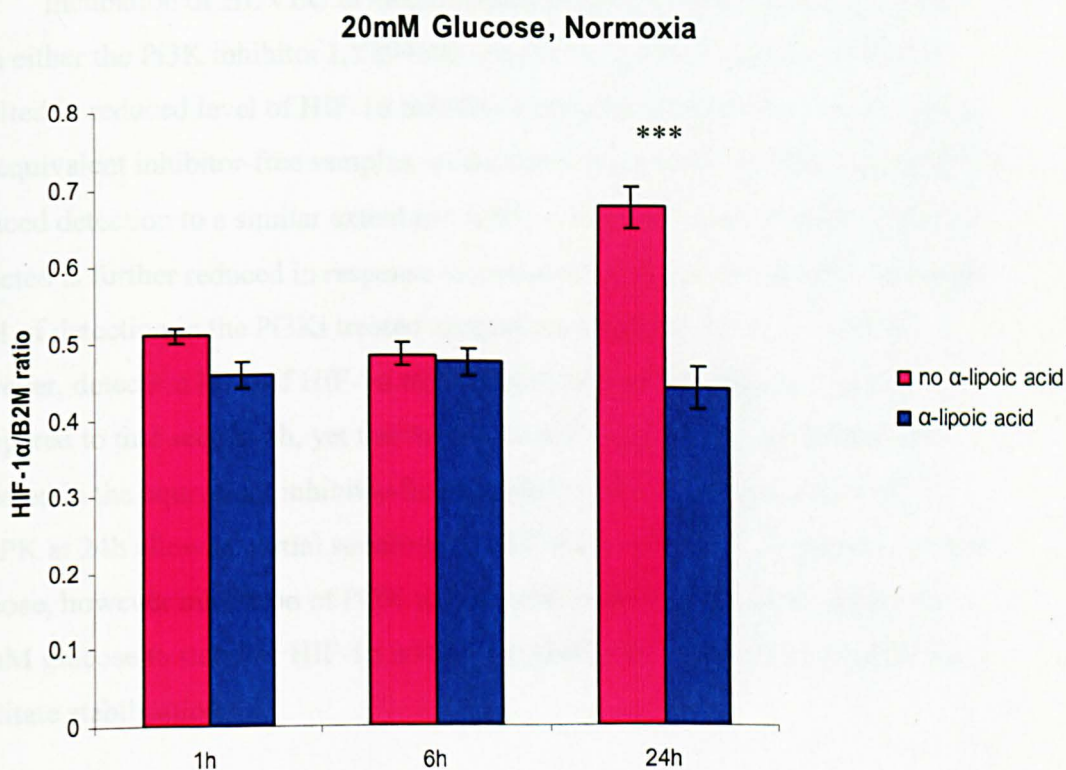


Figure 6.1: Effect of α -lipoic acid on HIF-1 α mRNA level detected. HUVEC were incubated in media containing 20mM glucose with or without α -lipoic acid, under normoxic conditions for 1, 6 and 24 hours. Total RNA was then extracted and used for reverse transcription. The resultant cDNAs were subsequently primed for HIF-1 α and B₂M (internal control) amplification by PCR, which was measured quantitatively on a plate reader using Picogreen detection. Treatment with α -lipoic acid resulted in reduced HIF-1 α mRNA detected at 24h ($p < 0.001$). Results shown are expressed as the ratio of HIF-1 α PCR product measured (ng) to that of B₂M (ng), and is representative of 3 separate experiments.

6.3.2 Effect of protein kinase inhibition on level of HIF-1 α mRNA detected

Incubation of HUVEC in media containing 20mM glucose supplemented with either the Pi3K inhibitor LY294002 or p42/44 MAPK inhibitor PD98059, resulted in reduced level of HIF-1 α mRNA detected at all time points compared to the equivalent inhibitor-free samples, as shown in figure 6.2. At 1h, both inhibitors reduced detection to a similar extent ($p < 0.01$). At 6h, the level of HIF-1 α mRNA detected is further reduced in response to treatment with p42/44 MAPKi, although level of detection in the Pi3Ki treated sample is unchanged from 1h. At 24h, however, detection level of HIF-1 α mRNA with p42/44 MAPKi was raised compared to that seen at 6h, yet this level was still significantly lower than that detected in the equivalent inhibitor-free sample ($p < 0.01$). Inhibition of p42/44 MAPK at 24h allowed partial stabilisation of HIF-1 α mRNA in response to 20mM glucose, however inhibition of Pi3K at 24h substantially reduced the ability of 20mM glucose to stabilise HIF-1 α mRNA ($p < 0.001$) or inhibited the signals the facilitate stabilisation.

20mM Glucose, Normoxia

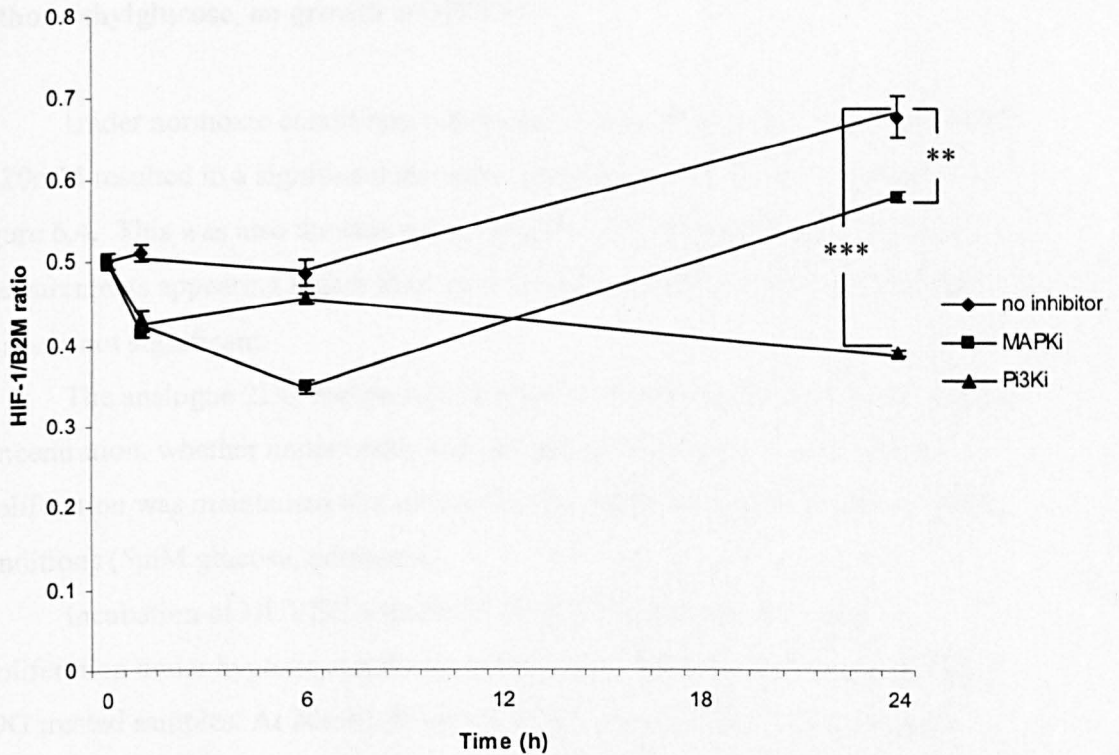


Figure 6.2: Effect of Pi3Ki and p42/44 MAPKi on HIF-1 α mRNA level detected. HUVEC were exposed media containing 20mM glucose with or without Pi3K inhibitor (Pi3Ki) or p42/44 MAPK inhibitor (MAPKi) under normoxic conditions for 0, 1, 6 and 24 hours. Total RNA was then extracted and used for reverse transcription. The resultant cDNAs were subsequently primed for HIF-1 α and B₂M amplification by PCR, which was measured quantitatively on a plate reader using Picogreen detection. At 24h, HIF-1 α mRNA detected in both Pi3Ki ($p < 0.001$) and p42/44 MAPKi ($p < 0.01$) treated samples was significantly lower than in the inhibitor free sample. Results shown are expressed as the ratio of HIF-1 α PCR product measured (ng) to that of B₂M (ng), and are representative of 3 separate experiments.

6.3.3 Effect of the glucose analogues, 2-deoxyglucose and 3-orthomethylglucose, on growth of HUVEC

Under normoxic conditions, increasing D-glucose concentration from 5mM to 20mM resulted in a significant increase in proliferation ($p<0.001$), as shown in figure 6.4. This was also the case under hypoxic conditions ($p<0.01$), with both measurements appearing higher than the equivalent normoxic samples, although this was not significant.

The analogue 2DG had no significant effect on cell growth at 24h at either concentration, whether under normoxic or hypoxic conditions. Furthermore, proliferation was maintained at a similar level to that seen under standard growth conditions (5mM glucose, normoxia).

Incubation of HUVEC with 5mM 3OMG did result in increased proliferation under hypoxic conditions compared to the equivalent D-glucose and 2DG treated samples. At 20mM, however, 3OMG had no significant effect on proliferation in normoxia or hypoxia compared to equivalent samples with the other two analogues. This was also significantly lower than that seen under hypoxic conditions with 5mM 3OMG ($p<0.01$).

6.3.4 Effect of the glucose analogues on HIF-1 α mRNA expression at 24 hours

As demonstrated in figure 6.4, HUVEC incubated for 24h with media containing 20mM of either 2-DG or 3-OMG in place of D-glucose under normoxic conditions, did not display stabilisation of HIF-1 α mRNA, as was observed in response to the equivalent sample incubated with D-glucose. Furthermore, no difference was observed in the level of detection in either of the 20mM analogue treated samples under hypoxic conditions compared to the D-glucose equivalent.

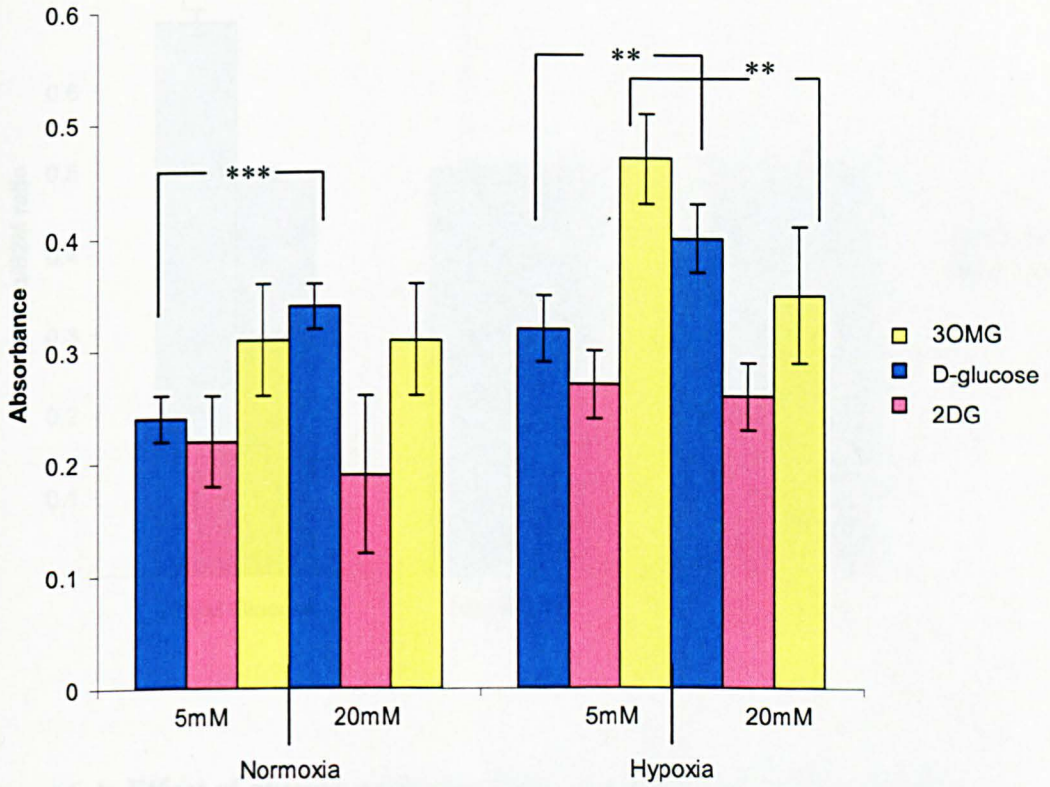


Figure 6.3. HUVEC growth in response to glucose analogues at 24h. HUVEC were seeded at a density of 0.025×10^6 cells/ml on a microtitre plate and allowed to grow overnight under standard conditions. Cells were then incubated with fresh growth media supplemented with D-glucose, 2DG or 3OMG and 10% (w/v) Alamar blue substrate. Plates were subsequently incubated under normoxic conditions, and cell proliferation measured at 24h on a colorimetric microplate reader as absorbance. Results shown are representative of $n=3$.

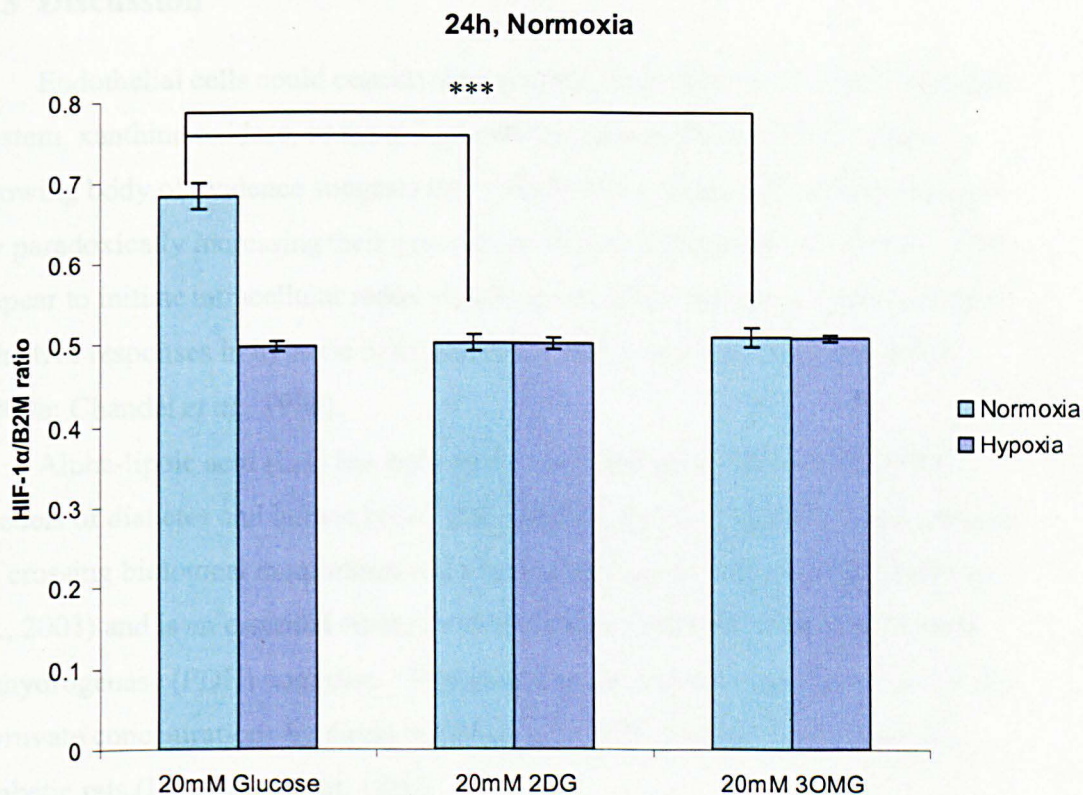


Figure 6.4: Effect of glucose analogues 2DG and 3OMG on HIF-1 α mRNA detection HUVEC were exposed to 5mM or 20mM of the glucose analogues 2-deoxyglucose (2DG) and 3-orthomethylglucose (3OMG), under normoxia for 24 hours. Total RNA was then extracted and used for reverse transcription. The resultant cDNAs were subsequently primed for HIF-1 α and B₂M (internal control) amplification by PCR, which was measured quantitatively on a plate reader using Picogreen detection. Neither analogue was capable of recreating the increase in HIF-1 α mRNA level detected in response to D-glucose ($p > 0.001$). Results shown are expressed as the ratio of HIF-1 α PCR product measured (ng) to that of B₂M (ng), and representative of $n=3$.

6.3 Discussion

Endothelial cells could conceivably generate ROS from an NAD(P)H oxidase system, xanthine oxidase, or the mitochondrial electron transport (ET) chain. A growing body of evidence suggests that mitochondria respond to cellular hypoxia by paradoxically increasing their generation of ROS (Chandel *et al.*, 2000a). ROS appear to initiate intracellular redox signaling and to contribute to a broad range of adaptive responses in hypoxic cells, including HIF-1 activation (Chandel *et al.*, 2000b; Chandel *et al.*, 1998).

Alpha-lipoic acid (LA) has been shown to lower glucose levels in animal models of diabetes and human type 2 diabetes (Packer *et al.*, 2001). LA is capable of crossing biological membranes and altering the redox status of cells (Tirosh *et al.*, 2003) and is an essential co-factor in oxidative metabolism via the pyruvate dehydrogenase (PDH) complex. This results in the reduction of serum lactate and pyruvate concentrations by direct stimulation of PDH activity, as observed in diabetic rats (Large & Beylot, 1999).

Lu and colleagues reported that pyruvate inhibits the activity of prolyl hydroxylases which degrade HIF-1 α protein under normoxic conditions, therefore maintaining the stability of HIF-1 α protein (Lu *et al.*, 2005). Therefore, our findings of reduced HIF-1 α mRNA stability in HUVEC incubated in 20mM glucose in the presence of LA may demonstrate that pyruvate is also capable of controlling HIF-1 α stability at the level of mRNA. However, this does not explain why the same effect is not seen in response to hypoxia, as anaerobic respiration due to lowered oxygen will also result in production of pyruvate.

LA is known to activate several components of the insulin signalling pathway including Pi3K and MAPK (Konrad *et al.*, 2001). Both Pi3K and MAPK pathways are implicated in enhancing HIF-1 protein expression and activity in tumour cells or cells stimulated by mitogenic signalling under normoxic conditions (Stiehl *et al.*, 2002; Zhong *et al.*, 2000). Of the few reports which detail the effect of such signalling on HIF-1 α mRNA, Pi3K is highlighted as an essential pathway in various

cell lines, while MAPK signalling appears to be of less significance (Tacchini *et al.*, 2001; Moeller *et al.*, 2005). In this study, Pi3K signalling was also seen to have a significant effect on the level of HIF-1 α mRNA in 20mM glucose with normoxia, as mRNA level detected at all time points was lower than in the equivalent inhibitor free sample. Increased HIF-1 α mRNA level was observed in response to high glucose at 24h with inhibition of p42/44 MAPK. In this case, absolute level of mRNA detected was not as high as that in the equivalent inhibitor free sample; however, the increase noted in the MAPKi sample was preceded by a marked reduction at 1 and 6h, therefore the magnitude of the increase was similar to that detected without inhibitor. This suggests that Pi3K signalling is necessary for the response to high glucose at 24h, and although p42/44 MAPK would appear to also be involved, inhibition of the p42/44 MAPK pathway does not actually prevent the increase in HIF-1 α mRNA.

At 24h, cell proliferation in the presence of 20mM D-glucose was increased compared to 5mM, in both normoxic and hypoxic samples, with hypoxia generally increasing cell growth compared to normoxia. In normoxia or hypoxia, increasing the concentration of 2DG from 5mM to 20mM had no significant effect on cell growth, which is not surprising, as the cell can't fully metabolise this analogue. Interestingly, all 2DG treatments at 24h resulted in proliferation rates which were not significantly different to that observed under standard growth conditions (5mM D-glucose, normoxia). It would seem, therefore, that 2DG despite only being recognised by hexokinase and trapped in the cell at that point, is not having a detrimental effect on cell growth. 3OMG, due to the methylation at position 3 is not recognised by hexokinase, not metabolised and free to leave the cell (Bessel *et al.*, 1972). Under normoxic conditions, 5mM 3OMG increased cell proliferation compared to its D-glucose equivalent. At 20mM, proliferation was equal to its D-glucose equivalent. This was also the case under hypoxic conditions.

Neither 2DG or 3OMG could recreate the increase in HIF-1 α mRNA stability seen at 24h in 20mM D-glucose with normoxia. As it has already been determined that cells are actively proliferating under conditions where D-glucose is replaced by a non-metabolizable analogue, the inability of either analogue to stabilise HIF-1 α

mRNA is not likely caused by any adverse effect on cell growth, but rather a product of hexose metabolism mediating the permissive effect of high glucose. Specifically, it appears that metabolism of glucose beyond glucose-6 phosphate is a necessary step. Therefore, it could be postulated that a metabolite of glucose beyond the first step, or perhaps energy or ROS generated as a result of glucose metabolism, is responsible for its effects on the stability of HIF-1 α mRNA.

HIF-1 itself promotes glycolytic metabolism through the induction of target genes such as GLUT-1, PFKF and MCT4. In HUVEC, this study has found that enhancement of the stability of HIF-1 α mRNA by glucose metabolites, or indeed the mediators of glycolysis, is coincident with reduced HIF-1 α protein expression. Therefore, metabolism of large amounts of glucose, along with the by products and/or enzymes involved in that process, may reduce the cells' ability to cope with an emerging state of pseudohypoxia.

Chapter 7

General Discussion

7.1 Summary of findings

This study has shown HIF-1 α protein to be expressed in the vasculature accompanying the sciatic nerve of a streptozotocin (STZ) rat model of diabetes. The increased HIF-1 α protein expression represented a chronic response to the disease, with elevated expression detected at 10 weeks disease duration. Expression was confined to the vasculature, and at 24 weeks, in addition to expression in vasculature surrounding the nerve, HIF-1 α was also detected within the intraneural vasculature of the sciatic nerve. Furthermore, supplementation of the STZ rat with α -lipoic acid visibly reduced the expression of HIF-1 α protein in the vasculature surrounding the sciatic nerve at 24 weeks.

Due to the location of the endothelium within the vessel as primary intimal contact for substances contained within the blood, an *in vitro* cell culture model of diabetes using HUVEC was employed in order to investigate the role of glucose in the induction of HIF-1 α expression in the diabetic vasculature. At 24h, the level of HIF-1 α mRNA detected increased significantly in response to incubation with 20mM glucose under normoxic conditions. This response appeared to arise from enhanced stability of the mRNA which was dependent upon *de novo* protein synthesis, as opposed to increased transcription.

Despite the enhanced stability of HIF-1 α mRNA in response to high glucose at 24h in HUVEC, HIF-1 α protein expression appeared to be reduced at this time point compared to that detected under normal growth conditions (5mM glucose, normoxia). Furthermore, expression of HIF-1 α protein also appeared to be reduced in the 20mM hypoxia sample compared to its 5mM equivalent, although no difference in mRNA levels were detected.

No change in mRNA level was detected in the HIF-1 α regulated genes GLUT-1 or IGF-1R at 24h in response to 20mM glucose in normoxia. At 6h incubation in 20mM glucose combined with normoxia, a small but significant increase in the level of the natural antisense of HIF-1 α mRNA (aHIF) was detected; however, this increase was not seen at 24h.

The mechanism by which high glucose concentration elicited increased stability of HIF-1 α mRNA expression appeared to be dependent upon signalling through Pi3K-dependent pathway/s and the presence of ROS, as indicated by the application α -lipoic acid preventing the increase in HIF-1 α mRNA level observed in response to high glucose alone.

The effect of D-glucose on HIF-1 α mRNA, as detailed above, was also observed to be directly attributable to the metabolizable nature of the hexose, as partial or non metabolizable analogues of D-glucose were incapable of conferring enhanced stability upon HIF-1 α mRNA at 24h under the same conditions.

7.2 Discussion

Hypoxic regulation of HIF-1 α expression has been well documented since the discovery of the transcription factor by Semenza and Wang in 1992. It is also appreciated that HIF-1 is subject to complex modulation in normoxia, and in contrast to the post-transcriptional control of hypoxia-induced HIF-1 α stability, non-hypoxic stimuli have been reported to regulate HIF-1 α through transcriptional and translational mechanisms involving ROS, PKC and Pi3K signalling (BelAiba *et al.*, 2004; Page *et al.*, 2002; Sandau *et al.*, 2001; Zelzer *et al.*, 1998).

Chronic expression of HIF-1 α protein may indicate a crucial role for HIF-1 α in mediating endothelial cell damage elicited by high circulatory concentrations of glucose, such as that experienced in poorly controlled diabetes. In this study, HIF-1 α protein expression was not found to be increased before 10 weeks disease duration in the rat model, therefore, we can postulate that hypoxia resulting from ischemia is not the sole cause, as hyperglycaemia-induced sciatic nerve blood flow reductions (Cameron *et al.*, 1991) result in tissue hypoxia at a much earlier stage of disease (Young *et al.*, 1992). Therefore, it would seem likely that upregulation is caused by hyperglycaemia in conjunction with hypoxia, which would suggest a level of cross-talk or interference between oxygen and glucose signalling, such as that demonstrated in the regulation of the glycolytic enzyme L-type pyruvate kinase

(L-PK) gene expression in the liver (Krones *et al.*, 2001), in which HIF-1 α may have a central role.

Although poor perfusion can't be ruled out as an explanation for the upregulation of HIF-1 α protein expression detected in the intraneural vasculature at 24 weeks, the persistence of hyperglycaemia-induced metabolic disruption may also contribute to this observation. Intraneural vascular expression of HIF-1 α may also serve as a marker of poor prognosis, indicating thickening of the intraneural vessel wall associated with progression of diabetic peripheral neuropathy.

While preparing this thesis, a study was published suggesting that HIF-1 α protein detected by Western blotting is transiently expressed within diabetic nerves, peaking at between 4 and 6 weeks and declining at 8 weeks after induction of diabetes (Chavez *et al.*, 2005). This group conclude that expression of HIF-1 α and its target genes do not represent a sustained response to chronic injury. However, the duration of the Chavez study was only 10 weeks, and did not take into account the influence of the vasculature supplying the nerves. Using IHC, we saw no non-vascular HIF-1 α protein expression within the nerve at any time point, but rather confined to the vessels surrounding the nerve at 10 weeks, which then progressed to vessels within the nerve at 24 weeks.

Despite reports of oxygen sensing and HIF-1 stabilization not involving the mitochondria (Srinivas *et al.*, 2001; Vaux *et al.*, 2001) it has been indicated that a functional electron transport chain (ETC) is required for the hypoxic stabilization of HIF-1 α protein via increased ROS (Chandel *et al.*, 2000). Increased levels of ROS reduce nitric oxide (NO) and compromise the perfusion of the peripheral nerve (Cameron *et al.*, 1991; Cameron and Cotter, 1997). Paradoxically, HIF-1 α has also been found to be essential for the hypoxic regulation of inducible NO synthase (iNOS) gene transcription in endothelial cells (Palmer & Johns, 1998).

Under hypoxic conditions, HIF-1 α and ROS may be involved in reciprocal regulation, whereby induction of HIF-1 α by ROS decreases mitochondrial oxygen consumption, ultimately leading to reduction of ROS (Papandreou *et al.*, 2006). This may be as a result of the ability of HIF-1 to trans-activate pyruvate dehydrogenase kinase 1 (PDK1), thereby reducing production of ROS by

preventing pyruvate from being metabolised by pyruvate dehydrogenase during the tricarboxylic acid cycle (TCA) (Kim *et al.*, 2006), while maintaining ATP production via glycolysis. Therefore, hypoxic activation of HIF-1 α acts as a metabolic switch which shunts glucose metabolites from the mitochondria to glycolysis (Guzy *et al.*, 2005).

The action of ROS scavengers such as α -lipoic acid, are markedly attenuated by NOS inhibitor co-treatment, therefore antioxidant repair of ROS mediated damage may potentially be dependent upon the induction of NOS by HIF-1 α . Thomsen *et al.* (2002) saw a transient increase in NOS within streptozotocin-induced diabetic rat sciatic nerve at 8-10 weeks, which coincides with the time point at which upregulation of HIF-1 α protein was first noted in this study.

It would also seem that when NO is present in increased concentrations, it then has a negative feed-back effect on HIF-1 α . This may be accounted for by the fact that NO is also able to inhibit mitochondrial respiration, thus increasing the availability of free oxygen (Mateo *et al.*, 2003) which can then be redistributed throughout the cell, and utilised by PHDs to degrade HIF-1 α in hypoxia (Hagen *et al.*, 2003).

The antioxidant α -lipoic acid has been shown to lower glucose levels in animal models of diabetes and human type 2 diabetes (Packer *et al.*, 2001). One hypothesis involves the stimulation of glucose transport by α -lipoic acid (Greene *et al.*, 2001) yet the mechanism of action and fate of glucose in the presence of α -lipoic acid remains to be elucidated. The effect of α -lipoic acid on blood glucose level at 24 weeks for the animals used in this study is not known, however at 8 weeks there was no significant reduction in blood glucose level in α -lipoic acid treated animals compared to diabetic control (Gibson *et al.*, 2003).

Results generated for this thesis have demonstrated inhibition of HIF-1 α protein accumulation in the 24 week diabetic rat in response to supplementation with α -lipoic acid, suggesting that expression of HIF-1 α in the diabetic rat vasculature may also be associated with induction of ROS by high glucose. As such, it is perhaps the ability of α -lipoic acid to correct redox imbalance, rather than reduce elevated glucose level *per se*, which is abrogating HIF-1 α protein expression in the vasculature. Furthermore, this regulation may be occurring prior to the

translation of HIF-1 α protein, as α -lipoic acid is also known to act as an effective iron chelator (Coleman & Walker, 2000; Packer *et al.*, 2001). As previously discussed, iron chelators are potent inducers of HIF-1 α protein stability; therefore reduction of HIF-1 α protein expression in the vasculature suggests that α -lipoic acid may actually be affecting HIF-1 α at a pre-translational level. Results obtained from the HUVEC model did indeed show α -lipoic acid to prevent increased HIF-1 α mRNA level in response to high glucose, although it is as yet unknown what effect this had on the expression of HIF-1 α protein.

A potential cause of peripheral neuropathy is endothelial cell hyperplasia (Britland *et al.*, 1990). Endothelial cells are highly predisposed to glucose induced injury, as demonstrated by previous groups (Knott *et al.*, 1996; Hammes, 2003; Creager *et al.*, 2003). However, just what effect such injury has on cell proliferation is subject to debate, and likely affected by the micro or macrovascular origin of the endothelial cell line. It has been reported that high glucose is toxic to micro and macrovascular endothelial cells *in vitro*, resulting in retarded cell proliferation (Ceriello *et al.*, 1996), disturbed cell cycle and increased DNA damage (Lorenzi *et al.*, 1986; Lorenzi *et al.*, 1987). In BREC, high glucose has been seen to result in decreased DNA synthesis, yet this was not accompanied by any change in proliferation (Knott *et al.*, 1998). This study demonstrated proliferation of HUVEC to increase in response to high glucose to a similar extent as in response to hypoxia, both of which were significantly higher than under normal growth conditions. Zanetti *et al.* (2001) and Wu *et al.* (1999) both detected increased HUVEC cell death on incubation with 28mM and 30mM glucose, respectively, following an incubation period of 48h. These observations, however, may be due to the build up of toxic by-products resulting from the metabolism of very high concentrations of glucose. Furthermore, cell death may also arise from overcrowding after such an extended growth period, as our investigation showed cell proliferation in 20mM glucose approaching a plateau at 29h. The concentration of glucose used in the afore-mentioned study is also very high, while we feel justified in the use of 20mM, as a physiological blood glucose level of just 8.3mM is considered high enough to put the person with diabetes at risk of serious

complications (Service & O'Brien, 2001). Increased cell growth may even be attributable to HIF-1 α expression in certain cases, as Yu and colleagues (2004) reported that HIF-1 α does actually exert an anti-apoptotic effect in HUVEC stressed by severe hypoxia.

Under normoxic conditions, ROS formation has been shown to destabilize HIF-1 α protein (Kietzmann *et al.*, 2000; Yang *et al.*, 2003) which may account for the reduced HIF-1 α protein expression observed in this study in HUVEC exposed to high glucose. Callapina and colleagues (2005) reported that induction of ROS in fact had a differential effect upon HIF-1 α stability in normoxic conditions, where high concentrations of superoxide blocked prolyl hydroxylase (PHD) activity and induced HIF-1 α accumulation under normoxic conditions, while low concentrations had the opposite effect. If this is the case in HUVEC, the observation of no increase in protein expression in the 24h normoxic and hypoxic samples treated with high glucose may indicate a lesser accumulation of ROS than that found in a 10 or 24 week diabetic animal, where protein was seen to increase. This would seem logical, and therefore account for the opposing effect of high glucose combined with hypoxia on HIF-1 α protein expression in the rat and HUVEC models of diabetes.

Several studies have indicated that chemically diverse nitric oxide (NO) donors also induce HIF-1 α stabilization, HIF-1 DNA binding and HIF-1 transactivation under normoxic conditions (Brune & Zhou, 2003). Similar to ROS, they achieve this effect by targeting the PHDs (Metzen *et al.*, 2003). In bovine aortic endothelial cells, high glucose has been shown to decrease the expression of constitutive NOS (cNOS) and iNOS, thus decreasing NO (Guo *et al.*, 2000). Although NO and peroxynitrite (ONOO) (formed on reaction of NO with superoxide) can cause endothelial and neuronal cell death in vitro, in animal models of diabetes, reductions in endothelial NO production can inhibit vasodilatation and cause nerve ischemia. Therefore, ideal therapeutic approaches should limit the formation of superoxides and ONOO while preventing reductions in vascular NO.

Although pre-translational regulation of HIF-1 α has been demonstrated in carcinogenesis (Jiang *et al.*, 2003) and wound healing (Zhong *et al.*, 1999), a novel

observation to arise from this study was the increase of HIF-1 α mRNA stability at 24h in HUVEC exposed to high glucose in normoxia. The increase in mRNA detected was not due to increased transcription, shown through the transcription inhibitor actinomycin D (Act D) having no effect on the level detected under high glucose conditions. However, the protein synthesis inhibitor cyclohexamide (CHX) was seen to prevent increase of HIF-1 α mRNA levels in response to high glucose. This indicated the necessity for de novo synthesis of a protein, which may be an RNA-binding protein, a protein kinase or phosphatase involved in signalling, or the HIF-1 α protein itself. This is in agreement with previous findings in retinal pigment epithelial cell lines (Treins *et al.*, 2002) whereby protein translation was considered to be a key factor in stabilisation of HIF-1 α mRNA.

In cortical neurones, such a response represents a protective mechanism in response to oxidative stress, leading to enhanced DNA binding of HIF-1 α and increased expression of glycolytic enzymes (Zaman *et al.*, 1999). In this case, regulation of HIF-1 α mRNA stability at 24h in high glucose is also likely to be dependent upon oxidative stress, shown by the ability of α -lipoic acid to prevent this stability.

The observations made were likely occurring via regulation of certain protein kinase signalling pathways activated by high glucose concentrations (Srivastava *et al.*, 2002). Campbell & Trimble (2005) have shown phosphorylation of Akt (downstream of Pi3K) and p42/44 MAPK to increase after 24h in VSMC exposed to high glucose. Potential signalling pathways regulating the expression of HIF-1 α under hypoxic and normoxic conditions at the level of transcription and translation are still subject to debate, however, p42/p44 MAPK has been implicated in HIF-1 α phosphorylation and promotion of transcriptional activation by HIF-1 (Conrad *et al.*, 1999, Richard *et al.*, 1999). MAPK also seems to regulate the basal activity of HIF-1 expression under normoxic conditions (Sang *et al.*, 2003). On the other hand, induction of HIF-1 α mRNA has been observed to be dependent upon the Akt-Pi3K pathway, but not p42/44 MAPK in human skin fibroblasts (Moeller *et al.*, 2005) and HepG2 cells (Tacchini *et al.*, 2001).

At 24h exposure of HUVEC to high glucose, this study found that inhibition of p42/44 MAPK reduced but did not abolish the stability of HIF-1 α mRNA in response to high glucose, while inhibition of Pi3K not only abolished increased stability, but also lowered basal levels. Under high glucose conditions, Akt activates the MAPK pathway (Campbell *et al.*, 2004). Therefore, by inhibiting Akt, this will also reduce the activity of MAPK and its downstream targets, which may explain why we found inhibition of Pi3K to have the greater effect. It is therefore possible to correlate our finding to those of Moeller and colleagues (2005) who determined induction of HIF-1 and subsequent activation of transporters and enzymes involved in glucose metabolism to be completely abrogated by inhibition of the Pi3K pathway, yet preserved under inhibition of the MAPK pathway.

McBain *et al.*, (2003) reported that BRECs exposed to high glucose concentrations are not sensitive to the HIF-1 regulated gene IGF-1 when compared to 5mM controls, and that this was in part due to a reduced activation of the p42/44 MAPK pathway. In this study, mRNA levels of other HIF-1 target genes, the IGF-1 receptor (IGF-1R) and glucose transporter GLUT-1, were found to be unaffected by high glucose after 24h incubation. This is not surprising, as the observation concurs with reduced HIF-1 α protein expression and aberrant sub-cellular location at this time, which would therefore result in disruption of the expression of glucose sensitive genes targeted by HIF-1.

Enhanced stability of HIF-1 α mRNA in response to high glucose in HUVEC may also have been attributable to altered expression of the natural antisense of HIF-1 α mRNA (aHIF), which binds to the instability element within the 3'UTR, targeting the mRNA for degradation (Thrash-Bingham *et al.*, 2002) and is expressed widely in normal and tumour tissue (Rossignol *et al.*, 2002). Observation of an increase in the level of aHIF preceding the increase in HIF-1 α mRNA at 24h, may indicate that at 6h the level of unbound aHIF is seen to increase due to it competing with something else which targets the 3'UTR of HIF-1 α mRNA, such as an RNA binding protein. Such a protein would require conditions of high glucose for production, and have the ability to bind the 3'UTR therefore modulating the ability of the mRNA to fold in stable secondary structures (Dreyfuss

et al., 1993). Any such disruption to the 3'UTR could prevent the binding of aHIF, and therefore prevent the mRNA being targeted for degradation.

The mRNA-stabilizing protein HuR, when expressed in the cytoplasm, is often accompanied by an increased association with the nucleocytoplasmic shuttling protein, pp32 (Cherradi *et al.*, 2006). If HuR were binding in this case, it may also rationalise the perinuclear location of HIF-1 α protein expression in addition to increased stability of the mRNA. The glycolytic enzyme, glyceraldehyde-3-phosphate dehydrogenase (GAPDH) is also known to be an RNA-binding protein (Nagy *et al.*, 1995). HIF-1 binding is necessary for the upregulation of GAPDH in EC under hypoxic conditions (Graven *et al.*, 1999) but nothing is known of GAPDHs effect on HIF-1 α . If GAPDH were found to be binding and having such an effect on HIF-1 α , this would enhance the theory that abundant GAPDH may also be involved in the regulation of a variety of cellular processes independently of its characteristic metabolic activity (Nagy *et al.*, 2000). Another glycolytic enzyme, lactate dehydrogenase (LDH) may also serve multiple roles in RNA metabolism beyond its role in glycolysis (Pioli *et al.*, 2002). Like GAPDH, LDH is known to be regulated by HIF-1 under hypoxic conditions (Firth *et al.*, 1995); however, we have no knowledge of how it may affect HIF-1 α in normoxia under conditions of high glucose, making these glycolytic enzymes ideal candidates for follow-up studies.

Expression of HIF-1 α protein in response to hypoxia was clearly evident at 24h in the nucleus of HUVEC. At the outset, this demonstrated HIF-1 α to be responsive to chronic hypoxia in endothelial cells, a trait which is not shared by all cell types, as lung epithelial cells are subject to acute regulation, shown by HIF-1 α protein peaking at 4h hypoxia, thereafter declining up to 12h (Uchida *et al.*, 2004).

In cells treated with high glucose for 24h, HIF-1 α protein expression was visibly decreased in both normoxic and hypoxic HUVEC compared to those treated with 5mM glucose, thus indicating glucose interfering not only with HIF-1 α mRNA expression, but extending to the level of protein expression. Furthermore, conditions of high glucose also resulted in the little expression which was evident being perinuclear. This is significant, because for HIF-1 to function as a

transcription factor, HIF-1 α requires to enter the nucleus in order to dimerize with HIF-1 β , thus forming the functional unit.

Reduced protein expression along with change in sub-cellular location at 24h in high glucose, may both result from the effect of regulatory protein binding to HIF-1 α mRNA, as described previously. Therefore, this suggests that the majority of HIF-1 α mRNA detected at 24h in high glucose may have accumulated as a result of its inability to be translated to protein. Furthermore, binding of RNA-regulatory protein/s, in addition to regulating stability, may also have a role in the trafficking of mRNA to the cytoplasm for packaging into protein (Tretyakova *et al.*, 2005). If this process is hampered in any way by elevated glucose, this could explain the reduced protein expression and aberrant sub-cellular location, all of which ties in with the earlier discussion of results relating to inhibition of translation, RNA binding proteins and induction of HIF-1 targeted genes.

Findings of reduced HIF-1 α protein expression are partially in accordance with those of Catrina and colleagues (2004), who reported hyperglycaemia to reduce hypoxia induced protein stability in human dermal microvascular endothelial cells (HDMEC). This study, however, reported that no effect on HIF-1 α protein expression was observed in HDMEC exposed to high glucose in the presence of normoxia. Observations made in the present study may therefore be organ specific rather than endothelium specific, as the kinetics of HIF-1 α expression are known to vary between organs (Stroka *et al.*, 2001). However, we can not directly compare the results from this study with that of Catrina, as we utilised a macrovascular cell line as opposed to microvascular. The actual stage of growth and conditions in which the cells were maintained in the Catrina study also differed quite considerably from this study. They exposed confluent cultures to media containing high glucose concentrations for 24 h preceding the experiment, whereas this study used 80% confluent cultures which had been incubated overnight in glucose free media in order to synchronize cell growth prior to applying the test conditions. These factors, therefore, may also account for the differences observed.

Considering the ability of HIF-1 to transactivate a variety of enzymes involved in the metabolism of glucose, it was prudent to question whether high

glucose *per se* or a product of its metabolism was responsible for the observations of increased HIF-1 α stability in response to high glucose concentration. Replacement of D-glucose with partially/non-metabolisable analogues did not mimic the effect of high D-glucose on mRNA stability at 24h under normoxic conditions. It has previously been reported that the end products of anaerobic glycolysis, lactate and pyruvate, are responsible for stabilization of HIF-1 α protein independently of hypoxia, whereas the citric acid cycle intermediates 2-oxoglutarate and succinate did not have this effect (Lu *et al.*, 2005). The observations of Lu *et al.* were made in a cancer cell line and were not in response to elevated glucose concentration, but neither were they in response to hypoxia, thereby providing evidence of the ability of the Warburg effect to regulate HIF-1 α . Therefore, in relation to this study, it presents the possibility of increased levels of pyruvate, resulting from increased metabolism of glucose, feeding into mitochondrial respiration with subsequent elevated production of ROS, as oxygen availability is not a limiting factor therefore the TCA cycle is not inhibited.

Previous investigation into the significance of HIF-1 expression in the diabetic microvasculature has highlighted the negative effect of its pro-angiogenic capabilities, such as is seen in diabetic retinopathy (Lukiw *et al.*, 2001) and tumour progression (Zhong *et al.*, 1998). However, induction of HIF-1 may also function as a metabolic switch which shunts glucose metabolites from the mitochondria to anaerobic glycolysis (Guzy *et al.*, 2005) thus reducing the production of ROS. Therefore, reducing the level of HIF-1 α protein within the nucleus may negate its protective effect in preventing induction of ROS via inhibition of mitochondrial respiration.

In the rat model, HIF-1 α protein expression was seen to increase in the vasculature after 10 weeks of diabetes. However, HUVEC treated with high glucose in the presence or absence of hypoxia did not show any upregulation of HIF-1 α protein expression, but rather increased the level of mRNA, but only in normoxic conditions. As discussed at the outset (section 1.6), these two models can not be directly compared. The complexity of the animal model does not allow

us to state whether glucose or hypoxia alone are the cause of changes observed, as the physiological system has many other factors impacting upon it.

Observations made in the rat model did, however, provide rationale for further investigation in the endothelial cell model of diabetes, due to the endothelium being in direct contact with the blood, although the results obtained appear conflicting. If conclusions can be drawn from the results obtained from these two models relating to the expression of HIF-1 α protein, it may be that vascular smooth muscle cells (VSMC) are in fact the primary source of elevated HIF-1 α protein expression in the rat model, as opposed to endothelial cells. A recent report has found that exposure of human VSMC to moderate hypoxia is sufficient to elicit increased cellular levels of HIF-1 α protein which then promote proliferative responses (Schultz *et al.*, 2006).

Excessive proliferation of VSMC in response to elevated HIF-1 arising from high glucose could therefore contribute to thickening of the vascular media, which would narrow the vessel lumen thus aggravating tissue ischaemia. It is possible, therefore, that the effects of pseudohypoxia arising from increased glucose levels and/or hypoxia experienced by the endothelium are magnified in VSMC. It is well known that EC and VSMC interactions play a critical role in the ability of the vessel to respond to vascular injury. Indeed, it was noted by Hodges and colleagues (2005) that chemical induction of HIF-1 α indirectly stimulated EC growth by directly stimulating VEGF production in VSMC, although there was no VEGF production detected in EC. This obviously highlights the caveats of working with isolated cell culture models, but also shows the individual responses of different vascular cell types to be working toward a common goal, in this case cell proliferation.

Antioxidant treatment reduced the appearance of HIF-1 α protein in the 24 week rat model of diabetes. Paradoxically, this may suggest that HIF-1 α has a protective role in the vasculature exposed to high glucose. The reasoning for this may lie in the ability of HIF-1 to act as a metabolic switch, which is capable of channelling glucose away from the mitochondria and into anaerobic respiration in a high ROS environment (Guzy *et al.*, 2005); therefore, reduction of ROS in response to antioxidant treatment would also result in reduction of HIF-1 α . In HUVEC, α -

lipoic acid may play a role in maintaining baseline level of HIF-1 α mRNA under conditions of high glucose, such as that seen in cardiomyocytes where reduction of oxidative stress inhibited the mitochondrial apoptotic pathway via maintenance of baseline HIF-1 α mRNA levels, as observed in cardiomyocytes exposed to hypoxia (Vassilopoulos & Papazafiri, 2005). Despite its reproducibility and relative ease of use, RT-PCR as a method of mRNA quantification is not without its limitations. As highlighted in chapter 4, RT-PCR does not directly measure mRNA expression, but rather amplification of the gene of interest reverse transcribed from cDNA.

Therefore, this must be recognised when interpreting mRNA data based solely on RT-PCR. Ideally, RT-PCR data should be verified using RPA, which is a method by which mRNA may be measured directly. In this study, attempts to detect mRNA by RPA were not successful. One reason for the lack of detection may have been the non-isotopic labelling of the probe. Indeed, available literature detailing HIF-1 α detection by RPA cites radioactive labelling (Ameri *et al.*, 2004), which is more sensitive for the detection of low abundance mRNAs.

By stabilizing HIF-1 α mRNA and allowing its accumulation in EC, high glucose may chronically reduce the expression of HIF-1 α protein below basal level in a normoxic environment to such an extent that the tissue becomes susceptible to oxidative damage. In a physiological system, this may be impacted upon by the responses of other vascular cell types, such as VSMC, which may potentially over-express HIF-1 α protein and its target genes in response to elevated glucose, the confirmation of which would be a primary aim of any future work.

Therefore, a scenario where EC already damaged by ROS are subject to excessive proliferation resulting from the production of factors such as VEGF by VSMC, would surely culminate in an endothelium which is seriously depleted of its ability to cope with unregulated blood glucose, thus perpetuating the chronic vascular complications associated with diabetes

7.3 Future work

Firstly, as discussed in the latter section of 7.2, the response of VSMC to elevated glucose must be considered in order to relate the events occurring in isolated EC to a realistic physiological situation, where these two vascular cell types are in permanent contact and able to communicate with one another.

In terms of extending existing data, it would be useful to validate the findings which relate to mRNA expression with *in situ* hybridisation (ISH). As discussed in chapter 4, the benefit of using ISH is that mRNA can be measured directly, which is not the case in Picogreen detection which measures mRNA indirectly as PCR product. Optimising the ISH protocol would in addition allow for the identification of exactly where in the cell the mRNA is being expressed, which could also have implications for binding of regulatory proteins

The majority of the published work within this field indicates that HIF-1 α mRNA levels do not change, despite the fact that the 3'UTR of the mRNA contains sequences known to be associated with mRNA stability. As we determined increased levels of HIF-1 α mRNA in response to high glucose to depend upon enhanced stability, it is necessary to establish what is the exact involvement of the 3'UTR. The significance of mRNA stability in terms of protein translation was also not fully addressed within this study, as the reduced expression of protein which is referred to in this report is not based upon quantitative measurements, but rather visual appreciation by IHC detection in HUVEC, therefore Western blotting would need to be employed to validate this. What was perhaps of greater significance to the interpretation of the results, was the subcellular location of the protein expression, as opposed to actual protein level, therefore it is also important to investigate the dual role of the 3'UTR in directing stability and subcellular localisation of the mRNA, and the consequence of protein binding on these processes.

The involvement of signalling pathways, including Pi3K and MAPK should also be verified at the level of HIF-1 α protein expression. We hypothesised that Pi3K may feed into p42/44 MAPK signalling; which could also be verified by dual

inhibition of both pathways. Furthermore, stabilization of mRNA often depends on activation of p38 mitogen-activated protein kinase (p38 MAPK) (Fechir *et al.*, 2005). Therefore it would be of interest to see what effect inhibition of p38 MAPK would have upon RNA-protein binding and subsequent expression of HIF-1 α mRNA and protein.

The contribution of mitochondrial generation of ROS to HIF-1 α expression should also be considered, as initial experimentation in both the rat and HUVEC model of diabetes implicated antioxidant treatment in the reduction of HIF-1 α protein and mRNA detection, respectively. At this point, it is essential to investigate HIF-1 α protein status in the HUVEC model of diabetes treated with antioxidant, and it would also be very interesting to look at the levels of expression in the 4 and 10 week rat model supplemented with α -lipoic acid. Further investigation into the role of the mitochondria would be possible by detecting the effect of the mitochondria-targeted antioxidant, mitoubiquinone (MitoQ) on HIF-1 α mRNA and protein under conditions of high glucose. An inhibitor of the TCA cycle, monofluoroacetate, could also be used to verify whether or not ROS of mitochondrial origin is central to any observation.

Our finding of the inability of the non-metabolizable analogues of glucose to induce stability of HIF-1 α mRNA must also be further investigated at the level of protein expression. By using inhibitors of the glycolytic enzymes, such as GAPDH or phosphoglycerate kinase, the critical point the metabolism of glucose which may dictate the observed effects on HIF-1 α expression could be predicted, or with the use of pyruvate dehydrogenase, whether these results are indeed dependent on the end product of anaerobic glycolysis.

In conclusion, regulation of HIF-1 α at the level of protein and mRNA has demonstrated a novel mechanism by which oxidative demand placed upon the cell through the need to metabolise high concentrations of glucose may be contributing to the progression of vascular complications. As such, this research requires to be validated and further extended, in order to explore whether targeting this mechanism could represent a therapeutic strategy for the reduction and prevention of chronic vascular disease associated with diabetes.

Appendix 1

References

AGANI, F. and SEMENZA, G.L., 1998. Mersalyl is a novel inducer of vascular endothelial growth factor gene expression and hypoxia-inducible factor 1 activity. *Molecular pharmacology*, 54(5), pp. 749-754

AGANI, F.H., PUCHOWICZ, M., CHAVEZ, J.C., PICHIULE, P. and LAMANNA, J., 2002. Role of nitric oxide in the regulation of HIF-1 alpha expression during hypoxia. *American Journal of Physiology. Cell physiology*, 283(1), pp. C178-86

AHN, S.J., COSTA, J. and EMANUEL, J.R., 1996. PicoGreen quantitation of DNA: effective evaluation of samples pre- or post-PCR. *Nucleic acids research*, 24(13), pp. 2623-2625

AI, E., 1992. Current management of diabetic retinopathy. *The Western journal of medicine*, 157(1), pp. 67-70

AKAKURA, N., KOBAYASHI, M., HORIUCHI, I., SUZUKI, A., WANG, J., CHEN, J., NIIZEKI, H., KAWAMURA, K., HOSOKAWA, M. and ASAKA, M., 2001. Constitutive expression of hypoxia-inducible factor-1alpha renders pancreatic cancer cells resistant to apoptosis induced by hypoxia and nutrient deprivation. *Cancer research*, 61(17), pp. 6548-6554

AKBARI, C.M., GIBBONS, G.W., HABERSHAW, G.M., LOGERFO, F.W. and VEVES, A., 1997. The effect of arterial reconstruction on the natural history of diabetic neuropathy. *Archives of Surgery (Chicago, Ill. : 1960)*, 132(2), pp. 148-152

ALBINA, J.E., MASTROFRANCESCO, B., VESSELLA, J.A., LOUIS, C.A., HENRY, W.L., JR and REICHNER, J.S., 2001. HIF-1 expression in healing wounds: HIF-1alpha induction in primary inflammatory cells by TNF-alpha. *American Journal of Physiology. Cell physiology*, 281(6), pp. C1971-7

ALFRANCA, A., GUTIERREZ, M.D., VARA, A., ARAGONES, J., VIDAL, F. and LANDAZURI, M.O., 2002. c-Jun and hypoxia-inducible factor 1 functionally cooperate in hypoxia-induced gene transcription. *Molecular and cellular biology*, 22(1), pp. 12-22

AMANO, K., OKIGAKI, M., ADACHI, Y., FUJIYAMA, S., MORI, Y., KOSAKI, A., IWASAKA, T. and MATSUBARA, H., 2004. Mechanism for IL-1 beta-mediated neovascularization unmasked by IL-1 beta knock-out mice. *Journal of Molecular and Cellular Cardiology*, 36(4), pp. 469-480

AMERI, K., LEWIS, C.E., RAIDA, M., SOWTER, H., HAI, T. and HARRIS, A.L., 2004. Anoxic induction of ATF-4 through HIF-1-independent pathways of protein stabilization in human cancer cells. *Blood*, 103(5), pp. 1876-1882

ANTONETTI, D.A., BARBER, A.J., HOLLINGER, L.A., WOLPERT, E.B. and GARDNER, T.W., 1999. Vascular endothelial growth factor induces rapid phosphorylation of tight junction proteins occludin and zonula occluden 1. A potential mechanism for vascular permeability in diabetic retinopathy and tumors. *Journal of Biological Chemistry*, 274(33), pp. 23463-23467

ARANY, Z., HUANG, L.E., ECKNER, R., BHATTACHARYA, S., JIANG, C., GOLDBERG, M.A., BUNN, H.F. and LIVINGSTON, D.M., 1996. An essential role for p300/CBP in the cellular response to hypoxia. *Proceedings of the National Academy of Sciences of the United States of America*, 93(23), pp. 12969-12973

ARSHAM, A.M., PLAS, D.R., THOMPSON, C.B. and SIMON, M.C., 2002. Phosphatidylinositol 3-kinase/Akt signaling is neither required for hypoxic stabilization of HIF-1 alpha nor sufficient for HIF-1-dependent target gene transcription. *Journal of Biological Chemistry*, 277(17), pp. 15162-15170

AUSSERER, W.A., BOURRAT-FLOECK, B., GREEN, C.J., LADEROUTE, K.R. and SUTHERLAND, R.M., 1994. Regulation of c-jun expression during hypoxic and low-glucose stress. *Molecular and cellular biology*, 14(8), pp. 5032-5042

BAYNES, J.W., 1991. Role of oxidative stress in development of complications in diabetes. *Diabetes*, 40(4), pp. 405-412

BELAIBA, R.S., DJORDJEVIC, T., BONELLO, S., FLUGEL, D., HESS, J., KIETZMANN, T. and GORLACH, A., 2004. Redox-sensitive regulation of the HIF pathway under non-hypoxic conditions in pulmonary artery smooth muscle cells. *Biological chemistry*, 385(3-4), pp. 249-257

BESSION, A., ROBBINS, S.M. and YONG, V.W., 1999. PTEN/MMAC1/TEP1 in signal transduction and tumorigenesis. *European journal of biochemistry / FEBS*, 263(3), pp. 605-611

BEVILACQUA, M.P., STENGELIN, S., GIMBRONE, M.A.,JR and SEED, B., 1989. Endothelial leukocyte adhesion molecule 1: an inducible receptor for neutrophils related to complement regulatory proteins and lectins. *Science*, 243(4895), pp. 1160-1165

BIEDERMAN, J., YEE, J. and CORTES, P., 2004. Validation of internal control genes for gene expression analysis in diabetic glomerulosclerosis. *Kidney international*, 66(6), pp. 2308-2314

BIJU, M.P., AKAI, Y., SHRIMANKER, N and HAASE, V.H., 2005. Protection of HIF-1-deficient primary renal tubular epithelial cells from hypoxia-induced cell death is glucose dependent. *American Journal of Physiology and Renal Physiology*, 289, pp. 1217-1226

BLANCHER, C., MOORE, J.W., TALKS, K.L., HOULBROOK, S., and HARRIS, A.L., 2000. Relationship of hypoxia-inducible factor (HIF)-1 α and HIF-2 α expression to vascular endothelial growth factor induction and hypoxia survival in human breast cancer cell lines. *Cancer Research*, 60, pp. 7106-7113

BOES, M., DAKE, B.L. and BAR, R.S., 1991. Interactions of cultured endothelial cells with TGF-beta, bFGF, PDGF and IGF-I. *Life Sciences*, 48(8), pp. 811-821

BONE, A.J., BANISTER, S.H. and ZHANG, S., 1997. The REG gene and islet cell repair and renewal in type 1 diabetes. *Advances in Experimental Medicine and Biology*, 426, pp. 321-327

BONNARDEL-PHU, E., WAUTIER, J.L., SCHMIDT, A.M., AVILA, C. and VICAUT, E., 1999. Acute modulation of albumin microvascular leakage by advanced glycation end products in microcirculation of diabetic rats in vivo. *Diabetes*, 48(10), pp. 2052-2058

BOOTH, G., STALKER, T.J., LEFER, A.M. and SCALIA, R., 2002. Mechanisms of amelioration of glucose-induced endothelial dysfunction following inhibition of protein kinase C in vivo. *Diabetes*, 51(5), pp. 1556-1564

BRAUN, L., KARDON, T., REISZ-PORSZASZ, Z.S., BANHEGYI, G. and MANDL, J., 2001. The regulation of the induction of vascular endothelial growth factor at the onset of diabetes in spontaneously diabetic rats. *Life Sciences*, 69(21), pp. 2533-2542

BRIAUD, I., LINGOHR, M.K., DICKSON, L.M., WREDE, C.E. and RHODES, C.J., 2003. Differential activation mechanisms of Erk-1/2 and p70(S6K) by glucose in pancreatic beta-cells. *Diabetes*, 52(4), pp. 974-983

BROOKS, G.A., HENDERSON, S.A. and DALLMAN, P.R., 1987. Increased glucose dependence in resting, iron-deficient rats. *The American Journal of Physiology*, 253(4 Pt 1), pp. E461-6

BROWNLEE, M., 2001. Biochemistry and molecular cell biology of diabetic complications. *Nature*, 414(6865), pp. 813-820

BRUICK, R.K., 2000. Expression of the gene encoding the proapoptotic Nip3 protein is induced by hypoxia. *Proceedings of the National Academy of Sciences of the United States of America*, 97(16), pp. 9082-9087

BRUICK, R.K. and MCKNIGHT, S.L., 2001. A conserved family of prolyl-4-hydroxylases that modify HIF. *Science*, 294(5545), pp. 1337-1340

BRUNE, B. and ZHOU, J., 2003. The role of nitric oxide (NO) in stability regulation of hypoxia inducible factor-1alpha (HIF-1alpha). *Current medicinal chemistry*, 10(10), pp. 845-855

BURATTI, E. and BARALLE, F.E., 2004. Influence of RNA secondary structure on the pre-mRNA splicing process. *Molecular and cellular biology*, 24(24), pp. 10505-10514

CALDWELL, R.B., BARTOLI, M., BEHZADIAN, M.A., EL-REMESSY, A.E., AL-SHABRAWAY, M., PLATT, D.H. and CALDWELL, R.W., 2003. Vascular endothelial growth factor and diabetic retinopathy: pathophysiological mechanisms and treatment perspectives. *Diabetes/metabolism research and reviews*, 19(6), pp. 442-455

CALLAPINA, M., ZHOU, J., SCHMID, T., KOHL, R. and BRUNE, B., 2005. NO restores HIF-1alpha hydroxylation during hypoxia: role of reactive oxygen species. *Free radical biology & medicine*, 39(7), pp. 925-936

CAMERON, N.E. and COTTER, M.A., 1992. Dissociation between biochemical and functional effects of the aldose reductase inhibitor, ponalrestat, on peripheral nerve in diabetic rats. *British journal of pharmacology*, 107(4), pp. 939-944

CAMERON, N.E. and COTTER, M.A., 1997. Metabolic and vascular factors in the pathogenesis of diabetic neuropathy. *Diabetes*, 46 Suppl 2, pp. S31-7

CAMERON, N.E. and COTTER, M.A., 1999. Effects of antioxidants on nerve and vascular dysfunction in experimental diabetes. *Diabetes research and clinical practice*, 45(2-3), pp. 137-146

CAMERON, N.E. and COTTER, M.A., 2003. The effects of 5-hydroxytryptamine 5-HT₂ receptor antagonists on nerve conduction velocity and endoneurial perfusion in diabetic rats. *Naunyn-Schmiedeberg's archives of pharmacology*, 367(6), pp. 607-614

CAMERON, N.E., COTTER, M.A., JACK, A.M., BASSO, M.D. and HOHMAN, T.C., 1999. Protein kinase C effects on nerve function, perfusion, Na(+), K(+)-ATPase activity and glutathione content in diabetic rats. *Diabetologia*, 42(9), pp. 1120-1130

CAMERON, N.E., COTTER, M.A. and LOW, P.A., 1991. Nerve blood flow in early experimental diabetes in rats: relation to conduction deficits. *The American Journal of Physiology*, 261(1 Pt 1), pp. E1-8

CAMERON, N.E., COTTER, M.A. and MAXFIELD, E.K., 1993. Anti-oxidant treatment prevents the development of peripheral nerve dysfunction in streptozotocin-diabetic rats. *Diabetologia*, 36(4), pp. 299-304

CAMERON, N.E., EATON, S.E., COTTER, M.A. and TESFAYE, S., 2001. Vascular factors and metabolic interactions in the pathogenesis of diabetic neuropathy. *Diabetologia*, 44(11), pp. 1973-1988

CAMPBELL, M., ALLEN, W.E., SAWYER, C., VANHAESEBROECK, B. and TRIMBLE, E.R., 2004. Glucose-potentiated chemotaxis in human vascular smooth muscle is dependent on cross-talk between the PI3K and MAPK signaling pathways. *Circulation research*, 95(4), pp. 380-388

CAMPBELL, M., ALLEN, W.E., SILVERSIDES, J.A. and TRIMBLE, E.R., 2003. Glucose-induced phosphatidylinositol 3-kinase and mitogen-activated protein kinase-dependent upregulation of the platelet-derived growth factor-beta receptor potentiates vascular smooth muscle cell chemotaxis. *Diabetes*, 52(2), pp. 519-526

CAMPBELL, M. and TRIMBLE, E.R., 2005. Modification of PI3K- and MAPK-dependent chemotaxis in aortic vascular smooth muscle cells by protein kinase CbetaII. *Circulation research*, 96(2), pp. 197-206

CANIGGIA, I., WINTER, J., LYE, S.J. and POST, M., 2000. Oxygen and placental development during the first trimester: implications for the pathophysiology of pre-eclampsia. *Placenta*, 21 Suppl A, pp. S25-30

CANTLEY, L.C. and NEEL, B.G., 1999. New insights into tumor suppression: PTEN suppresses tumor formation by restraining the phosphoinositide 3-kinase/AKT pathway. *Proceedings of the National Academy of Sciences of the United States of America*, 96(8), pp. 4240-4245

CAPUTI, M. and ZAHLER, A.M., 2002. SR proteins and hnRNP H regulate the splicing of the HIV-1 tev-specific exon 6D. *The EMBO journal*, 21(4), pp. 845-855

CARBALLO, E., LAI, W.S. and BLACKSHEAR, P.J., 2000. Evidence that tristetraprolin is a physiological regulator of granulocyte-macrophage colony-stimulating factor messenger RNA deadenylation and stability. *Blood*, 95(6), pp. 1891-1899

CARRERO, P., OKAMOTO, K., COUMAILLEAU, P., O'BRIEN, S., TANAKA, H. and POELLINGER, L., 2000. Redox-regulated recruitment of the transcriptional coactivators CREB-binding protein and SRC-1 to hypoxia-inducible factor 1alpha. *Molecular and cellular biology*, 20(1), pp. 402-415

CARROLL, V.A., and ASHCROFT, M., 2006. Role of hypoxia-inducible factor (HIF)-1alpha versus HIF-2alpha in the regulation of HIF target genes in response to hypoxia, insulin-like growth factor-1, or loss of von Hippel-Lindau function: implications for targeting the HIF pathway. *Cancer Research*, 66(12), pp. 6264-6270

CARROZZA, M.J., UTLEY, R.T., WORKMAN, J.L. and COTE, J., 2003. The diverse functions of histone acetyltransferase complexes. *Trends in genetics : TIG*, 19(6), pp. 321-329

CATRINA, S.B., OKAMOTO, K., PEREIRA, T., BRISMAR, K. and POELLINGER, L., 2004. Hyperglycemia regulates hypoxia-inducible factor-1alpha protein stability and function. *Diabetes*, 53(12), pp. 3226-3232

CAYRE, A., ROSSIGNOL, F., CLOTTE, E. and PENAULT-LLORCA, F., 2003. aHIF but not HIF-1alpha transcript is a poor prognostic marker in human breast cancer. *Breast cancer research (Print)*, 5(6), pp. R223-30

CERIELLO, A., DELLO RUSSO, P., AMSTAD, P. and CERUTTI, P., 1996. High glucose induces antioxidant enzymes in human endothelial cells in culture. Evidence linking hyperglycemia and oxidative stress. *Diabetes*, 45(4), pp. 471-477

CERIELLO, A., QUATRARO, A. and GIUGLIANO, D., 1993. Diabetes mellitus and hypertension: the possible role of hyperglycaemia through oxidative stress. *Diabetologia*, 36(3), pp. 265-266

CHAN, T.O., RITTENHOUSE, S.E. and TSICHLIS, P.N., 1999. AKT/PKB and other D3 phosphoinositide-regulated kinases: kinase activation by phosphoinositide-dependent phosphorylation. *Annual Review of Biochemistry*, 68, pp. 965-1014

CHANDEL, N.S., MCCLINTOCK, D.S., FELICIANO, C.E., WOOD, T.M., MELENDEZ, J.A., RODRIGUEZ, A.M. and SCHUMACKER, P.T., 2000. Reactive oxygen species generated at mitochondrial complex III stabilize hypoxia-inducible factor-1alpha during hypoxia: a mechanism of O₂ sensing. *Journal of Biological Chemistry*, 275(33), pp. 25130-25138

CHANDEL, N.S., TRZYNA, W.C., MCCLINTOCK, D.S. and SCHUMACKER, P.T., 2000. Role of oxidants in NF-kappa B activation and TNF-alpha gene transcription induced by hypoxia and endotoxin. *Journal of immunology (Baltimore, Md. : 1950)*, 165(2), pp. 1013-1021

CHANG, H., SHYU, K.G., LIN, S., TSAI, S.C., WANG, B.W., LIU, Y.C., SUNG, Y.L. and LEE, C.C., 2003. The plasminogen activator inhibitor-1 gene is induced by cell adhesion through the MEK/ERK pathway. *Journal of Biomedical Science*, 10(6 Pt 2), pp. 738-745

CHANG, T.C., HUANG, C.J., TAM, K., CHEN, S.F., TAN, K.T., TSAI, M.S., LIN, T.N. and SHYUE, S.K., 2005. Stabilization of hypoxia-inducible factor-1 {alpha} by prostacyclin under prolonged hypoxia via reducing reactive oxygen species level in endothelial cells. *Journal of Biological Chemistry*, 280(44), pp. 36567-36574

CHAVEZ, J.C., ALMHANNA, K. and BERTI-MATTERA, L.N., 2005. Transient expression of hypoxia-inducible factor-1 alpha and target genes in peripheral nerves from diabetic rats. *Neuroscience letters*, 374(3), pp. 179-182

CHAVEZ, J.C., BARANOVA, O., LIN, J., PICHIULE, P., 2006. The transcriptional activator hypoxia inducible factor 2 (HIF-2/EPAS-1) regulates the oxygen-dependent expression of erythropoietin in cortical astrocytes. *The Journal of Neuroscience*, 26(37), pp. 9471-9481

CHEN, C., PORE, N., BEHROOZ, A., ISMAIL-BEIGI, F. and MAITY, A., 2001. Regulation of glut1 mRNA by hypoxia-inducible factor-1. Interaction between H-ras and hypoxia. *Journal of Biological Chemistry*, 276(12), pp. 9519-9525

CHERRADI, N., LEJCZAK, C., DESROCHES-CASTAN, A. and FEIGE, J.J., 2006. Antagonistic functions of tetradecanoyl phorbol acetate-inducible-sequence 11b and HuR in the hormonal regulation of vascular endothelial growth factor messenger ribonucleic acid stability by adrenocorticotropin. *Molecular endocrinology (Baltimore, Md.)*, 20(4), pp. 916-930

CHISALITA, S.I. and ARNQVIST, H.J., 2004. Insulin-like growth factor I receptors are more abundant than insulin receptors in human micro- and macrovascular endothelial cells. *American Journal of Physiology. Endocrinology and Metabolism*, 286(6), pp. E896-901

COLEMAN, M.D. and WALKER, C.L., 2000. Effects of oxidised alpha-lipoic acid and alpha-tocopherol on xenobiotic-mediated methaemoglobin formation in diabetic and non-diabetic human erythrocytes in-vitro. *Environmental toxicology and pharmacology*, 8(2), pp. 127-132

COLLIER, A. and SMALL, M., 1991. The role of the polyol pathway in diabetes mellitus. *British journal of hospital medicine*, 45(1), pp. 38-40

CONRAD, P.W., FREEMAN, T.L., BEITNER-JOHNSON, D. and MILLHORN, D.E., 1999. EPAS1 trans-activation during hypoxia requires p42/p44 MAPK. *Journal of Biological Chemistry*, 274(47), pp. 33709-33713

COPPEY, L.J., GELLETT, J.S., DAVIDSON, E.P., DUNLAP, J.A., LUND, D.D. and YOREK, M.A., 2001. Effect of antioxidant treatment of streptozotocin-induced diabetic rats on endoneurial blood flow, motor nerve conduction velocity, and vascular reactivity of epineurial arterioles of the sciatic nerve. *Diabetes*, 50(8), pp. 1927-1937

CREAGER, M.A., LUSCHER, T.F., COSENTINO, F. and BECKMAN, J.A., 2003. Diabetes and vascular disease: pathophysiology, clinical consequences, and medical therapy: Part I. *Circulation*, 108(12), pp. 1527-1532

DAHLFORS, G. and ARNQVIST, H.J., 2000. Vascular endothelial growth factor and transforming growth factor-beta1 regulate the expression of insulin-like growth factor-binding protein-3, -4, and -5 in large vessel endothelial cells. *Endocrinology*, 141(6), pp. 2062-2067

DAKO CORPORATION. 1989. *Immunochemical Staining Methods Handbook*.

DAMES, S.A., MARTINEZ-YAMOUT, M., DE GUZMAN, R.N., DYSON, H.J. and WRIGHT, P.E., 2002. Structural basis for Hif-1 alpha /CBP recognition in the cellular hypoxic response. *Proceedings of the National Academy of Sciences of the United States of America*, 99(8), pp. 5271-5276

- DEBOSCH, B.J., BAUR, E., DEO, B.K., HIRAOKA, M. and KUMAGAI, A.K., 2001. Effects of insulin-like growth factor-1 on retinal endothelial cell glucose transport and proliferation. *Journal of neurochemistry*, 77(4), pp. 1157-1167
- DECKERT, T., KOFOED-ENEVOLDSEN, A., NORGAARD, K., BORCH-JOHNSEN, K., FELDT-RASMUSSEN, B. and JENSEN, T., 1992. Microalbuminuria. Implications for micro- and macrovascular disease. *Diabetes care*, 15(9), pp. 1181-1191
- DIABETES UK, 2004. *Diabetes in the UK 2004. A report from Diabetes UK.*
- DIABETES UK, 2005. *Diabetes: State of the Nations 2005. Progress made in delivering the national diabetes frameworks.*
- DREYFUSS, G., MATUNIS, M.J., PINOL-ROMA, S. and BURD, C.G., 1993. hnRNP proteins and the biogenesis of mRNA. *Annual Review of Biochemistry*, 62, pp. 289-321
- DUYNDAM, M.C., HULSCHER, T.M., FONTIJN, D., PINEDO, H.M. and BOVEN, E., 2001. Induction of vascular endothelial growth factor expression and hypoxia-inducible factor 1alpha protein by the oxidative stressor arsenite. *Journal of Biological Chemistry*, 276(51), pp. 48066-48076
- DVORAK, H.F., NAGY, J.A., FENG, D., BROWN, L.F. and DVORAK, A.M., 1999. Vascular permeability factor/vascular endothelial growth factor and the significance of microvascular hyperpermeability in angiogenesis. *Current topics in microbiology and immunology*, 237, pp. 97-132
- DYCK, P.J. and GIANNINI, C., 1996. Pathologic alterations in the diabetic neuropathies of humans: a review. *Journal of neuropathology and experimental neurology*, 55(12), pp. 1181-1193
- ELSON, D.A., RYAN, H.E., SNOW, J.W., JOHNSON, R. and ARBEIT, J.M., 2000. Coordinate up-regulation of hypoxia inducible factor (HIF)-1alpha and HIF-1 target genes during multi-stage epidermal carcinogenesis and wound healing. *Cancer research*, 60(21), pp. 6189-6195
- EMA, M., HIROTA, K., MIMURA, J., ABE, H., YODOI, J., SOGAWA, K., POELLINGER, L. and FUJII-KURIYAMA, Y., 1999. Molecular mechanisms of transcription activation by HLF and HIF1alpha in response to hypoxia: their stabilization and redox signal-induced interaction with CBP/p300. *The EMBO journal*, 18(7), pp. 1905-1914

- EMERLING, B.M., PLATANIAS, L.C., BLACK, E., NEBREDA, A.R., DAVIS, R.J. and CHANDEL, N.S., 2005. Mitochondrial reactive oxygen species activation of p38 mitogen-activated protein kinase is required for hypoxia signaling. *Molecular and cellular biology*, 25(12), pp. 4853-4862
- EPSTEIN, A.C., GLEADLE, J.M., MCNEILL, L.A., HEWITSON, K.S., O'ROURKE, J., MOLE, D.R., MUKHERJI, M., METZEN, E., WILSON, M.I., DHANDA, A., TIAN, Y.M., MASSON, N., HAMILTON, D.L., JAAKKOLA, P., BARSTEAD, R., HODGKIN, J., MAXWELL, P.H., PUGH, C.W., SCHOFIELD, C.J. and RATCLIFFE, P.J., 2001. C. elegans EGL-9 and mammalian homologs define a family of dioxygenases that regulate HIF by prolyl hydroxylation. *Cell*, 107(1), pp. 43-54
- FACCHINI, F.S., CARANTONI, M., JEPPESEN, J. and REAVEN, G.M., 1998. Hematocrit and hemoglobin are independently related to insulin resistance and compensatory hyperinsulinemia in healthy, non-obese men and women. *Metabolism: clinical and experimental*, 47(7), pp. 831-835
- FATYOL, K. and SZALAY, A.A., 2001. The p14ARF tumor suppressor protein facilitates nucleolar sequestration of hypoxia-inducible factor-1alpha (HIF-1alpha) and inhibits HIF-1-mediated transcription. *Journal of Biological Chemistry*, 276(30), pp. 28421-28429
- FECHIR, M., LINKER, K., PAUTZ, A., HUBRICH, T., FORSTERMANN, U., RODRIGUEZ-PASCUAL, F. and KLEINERT, H., 2005. Tristetraprolin regulates the expression of the human inducible nitric-oxide synthase gene. *Molecular pharmacology*, 67(6), pp. 2148-2161
- FELDSER, D., AGANI, F., IYER, N.V., PAK, B., FERREIRA, G. and SEMENZA, G.L., 1999. Reciprocal positive regulation of hypoxia-inducible factor 1alpha and insulin-like growth factor 2. *Cancer research*, 59(16), pp. 3915-3918
- FIRTH, J.D., EBERT, B.L. and RATCLIFFE, P.J., 1995. Hypoxic regulation of lactate dehydrogenase A. Interaction between hypoxia-inducible factor 1 and cAMP response elements. *Journal of Biological Chemistry*, 270(36), pp. 21021-21027
- FORRESTER, J.V., SHAFIEE, A., SCHRODER, S., KNOTT, R. and MCINTOSH, L., 1993. The role of growth factors in proliferative diabetic retinopathy. *Eye (London, England)*, 7 (Pt 2)(Pt 2), pp. 276-287

FORSYTHE, J.A., JIANG, B.H., IYER, N.V., AGANI, F., LEUNG, S.W., KOOS, R.D. and SEMENZA, G.L., 1996. Activation of vascular endothelial growth factor gene transcription by hypoxia-inducible factor 1. *Molecular and cellular biology*, 16(9), pp. 4604-4613

FRANK, S., HUBNER, G., BREIER, G., LONGAKER, M.T., GREENHALGH, D.G. and WERNER, S., 1995. Regulation of vascular endothelial growth factor expression in cultured keratinocytes. Implications for normal and impaired wound healing. *Journal of Biological Chemistry*, 270(21), pp. 12607-12613

FREDE, S., FREITAG, P., OTTO, T., HEILMAIER, C. and FANDREY, J., 2005. The proinflammatory cytokine interleukin 1beta and hypoxia cooperatively induce the expression of adrenomedullin in ovarian carcinoma cells through hypoxia inducible factor 1 activation. *Cancer research*, 65(11), pp. 4690-4697

FREUND, M.C., STEURER, W., GASSNER, E.M., UNSINN, K.M., RIEGER, M., KOENIGSRAINER, A., MARGREITER, R. and JASCHKE, W.R., 2004. Spectrum of imaging findings after pancreas transplantation with enteric exocrine drainage: Part 1, posttransplantation anatomy. *AJR. American Journal of Roentgenology*, 182(4), pp. 911-917

FUMERON, F., REIS, A.F. and VELHO, G., 2006. Genetics of macrovascular complications in diabetes. *Curr.Diab Rep.*, 6(2), pp. 162-168

GADDIPATI, J.P., MADHAVAN, S., SIDHU, G.S., SINGH, A.K., SETH, P. and MAHESHWARI, R.K., 1999. Picroliv -- a natural product protects cells and regulates the gene expression during hypoxia/reoxygenation. *Molecular and cellular biochemistry*, 194(1-2), pp. 271-281

GAO, N., NESTER, R.A. and SARKAR, M.A., 2004. 4-Hydroxy estradiol but not 2-hydroxy estradiol induces expression of hypoxia-inducible factor 1alpha and vascular endothelial growth factor A through phosphatidylinositol 3-kinase/Akt/FRAP pathway in OVCAR-3 and A2780-CP70 human ovarian carcinoma cells. *Toxicology and applied pharmacology*, 196(1), pp. 124-135

GAO, W., FERGUSON, G., CONNELL, P., WASLSHE, T., MURPHY, R., BIRNEY, Y.A., O'BRIEN, C. and CAHILL, P.A., 2007. High glucose concentrations alter hypoxia-induced control of vascular smooth muscle cell growth via a HIF-1 α -dependent pathway. *Journal of Molecular and Cellular Cardiology*, 42, pp. 609-619

GERALD, D., BERRA, E., FRAPART, Y.M., CHAN, D.A., GIACCIA, A.J., MANSUY, D., POUYSSEGUR, J., YANIV, M. and MECHTA-GRIGORIOU, F., 2004. JunD reduces tumor angiogenesis by protecting cells from oxidative stress. *Cell*, 118(6), pp. 781-794

GERHARDINGER, C., MCCLURE, K.D., ROMEO, G., PODESTA, F. and LORENZI, M., 2001. IGF-I mRNA and signaling in the diabetic retina. *Diabetes*, 50(1), pp. 175-183

GIANNINI, C. and DYCK, P.J., 1995. Basement membrane reduplication and pericyte degeneration precede development of diabetic polyneuropathy and are associated with its severity. *Annals of Neurology*, 37(4), pp. 498-504

GIANNINI, S., CRESCI, B., PALA, L., CIUCCI, A., FRANCHINI, A., MANUELLI, C., FUJITA-YAMAGUCHI, Y., CAPPUGI, P., ZONEFRATI, R. and ROTELLA, C.M., 2001. IGFBPs modulate IGF-I- and high glucose-controlled growth of human retinal endothelial cells. *The Journal of endocrinology*, 171(2), pp. 273-284

GIBSON, T.M., COTTER, M.A. and CAMERON, N.E., 2003. Effects of alpha-lipoic acid on impaired gastric fundus innervation in diabetic rats. *Free radical biology & medicine*, 35(2), pp. 160-168

GINIS, I. and FALLER, D.V., 1997. Protection from apoptosis in human neutrophils is determined by the surface of adhesion. *The American Journal of Physiology*, 272(1 Pt 1), pp. C295-309

GLEADLE, J.M. and RATCLIFFE, P.J., 1998. Hypoxia and the regulation of gene expression. *Molecular medicine today*, 4(3), pp. 122-129

GOLDBERG, M.A. and SCHNEIDER, T.J., 1994. Similarities between the oxygen-sensing mechanisms regulating the expression of vascular endothelial growth factor and erythropoietin. *Journal of Biological Chemistry*, 269(6), pp. 4355-4359

GOTHIE, E., RICHARD, D.E., BERRA, E., PAGES, G. and POUYSSEGUR, J., 2000. Identification of alternative spliced variants of human hypoxia-inducible factor-1 alpha. *Journal of Biological Chemistry*, 275(10), pp. 6922-6927

GRADIN, K., MCGUIRE, J., WENGER, R.H., KVIETIKOVA, I., FHITELAW, M.L., TOFTGARD, R., TORA, L., GASSMANN, M. and POELLINGER, L., 1996. Functional interference between hypoxia and dioxin signal transduction pathways: competition for

recruitment of the Arnt transcription factor. *Molecular and cellular biology*, 16(10), pp. 5221-5231

GRAIANI, G., EMANUELI, C., DESORTES, E., VAN LINTHOUT, S., PINNA, A., FIGUEROA, C.D., MANNI, L. and MADEDDU, P., 2004. Nerve growth factor promotes reparative angiogenesis and inhibits endothelial apoptosis in cutaneous wounds of Type 1 diabetic mice. *Diabetologia*, 47(6), pp. 1047-1054

GRAVEN, K.K., BELLUR, D., KLAHN, B.D., LOWREY, S.L. and AMBERGER, E., 2003. HIF-2 α regulates glyceraldehyde-3-phosphate dehydrogenase expression in endothelial cells. *Biochimica et biophysica acta*, 1626(1-3), pp. 10-18

GRAVEN, K.K. and FARBER, H.W., 1995. Hypoxia-associated proteins. *New horizons (Baltimore, Md.)*, 3(2), pp. 208-218

GRAVEN, K.K., YU, Q., PAN, D., RONCARATI, J.S. and FARBER, H.W., 1999. Identification of an oxygen responsive enhancer element in the glyceraldehyde-3-phosphate dehydrogenase gene. *Biochimica et biophysica acta*, 1447(2-3), pp. 208-218

GRAVEN, K.K., ZIMMERMAN, L.H., DICKSON, E.W., WEINHOUSE, G.L. and FARBER, H.W., 1993. Endothelial cell hypoxia associated proteins are cell and stress specific. *Journal of cellular physiology*, 157(3), pp. 544-554

GREENE, E.L., NELSON, B.A., ROBINSON, K.A. and BUSE, M.G., 2001. alpha-Lipoic acid prevents the development of glucose-induced insulin resistance in 3T3-L1 adipocytes and accelerates the decline in immunoreactive insulin during cell incubation. *Metabolism: clinical and experimental*, 50(9), pp. 1063-1069

GRUESSNER, A.C. and SUTHERLAND, D.E., 2005. Pancreas transplant outcomes for United States (US) and non-US cases as reported to the United Network for Organ Sharing (UNOS) and the International Pancreas Transplant Registry (IPTR) as of June 2004. *Clinical transplantation*, 19(4), pp. 433-455

GUO, X., CHEN, L.W., LIU, W.L. and GUO, Z.G., 2000. High glucose inhibits expression of inducible and constitutive nitric oxide synthase in bovine aortic endothelial cells. *Acta Pharmacologica Sinica*, 21(4), pp. 325-328

GUZY, R.D., HOYOS, B., ROBIN, E., CHEN, H., LIU, L., MANSFIELD, K.D., SIMON, M.C., HAMMERLING, U. and SCHUMACKER, P.T., 2005. Mitochondrial

complex III is required for hypoxia-induced ROS production and cellular oxygen sensing. *Cell.Metab.*, 1(6), pp. 401-408

HAGEN, T., TAYLOR, C.T., LAM, F. and MONCADA, S., 2003. Redistribution of intracellular oxygen in hypoxia by nitric oxide: effect on HIF1alpha. *Science*, 302(5652), pp. 1975-1978

HAMMES, H.P., 2003. Pathophysiological mechanisms of diabetic angiopathy. *Journal of diabetes and its complications*, 17(2 Suppl), pp. 16-19

HAQUE, K.A., PFEIFFER, R.M., BEERMAN, M.B., STRUEWING, J.P., CHANOCK, S.J. and BERGEN, A.W., 2003. Performance of high-throughput DNA quantification methods. *BMC biotechnology [computer file]*, 3, pp. 20

HARA, S., HAMADA, J., KOBAYASHI, C., KONDO, Y., and IMURA, N., 2001. *Biochemical and Biophysical Research Communications*, 287, pp. 808-813

HARA, S., KOBAYASHI, C. and IMURA, N., 1999. Molecular cloning of cDNAs encoding hypoxia-inducible factor (HIF)-1alpha and -2alpha of bovine arterial endothelial cells. *Biochimica et biophysica acta*, 1445(2), pp. 237-243

HAYASHI, M., SAKATA, M., TAKEDA, T., YAMAMOTO, T., OKAMOTO, Y., SAWADA, K., KIMURA, A., MINEKAWA, R., TAHARA, M., TASAKA, K. and MURATA, Y., 2004. Induction of glucose transporter 1 expression through hypoxia-inducible factor 1alpha under hypoxic conditions in trophoblast-derived cells. *The Journal of endocrinology*, 183(1), pp. 145-154

HELLWIG-BURGEL, T., STIEHL, D.P., KATSCHINSKI, D.M., MARXSEN, J., KREFT, B. and JELKMANN, W., 2005. VEGF production by primary human renal proximal tubular cells: requirement of HIF-1, PI3-kinase and MAPKK-1 signaling. *Cellular physiology and biochemistry : international journal of experimental cellular physiology, biochemistry, and pharmacology*, 15(1-4), pp. 99-108

HOSOMI, N., NOMA, T., OHYAMA, H., TAKAHASHI, T. and KOHNO, M., 2002. Vascular proliferation and transforming growth factor-beta expression in pre- and early stage of diabetes mellitus in Otsuka Long-Evans Tokushima fatty rats. *Atherosclerosis*, 162(1), pp. 69-76

HUANG, L.E., ARANY, Z., LIVINGSTON, D.M. and BUNN, H.F., 1996. Activation of hypoxia-inducible transcription factor depends primarily upon redox-sensitive

stabilization of its alpha subunit. *Journal of Biological Chemistry*, 271(50), pp. 32253-32259

HUANG, L.E., GU, J., SCHAU, M. and BUNN, H.F., 1998. Regulation of hypoxia-inducible factor 1alpha is mediated by an O₂-dependent degradation domain via the ubiquitin-proteasome pathway. *Proceedings of the National Academy of Sciences of the United States of America*, 95(14), pp. 7987-7992

HUANG, L.E., WILLMORE, W.G., GU, J., GOLDBERG, M.A. and BUNN, H.F., 1999. Inhibition of hypoxia-inducible factor 1 activation by carbon monoxide and nitric oxide. Implications for oxygen sensing and signaling. *Journal of Biological Chemistry*, 274(13), pp. 9038-9044

HUANG, S.S. and HUANG, J.S., 2005. TGF-beta control of cell proliferation. *Journal of cellular biochemistry*, 96(3), pp. 447-462

HUDLICKA, O., MILKIEWICZ, M., COTTER, M.A. and BROWN, M.D., 2002. Hypoxia and expression of VEGF-A protein in relation to capillary growth in electrically stimulated rat and rabbit skeletal muscles. *Experimental physiology*, 87(3), pp. 373-381

HUDSON, C.C., LIU, M., CHIANG, G.G., OTTERNESS, D.M., LOOMIS, D.C., KAPER, F., GIACCIA, A.J. and ABRAHAM, R.T., 2002. Regulation of hypoxia-inducible factor 1alpha expression and function by the mammalian target of rapamycin. *Molecular and cellular biology*, 22(20), pp. 7004-7014

IDRIS, I., GRAY, S. and DONNELLY, R., 2001. Protein kinase C activation: isozyme-specific effects on metabolism and cardiovascular complications in diabetes. *Diabetologia*, 44(6), pp. 659-673

IVAN, M. and KAELIN, W.G., JR, 2001. The von Hippel-Lindau tumor suppressor protein. *Current opinion in genetics & development*, 11(1), pp. 27-34

JAAKKOLA, P., MOLE, D.R., TIAN, Y.M., WILSON, M.I., GIELBERT, J., GASKELL, S.J., KRIEGSHEIM, A., HEBESTREIT, H.F., MUKHERJI, M., SCHOFIELD, C.J., MAXWELL, P.H., PUGH, C.W. and RATCLIFFE, P.J., 2001. Targeting of HIF-alpha to the von Hippel-Lindau ubiquitylation complex by O₂-regulated prolyl hydroxylation. *Science*, 292(5516), pp. 468-472

JACOB, S., HENRIKSEN, E.J., SCHIEMANN, A.L., SIMON, I., CLANCY, D.E., TRITSCHLER, H.J., JUNG, W.I., AUGUSTIN, H.J. and DIETZE, G.J., 1995.

Enhancement of glucose disposal in patients with type 2 diabetes by alpha-lipoic acid. *Arzneimittel-Forschung*, 45(8), pp. 872-874

JANSSENS, D., MICHIELS, C., DELAIVE, E., ELIAERS, F., DRIEU, K. and REMACLE, J., 1995. Protection of hypoxia-induced ATP decrease in endothelial cells by ginkgo biloba extract and bilobalide. *Biochemical pharmacology*, 50(7), pp. 991-999

JEONG, H.J., CHUNG, H.S., LEE, B.R., KIM, S.J., YOO, S.J., HONG, S.H. and KIM, H.M., 2003. Expression of proinflammatory cytokines via HIF-1alpha and NF-kappaB activation on desferrioxamine-stimulated HMC-1 cells. *Biochemical and biophysical research communications*, 306(4), pp. 805-811

JEWELL, U.R., KVIETIKOVA, I., SCHEID, A., BAUER, C., WENGER, R.H. and GASSMANN, M., 2001. Induction of HIF-1alpha in response to hypoxia is instantaneous. *The FASEB journal : official publication of the Federation of American Societies for Experimental Biology*, 15(7), pp. 1312-1314

JIANG, B.H., JIANG, G., ZHENG, J.Z., LU, Z., HUNTER, T. and VOGT, P.K., 2001. Phosphatidylinositol 3-kinase signaling controls levels of hypoxia-inducible factor 1. *Cell growth & differentiation : the molecular biology journal of the American Association for Cancer Research*, 12(7), pp. 363-369

JIANG, B.H., RUE, E., WANG, G.L., ROE, R. and SEMENZA, G.L., 1996. Dimerization, DNA binding, and transactivation properties of hypoxia-inducible factor 1. *Journal of Biological Chemistry*, 271(30), pp. 17771-17778

JIANG, K., ZHONG, B., GILVARY, D.L., CORLISS, B.C., HONG-GELLER, E., WEI, S. and DJEU, J.Y., 2000. Pivotal role of phosphoinositide-3 kinase in regulation of cytotoxicity in natural killer cells. *Nature immunology*, 1(5), pp. 419-425

JIANG, Y.A., FAN, L.F., JIANG, C.Q., ZHANG, Y.Y., LUO, H.S., TANG, Z.J., XIA, D. and WANG, M., 2003. Expression and significance of PTEN, hypoxia-inducible factor-1 alpha in colorectal adenoma and adenocarcinoma. *World J.Gastroenterol.*, 9(3), pp. 491-494

JONES, A., FUJIYAMA, C., BLANCHER, C., MOORE, J.W., FUGGLE, S., CRANSTON, D., BICKNELL, R., HARRIS, A.L., 2001. Relation of vascular endothelial growth factor production to expression and regulation of hypoxia-inducible factor-1 α and hypoxia-inducible factor-2 α in human bladder tumours and cell lines. *Clinical Cancer Research.*, 7, pp. 1263-1272

JOUSSEN, A.M., POULAKI, V., QIN, W., KIRCHHOF, B., MITSIADES, N., WIEGAND, S.J., RUDGE, J., YANCOPOULOS, G.D. and ADAMIS, A.P., 2002. Retinal vascular endothelial growth factor induces intercellular adhesion molecule-1 and endothelial nitric oxide synthase expression and initiates early diabetic retinal leukocyte adhesion in vivo. *American Journal of Pathology*, 160(2), pp. 501-509

KAISER, N., SASSON, S., FEENER, E.P., BOUKOBZA-VARDI, N., HIGASHI, S., MOLLER, D.E., DAVIDHEISER, S., PRZYBYLSKI, R.J. and KING, G.L., 1993. Differential regulation of glucose transport and transporters by glucose in vascular endothelial and smooth muscle cells. *Diabetes*, 42(1), pp. 80-89

KATAVETIN, P., MIYATA, T., INAGI, R., TANAKA, T., SASSA, R., INGLEFINGER, J.R., FUJITA, T. and NANGAKU, M., 2006. High glucose blunts vascular endothelial growth factor response to hypoxia via the oxidative stress-regulated hypoxia-inducible factor/hypoxia-response element pathway. *Journal of the American Society of Nephrology*, 15(5), pp. 1405-1413

KAWAGUCHI, T., VEECH, R.L. and UYEDA, K., 2001. Regulation of energy metabolism in macrophages during hypoxia. Roles of fructose 2,6-bisphosphate and ribose 1,5-bisphosphate. *Journal of Biological Chemistry*, 276(30), pp. 28554-28561

KELLY, W.D., LILLEHEI, R.C., MERKEL, F.K., IDEZUKI, Y. and GOETZ, F.C., 1967. Allograft transplantation of the pancreas and duodenum along with the kidney in diabetic nephropathy. *Surgery*, 61(6), pp. 827-837

KEWLEY, R.J., WHITELAW, M.L. and CHAPMAN-SMITH, A., 2004. The mammalian basic helix-loop-helix/PAS family of transcriptional regulators. *The international journal of biochemistry & cell biology*, 36(2), pp. 189-204

KIETZMANN, T., FANDREY, J. and ACKER, H., 2000. Oxygen Radicals as Messengers in Oxygen-Dependent Gene Expression. *News in physiological sciences : an international journal of physiology produced jointly by the International Union of Physiological Sciences and the American Physiological Society*, 15, pp. 202-208

KIETZMANN, T., KRONES-HERZIG, A. and JUNGERMANN, K., 2002. Signaling cross-talk between hypoxia and glucose via hypoxia-inducible factor 1 and glucose response elements. *Biochemical pharmacology*, 64(5-6), pp. 903-911

KIM, C.H., CHO, Y.S., CHUN, Y.S., PARK, J.W. and KIM, M.S., 2002. Early expression of myocardial HIF-1 α in response to mechanical stresses: regulation by

stretch-activated channels and the phosphatidylinositol 3-kinase signaling pathway. *Circulation research*, 90(2), pp. E25-33

KIM, J.W., TCHERNYSHYOV, I., SEMENZA, G.L. and DANG, C.V., 2006. HIF-1-mediated expression of pyruvate dehydrogenase kinase: a metabolic switch required for cellular adaptation to hypoxia. *Cell.Metab.*, 3(3), pp. 177-185

KIM, J.Y., KIM, S.M., KO, J.H., YIM, J.H., PARK, J.H. and PARK, J.H., 2006. Interaction of pro-apoptotic protein HGTD-P with heat shock protein 90 is required for induction of mitochondrial apoptotic cascades. *FEBS letters*, 580(13), pp. 3270-3275

KIMURA, H., WEISZ, A., KURASHIMA, Y., HASHIMOTO, K., OGURA, T., D'ACQUISTO, F., ADDEO, R., MAKUUCHI, M. and ESUMI, H., 2000. Hypoxia response element of the human vascular endothelial growth factor gene mediates transcriptional regulation by nitric oxide: control of hypoxia-inducible factor-1 activity by nitric oxide. *Blood*, 95(1), pp. 189-197

KNOTT, R.M., 1998. Insulin-like growth factor type 1--friend or foe? *The British journal of ophthalmology*, 82(7), pp. 719-720

KNOTT, R.M., ROBERTSON, M. and FORRESTER, J.V., 1993. Regulation of glucose transporter (GLUT 3) and aldose reductase mRNA in bovine retinal endothelial cells and retinal pericytes in high glucose and high galactose culture. *Diabetologia*, 36(9), pp. 808-812

KNOTT, R.M., ROBERTSON, M., MUCKERSIE, E., FOLEFAC, V.A., FAIRHURST, F.E., WILEMAN, S.M. and FORRESTER, J.V., 1999. A model system for the study of human retinal angiogenesis: activation of monocytes and endothelial cells and the association with the expression of the monocarboxylate transporter type 1 (MCT-1). *Diabetologia*, 42(7), pp. 870-877

KNOTT, R.M., ROBERTSON, M., MUCKERSIE, E. and FORRESTER, J.V., 1996a. Glucose-mediated regulation of GLUT-1 and GLUT-3 mRNA in human retinal endothelial cells. *Biochemical Society transactions*, 24(2), pp. 216S

KNOTT, R.M., ROBERTSON, M., MUCKERSIE, E. and FORRESTER, J.V., 1996b. Regulation of glucose transporters (GLUT-1 and GLUT-3) in human retinal endothelial cells. *The Biochemical journal*, 318 (Pt 1)(Pt 1), pp. 313-317

- KOBAYASHI, T. and KAMATA, K., 2002. Short-term insulin treatment and aortic expressions of IGF-1 receptor and VEGF mRNA in diabetic rats. *American Journal of Physiology. Heart and Circulatory Physiology*, 283(5), pp. H1761-8
- KONRAD, D., SOMWAR, R., SWEENEY, G., YAWORSKY, K., HAYASHI, M., RAMLAL, T. and KLIP, A., 2001. The antihyperglycemic drug alpha-lipoic acid stimulates glucose uptake via both GLUT4 translocation and GLUT4 activation: potential role of p38 mitogen-activated protein kinase in GLUT4 activation. *Diabetes*, 50(6), pp. 1464-1471
- KOUREMBANAS, S. and BERNFIELD, M., 1994. Hypoxia and endothelial-smooth muscle cell interactions in the lung. *American Journal of Respiratory Cell and Molecular Biology : An Official Journal of the American Thoracic Society, Medical Section of the American Lung Association*, 11(4), pp. 373-374
- KRONES, A., JUNGERMANN, K. and KIETZMANN, T., 2001. Cross-talk between the signals hypoxia and glucose at the glucose response element of the L-type pyruvate kinase gene. *Endocrinology*, 142(6), pp. 2707-2718
- KUHNE, W., BESSELMANN, M., NOLL, T., MUHS, A., WATANABE, H. and PIPER, H.M., 1993. Disintegration of cytoskeletal structure of actin filaments in energy-depleted endothelial cells. *The American Journal of Physiology*, 264(5 Pt 2), pp. H1599-608
- KUMAGAI, A.K., GLASGOW, B.J. and PARDRIDGE, W.M., 1994. GLUT1 glucose transporter expression in the diabetic and nondiabetic human eye. *Investigative ophthalmology & visual science*, 35(6), pp. 2887-2894
- LADEROUTE, K.R., CALAOAGAN, J.M., KNAPP, M. and JOHNSON, R.S., 2004. Glucose utilization is essential for hypoxia-inducible factor 1 alpha-dependent phosphorylation of c-Jun. *Molecular and cellular biology*, 24(10), pp. 4128-4137
- LANDO, D., PEET, D.J., WHELAN, D.A., GORMAN, J.J. and WHITELAW, M.L., 2002. Asparagine hydroxylation of the HIF transactivation domain a hypoxic switch. *Science*, 295(5556), pp. 858-861
- LARGE, V. and BEYLOT, M., 1999. Modifications of citric acid cycle activity and gluconeogenesis in streptozotocin-induced diabetes and effects of metformin. *Diabetes*, 48(6), pp. 1251-1257

- LAUGHNER, E., TAGHAVI, P., CHILES, K., MAHON, P.C. and SEMENZA, G.L., 2001. HER2 (neu) signaling increases the rate of hypoxia-inducible factor 1alpha (HIF-1alpha) synthesis: novel mechanism for HIF-1-mediated vascular endothelial growth factor expression. *Molecular and cellular biology*, 21(12), pp. 3995-4004
- LAVIE, L., 2003. Obstructive sleep apnoea syndrome--an oxidative stress disorder. *Sleep Med.Rev.*, 7(1), pp. 35-51
- LEE, M.J., KIM, J.Y., SUK, K. and PARK, J.H., 2004. Identification of the hypoxia-inducible factor 1 alpha-responsive HGTD-P gene as a mediator in the mitochondrial apoptotic pathway. *Molecular and cellular biology*, 24(9), pp. 3918-3927
- LEE, S.H., WOLF, P.L., ESCUDERO, R., DEUTSCH, R., JAMIESON, S.W. and THISTLETHWAITE, P.A., 2000. Early expression of angiogenesis factors in acute myocardial ischemia and infarction. *The New England journal of medicine*, 342(9), pp. 626-633
- LEROITH, D., WERNER, H., BEITNER-JOHNSON, D. and ROBERTS, C.T.,JR, 1995. Molecular and cellular aspects of the insulin-like growth factor I receptor. *Endocrine reviews*, 16(2), pp. 143-163
- LI, Y., ZHOU, C., CALVERT, J.W., COLOHAN, A.R. and ZHANG, J.H., 2005. Multiple effects of hyperbaric oxygen on the expression of HIF-1 alpha and apoptotic genes in a global ischaemia-hypotension rat model. *Experimental Neurology*, 191(1), pp. 198-210.
- LIU, L.X., LU, H., LUO, Y., DATE, T., BELANGER, A.J., VINCENT, K.A., AKITA, G.Y., GOLDBERG, M., CHENG, S.H., GREGORY, R.J. and JIANG, C., 2002. Stabilization of vascular endothelial growth factor mRNA by hypoxia-inducible factor 1. *Biochemical and biophysical research communications*, 291(4), pp. 908-914
- LIU, W., LIU, Y. and LOWE JR, W.L.,JR, 2001. The role of phosphatidylinositol 3-kinase and the mitogen-activated protein kinases in insulin-like growth factor-I-mediated effects in vascular endothelial cells. *Endocrinology*, 142(5), pp. 1710-1719
- LORENZI, M., MONTISANO, D.F., TOLEDO, S. and BARRIEUX, A., 1986. High glucose induces DNA damage in cultured human endothelial cells. *The Journal of clinical investigation*, 77(1), pp. 322-325

- LORENZI, M., NORDBERG, J.A. and TOLEDO, S., 1987. High glucose prolongs cell-cycle traversal of cultured human endothelial cells. *Diabetes*, 36(11), pp. 1261-1267
- LU, H., DALGARD, C.L., MOHYELDIN, A., MCFATE, T., TAIT, A.S. and VERMA, A., 2005. Reversible inactivation of HIF-1 prolyl hydroxylases allows cell metabolism to control basal HIF-1. *Journal of Biological Chemistry*, 280(51), pp. 41928-41939
- LU, H., FORBES, R.A. and VERMA, A., 2002. Hypoxia-inducible factor 1 activation by aerobic glycolysis implicates the Warburg effect in carcinogenesis. *Journal of Biological Chemistry*, 277(26), pp. 23111-23115
- LUKIW, W.J., GORDON, W.C., ROGAEV, E.I., THOMPSON, H. and BAZAN, N.G., 2001. Presenilin-2 (PS2) expression up-regulation in a model of retinopathy of prematurity and pathoangiogenesis. *Neuroreport*, 12(1), pp. 53-57
- MA, Y.Y., WEI, S.J., LIN, Y.C., LUNG, J.C., CHANG, T.C., WHANG-PENG, J., LIU, J.M., YANG, D.M., YANG, W.K. and SHEN, C.Y., 2000. PIK3CA as an oncogene in cervical cancer. *Oncogene*, 19(23), pp. 2739-2744
- MAHON, P.C., HIROTA, K. and SEMENZA, G.L., 2001. FIH-1: a novel protein that interacts with HIF-1 α and VHL to mediate repression of HIF-1 transcriptional activity. *Genes & development*, 15(20), pp. 2675-2686
- MAHONEY, D.J., CAREY, K., FU, M.H., SNOW, R., CAMERON-SMITH, D., PARISE, G. and TARNOPOLSKY, M.A., 2004. Real-time RT-PCR analysis of housekeeping genes in human skeletal muscle following acute exercise. *Physiological Genomics (Online)*, 18(2), pp. 226-231
- MALIK, R.A., 1997. The pathology of human diabetic neuropathy. *Diabetes*, 46 Suppl 2, pp. S50-3
- MALIK, R.A., TEFAYE, S., THOMPSON, S.D., VEVES, A., SHARMA, A.K., BOULTON, A.J. and WARD, J.D., 1993. Endoneurial localisation of microvascular damage in human diabetic neuropathy. *Diabetologia*, 36(5), pp. 454-459
- MANDARINO, L.J., FINLAYSON, J. and HASSELL, J.R., 1994. High glucose downregulates glucose transport activity in retinal capillary pericytes but not endothelial cells. *Investigative ophthalmology & visual science*, 35(3), pp. 964-972

MANSKE, C.L., 1993. Coronary artery disease in diabetic patients with nephropathy. *American Journal of Hypertension : Journal of the American Society of Hypertension*, 6(11 Pt 2), pp. 367S-374S

MARFELLA, R., D'AMICO, M., ESPOSITO, K., BALDI, A., DI FILIPPO, C., SINISCALCHI, M., SASSO, F.C., PORTOGHESE, M., CIRILLO, F., CACCIAPUOTI, F., CARBONARA, O., CRESCENZI, B., BALDI, F., CERIELLO, A., NICOLETTI, G.F., D'ANDREA, F., VERZA, M., COPPOLA, L., ROSSI, F. and GIUGLIANO, D., 2006. The ubiquitin-proteasome system and inflammatory activity in diabetic atherosclerotic plaques: effects of rosiglitazone treatment. *Diabetes*, 55(3), pp. 622-632

MARTI, H.J., BERNAUDIN, M., BELLAIL, A., SCHOCH, H., EULER, M., PETIT, E. and RISAU, W., 2000. Hypoxia-induced vascular endothelial growth factor expression precedes neovascularization after cerebral ischemia. *American Journal of Pathology*, 156(3), pp. 965-976

MATEO, J., GARCIA-LECEA, M., CADENAS, S., HERNANDEZ, C. and MONCADA, S., 2003. Regulation of hypoxia-inducible factor-1 alpha by nitric oxide through mitochondria-dependent and -independent pathways. *The Biochemical journal*, 376(Pt 2), pp. 537-544

MATHUPALA, S.P., REMPEL, A. and PEDERSEN, P.L., 2001. Glucose catabolism in cancer cells: identification and characterization of a marked activation response of the type II hexokinase gene to hypoxic conditions. *Journal of Biological Chemistry*, 276(46), pp. 43407-43412

MAXWELL, P.H., WIESENER, M.S., CHANG, G.W., CLIFFORD, S.C., VAUX, E.C., COCKMAN, M.E., WYKOFF, C.C., PUGH, C.W., MAHER, E.R. and RATCLIFFE, P.J., 1999. The tumour suppressor protein VHL targets hypoxia-inducible factors for oxygen-dependent proteolysis. *Nature*, 399(6733), pp. 271-275

MAYNARD, M.A., QI, H., CHUNG, J., LEE, E.H.L., KONDO, Y., HARA, S., CONAWAY, J.W. and OHH, M., 2003. Multiple splice variants of the human HIF-3 α locus are targets of the von Hippel-Lindau E3 ubiquitin ligase complex. *The Journal of Biological Chemistry*, 278(13), pp. 11032-11040

MAZURE, N.M., CHEN, E.Y., LADEROUTE, K.R. and GIACCIA, A.J., 1997. Induction of vascular endothelial growth factor by hypoxia is modulated by a phosphatidylinositol 3-kinase/Akt signaling pathway in Ha-ras-transformed cells through a hypoxia inducible factor-1 transcriptional element. *Blood*, 90(9), pp. 3322-3331

- MAZURE, N.M., CHEN, E.Y., YEH, P., LADEROUTE, K.R. and GIACCIA, A.J., 1996. Oncogenic transformation and hypoxia synergistically act to modulate vascular endothelial growth factor expression. *Cancer research*, 56(15), pp. 3436-3440
- MCBAIN, V.A., ROBERTSON, M., MUCKERSIE, E., FORRESTER, J.V. and KNOTT, R.M., 2003. High glucose concentration decreases insulin-like growth factor type 1-mediated mitogen-activated protein kinase activation in bovine retinal endothelial cells. *Metabolism: clinical and experimental*, 52(5), pp. 547-551
- MCCARTY, M.F., 2003. Hyperinsulinemia may boost both hematocrit and iron absorption by up-regulating activity of hypoxia-inducible factor-1alpha. *Medical hypotheses*, 61(5-6), pp. 567-573
- METZEN, E., ZHOU, J., JELKMANN, W., FANDREY, J. and BRUNE, B., 2003. Nitric oxide impairs normoxic degradation of HIF-1alpha by inhibition of prolyl hydroxylases. *Molecular biology of the cell*, 14(8), pp. 3470-3481
- MICHIELS, C., ARNOULD, T. and REMACLE, J., 2000. Endothelial cell responses to hypoxia: initiation of a cascade of cellular interactions. *Biochimica et biophysica acta*, 1497(1), pp. 1-10
- MINCHENKO, A., LESHCHINSKY, I., OPENTANOVA, I., SANG, N., SRINIVAS, V., ARMSTEAD, V. and CARO, J., 2002. Hypoxia-inducible factor-1-mediated expression of the 6-phosphofructo-2-kinase/fructose-2,6-bisphosphatase-3 (PFKFB3) gene. Its possible role in the Warburg effect. *Journal of Biological Chemistry*, 277(8), pp. 6183-6187
- MOELLER, L.C., DUMITRESCU, A.M. and REFETOFF, S., 2005. Cytosolic action of thyroid hormone leads to induction of hypoxia-inducible factor-1alpha and glycolytic genes. *Molecular endocrinology (Baltimore, Md.)*, 19(12), pp. 2955-2963
- MOSER, D.R., LOWE, W.L., JR, DAKE, B.L., BOOTH, B.A., BOES, M., CLEMMONS, D.R. and BAR, R.S., 1992. Endothelial cells express insulin-like growth factor-binding proteins 2 to 6. *Molecular endocrinology (Baltimore, Md.)*, 6(11), pp. 1805-1814
- MU, D., JIANG, X., SHELDON, R.A., FOX, C.K., HAMRICK, S.E., VEXLER, Z.S. and FERRIERO, D.M., 2003. Regulation of hypoxia-inducible factor 1alpha and induction of vascular endothelial growth factor in a rat neonatal stroke model. *Neurobiology*, 14(3), pp. 524-34

MURPHY, M.P., 2003. Does interplay between nitric oxide and mitochondria affect hypoxia-inducible transcription factor-1 activity? *The Biochemical journal*, 376(Pt 2), pp. e5-6

MYER, V.E., FAN, X.C. and STEITZ, J.A., 1997. Identification of HuR as a protein implicated in AUUUA-mediated mRNA decay. *The EMBO journal*, 16(8), pp. 2130-2139

NAGY, E., HENICS, T., ECKERT, M., MISETA, A., LIGHTOWLERS, R.N. and KELLERMAYER, M., 2000. Identification of the NAD(+)-binding fold of glyceraldehyde-3-phosphate dehydrogenase as a novel RNA-binding domain. *Biochemical and biophysical research communications*, 275(2), pp. 253-260

NAGY, E. and RIGBY, W.F., 1995. Glyceraldehyde-3-phosphate dehydrogenase selectively binds AU-rich RNA in the NAD(+)-binding region (Rossmann fold). *Journal of Biological Chemistry*, 270(6), pp. 2755-2763

NAKAMURA, J., KASUYA, Y., HAMADA, Y., NAKASHIMA, E., NARUSE, K., YASUDA, Y., KATO, K. and HOTTA, N., 2001. Glucose-induced hyperproliferation of cultured rat aortic smooth muscle cells through polyol pathway hyperactivity. *Diabetologia*, 44(4), pp. 480-487

NAKAYAMA, K., KANZAKI, A., HATA, K., KATABUCHI, H., OKAMURA, H., MIYAZAKI, K., FUKUMOTO, M. and TAKEBAYASHI, Y., 2002. Hypoxia-inducible factor 1 alpha (HIF-1 alpha) gene expression in human ovarian carcinoma. *Cancer letters*, 176(2), pp. 215-223

NG, D.P. and KROLEWSKI, A.S., 2005. Molecular genetic approaches for studying the etiology of diabetic nephropathy. *Current Molecular Medicine*, 5(5), pp. 509-525

OBROSOVA, I.G., VAN HUYSEN, C., FATHALLAH, L., CAO, X.C., GREENE, D.A. and STEVENS, M.J., 2002. An aldose reductase inhibitor reverses early diabetes-induced changes in peripheral nerve function, metabolism, and antioxidative defense. *The FASEB journal : official publication of the Federation of American Societies for Experimental Biology*, 16(1), pp. 123-125

ORANGE, S.J., PAINTER, D., HORVATH, J., YU, B., TRENT, R. and HENNESSY, A., 2003. Placental endothelial nitric oxide synthase localization and expression in normal human pregnancy and pre-eclampsia. *Clinical and experimental pharmacology & physiology*, 30(5-6), pp. 376-381

OZAKI, H., YU, A.Y., DELLA, N., OZAKI, K., LUNA, J.D., YAMADA, H., HACKETT, S.F., OKAMOTO, N., ZACK, D.J., SEMENZA, G.L. and CAMPOCHIARO, P.A., 1999. Hypoxia inducible factor-1 alpha is increased in ischemic retina: temporal and spatial correlation with VEGF expression. *Investigative ophthalmology & visual science*, 40(1), pp. 182-189

PACKER, L., KRAEMER, K. and RIMBACH, G., 2001. Molecular aspects of lipoic acid in the prevention of diabetes complications. *Nutrition (Burbank, Los Angeles County, Calif.)*, 17(10), pp. 888-895

PAGE, E.L., ROBITAILLE, G.A., POUYSSEGUR, J. and RICHARD, D.E., 2002. Induction of hypoxia-inducible factor-1alpha by transcriptional and translational mechanisms. *Journal of Biological Chemistry*, 277(50), pp. 48403-48409

PALMER, L.A. and JOHNS, R.A., 1998. Hypoxia upregulates inducible (Type II) nitric oxide synthase in an HIF-1 dependent manner in rat pulmonary microvascular but not aortic smooth muscle cells. *Chest*, 114(1 Suppl), pp. 33S-34S

PANDOLFI, A., CETRULLO, D., POLISHUCK, R., ALBERTA, M.M., CALAFIORE, A., PELLEGRINI, G., VITACOLONNA, E., CAPANI, F. and CONSOLI, A., 2001. Plasminogen activator inhibitor type 1 is increased in the arterial wall of type II diabetic subjects. *Arteriosclerosis, Thrombosis, and Vascular Biology*, 21(8), pp. 1378-1382

PAPANDREOU, I., CAIRNS, R.A., FONTANA, L., LIM, A.L. and DENKO, N.C., 2006. HIF-1 mediates adaptation to hypoxia by actively downregulating mitochondrial oxygen consumption. *Cell.Metab.*, 3(3), pp. 187-197

PASCAL, M.M., FORRESTER, J.V. and KNOTT, R.M., 1999. Glucose-mediated regulation of transforming growth factor-beta (TGF-beta) and TGF-beta receptors in human retinal endothelial cells. *Current eye research*, 19(2), pp. 162-170

PFAFFLIN, A., BRODBECK, K., HEILIG, C.W., HARING, H.U., SCHLEICHER, E.D. and WEIGERT, C., 2006. Increased glucose uptake and metabolism in mesangial cells overexpression glucose transporter 1 increases interleukin-6 and vascular endothelial growth factor production: role of AP-1 and HIF-1 α . *Cellular Physiology and Biochemistry*, 18, pp. 199-210

PINTER, E., HAIGH, J., NAGY, A. and MADRI, J.A., 2001. Hyperglycemia-induced vasculopathy in the murine conceptus is mediated via reductions of VEGF-A expression and VEGF receptor activation. *American Journal of Pathology*, 158(4), pp. 1199-1206

PIOLI, P.A., HAMILTON, B.J., CONNOLLY, J.E., BREWER, G. and RIGBY, W.F., 2002. Lactate dehydrogenase is an AU-rich element-binding protein that directly interacts with AUF1. *Journal of Biological Chemistry*, 277(38), pp. 35738-35745

POULAKI, V., QIN, W., JOUSSEN, A.M., HURLBUT, P., WIEGAND, S.J., RUDGE, J., YANCOPOULOS, G.D. and ADAMIS, A.P., 2002. Acute intensive insulin therapy exacerbates diabetic blood-retinal barrier breakdown via hypoxia-inducible factor-1 alpha and VEGF. *The Journal of clinical investigation*, 109(6), pp. 805-815

POWELL, L.A., NALLY, S.M., MCMASTER, D., CATHERWOOD, M.A. and TRIMBLE, E.R., 2001. Restoration of glutathione levels in vascular smooth muscle cells exposed to high glucose conditions. *Free radical biology & medicine*, 31(10), pp. 1149-1155

POWELL, L.A., WARPEHA, K.M., XU, W., WALKER, B. and TRIMBLE, E.R., 2004. High glucose decreases intracellular glutathione concentrations and upregulates inducible nitric oxide synthase gene expression in intestinal epithelial cells. *Journal of Molecular Endocrinology*, 33(3), pp. 797-803

RAJAKUMAR, A., DOTY, K., DAFTARY, A., HARGER, G. and CONRAD, K.P., 2003. Impaired oxygen-dependent reduction of HIF-1 alpha and -2alpha proteins in pre-eclamptic placentae. *Placenta*, 24(2-3), pp. 199-208

RATCLIFFE, P.J., O'ROURKE, J.F., MAXWELL, P.H. and PUGH, C.W., 1998. Oxygen sensing, hypoxia-inducible factor-1 and the regulation of mammalian gene expression. *The Journal of experimental biology*, 201(Pt 8), pp. 1153-1162

RAVI, R., MOOKERJEE, B., BHUJWALLA, Z.M., SUTTER, C.H., ARTEMOV, D., ZENG, Q., DILLEHAY, L.E., MADAN, A., SEMENZA, G.L. and BEDI, A., 2000. Regulation of tumor angiogenesis by p53-induced degradation of hypoxia-inducible factor 1alpha. *Genes & development*, 14(1), pp. 34-44

RICHARD, D.E., BERRA, E., GOTHIE, E., ROUX, D. and POUYSSEGUR, J., 1999. p42/p44 mitogen-activated protein kinases phosphorylate hypoxia-inducible factor 1 alpha (HIF-1 alpha) and enhance the transcriptional activity of HIF-1. *Journal of Biological Chemistry*, 274(46), pp. 32631-32637

RICHARD, D.E., BERRA, E. and POUYSSEGUR, J., 1999. Angiogenesis: how a tumor adapts to hypoxia. *Biochemical and biophysical research communications*, 266(3), pp. 718-722

RIDDLE, S.R., AHMAD, A., AHMAD, S., DEEB, S.S., MALKKI, M., SCHNEIDER, B.K., ALLEN, C.B. and WHITE, C.W., 2000. Hypoxia induces hexokinase II gene expression in human lung cell line A549. *American Journal of Physiology. Lung Cellular and Molecular Physiology*, 278(2), pp. L407-16

RIVARD, A., SILVER, M., CHEN, D., KEARNEY, M., MAGNER, M., ANNEX, B., PETERS, K. and ISNER, J.M., 1999. Rescue of diabetes-related impairment of angiogenesis by intramuscular gene therapy with adeno-VEGF. *American Journal of Pathology*, 154(2), pp. 355-363

RODRIGUEZ-MANAS, L., ANGULO, J., PEIRO, C., LLERGO, J.L., SANCHEZ-FERRER, A., LOPEZ-DORIGA, P. and SANCHEZ-FERRER, C.F., 1998. Endothelial dysfunction and metabolic control in streptozotocin-induced diabetic rats. *British journal of pharmacology*, 123(8), pp. 1495-1502

ROSSIGNOL, F., VACHE, C. and CLOTTE, E., 2002. Natural antisense transcripts of hypoxia-inducible factor 1alpha are detected in different normal and tumour human tissues. *Gene*, 299(1-2), pp. 135-140

ROTTMAN, J.B., 2002. The ribonuclease protection assay: a powerful tool for the veterinary pathologist. *Veterinary pathology*, 39(1), pp. 2-9

RUHE, R.C. and MCDONALD, R.B., 2001. Use of antioxidant nutrients in the prevention and treatment of type 2 diabetes. *Journal of the American College of Nutrition*, 20(5 Suppl), pp. 363S-369S; discussion 381S-383S

SAFRAN, M. and KAELIN, W.G.,JR, 2003. HIF hydroxylation and the mammalian oxygen-sensing pathway. *The Journal of clinical investigation*, 111(6), pp. 779-783

SALCEDA, S., BECK, I., SRINIVAS, V. and CARO, J., 1997. Complex role of protein phosphorylation in gene activation by hypoxia. *Kidney international*, 51(2), pp. 556-559

SALNIKOW, K., SU, W., BLAGOSKLONNY, M.V. and COSTA, M., 2000. Carcinogenic metals induce hypoxia-inducible factor-stimulated transcription by reactive oxygen species-independent mechanism. *Cancer research*, 60(13), pp. 3375-3378

SANDAU, K.B., ZHOU, J., KIETZMANN, T. and BRUNE, B., 2001. Regulation of the hypoxia-inducible factor 1alpha by the inflammatory mediators nitric oxide and tumor necrosis factor-alpha in contrast to desferrioxamine and phenylarsine oxide. *Journal of Biological Chemistry*, 276(43), pp. 39805-39811

SASSO, F.C., TORELLA, D., CARBONARA, O., ELLISON, G.M., TORELLA, M., SCARDONE, M., MARRA, C., NASTI, R., MARFELLA, R., COZZOLINO, D., INDOLFI, C., COTRUFO, M., TORELLA, R. and SALVATORE, T., 2005. Increased vascular endothelial growth factor expression but impaired vascular endothelial growth factor receptor signaling in the myocardium of type 2 diabetic patients with chronic coronary heart disease. *Journal of the American College of Cardiology*, 46(5), pp. 827-834

SCHMEDTJE, J.F.,JR, JI, Y.S., LIU, W.L., DUBOIS, R.N. and RUNGE, M.S., 1997. Hypoxia induces cyclooxygenase-2 via the NF-kappaB p65 transcription factor in human vascular endothelial cells. *Journal of Biological Chemistry*, 272(1), pp. 601-608

SEMENZA, G.L., 1998. Hypoxia-inducible factor 1 and the molecular physiology of oxygen homeostasis. *The Journal of laboratory and clinical medicine*, 131(3), pp. 207-214

SEMENZA, G.L., 1999. Regulation of mammalian O₂ homeostasis by hypoxia-inducible factor 1. *Annual Review of Cell and Developmental Biology*, 15, pp. 551-578

SEMENZA, G.L., 2000. HIF-1: mediator of physiological and pathophysiological responses to hypoxia. *Journal of applied physiology: respiratory, environmental and exercise physiology*, 88(4), pp. 1474-1480

SEMENZA, G.L., 2000. Hypoxia, clonal selection, and the role of HIF-1 in tumor progression. *Critical reviews in biochemistry and molecular biology*, 35(2), pp. 71-103

SEMENZA, G.L. and WANG, G.L., 1992. A nuclear factor induced by hypoxia via de novo protein synthesis binds to the human erythropoietin gene enhancer at a site required for transcriptional activation. *Molecular and cellular biology*, 12(12), pp. 5447-5454

SERVICE, F.J. and O'BRIEN, P.C., 2001. The relation of glycaemia to the risk of development and progression of retinopathy in the Diabetic Control and Complications Trial. *Diabetologia*, 44(10), pp. 1215-1220

SHI, Y.H., WANG, Y.X., BINGLE, L., GONG, L.H., HENG, W.J., LI, Y. and FANG, W.G., 2005. In vitro study of HIF-1 activation and VEGF release by bFGF in the T47D breast cancer cell line under normoxic conditions: involvement of PI-3K/Akt and MEK1/ERK pathways. *The Journal of pathology*, 205(4), pp. 530-536

SHIBA, T., INOBUCHI, T., SPORTSMAN, J.R., HEATH, W.F., BURSELL, S. and KING, G.L., 1993. Correlation of diacylglycerol level and protein kinase C activity in rat retina to retinal circulation. *The American Journal of Physiology*, 265(5 Pt 1), pp. E783-93

SHIGEMATSU, S., YAMAUCHI, K., NAKAJIMA, K., IJIMA, S., AIZAWA, T. and HASHIZUME, K., 1999. D-Glucose and insulin stimulate migration and tubular formation of human endothelial cells in vitro. *The American Journal of Physiology*, 277(3 Pt 1), pp. E433-8

SHIMA, D.T., ADAMIS, A.P., FERRARA, N., YEO, K.T., YEO, T.K., ALLENDE, R., FOLKMAN, J. and D'AMORE, P.A., 1995. Hypoxic induction of endothelial cell growth factors in retinal cells: identification and characterization of vascular endothelial growth factor (VEGF) as the mitogen. *Molecular medicine (Cambridge, Mass.)*, 1(2), pp. 182-193

SHWEIKI, D., ITIN, A., SOFFER, D. and KESHET, E., 1992. Vascular endothelial growth factor induced by hypoxia may mediate hypoxia-initiated angiogenesis. *Nature*, 359(6398), pp. 843-845

SMITH-MCCUNE, K., ZHU, Y.H., HANAHAAN, D. and ARBEIT, J., 1997. Cross-species comparison of angiogenesis during the premalignant stages of squamous carcinogenesis in the human cervix and K14-HPV16 transgenic mice. *Cancer research*, 57(7), pp. 1294-1300

SOBEY, C.G. and FARACI, F.M., 1997. Effects of a novel inhibitor of guanylyl cyclase on dilator responses of mouse cerebral arterioles. *Stroke; a journal of cerebral circulation*, 28(4), pp. 837-42; discussion 842-3

SOBEY, C.G., WEILER, J.M., BOUJAOUDE, M. and WOODMAN, O.L., 2004. Effect of short-term phytoestrogen treatment in male rats on nitric oxide-mediated responses of carotid and cerebral arteries: comparison with 17beta-estradiol. *The Journal of pharmacology and experimental therapeutics*, 310(1), pp. 135-140

SODHI, C.P., PHADKE, S.A., BATLLE, D. and SAHAI, A., 2001. Hypoxia and high glucose cause exaggerated mesangial cell growth and collagen synthesis: role of osteopontin. *American Journal of Physiology. Renal Physiology*, 280(4), pp. F667-74

SOGAWA, K., NUMAYAMA-TSURUTA, K., EMA, M., ABE, M., ABE, H. and FUJII-KURIYAMA, Y., 1998. Inhibition of hypoxia-inducible factor 1 activity by nitric oxide

donors in hypoxia. *Proceedings of the National Academy of Sciences of the United States of America*, 95(13), pp. 7368-7373

SONDERGAARD, K.L., HILTON, D.A., PENNEY, M., OLLERENSHAW, M. and DEMAINE, A.G., 2002. Expression of hypoxia-inducible factor 1alpha in tumours of patients with glioblastoma. *Neuropathology and applied neurobiology*, 28(3), pp. 210-217

SOULIS, T., SASTRA, S., THALLAS, V., MORTENSEN, S.B., WILKEN, M., CLAUSEN, J.T., BJERRUM, O.J., PETERSEN, H., LAU, J., JERUMS, G., BOEL, E. and COOPER, M.E., 1999. A novel inhibitor of advanced glycation end-product formation inhibits mesenteric vascular hypertrophy in experimental diabetes. *Diabetologia*, 42(4), pp. 472-479

SOWTER, H.M., RAVAL, R., MOORE, J., RATCLIFFE, P.J. and HARRIS, A.L., 2003. Predominant role of hypoxia-inducible transcription factor (Hif)-1 α versus Hif-2 α in regulation of the transcriptional response to hypoxia. *Cancer Research*, 63, pp. 6130-6134

SRINIVAS, V., LESHCHINSKY, I., SANG, N., KING, M.P., MINCHENKO, A. and CARO, J., 2001. Oxygen sensing and HIF-1 activation does not require an active mitochondrial respiratory chain electron-transfer pathway. *Journal of Biological Chemistry*, 276(25), pp. 21995-21998

SRINIVAS, V., LESHCHINSKY, I., SANG, N., KING, M.P., MINCHENKO, A. and CARO, J., 2001. Oxygen sensing and HIF-1 activation does not require an active mitochondrial respiratory chain electron-transfer pathway. *Journal of Biological Chemistry*, 276(25), pp. 21995-21998

SRIVASTAVA, K.D., ROM, W.N., JAGIRDAR, J., YIE, T.A., GORDON, T. and TCHOU-WONG, K.M., 2002. Crucial role of interleukin-1beta and nitric oxide synthase in silica-induced inflammation and apoptosis in mice. *American Journal of Respiratory and Critical Care Medicine : An Official Journal of the American Thoracic Society, Medical Section of the American Lung Association*, 165(4), pp. 527-533

STEHOUWER, C.D., LAMBERT, J., DONKER, A.J. and VAN HINSBERGH, V.W., 1997. Endothelial dysfunction and pathogenesis of diabetic angiopathy. *Cardiovascular research*, 34(1), pp. 55-68

STEVENS, M.J., DANANBERG, J., FELDMAN, E.L., LATTIMER, S.A., KAMIJO, M., THOMAS, T.P., SHINDO, H., SIMA, A.A. and GREENE, D.A., 1994. The linked roles of nitric oxide, aldose reductase and, (Na⁺,K⁺)-ATPase in the slowing of nerve conduction in the streptozotocin diabetic rat. *The Journal of clinical investigation*, 94(2), pp. 853-859

STIEHL, D.P., JELKMANN, W., WENGER, R.H. and HELLWIG-BURGEL, T., 2002. Normoxic induction of the hypoxia-inducible factor 1alpha by insulin and interleukin-1beta involves the phosphatidylinositol 3-kinase pathway. *FEBS letters*, 512(1-3), pp. 157-162

STROKA, D.M., BURKHARDT, T., DESBAILLETS, I., WENGER, R.H., NEIL, D.A., BAUER, C., GASSMANN, M. and CANDINAS, D., 2001. HIF-1 is expressed in normoxic tissue and displays an organ-specific regulation under systemic hypoxia. *The FASEB journal : official publication of the Federation of American Societies for Experimental Biology*, 15(13), pp. 2445-2453

TACCHINI, L., DANSI, P., MATTEUCCI, E. and DESIDERIO, M.A., 2001. Hepatocyte growth factor signalling stimulates hypoxia inducible factor-1 (HIF-1) activity in HepG2 hepatoma cells. *Carcinogenesis*, 22(9), pp. 1363-1371

TEICHERT, J., KERN, J., TRITSCHLER, H.J., ULRICH, H. and PREISS, R., 1998. Investigations on the pharmacokinetics of alpha-lipoic acid in healthy volunteers. *International journal of clinical pharmacology and therapeutics*, 36(12), pp. 625-628

TERATA, K., COPPEY, L.J., DAVIDSON, E.P., DUNLAP, J.A., GUTTERMAN, D.D. and YOREK, M.A., 1999. Acetylcholine-induced arteriolar dilation is reduced in streptozotocin-induced diabetic rats with motor nerve dysfunction. *British journal of pharmacology*, 128(3), pp. 837-843

TESFAYE, S., STEVENS, L.K., STEPHENSON, J.M., FULLER, J.H., PLATER, M., IONESCU-TIRGOVISTE, C., NUBER, A., POZZA, G. and WARD, J.D., 1996. Prevalence of diabetic peripheral neuropathy and its relation to glycaemic control and potential risk factors: the EURODIAB IDDM Complications Study. *Diabetologia*, 39(11), pp. 1377-1384

THE DIABETES CONTROL AND COMPLICATIONS TRIAL RESEARCH GROUP, 1993. The effect of intensive treatment of diabetes on the development and progression of long-term complications in insulin-dependent diabetes mellitus. *The Diabetes Control*

and Complications Trial Research Group. *The New England journal of medicine*, 329(14), pp. 977-986

THOMAS, P.K., 1993. A critical assessment of vascular factors in the causation of diabetic polyneuropathy. *Diabetic medicine : a journal of the British Diabetic Association*, 10 Suppl 2, pp. 62S-63S

THOMSEN, K., RUBIN, I. and LAURITZEN, M., 2002. NO- and non-NO-, non-prostanoid-dependent vasodilatation in rat sciatic nerve during maturation and developing experimental diabetic neuropathy. *The Journal of physiology*, 543(Pt 3), pp. 977-993

THRASH-BINGHAM, C.A. and TARTOF, K.D., 1999. aHIF: a natural antisense transcript overexpressed in human renal cancer and during hypoxia. *Journal of the National Cancer Institute*, 91(2), pp. 143-151

TIROSH, O., SHILO, S., ARONIS, A. and SEN, C.K., 2003. Redox regulation of mitochondrial permeability transition: effects of uncoupler, lipoic acid and its positively charged analog LA-plus and selenium. *BioFactors (Oxford, England)*, 17(1-4), pp. 297-306

TREINS, C., GIORGETTI-PERALDI, S., MURDACA, J., SEMENZA, G.L. and VAN OBBERGHEN, E., 2002. Insulin stimulates hypoxia-inducible factor 1 through a phosphatidylinositol 3-kinase/target of rapamycin-dependent signaling pathway. *Journal of Biological Chemistry*, 277(31), pp. 27975-27981

TREINS, C., GIORGETTI-PERALDI, S., MURDACA, J. and VAN OBBERGHEN, E., 2001. Regulation of vascular endothelial growth factor expression by advanced glycation end products. *Journal of Biological Chemistry*, 276(47), pp. 43836-43841

TRETYAKOVA, I., ZOLOTUKHIN, A.S., TAN, W., BEAR, J., PROPST, F., RUTHEL, G. and FELBER, B.K., 2005. Nuclear export factor family protein participates in cytoplasmic mRNA trafficking. *Journal of Biological Chemistry*, 280(36), pp. 31981-31990

TUCCI, M., MCDONALD, R.J., AARONSON, R., GRAVEN, K.K. and FARBER, H.W., 1996. Specificity and uniqueness of endothelial cell stress responses. *The American Journal of Physiology*, 271(3 Pt 1), pp. L341-8

TUCCI, M., NYGARD, K., TANSWELL, B.V., FARBER, H.W., HILL, D.J. and HAN, V.K., 1998. Modulation of insulin-like growth factor (IGF) and IGF binding protein

biosynthesis by hypoxia in cultured vascular endothelial cells. *The Journal of endocrinology*, 157(1), pp. 13-24

UCHIDA, T., ROSSIGNOL, F., MATTHAY, M.A., MOUNIER, R., COUETTE, S., CLOTTE, E. and CLERICI, C., 2004. Prolonged hypoxia differentially regulates hypoxia-inducible factor (HIF)-1alpha and HIF-2alpha expression in lung epithelial cells: implication of natural antisense HIF-1alpha. *Journal of Biological Chemistry*, 279(15), pp. 14871-14878

UK PROSPECTIVE DIABETES STUDY (UKPDS) GROUP, 1998. Effect of intensive blood-glucose control with metformin on complications in overweight patients with type 2 diabetes (UKPDS 34). UK Prospective Diabetes Study (UKPDS) Group. *Lancet*, 352(9131), pp. 854-865

VANHAESEBROECK, B. and ALESSI, D.R., 2000. The PI3K-PDK1 connection: more than just a road to PKB. *The Biochemical journal*, 346 Pt 3, pp. 561-576

VANNUCCI, S.J., SEAMAN, L.B. and VANNUCCI, R.C., 1996. Effects of hypoxia-ischemia on GLUT1 and GLUT3 glucose transporters in immature rat brain. *Journal of cerebral blood flow and metabolism : official journal of the International Society of Cerebral Blood Flow and Metabolism*, 16(1), pp. 77-81

VAUX, E.C., METZEN, E., YEATES, K.M. and RATCLIFFE, P.J., 2001. Regulation of hypoxia-inducible factor is preserved in the absence of a functioning mitochondrial respiratory chain. *Blood*, 98(2), pp. 296-302

VERROTTI, A., GRECO, R., BASCIANI, F., MORGESE, G. and CHIARELLI, F., 2003. von Willebrand factor and its propeptide in children with diabetes. Relation between endothelial dysfunction and microalbuminuria. *Pediatric research*, 53(3), pp. 382-386

VEVES, A., DONAGHUE, V.M., SARNOW, M.R., GIURINI, J.M., CAMPBELL, D.R. and LOGERFO, F.W., 1996. The impact of reversal of hypoxia by revascularization on the peripheral nerve function of diabetic patients. *Diabetologia*, 39(3), pp. 344-348

VIHANTO, M.M., PLOCK, J., ERNI, D., FREY, B.M., FREY, F.J., HUYNH-DO, U., 2005. Hypoxia up-regulates expression of Eph receptors and ephrins in mouse skin. *The FASEB Journal*

VOGEL, T., BLAKE, D.A., WHIKEHART, D.R., GUO, N.H., ZABRENETZKY, V.S. and ROBERTS, D.D., 1993. Specific simple sugars promote chemotaxis and chemokinesis of corneal endothelial cells. *Journal of cellular physiology*, 157(2), pp. 359-366

VORDERMARK, D., KRAFT, P., KATZER, A., BOLLING, T., WILLNER, J. and FLENTJE, M., 2005. Glucose requirement for hypoxic accumulation of hypoxia-inducible factor-1 α . *Cancer Letters*, 230, pp. 122-133

WAHL, S.M., HUNT, D.A., WAKEFIELD, L.M., MCCARTNEY-FRANCIS, N., WAHL, L.M., ROBERTS, A.B. and SPORN, M.B., 1987. Transforming growth factor type beta induces monocyte chemotaxis and growth factor production. *Proceedings of the National Academy of Sciences of the United States of America*, 84(16), pp. 5788-5792

WANG, G.L., JIANG, B.H., RUE, E.A. and SEMENZA, G.L., 1995. Hypoxia-inducible factor 1 is a basic-helix-loop-helix-PAS heterodimer regulated by cellular O₂ tension. *Proceedings of the National Academy of Sciences of the United States of America*, 92(12), pp. 5510-5514

WANG, G.L. and SEMENZA, G.L., 1993. General involvement of hypoxia-inducible factor 1 in transcriptional response to hypoxia. *Proceedings of the National Academy of Sciences of the United States of America*, 90(9), pp. 4304-4308

WANG, G.L. and SEMENZA, G.L., 1995. Purification and characterization of hypoxia-inducible factor 1. *Journal of Biological Chemistry*, 270(3), pp. 1230-1237

WANG, Q., DILLS, D.G., KLEIN, R., KLEIN, B.E. and MOSS, S.E., 1995. Does insulin-like growth factor I predict incidence and progression of diabetic retinopathy? *Diabetes*, 44(2), pp. 161-164

WANG, T., FOKER, J.E. and TSAI, M.Y., 1980. The shift of an increase in phosphofructokinase activity from protein synthesis-dependent to -independent mode during concanavalin A induced lymphocyte proliferation. *Biochemical and biophysical research communications*, 95(1), pp. 13-19

WATKINS, P.J., 2003. *ABC of diabetes*. London: BMJ Books.

WAUTIER, J.L., ZOUKOURIAN, C., CHAPPEY, O., WAUTIER, M.P., GUILLAUSSEAU, P.J., CAO, R., HORI, O., STERN, D. and SCHMIDT, A.M., 1996. Receptor-mediated endothelial cell dysfunction in diabetic vasculopathy. Soluble receptor

for advanced glycation end products blocks hyperpermeability in diabetic rats. *The Journal of clinical investigation*, 97(1), pp. 238-243

WEBSTER, K.A., 1987. Regulation of glycolytic enzyme RNA transcriptional rates by oxygen availability in skeletal muscle cells. *Molecular and cellular biochemistry*, 77(1), pp. 19-28

WENGER, R.H., 2000. Mammalian oxygen sensing, signalling and gene regulation. *The Journal of experimental biology*, 203(Pt 8), pp. 1253-1263

WENGER, R.H., KVIETIKOVA, I., ROLFS, A., GASSMANN, M. and MARTI, H.H., 1997. Hypoxia-inducible factor-1 alpha is regulated at the post-mRNA level. *Kidney international*, 51(2), pp. 560-563

WHITESSELL, R.R., REGEN, D.M., PELLETIER, D. and ABUMRAD, N.A., 1990. Evidence that downregulation of hexose transport limits intracellular glucose in 3T3-L1 fibroblasts. *Diabetes*, 39(10), pp. 1228-1234

WIENER, C.M., BOOTH, G. and SEMENZA, G.L., 1996. In vivo expression of mRNAs encoding hypoxia-inducible factor 1. *Biochemical and biophysical research communications*, 225(2), pp. 485-488

WEISNER, M.S., JURGENSEN, J.S., ROSENBERGER, C., SCHOLZE, C., HORSTRUP, J.H., WARNECKE, C., MANDRIOTA, S., BECHMANN, I., FREI, U.A., PUGH, C.W., RATCLIFFE, P.J., BACHMANN, S., MAXWELL, P.H., ECKARDT, K., 2002. Widespread, hypoxia-inducible expression of HIF-2 α in distinct cell populations of different organs. *The FASEB Journal*.

WILLIAMSON, J.R. and ARRIGONI-MARTELLI, E., 1992. The roles of glucose-induced metabolic hypoxia and imbalances in carnitine metabolism in mediating diabetes-induced vascular dysfunction. *International journal of clinical pharmacology research*, 12(5-6), pp. 247-252

WILLIAMSON, J.R., CHANG, K., FRANGOS, M., HASAN, K.S., IDO, Y., KAWAMURA, T., NYENGAARD, J.R., VAN DEN ENDEN, M., KILO, C. and TILTON, R.G., 1993. Hyperglycemic pseudohypoxia and diabetic complications. *Diabetes*, 42(6), pp. 801-813

WENGER, R.H. and GASSMANN, M., 1997. Oxygen(es) and the hypoxia-inducible-factor-1. *Biological Chemistry*, 378. pp. 609-616.

WILSON, W.J. and POELLINGER, L., 2002. The dietary flavonoid quercetin modulates HIF-1 alpha activity in endothelial cells. *Biochemical and biophysical research communications*, 293(1), pp. 446-450

WINTERS, S. and JERNIGAN, V., 2000. Vascular disease risk markers in diabetes: monitoring & intervention. *The Nurse practitioner*, 25(6 Pt 1), pp. 40, 43-6, 49 passim; quiz 65-7

WU, Q.D., WANG, J.H., FENNESSY, F., REDMOND, H.P. and BOUCHIER-HAYES, D., 1999. Taurine prevents high-glucose-induced human vascular endothelial cell apoptosis. *The American Journal of Physiology*, 277(6 Pt 1), pp. C1229-38

XU, Q., SIMPSON, S.E., SCIALLA, T.J., BAGG, A. and CARROLL, M., 2003. Survival of acute myeloid leukemia cells requires PI3 kinase activation. *Blood*, 102(3), pp. 972-980

YAGIHASHI, S., YAMAGISHI, S.I., WADA RI, R., BABA, M., HOHMAN, T.C., YABE-NISHIMURA, C. and KOKAI, Y., 2001. Neuropathy in diabetic mice overexpressing human aldose reductase and effects of aldose reductase inhibitor. *Brain; a journal of neurology*, 124(Pt 12), pp. 2448-2458

YAMAGISHI, S. and TAKEUCHI, M., 2004. Inhibition of protein kinase C might be harmful to diabetic retinopathy. *Medical hypotheses*, 63(1), pp. 135-137

YAMAKAWA, M., LIU, L.X., DATE, T., BELANGER, A.J., VINCENT, K.A., AKITA, G.Y., KURIYAMA, T., CHENG, S.H., GREGORY, R.J. and JIANG, C., 2003. Hypoxia-inducible factor-1 mediates activation of cultured vascular endothelial cells by inducing multiple angiogenic factors. *Circulation research*, 93(7), pp. 664-673

YANG, Z.Z., ZHANG, A.Y., YI, F.X., LI, P.L. and ZOU, A.P., 2003. Redox regulation of HIF-1alpha levels and HO-1 expression in renal medullary interstitial cells. *American Journal of Physiology. Renal Physiology*, 284(6), pp. F1207-15

YASUDA, S., ARII, S., MORI, A., ISOBE, N., YANG, W., OE, H., FUJIMOTO, A., YONENAGA, Y., SAKASHITA, H. and IMAMURA, M., 2004. Hexokinase II and VEGF expression in liver tumors: correlation with hypoxia-inducible factor 1 alpha and its significance. *Journal of hepatology*, 40(1), pp. 117-123

YIN, Z., HAYNIE, J., YANG, X., HAN, B., KIATCHOOSAKUN, S., RESTIVO, J., YUAN, S., PRABHAKAR, N.R., HERRUP, K., CONLON, R.A., HOIT, B.D.,

- WATANABE, M. and YANG, Y.C., 2002. The essential role of Cited2, a negative regulator for HIF-1alpha, in heart development and neurulation. *Proceedings of the National Academy of Sciences of the United States of America*, 99(16), pp. 10488-10493
- YOREK, M.A., 2003. The role of oxidative stress in diabetic vascular and neural disease. *Free radical research*, 37(5), pp. 471-480
- YOUNG, M.J., VEVES, A., WALKER, M.G. and BOULTON, A.J., 1992. Correlations between nerve function and tissue oxygenation in diabetic patients: further clues to the aetiology of diabetic neuropathy? *Diabetologia*, 35(12), pp. 1146-1150
- YU, A.Y., FRID, M.G., SHIMODA, L.A., WIENER, C.M., STENMARK, K. and SEMENZA, G.L., 1998. Temporal, spatial, and oxygen-regulated expression of hypoxia-inducible factor-1 in the lung. *The American Journal of Physiology*, 275(4 Pt 1), pp. L818-26
- YU, D.Y., CRINGLE, S.J., SU, E.N., YU, P.K., JERUMS, G. and COOPER, M.E., 2001. Pathogenesis and intervention strategies in diabetic retinopathy. *Clinical & experimental ophthalmology*, 29(3), pp. 164-166
- YU, E.Z., LI, Y.Y., LIU, X.H., KAGAN, E. and MCCARRON, R.M., 2004. Antiapoptotic action of hypoxia-inducible factor-1 alpha in human endothelial cells. *Laboratory investigation; a journal of technical methods and pathology*, 84(5), pp. 553-561
- ZAMAN, K., RYU, H., HALL, D., O'DONOVAN, K., LIN, K.I., MILLER, M.P., MARQUIS, J.C., BARABAN, J.M., SEMENZA, G.L. and RATAN, R.R., 1999. Protection from oxidative stress-induced apoptosis in cortical neuronal cultures by iron chelators is associated with enhanced DNA binding of hypoxia-inducible factor-1 and ATF-1/CREB and increased expression of glycolytic enzymes, p21(waf1/cip1), and erythropoietin. *The Journal of neuroscience : the official journal of the Society for Neuroscience*, 19(22), pp. 9821-9830
- ZANETTI, M., ZWACKA, R., ENGELHARDT, J., KATUSIC, Z. and O'BRIEN, T., 2001. Superoxide anions and endothelial cell proliferation in normoglycemia and hyperglycemia. *Arteriosclerosis, Thrombosis, and Vascular Biology*, 21(2), pp. 195-200
- ZELZER, E., LEVY, Y., KAHANA, C., SHILO, B.Z., RUBINSTEIN, M. and COHEN, B., 1998. Insulin induces transcription of target genes through the hypoxia-inducible factor HIF-1alpha/ARNT. *The EMBO journal*, 17(17), pp. 5085-5094

ZHONG, H., AGANI, F., BACCALA, A.A., LAUGHNER, E., RIOSECO-CAMACHO, N., ISAACS, W.B., SIMONS, J.W. and SEMENZA, G.L., 1998. Increased expression of hypoxia inducible factor-1alpha in rat and human prostate cancer. *Cancer research*, 58(23), pp. 5280-5284

ZHONG, H., CHILES, K., FELDSER, D., LAUGHNER, E., HANRAHAN, C., GEORGESCU, M.M., SIMONS, J.W. and SEMENZA, G.L., 2000. Modulation of hypoxia-inducible factor 1alpha expression by the epidermal growth factor/phosphatidylinositol 3-kinase/PTEN/AKT/FRAP pathway in human prostate cancer cells: implications for tumor angiogenesis and therapeutics. *Cancer research*, 60(6), pp. 1541-1545

ZHONG, H., DE MARZO, A.M., LAUGHNER, E., LIM, M., HILTON, D.A., ZAGZAG, D., BUECHLER, P., ISAACS, W.B., SEMENZA, G.L. and SIMONS, J.W., 1999. Overexpression of hypoxia-inducible factor 1alpha in common human cancers and their metastases. *Cancer research*, 59(22), pp. 5830-5835

ZHOU, J., FANDREY, J., SCHUMANN, J., TIEGS, G. and BRUNE, B., 2003. NO and TNF-alpha released from activated macrophages stabilize HIF-1alpha in resting tubular LLC-PK1 cells. *American Journal of Physiology. Cell physiology*, 284(2), pp. C439-46

ZIEGLER, D., HANEFELD, M., RUHNAU, K.J., HASCHE, H., LOBISCH, M., SCHUTTE, K., KERUM, G. and MALESSA, R., 1999. Treatment of symptomatic diabetic polyneuropathy with the antioxidant alpha-lipoic acid: a 7-month multicenter randomized controlled trial (ALADIN III Study). ALADIN III Study Group. Alpha-Lipoic Acid in Diabetic Neuropathy. *Diabetes care*, 22(8), pp. 1296-1301

ZIEL, K.A., GRISHKO, V., CAMPBELL, C.C., BREIT, J.F., WILSON, G.L. and GILLESPIE, M.N., 2005. Oxidants in signal transduction: impact on DNA integrity and gene expression. *The FASEB journal : official publication of the Federation of American Societies for Experimental Biology*, 19(3), pp. 387-394

ZUND, G., NELSON, D.P., NEUFELD, E.J., DZUS, A.L., BISCHOFF, J., MAYER, J.E. and COLGAN, S.P., 1996. Hypoxia enhances stimulus-dependent induction of E-selectin on aortic endothelial cells. *Proceedings of the National Academy of Sciences of the United States of America*, 93(14), pp. 7075-7080

ZUNDEL, W., SCHINDLER, C., HAAS-KOGAN, D., KOONG, A., KAPER, F., CHEN, E., GOTTSCHALK, A.R., RYAN, H.E., JOHNSON, R.S., JEFFERSON, A.B.,

STOKOE, D. and GIACCIA, A.J., 2000. Loss of PTEN facilitates HIF-1-mediated gene expression. *Genes & development*, 14(4), pp. 391-396

Appendix 2

Buffers and solutions

Buffers and solutions

All reagents were purchased from Sigma, unless stated otherwise.

ABC/AP substrate buffer

1.7ml Naphtol AS-MX Phosphate sodium salt
1mM Levamisol
3.5mM Fast red TR salt
in Veronal acetate buffer

Bacterial cell lysis buffer

200mM NaOH
1% SDS

Blocking solution

1% (w/v) blocking reagent (Roche)
0.1M maleic acid
0.15M NaCl, pH 7.5

Chemiluminescent detection washing buffer

0.1M maleic acid
0.15M NaCl, pH 7.5
0.3% Tween

50x Derrhardt's reagent

1% w/v Ficoll
1% w/v PVP
1% w/v BSA
800µl denatured salmon sperm
10% SDS

Detection buffer

0.1M Tris-HCl

0.1M NaCl, pH 9.5

DIG-AP antibody solution

75 mU/ml anti-DIG-AP (Roche)

1% (w/v) blocking reagent (Roche)

0.1M maleic acid

0.15M NaCl, pH 7.5

DIG detection blocking buffer

5% BSA

0.1M Tris-HCl

0.15 NaCl, pH 7.5

DIG detection substrate buffer

0.1M Tris-HCl

0.1M NaCl

0.05M MgCl₂

DIG detection wash buffer

0.1M Tris-HCl

0.15M NaCl, pH 7.5

DNA loading dye

50% Glycerol

100mM Na EDTA 2H₂O

1% SDS

0.1% Bromophenol blue

Equilibration buffer

750mM NaCl

50mM MOPS

15% isopropanol

0.15% Triton-X100, pH 7.0

GMEM

3mM Glutamine (Gibco BRL)

10% Tryptose phosphate broth (Gibco BRL)

100U/ml Penicillin (Gibco BRL)

100µg/ml Streptomycin (Gibco BRL)

1mM HEPES (Gibco BRL)

1.8% NaHCO₃ (Gibco BRL)

HUVEC lysis buffer

1% w/v SDS

1mM sodium orthovanadate

0.01M Tris-HCl, pH 7.4

ISH wash buffer

0.4M NaCl

10mM Tris-HCl

5mM EDTA

LB-1.5% agarose/ampicillin/IPTG/X-gal

1.5% agar (Oxoid)

1% Bacto-tryptone (Oxoid)

0.5% Bacto-yeast extract (Oxoid)

0.5% NaCl, pH 7.0

100µg/ml ampicillin

0.5mM IPTG

80µg/ml X-gal

10x PCR reaction buffer

50mM KCl

10mM Tris-HCl, pH 8.3

1.5mM MgCl₂

Plasmid elution buffer

1.25mM NaCl

50mM MOPS

15% isopropanol, pH 7.0

Plasmid purification neutralisation buffer

3M potassium acetate, pH 5.5

Plasmid purification resuspension buffer

50mM Tris-HCl

10mM EDTA

100µg/ml RNase, pH8.0 (Ambion)

Plasmid purification wash buffer

1M NaCl

50mM MOPS

15% isopropanol, pH 7.0

10 x Restriction enzyme buffer

60mM Tris-HCl pH 9.7,

1.5M NaCl

60mM MgCl₂

10mM DTT (Promega)

RNA loading dye

50% Glycerol

1mM EDTA

0.4% Bromophenol blue

0.4% Xylene cyanol

SOC growth medium

2% Bacto-tryptone (Oxoid)

0.5% Bacto-yeast extract (Oxoid)

10mM NaCl

2.5mM KCl

20mM Mg²⁺

20mM glucose

20X SSC buffer

3M NaCl

0.4M Citric acid

pH to 7.0

TAE buffer

40mM Tris-acetate

1mM EDTA, pH 8.3

TBE buffer

130mM Tris

35mM boric acid

2.5mM EDTA

TE buffer

10mM Tris-HCl, pH 7.4

1mM EDTA

TBS buffer

0.05M Tris-HCl, pH 7.6

0.15M NaCl

Veronal acetate buffer

0.028M Sodium acetate (trihydrate)

0.28M Sodium diethyl barbiturate

pH 9.2, store at 4°C